



**Phosphatidylinositol (3,5) bisphosphate dependent
membrane trafficking in *S. cerevisiae*.**

By

Fay Kathleen Williams

A thesis submitted to the University of Birmingham

for the degree of

DOCTOR OF PHILOSOPHY

School of Biosciences

College of life and environmental sciences

University of Birmingham

B15 2TT

September 2011

Supervisors: Dr. Stephen K. Dove and Professor Robert H. Michell

UNIVERSITY OF
BIRMINGHAM

University of Birmingham Research Archive

e-theses repository

This unpublished thesis/dissertation is copyright of the author and/or third parties. The intellectual property rights of the author or third parties in respect of this work are as defined by The Copyright Designs and Patents Act 1988 or as modified by any successor legislation.

Any use made of information contained in this thesis/dissertation must be in accordance with that legislation and must be properly acknowledged. Further distribution or reproduction in any format is prohibited without the permission of the copyright holder.

ABSTRACT

Phosphoinositides are lipid signals that control cellular processes and are particularly closely associated with the control of membrane trafficking. PtdIns(3,5) P_2 is the most recently identified phosphoinositide and was previously recognised as controlling events in the late endocytic system, between the late endosome and the vacuole/lysosome. Primarily associated with retrograde trafficking from the vacuole/lysosome to the late endosome/MVB, PtdIns(3,5) P_2 is generated by the kinase Fab1p (PIKfyve in animals).

In mammalian cells, PtdIns(3,5) P_2 has also been implicated in control of ill-defined trafficking pathways close to the Golgi; for example, the recycling of mannose-6-phosphate receptor (M6R) back to the Golgi and also the trafficking of some types of ion and nutrient channels from the Golgi to the cell surface.

This thesis describes attempts to study putative PtdIns(3,5) P_2 dependent trafficking in the early endocytic system of *S cerevisiae* using two model proteins; the recycling of Vps10p from late endosome to Golgi and of Chs3p from recycling endosome to Golgi.

Vps10p is a membrane ‘receptor’ for the vacuolar carboxypeptidase Y (CPY) protein that directs this soluble hydrolyase out of the secretory pathway, so that it is correctly sorted into the vacuole. Once it has performed this job, Vps10p recycles back to the Golgi, in a retromer dependent fashion, to bind more CPY cargo for successive rounds of sorting. This study examined recycling of Vps10-GFP, expressed at native levels in wild-type cells and in cells that cannot synthesize PtdIns(3,5) P_2 ($\Delta fab1$) by co-localisation with red fluorescent protein tagged markers for the yeast TGN and

early endosome. By fluorescent microscopy it was shown that neither Fab1p or PtdIns(3,5) P_2 have an affect on recycling of Vps10p, However the process was demonstrated to be dependent upon Vac14p; a protein involved in production of PtdIns(3,5) P_2 but which this thesis shows has independent functions. The trafficking of other cargoes was also examined, including Mrl1p: a protein that shares homology with M6Rs. PtdIns(3,5) P_2 appears to be involved in localisation of this protein, suggesting that PtdIns(3,5) P_2 is important for the recycling of some cargoes and that Mrl1p trafficking could be used as screen to isolate mutants involved in PtdIns(3,5) P_2 dependent late endosome to Golgi recycling.

Chs3p is a protein involved in chitin biosynthesis that traffics from internal stores to the plasma membrane. Deletion of Chs6p traps Chs3p inside the cell because the protein becomes enmeshed in an ‘intracellular treadmill’ of futile recycling between the recycling endosome and Golgi. Part of this recycling is dependent on PtdIns(3,5) P_2 as disruption of PtdIns(3,5) P_2 synthesis frees Chs3p from this futile cycling and allows it to access the cell surface again. When Chs3p is present at the cell surface, the structure of the cell wall changes and can be detected using FACS analysis. FACS analysis was used to isolate mutants that act in the same trafficking pathway as PtdIns(3,5) P_2 . Vps13p was found to be a novel component of Fab1p dependent trafficking at the early endosome and to link to Chs3p trafficking.

ACKNOWLEDGEMENTS

Throughout the time spent doing my PhD I have encountered many people who have infused and encouraged me. First of all I would like to thank my PhD supervisor Dr Stephen K. Dove. During my studies he has been an inspiration to me. He has guided me through the ups and downs, with much patience and advice. I am extremely grateful for the time he has spent helping me produce this thesis, and his kindness throughout the years.

I would also like to gratefully thank Professor Bob Michell. His insights into the area of phosphoinositides have been invaluable, and provided much stimulation.

Dr Tim Overton, has provided much help in the FACS analysis carried out in this thesis and I would like to thank him for his time, patience and expertise in this area.

Past and present members of the Dove lab have provided much support throughout my PhD studies and for this I am extremely grateful. I would also like to mention members of the 6th floor Bioscience labs who have kept me going and provided much laughter, I will miss you all.

To my friends and family, I really would not have been able to complete my thesis without your help. Thank you for your love, support and the endless tea that have kept me going.

Finally I would like to thank the University of Birmingham and the Adrian Brown Scholarship who have provided financial support for my PhD.

Dedication

I would like to dedicate this thesis in memory of my ‘mom’. Not a day passes by where I don’t think of you. I am so sad you cannot be here to share in this moment, but I hope you are proud of what I have achieved.

CONTENTS

Chapter 1: Introduction

1.1 Membrane trafficking.....	1
1.2 Compartment identity	6
1.3 Yeast in trafficking research.....	8
1.4 Routes to the Vacuole/Lysosome.....	10
1.4.1 Endocytosis.....	12
1.4.2 The AP-3 Pathway.....	12
1.4.3 The Cytoplasm to vacuole (CVT) pathway and Autophagy.....	13
1.5 Phosphoinositide-based regulatory systems.....	13
1.6 Phosphoinositide binding domains.....	14
1.6.1. PX domains.....	14
1.6.2. PH domains.....	15
1.6.3. FYVE domains.....	15
1.7 Metabolism of phosphoinositides.....	16
1.8. Seven Species of phosphoinositides and their function.....	19
1.8.1 PtdIns3P.....	20
1.8.2 PtdIns(3,4) P_2	20
1.8.3 PtdIns(3,4,5) P_3	21
1.8.4 PtdIns4P.....	22

1.8.5 PtdIns(4,5) P_2	22
1.8.6 PtdIns5 P	23
1.8.7 PtdIns(3,5) P_2	24
1.9. Discovery of PtdIns(3,5) P_2	24
1.10 Regulation of PtdIns(3,5) P_2 metabolism.....	25
1.11. Fab1p; the PtdIns3 P 5- kinase.....	26
1.12 Phenotypes of $\Delta fab1$ in <i>S. cerevisiae</i>	28
1.13. Evidence for the role of Fab1p/PIKfyve in other systems.....	29
1.14. Regulation of Fab1p.....	32
1.15. Degradation of PtdIns(3,5) P_2	35
1.15.1 Negative Feedback regulation.....	37
1.15.2 Svp3p/Art1p.....	38
1.16. Functional interactions of PtdIns(3,5) P_2	38
1.16.1. Atg18p/Svp1p.....	39
1.16.2. Hsv1p/Atg21p and Hsv2p.....	41
1.16.3 Tup1p and Cti6p.....	41
1.16.4. Ent3p and Ent5p.....	42
1.16.5. Vps24p.....	43
1.17. Roles of PtdIns(3,5) P_2 that lack effector proteins.....	44
1.17.1. PtdIns(3,5) P_2 in stress responses.....	44
1.17.2. Vacuolar acidification.....	45

1.17.3. Roles in autophagy.....	46
1.17.4 PIKfyve regulation of ion channels.....	48
1.17.5. Exocytosis.....	50
1.18 Aims.....	51

Chapter 2: Materials and methods

2.1.1. Plasmid and <i>S. cerevisiae</i> strains.....	53
2.1.2. Reagents for culture of <i>S. cerevisiae</i> and <i>E. coli</i>	63
2.1.3. Reagents for molecular biology.....	63
2.1.4. Materials for Microscopy.....	63
2.1.5. Materials for high efficiency transformation of Yeast and <i>E. coli</i>	64
2.1.6 Media composition and solutions.....	64

2.2. METHODS

2.3. High efficiency transformation of yeast.....	66
2.4. Extraction of Genomic DNA from <i>S. cerevisiae</i>	67
2.5 Changing the mating type of <i>S. cerevisiae</i> cells.....	68
2.5.1 Mating of haploid cells to form a diploid....	68
2.5.2 Sporulation.....	68
2.5.3 Tetrad dissection.....	69
2.6. Preparation of competent <i>E. coli</i> cells.....	69

2.7. Transformation of competent <i>E. coli</i> cells.....	70
2.8. Purification of plasmids from <i>E. coli</i>	70
2.9 Extraction of plasmids from <i>S. cerevisiae</i>	71
2.10 Polymerase chain reaction (PCR).....	72
2.11. Purification and concentration of DNA after PCR.....	72
2.12. Plasmid construction and GFP tagging of proteins.....	73
2.12.1. VPS10-GFP, CHS3-GFP and MRL1- GFP.....	73
2.12.2. pUG36- <i>YIF1</i>	75
2.12.4. pUG23- <i>MRL1</i> and pUG34- <i>MRL1</i>	76
2.12.5. Construction of pGEX6Pk-1 VMA1, pGEX6Pk-1 VMA2, pGEX6Pk-1 VMA4 and pGEX6Pk-1 VMA5.....	77
2.12.6 Creation of pUG36-SVP3 plasmids.....	80
2.12.7 Creation of <i>VPS13</i> ^{E003K}	84
2.13. Transfer of deletions.....	86
2.14. Creation of BY4742 Δ <i>chs6::LYS2</i>	89
2.15. DNA Sequencing.....	91
2.16. Visualisation of GFP and RFP tagged proteins.....	91
2.17. Co-localisation of RFP and GFP tagged proteins.....	92

2.18. FM4-64 staining of vacuoles.....	93
2.19. Hyper osmotic stress.....	93
2.20.WGA-FITC staining of bud scars.....	94
2.21. Calcofluor staining of bud scars.....	95
2.22. Calcofluor resistance spot dilutions.....	95
2.23. Calcofluor resistance replica plating.....	95
2.24. EMS mutagenesis.....	95
2.25. Flow cytometry data collection and FACS sorts.....	96
2.26. Expression of GST-Vma1p, GST-Vma2p, GST-Vma4p and GST-Vma5p.....	97

Chapter 3-Endosome to TGN retrieval of cargo is Fab1p and PtdIns(3,5) P_2 independent in *S. cerevisiae* but requires Vac14p.

3.1 Introduction.....	99
3.2 Generation of an assay to assess retromer function.....	104
3.3 Sub-cellular localisation of Vps10-GFP.....	105
3.4 PtdIns (3,5) P_2 is not involved in retromer mediated recycling.....	110

3.5 Yif1p another mode of retrograde trafficking.....	120
3.6 Localisation of YIF1-GFP.....	120
3.7 Mr11p a homologue of the mammalian mannose-6-phosphate receptors.....	127
3.8 Localisation of MRL1	128
3.9 Discussion.....	133

Chapter 4: PtdIns(3,5) P_2 role in the early endosomal system

4.1 Introduction	137
4.2 Aim.....	143
4.3 Chs3-GFP localization.....	143
4.4 Calcofluor staining.....	147
4.5 Calcofluor resistance.....	152
4.6 Calcofluor sensitivity of $\Delta chs6\Delta fab1$ is PtdIns(3,5) P_2 dependent...162	
4.7 Fab1p and Apl4p are in the same pathway and perform the same role?.....	164
4.8 An alternative route for Chs3p to the cell surface.....	165
4.9 Mutagenesis.....	170

4.10 FACS sorting of strains.....	172
4.11 Characterisation of the EMS mutants.....	181
4.12 Rescue of large vacuolated EMS mutants with Fab1.....	183
4.13 Complementation analysis.....	184
4.14 Mutant 2-14 is <i>APL2</i>	189
4.15 Mutant 2-2 is <i>GUP1</i>	192
4.16 Mutant 2-27 is <i>VPS13</i>	199
4.17 Discussion.....	207

Chapter 5: Vacuole Fragmentation.

5.1 Introduction.....	214
5.2. Vacuole fission.....	214
5.3. Vacuole fragmentation in response to stress.....	216
5.4. Process of vacuole Fragmentation.....	218
5.5 The CORVET-HOPS complex.....	218
5.6. The V-ATPase.....	220
5.7. Maintaining vacuole fragmentation.....	222
5.8. Aims.....	222

5.9 Results.....	223
------------------	-----

5.10 Discussion.....	242
----------------------	-----

Chapter 6: PtdIns(3,5) P_2 and Svp3p/Art1p.

6.1 Introduction.....	245
-----------------------	-----

6.2 Localisation of Svp3p.....	247
--------------------------------	-----

6.3 Discussion.....	269
---------------------	-----

CHAPTER 7:Concluding remarks and future work.

7.1 Fab1p in the early endocytic system.....	271
--	-----

7.2 Role of Svp3p.....	273
------------------------	-----

References.....	276
-----------------	-----

Appendix

Appendix 1: Visualisation of mutants.....	287
---	-----

Appendix 2: Spot dilutions of Mutants.....	292
--	-----

Appendix 3: Complementation analysis of mutants.....	297
--	-----

ABBREVIATIONS

ANTH	AP180 N-Terminal Homology domain
AP1	Adaptin protein one
CCVs	Clathrin coated vesicles
CMT	Charcot-Marie-Tooth
CORVET	Class C core vacuole/endosome tethering
CPY	Carboxypeptidase Y
CVT	Cytosol-to-vacuole transport
DIC	Differential interference contrast
DMSO	Dimethyl sulfoxide
DTT	Dithiothreitol
<i>E. coli</i>	<i>Escherichia coli</i>
EM	Electron Microscopy
EMS	Ethyl methanesulfonate
ENTH	Epsin N-terminal homology
ER	Endoplasmic reticulum

FACS	Fluorescence-activated cell sorting
GFP	Green fluorescence protein
HOG pathway	Hyper-osmolarity glycerol pathway
HOPS	Homotypic fusion and protein sorting
HPLC	High Performance Liquid Chromatography
IPTG	Isopropyl β -D-1-thiogalactopyranoside
MTMR	Myotubularin related protein
MVB	Multivesicular body
M6R	Mannose-6-phosphate receptor
ORF	Open reading frame
PDGF	Platelet-derived growth factor
PEG	Polyethylene glycol
PGE	Post Golgi Endosome
PH domain	Pleckstrin homology domains
PIPKIII	Phosphatidylinositol monophosphate kinase type three
PM	Plasma membrane
PMSF	Phenylmethanesulfonyl fluoride
PIPn	Phosphoinositides

PROPPIN	β -propeller(s) that bind PPI _n
PtdIns	Phosphatidylinositol
PtdIns3P	Phosphatidylinositol 3-monophosphate
PtdIns4P	Phosphatidylinositol 4-monophosphate
PtdIns5P	Phosphatidylinositol 5-monophosphate
PtdIns(3,5)P₂	Phosphatidylinositol 3,5-bisphosphate
PtdIns(4,5)P₂	Phosphatidylinositol 4,5-bisphosphate
PtdIns(3,4,5)P₃	Phosphatidylinositol 3,4,5-trisphosphate
PTEN	Phosphatase and tensin homologue deleted on chromosome ten
PVE	Pre vacuolar endosome
PX domain	Phox homology domain
PY motif	PPxY site for binding of WW domain containing proteins
MTM	Myotubularins
RT	Room temperature
<i>S. cerevisiae</i>	<i>Saccharomyces cerevisiae</i>
SNARE	Soluble N-ethylmaleimide-sensitive factor attachment protein receptor

TGN	Trans-Golgi network
Tris	Tris (hydroxymethyl) aminomethane
ts	Temperature sensitive
V-ATPase	Vacuolar-type H ⁺ -ATPase
WT	Wild type
XLMTM	X-linked Myotublar Myopathy
YPD	Yeast extract- Peptone –Dextrose
YTD	Yeast extract- Tryptone –Dextrose
YXXØ	Tyrosine-based motif

Nomenclature used in *S. cerevisiae*

The standardised *S. cerevisiae* nomenclature has been used to refer to genes and protein names. However, when the abbreviation refers to a specific organism, that specific organisms nomenclature has been adhered to. Examples of *S. cerevisiae* nomenclature are as follows for ‘Gene of interest’;

Gene	<i>GOI</i>
Protein	Goi1p
Complete gene deletion from genome	Δgoi
Dominant mutant allele	<i>GOI</i>
Recessive mutant allele	<i>goi</i>

Chapter 1

Introduction.

1.1 Membrane trafficking

All living organisms are composed of cells, ‘the building blocks of complex life’. This fact has been known since Hook and Anton van Leeuwenhoek used the first microscopes to examine living things. We can recognise a cell from its boundary, the plasma membrane that divides and separates it from the environment. Somewhere in evolution this boundary membrane underwent hypertrophy, giving rise to internal structures and compartments that were each surrounded by their own membrane. At first these structures would have been simple, like the invaginations of the plasma membrane that are still the site of energy metabolism in bacteria today. Cells possessing this enhanced internal organisation could be termed ‘proto-eukaryotes’ because at this time the nucleus was not yet the fully formed structure we know today. As time went on however, these internal organelles became more and more elaborate until the point was reached where each compartment had a unique complement of proteins and lipids, both in the membranes and also in the organelle lumen. In this way the ER, the Golgi, the nucleus and the endosomal organelles are thought to have evolved (Warren and Wickner, 1996). Concurrently, the peroxisomes, mitochondria and other plastids became part of these already larger and more complex ‘proto-eukaryotic’ cells through the process of endosymbiosis. The fact that two disparate processes formed the organelles present in modern eukaryotes is reflected in the fact that the ER, Golgi, plasma membrane and endosomes continuously ‘communicate’ with each other by means of transport vesicles; constantly exchanging membrane and

luminal contents (Schekman, 1994, Farquhar and Palade, 1998). In contrast, the mitochondria and other organelles of endosymbiotic origin do not participate in vesicle trafficking and lie largely outside of the 'endomembrane system' (Haucke and Schatz, 1997).

One of the central problems in cell biology is to understand how each organelle in the endomembrane system can maintain its unique complement of membranes, proteins and lipids in the face of this constant exchange of material with other compartments (Bowers and Stevens, 2005). To begin to answer this question, it is necessary to understand how all membrane trafficking occurs. Much of what we know about the endomembrane system derives from research carried out in the 1950s by Porter, Palade, Novikoff, deDuve and Claude (De Duve, 1971, Palade, 1975). Porter used newly developed stains to examine thin sections of cells using the electron microscope, visualising organelles in unparalleled detail. Claude introduced the idea of cell fractionation, allowing isolated organelles to be studied; this led deDuve to study lysosomes and to develop ideas about endosymbiosis (De Duve, 1971).

Of them all, perhaps Palade's work is the most seminal, as he proposed, after studies on the Golgi, that the organelles of the endomembrane system exchanged material via 'transport intermediates' and went on to show that these were small vesicles (Palade, 1975). What emerged from this all this work was a unified view of membrane trafficking that essentially reduces all protein sorting to a series of regulated membrane fission and fusion events that are all fundamentally similar (Mellman and Warren, 2000).

In this theory, all compartments are reduced to 'donor' or 'acceptor' organelles, though in reality all organelles are both donors and acceptors. The 'donor'

compartment contains two types of proteins; those that reside in the donor organelle and those that are destined for another compartment; these latter proteins are designated as 'cargo' although they may have more than passive roles in the process of trafficking themselves (Palade, 1975, Rothman and Wieland, 1996). One important idea to emerge from Palade's work was that the sorting information necessary for a cargo protein to end up in the right compartment is often encoded in the protein itself. This sorting information, a kind of 'molecular postcode' can be a short linear sequence of amino-acids, such as the YXX Φ sequence necessary for AP-1 based sorting, or can also be more complex three dimensional structures, like the amphipathic helix required for protein sorting into mitochondria (Palade, 1975, Marks et al., 1997).

The first step in regulated transmembrane protein sorting at donor compartments is the association of cargo with an 'intermediary' protein that links it to so-called 'coat-proteins' (Schekman and Orci, 1996). This association is driven by the sorting information contained in the cargo protein. Hence at least one intermediary protein needs to exist for each acceptor compartment in the cell, since they are the specific component in the system that recognises the sorting information in cargo proteins (Schekman and Orci, 1996). The first intermediary proteins discovered were the adaptins, such as AP-1, but the general properties of most intermediary proteins are the same; they are soluble proteins that transiently associate with membranes, specifically bind cargos and cluster them into defined membrane microdomains, before recruiting a protein coat. Likewise, all protein coats seem to work in a fundamentally similar way; they are soluble, self associating proteins that spontaneously form spherical, cage-like structures. These coat proteins are recruited by the intermediary proteins to the membrane microdomain that is enriched in cargo.

This deforms the membrane, since the lattice structure of all known coat proteins has intrinsic curvature. Thus coat protein binding forms an invagination that contains the cargo linked through the intermediary protein, to the protein coat. More cargo can now be recruited as the invagination deepens and more coat and intermediary proteins are recruited to the forming vesicle (Schekman and Orci, 1996). Eventually, vesicle formation is terminated by membrane scission; the process whereby the vesicle is separated from the donor membrane. Sometimes the energy of coat protein polymerisation itself is sufficient for this function (e.g. for COPII vesicles) but sometimes an accessory protein is required (e.g. dynamin for clathrin) (Kirchhausen, 1999, Rothman and Wieland, 1996, Schmid, 1997).

Once the vesicle, a 'ball of membrane', sheathed in the basket-like lattice of the coat protein, has budded off from the donor compartment, it 'uncoats' to prepare it for fusion with the acceptor compartment. Uncoating requires energy; indeed this is usually the major step during which energy is supplied to this system, so it is carried out by ATPase enzymes that break the coat protein lattice down into monomers (Schekman and Orci, 1996).

Once uncoating has occurred, the vesicle trafficks along cytoskeletal elements, powered by motor proteins such as dynein and myosin, to the acceptor compartment. It is at this point that docking and fusion can occur. Docking allows a complex recognition system to determine if the vesicle is compatible with the acceptor organelle. This recognition step is principally mediated by SNARE proteins on both the vesicle and the acceptor compartment (Pelham, 1999). For successful recognition, the SNAREs on the vesicle must 'match' those on the acceptor compartment to form a stable four-helix bundle. Specific SNAREs are associated with each trafficking step in the cell; though some seem to be able to mediate more than one step. The correct

SNAREs are loaded onto a vesicle as if it were passive cargo, at the stage of vesicle formation, whereas SNAREs specific for each acceptor compartment are part of the unique protein complement of that compartment and contain specific sorting information that allows them to reside there (Pelham, 1999). Formation of the four-helix SNARE bundle is spontaneous for compatible SNAREs and drives membrane fusion, allowing the vesicle to deliver its cargo. Note that the machinery, such as vesicular SNAREs, and other transmembrane proteins that directed the vesicle to the acceptor compartment are now 'cargo' and must be recycled back to their correct compartment; so called retrograde trafficking (Pelham, 1999, Munier-Lehmann et al., 1996). Intermediary and coat proteins are both soluble and hence do not need to be recycled. This is likely to have evolved because the specificity in membrane trafficking comes, not from any one protein, but from the formation of specific complexes of proteins. Hence it is important that these complexes never form inappropriately.

The above picture is merely an outline of trafficking as many more proteins are involved, some of which are essential, but whose function is obscure. It is also true that for many trafficking steps, the coat and intermediary proteins have not yet been isolated. Indeed the above model raises more questions than it answers.

Note also that the above discussion of sorting relates to transmembrane protein cargo; the specific sorting of soluble, luminal cargo is similar, save that each soluble protein first associates with a transmembrane 'receptor' that then links the soluble cargo to an intermediary protein or sometimes directly to a coat protein. The first such transmembrane receptor for soluble cargo to be discovered was the Mannose-6-phosphate receptor (M6R), which links enzymes destined for the lysosome to the AP-1 adaptins and thence to clathrin (Munier-Lehmann et al., 1996, Schmid, 1997).

The caveat to the idea of regulated protein sorting is that of ‘default trafficking’; i.e. what happens to proteins that contain no recognisable sorting information? From studies in the yeast *S. cerevisiae*, we now know that the default destination for soluble proteins that contain no sorting information, yet reside in the lumen of an organelle, is to be secreted to the outside of the cell (Schekman, 1994). In contrast, transmembrane proteins that contain no recognisable sorting information are sent to the vacuole (lysosome in higher eukaryotes) to be degraded (Bowers and Stevens, 2005). This latter sorting bias is probably an evolutionary protection mechanism to prevent protein aggregation; since one of the commonest types of cargo without sorting information are proteins that have become unfolded where the sorting information is no longer recognisable or accessible. These membrane proteins pose a risk to the cell since they are thermodynamically driven to associate with other unfolded proteins and this can result in precipitation of the membrane, which often triggers apoptosis. Hence the cell has evolved to degrade them as rapidly as possible.

Much of our knowledge of membrane trafficking comes from studies of the yeast *S. cerevisiae*. This model eukaryotic organism is so useful because laboratory strains are haploid, grow rapidly in defined liquid or solid culture, possess a small and compact genome that encodes very few introns and boast a DNA repair system that is heavily biased towards homologous recombination; rendering the targeted deletion of any gene relatively trivial.

1.2 Compartment identity.

One thing that has made *S. cerevisiae* problematic for studies of membrane trafficking is the issue of compartment identity; yeast endosomal compartments have often been

defined on genetic rather than morphological criteria, making it hard to generalise observations made in yeast to higher eukaryotes because of uncertainties about which yeast compartment is homologous to the mammalian late endosome, for example. One reason this may be so problematic is the suspicion that the yeast endosomal system has become truncated throughout the course of evolution, when compared with slower growing, 'higher' eukaryotes. Indeed yeast seem to have lost many genes and pathways that they must once have possessed, not just in trafficking but across a wide spectrum of their cell physiology, based on evolutionary data. It has been proposed that by using SNARE and Rab proteins as markers for compartments, the issue may be made less ambiguous (Pelham, 2002, Dove et al., 2009) and this is the approach adopted in this work; the compartments are defined as follows:

The Snc1p (SNARE) positive compartment underlies the yeast plasma membrane, where FM4-64, an endocytosed lipophilic dye, appears at early time points. This indicates the compartment is either an early or recycling endosome (Dove et al., 2009). However from this compartment there is no direct trafficking pathway, to the cell surface and any cargo to be transported to the plasma membrane appears to first pass through the Golgi. So this compartment is sometimes named the 'post-Golgi endosome' or PGE to avoid confusion with true early or recycling endosomes in mammals (Dove et al., 2009).

The Pep12p (SNARE)-positive compartment has trafficking pathways to and from the plasma membrane, and is also the site of multi-vesicular body (MVB) formation and maturation in yeast (Ali et al., 2004), a function normally associated with mammalian 'late endosomes' (Dove et al., 2009). However entry into the yeast Pep12p-positive compartment is controlled by Vps21p; a Rab GTPase, most closely resembling mammalian Rab5, which resides on early endosomes (Schimmoller and Riezman,

1993). Therefore it has been proposed that the Pep12p positive compartment is an early endosome that can mature or acquire late endosomal characteristics. Indeed a recent immuno-EM study of Pep12p distribution suggests that this compartment loses Pep12p staining just around the time it starts to develop the intra-lumenal vesicles characteristic of MVBs (Prescianotto-Baschong and Riezman, 2002). To avoid confusion the Pep12p-positive compartment will be known as the 'pre-vacuolar endosome' or PVE (Dove et al., 2009).

It is often assumed that the yeast vacuole is homologous to the lysosome, due to its large size and acidity, with a pH of around 6.0. They appear to have a similar functions since both are home to many proteolytic enzymes (Rusten et al., 2007b) but the lysosome is even more acidic with a pH of 4-5 (Dove et al., 2009). Indeed a pH of 6.0 is characteristic of the mammalian late endosome. In addition, Ypt7p, which is homologous to mammalian Rab7, resides in the vacuole. In animal cells, Rab7 controls entry to late endosomes leading to the suggestion that the yeast vacuole may be more like a modified version of the mammalian late endosome, or an endosome-lysosome hybrid (Dove et al., 2009).

1.3 Yeast in trafficking research.

Much of the machinery for membrane trafficking was first isolated from studies of yeast *SEC* and *VPS* mutants; all of which possess defects in the sorting of soluble proteins. The *SEC* mutants have defects in the secretion of soluble proteins to the outside of the cell. The *VPS* mutants all missort a vacuolar hydrolyase, known as carboxypeptidase Y (CPY), and end up secreting it (Bowers and Stevens, 2005). Both

sets of mutants were identified by chemical mutagenesis of wild-type yeast and then the resulting pools of mutants were screened for either internal retention of normally secreted proteins or for secretion of the normally vacuolar enzyme, CPY respectively. The *VPS* mutants were then classified based on the morphology of their vacuoles, into a series of groupings (see table below) (Bowers and Stevens, 2005, Raymond et al., 1992, Banta et al., 1988). It later emerged, after the defective genes in these strains were isolated, that each class of *VPS* mutant represent disparate defects that are all blocked at the same step. For example, all class E *VPS* mutants have a defect in MVB formation and hence class E *VPS* genes encode components of the ESCRT sorting machinery required for MVB formation (Bowers and Stevens, 2005).

Table 1.1 Classification of *VPS* mutants (Bowers and Stevens, 2005).

Class	Vacuolar morphology
A	Wild-type with 3-10 spherical vacuoles that cluster in one area of the cytoplasm.
B	Fragmented vacuoles: more than 20 small, vacuole like compartments.
C	No identifiable vacuoles.
D	Single large vacuole that fails to extend into daughter cell buds.
E	Larger than wild-type, with a very large aberrant pre-vacuolar endosome.
F	One large vacuole surrounded by fragmented vacuolar structures.

Subsequently, the *END* screen, the *ALP* screen and the *ATG* screens revealed the genes involved in endocytosis, the AP-3 pathway and autophagy respectively in a similar way to the original *SEC* and *VPS* screens. Hence yeast have proved pivotal in

the isolation of components of nearly all the fundamental membrane trafficking pathways present in eukaryotes.

Figure 1.2 Diagram of the endocytic system in *S. cerevisiae*.

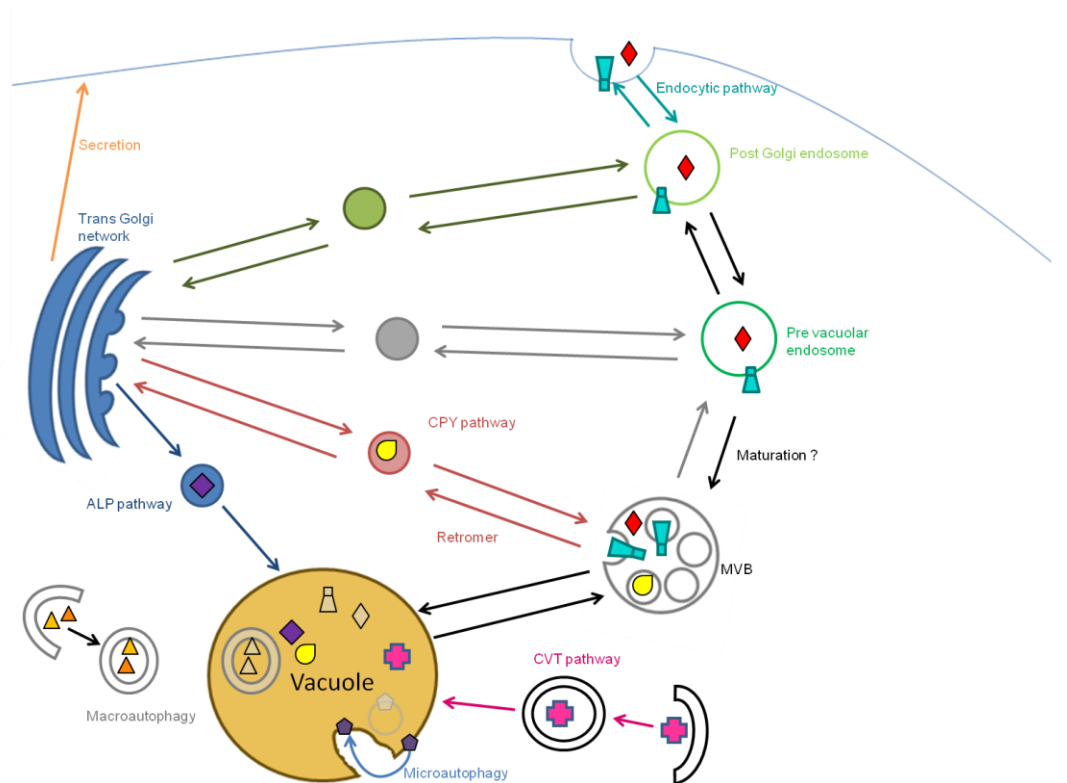


Diagram shows many of the common trafficking events, which take place inside the cell. There are multiple vesicular transport pathways that deliver proteins to and from the vacuole.

1.4 Routes to the Vacuole/Lysosome.

The major route into the vacuole is known as the ‘biosynthetic pathway’ and is primarily defined as the route followed by CPY, as elucidated by the *VPS* screen.

Newly synthesized soluble proteins travel non-specifically to the TGN where they

bind to a number of cargo receptors, such as Vps10p (Marcusson et al., 1994). The soluble proteins are then specifically sorted to the maturing PVE by these cargo receptors. These receptors are then recycled away from the PVE by means of a novel coat complex, known as Retromer, whilst the soluble proteins remain in the lumen of the PVE. The PVE then matures into an MVB by lipid partitioning that creates micro domains within the late endosome/PVE. These micro domains are rich in specific lipids including PtdIns3P (Vicinanza et al., 2008a, Odorizzi et al., 2000, Jeffries et al., 2004). Inward budding occurs to form intraluminal vesicles and is controlled by the Yeast class E *VPS* proteins. Specific trans-membrane domains can also direct sorting into the MVB (Urbanowski and Piper, 2001). Membrane proteins such as Cps1p (Carboxypeptidase S) or Phm5p (vacuolar polyphosphate phosphatase) that are transported into the vacuole lumen utilise this pathway; Cps1p is transported to the MVB as a membrane protein. It is then integrated into internal vesicles for delivery to the vacuole. Once at the vacuole it is processed to remove the membrane domain (Bowers and Stevens, 2005). Ubiquitinated proteins are also sorted into MVB luminal vesicles; indeed this is how many unfolded membrane proteins are degraded in yeast. In order to deliver proteins for degradation, the MVB undergoes homotypic and heterotypic fusion with vacuoles/lysosomes (Piper and Luzio, 2001) after maturation. Members of the V-ATPase also transit the biosynthetic pathway but do not enter the interluminal vesicles of the MVB (Piper et al., 1995, Bowers and Stevens, 2005) and so end up on the vacuole outer membrane when the MVB fuses with the vacuole.

1.4.1 Endocytosis.

The major route to internalise receptors is the clathrin coated vesicle pathway (CCV). Here, receptors are linked to the clathrin lattice by a variety of adapter proteins (Kirchhausen, 1999). In mammalian cells PtdIns(4,5) P_2 binds to Epsin through the ENTH domain (Vicinanza et al., 2008a, Odorizzi et al., 2000), and this allows recruitment of endocytic machinery to internalise the cargo.

Endocytosed receptors are delivered to the PVE/endosome, where sorting occurs, and proteins can be committed into a pathway to the vacuole for degradation (Vicinanza et al., 2008a). Carrier vesicles are also received from the Golgi in a clathrin dependent process. Outward recycling pathways are also present (Clague et al., 2009). The FYVE domain is recognised to act as an early endosomal localisation signal (Clague et al., 2009, Gaullier et al., 1998), implicating PtdIns3 P in the homotypic fusion of endosomes. This role is further supported by inhibition of PDGF receptor trafficking in wortmannin treated animal cells (Li et al., 1995, Joly et al., 1995).

1.4.2 The AP-3 Pathway.

The 'AP-3' or 'ALP pathway' controls direct trafficking from the TGN to the vacuole, in a clathrin independent process that bypasses the MVB completely (Cowles et al., 1997, Piper et al., 1997). Vps41p first associates with the AP-3 complex (an adapter complex, consisting of four class C VPS proteins) and later the HOPS complex (required for fusion), providing a link from cargo selection to eventual docking and fusion with the target membrane (Darsow et al., 2001).

1.4.3 The Cytoplasm to vacuole (Cvt) pathway and Autophagy.

In the Cvt pathway (see Figure 1.1), membrane of unknown origin creates an envelopment of API complexes (vacuolar amino-peptidase I) which delivers vesicles to the vacuole so that this hydrolyase is correctly targeted (Dove et al., 2009).

Autophagy is induced upon starvation, and delivers cytoplasm and organelles to the vacuole for amino acid recycling using a machinery that largely overlaps with that of the Cvt pathway but with additional components. In both the Cvt and autophagy pathways, double membrane vesicles are formed *de novo* in the cytoplasm (Teter and Klionsky, 2000).

As mentioned above lipids and particularly phosphoinositides are crucial for the function of membrane trafficking at various compartments within the cell. In order to understand membrane trafficking we must also understand phosphoinositides.

1.5 Phosphoinositide-based regulatory systems.

PPIn are a class of lipid signalling molecules that decorate different organelle membranes of all eukaryotic cells and seem to act as 'compartment markers' (Clague et al., 2009). PPIn also help regulate general homeostasis and stress responses of many types of cell (Michell et al., 2006). PPIn play diverse roles throughout the cellular system, and are essential mediators of a wide variety of cellular processes, including cytoskeletal rearrangements, membrane trafficking and stimulus-response coupling from cell surface receptors. This multitude of functions are instigated through interaction with specific effector proteins, which can either gain or lose a function as a result of the lipid-protein interaction (Michell et al., 2006).

1.6 Phosphoinositide binding domains.

Localisation of effector proteins to membrane surfaces occurs through association of specific protein domains on the effector that recognise and bind PPI_n. Several domains have been identified and are known to recognise specific PPI_n including, FYVE, PX (phox homology), PH (Pleckstrin homology), ENTH, ANTH, PROPPIN, Tubby and FERM domains (Cullen et al., 2001). Some domains can also have an effect on the properties of membranes with which they interact, such as the ENTH domain that causes curvature of its target membranes (Ford et al., 2002). Although a domain that binds PtdIns(3,5) P_2 remained elusive for many years, several proteins which will be discussed later, have now been shown to bind PtdIns(3,5) P_2 . These include binding through a PROPPIN motif (Han and Emr, 2011, Dove et al., 2004), an ENTH domain or directly, as in the case of the N terminus of TRPML1 (Dong et al., 2010).

1.6.1. PX domains

Phox homology or PX domains are mainly required for the binding of PtdIns3 P (Kanai et al., 2001), although it is possible that they may bind both PtdIns(3,5) P_2 and PtdIns(4,5) P_2 in some cases (Song et al., 2001, Kanai et al., 2001). Most proteins containing PX domains normally have roles in vesicular trafficking, protein sorting or lipid modification, e.g. the family of sorting nexins have roles in cargo receptor recycling in the endocytic system. PX domains are comprised of around 120 amino acids, with an N terminal 3-stranded β -sheet and a helical sub domain (Lemmon, 2008). Hydrogen bonds are made with the phosphoinositide head group PX domains, creating nine in total. Van der Waals contact with the glycerol backbone of the phosphoinositide increases membrane affinity of the protein (Lemmon, 2008).

1.6.2. PH domains

PH or Pleckstrin homology domains are present in large number of proteins, including both Protein kinase B and GRP1 (general receptor for phosphoinositides-1) (Lemmon and Ferguson, 2000, Isakoff et al., 1998). PH domains are structurally well characterised, and contain approximately 120 amino acids (Lemmon, 2008). They share a core fold consisting of a 7-stranded β -sandwich formed from two near-orthogonal β -sheets, this causes two corners to be 'open' and the two opposite corners to be 'closed' (Lemmon, 2008). A common C-terminus is shared and comprises an α -helix, this covers one of the open corners, whilst the other is covered by three interstrand loops that form much of the positively charged phosphoinositide-binding site (Lemmon, 2008, Lemmon and Ferguson, 2000). There is some understanding of PH domains and it is thought that specific sequence motifs exist to identify, and allow the domain to recognise and bind with a particular phosphoinositide. A sequence motif of basic residues exists at the loop between the first two strands of the domain, perhaps allowing recognition of $\text{PtdIns}(3,4,5)\text{P}_3$ (Isakoff et al., 1998). It also allows a spatial disposition of basic side-chains that complements the arrangement of phosphate groups in the head group to maximise hydrogen bonding.

1.6.3. FYVE domains

FYVE domains were named, by the Stenmark lab, after the proteins in which the domain was first identified; Fab1p, YOTB, Vac1p and EEA1 (Stenmark et al., 1996). Like PX domains, FYVE domains allow binding of $\text{PtdIns}3\text{P}$ (Sbrissa et al., 2002, Stenmark et al., 2002). FYVE domains contain approximately 60-70 amino acids and contain two β -hairpins and a C-terminal α -helix held together by two Zn^{2+} binding clusters creating a zinc finger like structure (Misra and Hurley, 1999). A basic

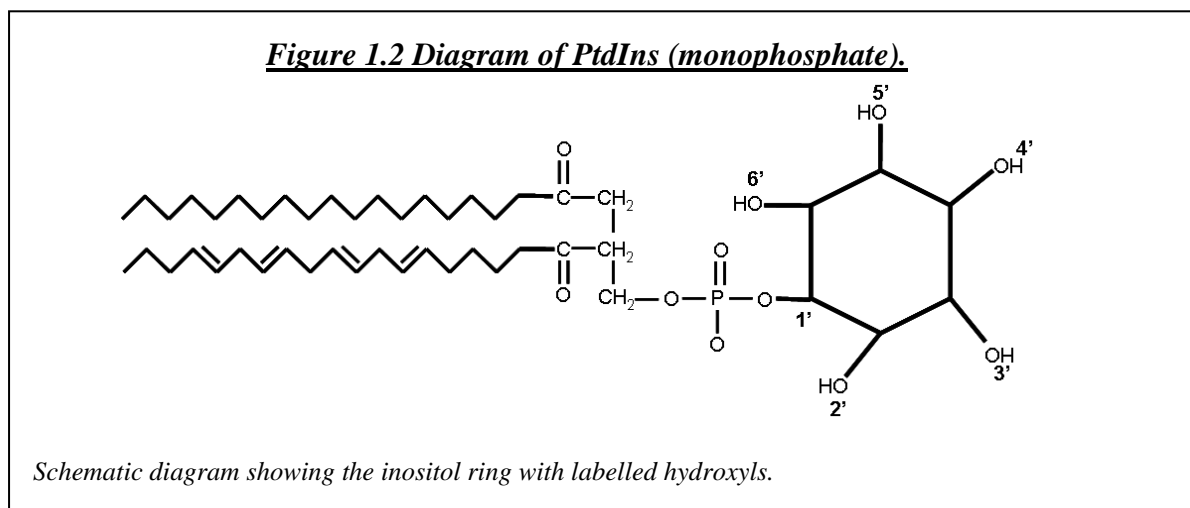
sequence motif is present in the first β -strand, creating a shallow positively charged pocket, that is responsible for PtdIns3P binding (Lemmon, 2008). Side-chains stemming from the basic motif are responsible for almost all hydrogen bonding with the head group (Lemmon, 2008, Dumas et al., 2001). Targeting of FYVE domains to membranes requires additional elements due to relatively weak hydrogen binding, and the low abundance of its target phosphoinositide, PtdIns3P making most FYVE domain proteins into ‘coincidence detectors’ that require binding to both lipid and protein binding partners before they can stably associate with membranes (Lemmon, 2008). FYVE domains are able to penetrate the membrane through insertion of non-polar side-chains from the membrane interaction loop into the membrane interior (Sankaran et al., 2001). Hydrogen bonding of the head group combines with these non-specific hydrophobic interactions in order to promote membrane targeting, however targeting of most FYVE proteins requires dimerisation of the FYVE domain (Lemmon, 2008, Gillooly et al., 2000).

1.7 Metabolism of phosphoinositides

Alterations in PPIIn signalling are common properties of many human diseases, particularly when the cellular levels of these lipids are inappropriately elevated, highlighting their importance throughout the cellular system (Vicinanza et al., 2008b). Turnover and levels of PPIIn are therefore tightly controlled. PPIIn appear very transiently during a cellular process and then rapidly disappear, with a lifetime that is often only a few seconds or minutes.

All PPIIn are generated through sequential phosphorylation of hydroxyls located on the inositol ring of the ubiquitous membrane lipid phosphatidylinositol (PtdIns) see

Figure 1.2. PtdIns is generated at the endoplasmic reticulum by phosphatidylinositol synthase, all other steps of phosphorylation take place in specific cell compartments.



Phosphorylations are mediated by four distinct families of highly regulated, ATP-dependent lipid kinases, which attack the D3, D4 and D5 hydroxyls (Michell et al., 2006). To date no PPIIn with phosphorylation at the D2 residue has been identified. Turnover is maintained by specific phosphatases that act to remove phosphates from the PPIIn (Michell et al., 2006) see Figure 1.3.

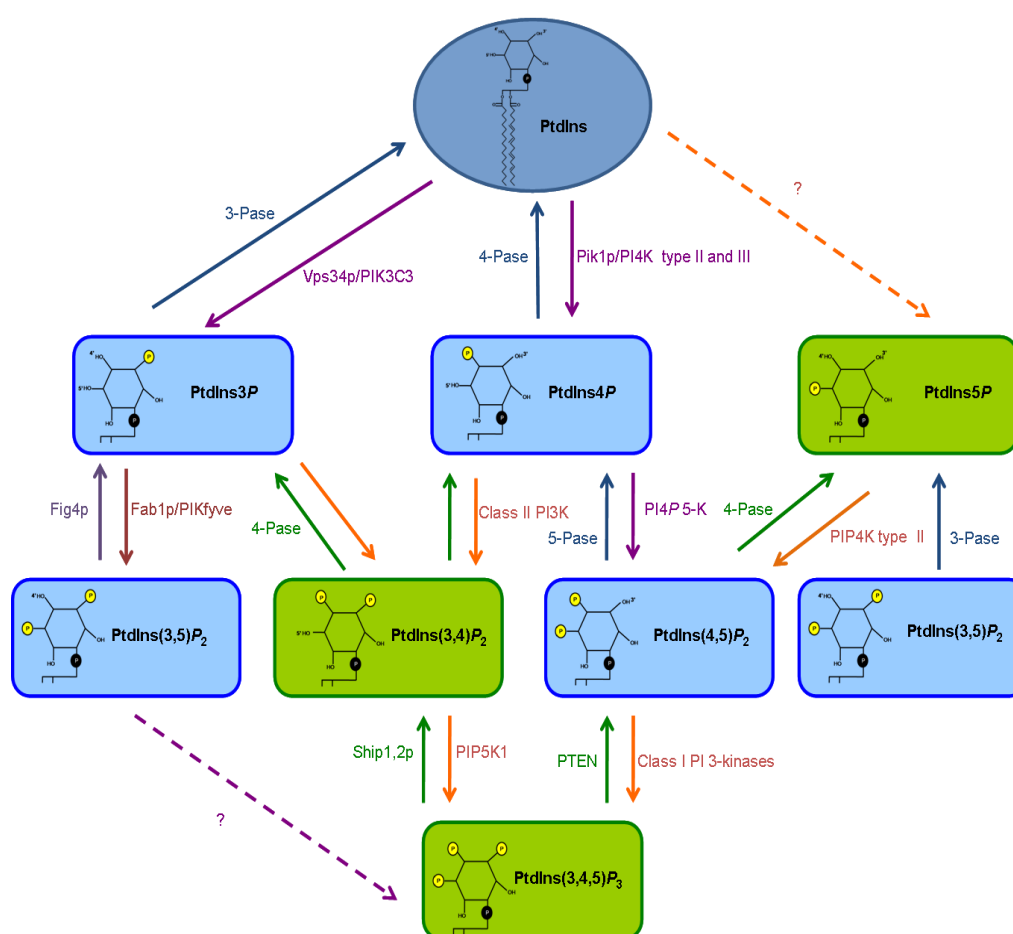
The specific kinases that produce phosphoinositides were separated into three groups: the Type I/III “PI-kinases”, the type II “PI-kinases” that share no sequence homology with the Type I/III enzymes and the PtdIns P kinases. However most of the inositol lipid kinases are specific, and phosphorylate only one lipid at one ring position (Balla, 2006). Therefore they are now classified according to the reactions they catalyse: phosphoinositide 3-kinases (PI3Ks), PtdIns 4-kinases (PI4Ks) and three types of PtdIns P kinases (PIPKs) (Strahl and Thorner, 2007).

The mechanism by which phosphoinositides function in trafficking is not always clear, however it is thought that they carry out their roles in a similar manner to the way in which Rab-GTPases function (Dove et al., 2009). PPIs seem to allow the formation of specific complexes at the membrane. When PPIs are absent, the protein-protein affinities of membrane proteins are too low for them to interact and form a complex. Specific PPI effector proteins, when able to interact with the membrane are then able to act as a 'bridge' binding both PPI and transmembrane proteins, allowing formation of a stable complex (Dove et al., 2009). Phosphatases that hydrolyse PPI act once the complex has served its purpose, causing disassembly.

This model can explain why PPIs are able to regulate many different functions at the same time. An individual effector can only be recruited to a protein complex if both its preferred PPI and its preferred protein are present (Efe et al., 2007, Dove et al., 2009). Therefore PPIs can regulate many different protein complexes by regulating several effectors that bind the same ligand but have different protein partners (Efe et al., 2007, Dove et al., 2009). This along with compartmentalisation allows PPIs to have many varied roles.

1.8. Seven Species of phosphoinositides and their function

Figure 1.4 Metabolism of the 7 species of PPI_n.



*Kinases and phosphatases act to convert specific PPI_n. Blue backgrounds indicate phosphoinositides present in both mammalian and yeast cells. Green backgrounds indicate those found only in higher eukaryotes, although PtdIns(3,4,5)P₃ and PtdIns5P have recently been detected in *S. pombe* mutants (Mitra et al., 2004).*

Seven PPI_n are currently known, four of which are found in yeast (depicted in Figure 1.4). As mentioned previously, they are present in transient but distinct pools throughout cellular membranes, and each phosphoinositide is associated with one compartment; e.g. PtdIns(4,5)P₂ with the plasma membrane, PtdIns3P with early endosomes and PtdIns4P with the Golgi (Odorizzi et al., 2000).

1.8.1 PtdIns3P.

PtdIns3P is constitutively present in eukaryotic cells (Auger et al., 1989) and is produced by the PI-3 kinase (PI3K) Vps34p in yeast. Vps34p is the sole class III enzyme in yeast, and was first found to function in the regulation of vesicular trafficking in the endosomal/lysosomal system, where it is responsible for the recruitment of proteins containing FYVE domains to intracellular membranes (Odorizzi et al., 2000, Lindmo and Stenmark, 2006). PtdIns3P is localised primarily to membranes of early endosomes and internal vesicles of multivesicular bodies (MVBs) in mammalian cells (Gillooly et al., 2000). In yeast it is also found on vacuolar membranes. It has important roles in the regulation of the early endocytic pathway (Corvera, 2001) and in Golgi to lysosome vacuolar sorting (Odorizzi et al., 2000). It is also required for autophagy, the Cvt pathway and glucose repression pathway (Backer, 2008, Odorizzi et al., 2000). PtdIns3P is also the precursor phosphoinositide to PtdIns(3,5)P₂.

1.8.2 PtdIns(3,4)P₂.

PtdIns(3,4)P₂ levels are increased after animal cells are stimulated with growth factors or agonists (Stephens et al., 1993) and is not found in Yeast. The main source of production for PtdIns(3,4)P₂ is from dephosphorylation of PtdIns(3,4,5)P₃ (Andrews et al., 2007). PtdIns(3,4)P₂ is a lipid second messenger and functions by recruitment of a large number of effector proteins to the membrane through PH domains. PtdIns(3,4)P₂ is known to activate the serine/threonine kinase Akt (Franke et al., 1997), which is involved in cell survival mechanisms and can inhibit apoptosis through phosphorylation leading to inactivation of Bad; a factor that promotes cell

death (Franke and Cantley, 1997). $\text{PtdIns}(3,4)P_2$ is also known to have roles in gluconeogenesis and glycolysis, again through interaction with the Akt pathway.

1.8.3 $\text{PtdIns}(3,4,5)P_3$.

$\text{PtdIns}(3,4,5)P_3$ is only found in animals and slime molds, and is the major product of agonist-stimulated PI-3-kinases (Stephens et al., 1993). Stimulation increases levels by 40-fold within seconds; basal levels of the phosphoinositide are normally very low. $\text{PtdIns}(3,4,5)P_3$ also acts as a second messenger to control many cellular functions and is downstream of the Akt pathway which has an important role in stimulating cell proliferation and suppression of apoptosis (Franke et al., 1997). Following activation, PDK (Phosphoinositide dependent kinase) and Akt are recruited to the plasma membrane by $\text{PtdIns}(3,4,5)P_3$. Akt is then phosphorylated and activated by PDK to interact with other important signalling pathways. Akt can also phosphorylate forkhead transcription factors, such as FKHR seen in breast cancers (Jackson et al., 2000). These pathways are often mutated in various cancers and are negatively regulated by PTEN, a phosphatase that removes the D3 phosphate group, and SHIP-1 and 2. These phosphatases are therefore tumour suppressors and the targets for cancer drug development (Cantley, 2002, Czech, 2003). $\text{PtdIns}(3,4,5)P_3$, Akt, PTEN and the PI3Ks have all been identified within the nucleus and research has identified that they may regulate cell survival by pathways from within the nuclear membrane (Martelli et al., 2007). $\text{PtdIns}(3,4,5)P_3$ has also been shown to stimulate actin polymerisation and controls the cytoskeleton (Funamoto et al., 2001).

1.8.4 PtdIns4P.

PtdIns4P is the most abundant monophosphorylated derivative of PtdIns present in both yeast and mammalian cells (Lemmon, 2008). For many years PtdIns4P was considered to just be a precursor for PtdIns(4,5)P₂ with no specific cellular role. However recent work using yeast has suggested that it controls many cellular processes (D'Angelo et al., 2008). A large concentration of PtdIns4P is observed at the Golgi and this is where many of its functions are based, new work however suggests it may play a wider role throughout the cell (D'Angelo et al., 2008, Vicinanza et al., 2008a). PtdIns4P is generated from PtdIns by members of the family of PI-4 kinases (PI4Ks) (Vicinanza et al., 2008a). Yeast have three PI4Ks; Pik1p, Stt4p and Lsb6p. Effectors of PtdIns4P have been identified and they fall into two main groups, with a role in adapter and coat complexes e.g. AP-1, GGA and EpsinR or a role in non-vesicular lipid transfer e.g. OBSP, CERT and FAPP proteins (D'Angelo et al., 2008). In both cases PtdIns4P is used as part of a complex Golgi-membrane localisation code (D'Angelo et al., 2008).

1.8.5 PtdIns(4,5)P₂.

PtdIns(4,5)P₂ is present in both yeast and mammalian cells. It is the most abundant phosphoinositide at the plasma membrane, where it is responsible for the recruitment of the AP-2 complex, which promotes clathrin coated vesicle formation and internalisation of cell surface receptors (Vicinanza et al., 2008a). PtdIns(4,5)P₂ can also bind to ENTH domains and therefore, can indirectly recruit components of the endocytic machinery. It is generated from PtdIns4P e.g. by Mss4p in yeast (Odorizzi et al., 2000). PtdIns(4,5)P₂ has a role in regulating many important cellular pathways including exocytosis, endocytosis and recycling. It is also known to regulate cadherin

trafficking in epithelial morphogenesis (Schill and Anderson, 2009). PtdIns(4,5) P_2 is also the precursor of both IP₃; an inositol phosphate that can function as a second messenger in Ca²⁺ release; and of PtdIns(3,4,5) P_3 .

1.8.6 PtdIns5P.

PtdIns5P was first discovered in mammalian fibroblasts as a source for PtdIns(4,5) P_2 (Rameh et al., 1997), and is probably the least characterised phosphoinositide. It has yet to be reported in yeast. Synthesis of PtdIns5P has not been demonstrated directly in cells, and it could be produced from three different precursors, PtdIns, PtdIns(3,5) P_2 or PtdIns(4,5) P_2 , with a mechanism of production from PtdIns(3,5) P_2 being favoured (Lecompte et al., 2008). This would be catalysed through the removal of the D3 phosphate group by myotubularins. A role in signal transduction is beginning to emerge, with its regulatory genes are often disrupted in a variety of human diseases (Lecompte et al., 2008). Nuclear levels of PtdIns5P are known to increase under cellular stress, and it can then bind to the plant homeodomain (PHD) domain of ING2 a tumour suppressor which promotes p53- dependent apoptosis (Lecompte et al., 2008, Jones et al., 2006). PtdIns5P may also help to regulate PtdIns(3,4,5) P_3 levels (Carricaburu et al., 2003), and a role in membrane trafficking from the late endosome to plasma membrane has also been proposed (Lecompte et al., 2008).

1.8.7 PtdIns(3,5) P_2

PtdIns(3,5) P_2 is the focus of this thesis, it will be discussed in detail below.

1.9. Discovery of PtdIns(3,5) P_2 .

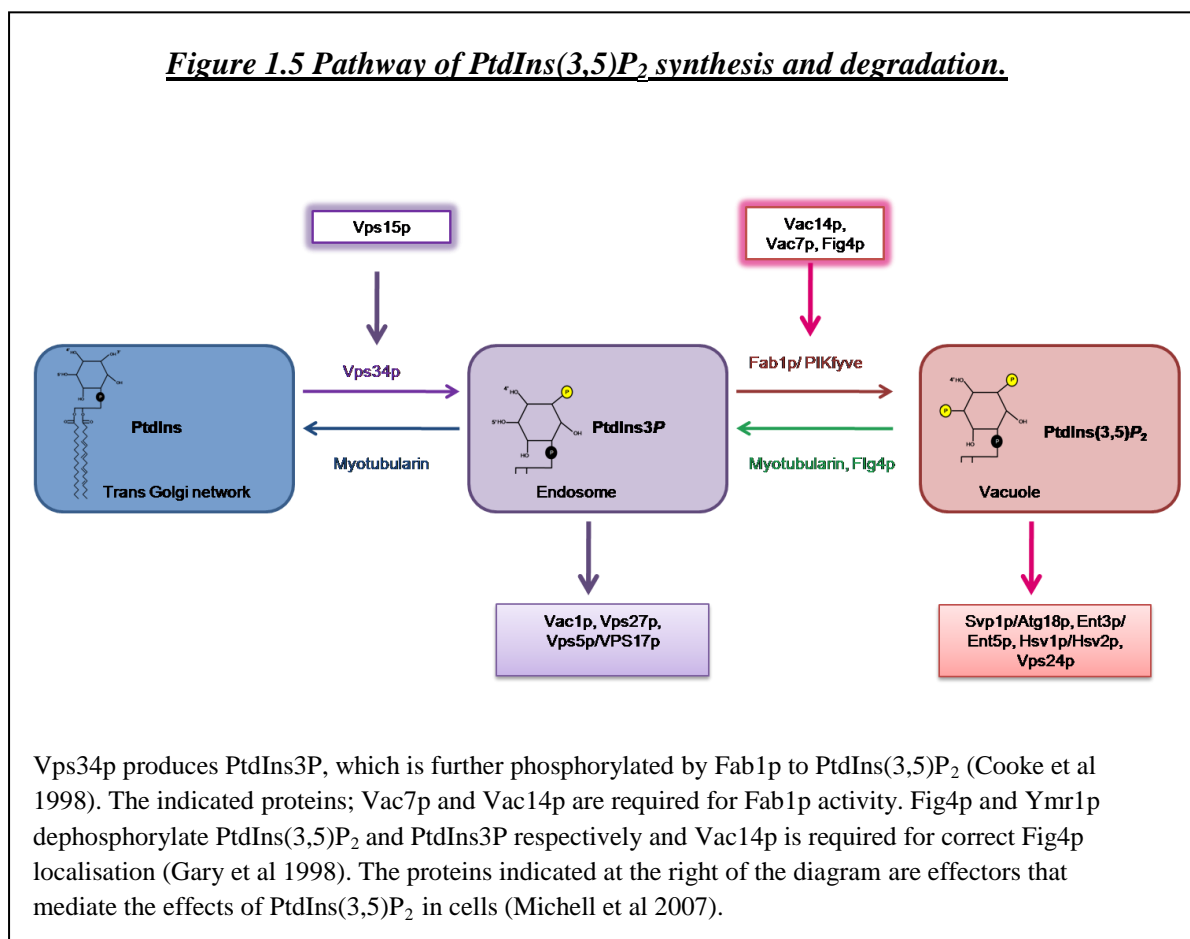
Phosphatidylinositol 3,5-bisphosphate is the most recently discovered PPI_n, first identified in *S.cerevisiae* in 1997 through HPLC analysis of [³H]inositol radiolabelled lipids (Dove et al., 1997). PtdIns(3,5) P_2 , along with the components controlling its production, are conserved amongst all major eukaryotes from fungi to animals, indicating a function for PtdIns(3,5) P_2 required throughout evolution (Michell et al., 2006) . Perhaps one reason why PtdIns(3,5) P_2 remained elusive is because of its steady state levels; in normal unstressed *S. cerevisiae* cells, PtdIns(3,5) P_2 levels are around 20-fold lower than that of the other identified yeast phosphoinositides. However, this basal level of PtdIns(3,5) P_2 is vital for many cellular functions in yeast (Dove and Johnson, 2007). Even a small decrease in the levels of PtdIns(3,5) P_2 in unstressed cells can create defects. Different processes require different amounts of the lipid; only a small amount is required for acidification of the vacuole, but more is necessary for vacuole fragmentation. Hyper-osmotic stress with 1.4M sorbitol or 0.9M NaCl triggers a rapid (5-15 minutes) but transient increase (up to 20-fold), in the levels of PtdIns(3,5) P_2 that is not observed for other phospholipids or PPI_ns (Dove et al., 1997), so levels of PtdIns(3,5) P_2 are of a similar concentration to that of PtdIns(4,5) P_2 . Both the magnitude and the duration of the increase in PtdIns(3,5) P_2 are proportional to the molarity of the hyperosmotic stress given, indicating that this is likely to represent an adaptive response (Dove et al., 1997).

Where the extra stress-induced PtdIns(3,5) P_2 is synthesized, and how it is degraded are both unclear. Neither an increase in PtdIns3 P or PtdIns5 P levels after treatment with a stress is observed. The increase in PtdIns(3,5) P_2 does however, coincide with

fragmentation of the yeast lysosome-like vacuole into many smaller vesicles, although the adaptive advantage this confers is not clear (Dove et al., 1999) (discussed below).

1.10 Regulation of PtdIns(3,5) P_2 metabolism

PtdIns(3,5) P_2 is synthesised through two tightly controlled sequential phosphorylation events, as shown in Figure 1.5. The PtdIns-specific PI 3-kinase, Vps34p, first produces PtdIns3P which is then further phosphorylated by a PtdIns3P 5-kinase, to generate PtdIns(3,5) P_2 (Cooke et al., 1998)



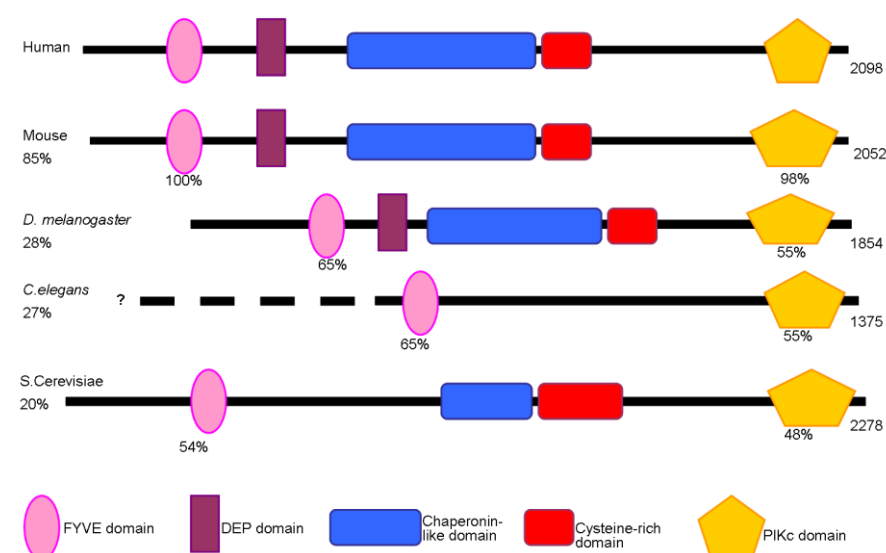
Although hyper-osmotic stress can generate PtdIns(3,5) P_2 , the pathway doesn't interact with the well characterised Hyper-osmolarity glycerol (HOG)

pathway, mutants of HOG components show normal PtdIns(3,5) P_2 accumulation. To date there is no specific probe for PtdIns(3,5) P_2 so its localisation remains uncertain. Generation of PtdIns(3,5) P_2 in response to hyperosmotic stress and the resulting vacuole fragmentation is rapid, and all components of the Fab1p pathway reside on the vacuole membrane, so PtdIns(3,5) P_2 generation is probably at least partially vacuolar (Dove et al., 2009). However, there is evidence for discrete extra-vacuolar pools of PtdIns(3,5) P_2 (Shaw et al., 2003).

1.11. Fab1p; the PtdIns3P 5- kinase

In yeast, the PtdIns3P 5-kinase has been demonstrated to be Fab1p; through *in vitro* kinase assays and because cells with a deletion of the *FAB1* gene are unable to synthesise PtdIns(3,5) P_2 (Dove et al., 1997).

Figure 1.6 Schematic diagrams of Fab1p mRNA structure and its putative homologs in other species.



Adapted from (Cabezas et al., 2006). Not drawn to scale

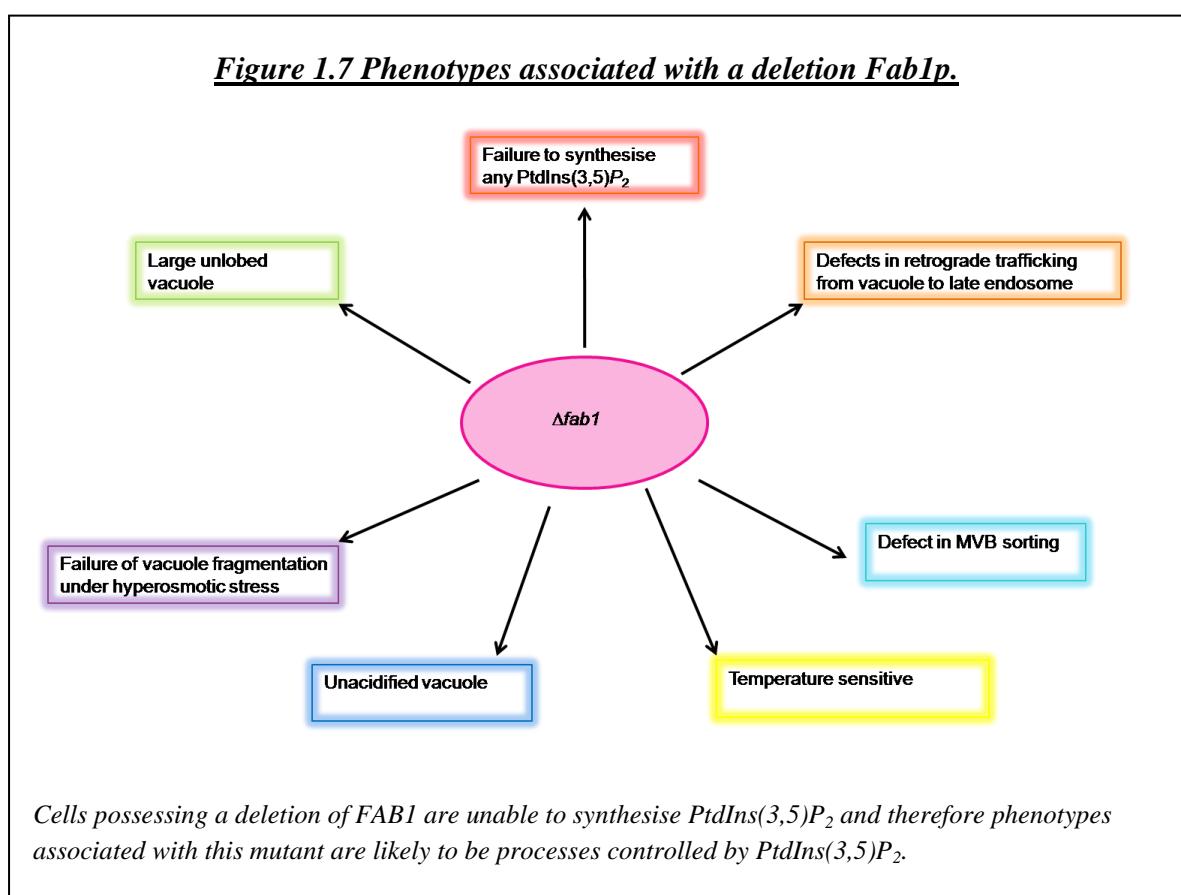
As shown in Figure 1.6, the genes for Fab1p-type PtdIns3P 5-kinases encode large 150-250 kD proteins, which all contain a kinase domain at the C terminus and a

cysteine rich FYVE zinc finger domain at their NH₂ terminus. The central domain of Fab1p encodes a regulatory CCT-like chaperone domain of unknown function as well as a “Fab1p unique” histidine and cysteine rich PtdIns3P 5-kinase specific domain (Michell et al., 2006). Constitutively activated mutants of Fab1p all have mutations within this regulatory region suggesting that this might represent some kind of autoinhibitory centre, though this remains speculation at the present time (Bonangelino et al., 2002, Gary et al., 2002).

FAB1 was first discovered during a screen for mutants that possess a nuclear segregation defect and so was designated *FAB1* for formation of aploid and binucleate cells (Yamamoto et al., 1995). However, it was subsequently discovered that the reason the nucleus was not correctly segregating in *fab1* cells was because of the enormously enlarged vacuole and not because of a specific karyokinesis defect. It was the sequence of Fab1p kinase domain that originally lead to the belief that it was a PtdIns4P 5-kinase before the subsequent discovery of PtdIns(3,5)*P*₂ in 1997 (Yamamoto et al., 1995). Additional sequence analysis of the kinase domain later revealed that Fab1p defines a subfamily of putative PtdIns*P* kinases that are distinct from those that synthesise PtdIns(4,5)*P*₂ and so have been designated as ‘type III PtdIns*P* kinases’ (PIPkIII) (Gary et al., 1998). *In vivo* analysis of phosphoinositides revealed that strains bearing point mutations in the Fab1p kinase domain lack detectable levels of PtdIns(3,5)*P*₂ but levels of PtdIns(4,5)*P*₂ are unaffected (Gary et al., 1998, Dove et al., 1997, Cooke et al., 1998). This indicates that Fab1p provides the only route to PtdIns(3,5)*P*₂ in yeast. The FYVE domain as mentioned above is not required for Fab1p function as expression of a *fab1* mutant with no FYVE domain can recover the phenotypes associated with *FAB1* deletion (Efe et al., 2007). It is however

required for Fab1p localisation to the vacuole, and so may play a part in the hyperosmotic stress response (Dove et al., 2009).

1.12 Phenotypes of $\Delta fab1$ in *S. cerevisiae*.



Fab1p inactivated cells display many characteristic phenotypes; including no $PtdIns(3,5)P_2$ synthesis, temperature sensitive growth, and a very large, unlobed unacidified vacuole (Bryant et al., 1998, Dove et al., 2004) which does not decrease in size when treated with a hyper-osmotic stress (Dove and Johnson, 2007, Shaw et al., 2003). These characteristic phenotypes suggest that $PtdIns(3,5)P_2$ is a regulator of vacuole volume, morphology, acidity and membrane potential (Cooke et al., 1998). Defects are also observed in retrograde trafficking from the vacuole to the late

endosome, suggesting a role for PtdIns(3,5) P_2 in the recycling of membranes and cargo receptors. Vps34p and PtdIns3P have already been shown to be essential for anterograde trafficking of membrane and protein cargos to the vacuole, possibly suggesting a mechanism by which a balance of membrane flow into and out of the vacuole is achieved (Lindmo and Stenmark, 2006). Ubiquitin-dependent protein sorting to the vacuole lumen via the multivesicular body is also affected in strains possessing a *FAB1* deletion (Shaw et al., 2003), with certain cargoes failing to enter intraluminal vesicles in the absence of this lipid, though the vesicles themselves form normally. The various homologs of *FAB1* also display similar defects when inactivated in the appropriate organism, suggesting close conservation of the pathway between species, such as vacuolation observed in mammalian cells without PIKfyve (Dove and Johnson, 2007, Ikononov et al., 2001).

1.13. Evidence for the role of Fab1p/PIKfyve in other systems

The mammalian homolog of Fab1p is PIKfyve, which has been shown to rescue the defects associated with *fab1* mutants when it is expressed in yeast, demonstrating that this pathway is conserved between yeast and mammals (Mitchell et al., 2006, Shisheva, 2001, Mitchell et al., 2008). Over-expression of Fab1p or PIKfyve in yeast does not result in increased PtdIns(3,5) P_2 synthesis, which has led to the suggestion that its kinase activity is somehow tightly controlled, possibly via auto-inhibition, although this has yet to be formally shown (Gary et al., 1998).

The DEP domain, present in PIKfyve, is only observed in higher eukaryotic Fab1s (see Figure 1.6). The purpose of the domain is unclear as it was first identified via

bioinformatics screening, hence its name (Disheveled, Egl-10, Pleckstrin) and is found in over 50 proteins involved in G-coupled receptor pathways. It has also been shown to be implicated in membrane binding, both through direct interaction or by contacts with other membrane associated proteins. The domain is not essential for activity in PIKfyve, as it is not evolutionary conserved (Cabezas et al., 2006), however it may be responsible for some of the more recently evolved functions of PIKfyve. Human PIKfyve has been shown to co localise with early endosomal markers such as EEA1 and Hrs but a small amount is also found in late endosomal compartments (Cabezas et al., 2006). This may indicate a role for the protein in multiple steps of the endocytic pathway.

Table 1.2 Mammalian homologs of yeast proteins.

Yeast gene product	Mammalian gene product	Function
Fab1p	PIKfyve/PIP5K3	Kinase that produces PtdIns(3,5) P_2 from PtdIns3P
Vac14p	ArPIKfyve	Activator of Fab1p, composed of HEAT repeats and acts as a scaffold for the formation of a complex essential for PtdIns(3,5) P_2 formation.
Fig4p	Sac3	PtdIns(3,5) P_2 phosphatase that regulates cellular levels.
Svp1p/Atg18p	WIPI-1 /	β - Propeller protein that is a known effector of PtdIns(3,5) P_2 . Known roles in autophagy, and as an inhibitor of Fab1p.
Hsv1p/Atg21p	WIPI-3 / WIPI-49	β - Propeller protein that is a known effector of

Hsv2p		PtdIns(3,5) P_2
Tup1p	Human- TLE Drosophila- Groucho	β - Propeller protein that is known to bind PtdIns(3,5) P_2 . Roles in transcriptional regulation.
Ent3p /Ent5p	EpsinR	ENTH like protein, potential effectors of PtdIns(3,5) P_2 . Associates with Clathrin adapter Gga2p
Vps10p	Homolog of mannose-6-phosphate receptors	Receptor for trafficking of CPY.

Mutation of PIKfyve leads to similar phenotypes as those associated with loss of Fab1p (see above). A dominant negative or kinase dead form of the PIKfyve results in extensive vacuolation of animal cells, as does treatment with a cell permeant kinase inhibitor, YM201636 (Ikonomov et al., 2001, Dove and Johnson, 2007). PIKfyve can also recover hyper-osmotically- stress-stimulated PtdIns(3,5) P_2 synthesis (McEwen et al., 1999), suggesting the two enzymes are conserved (Michell et al., 2006). Both kinases can produce PtdIns(3,5) P_2 *in vitro* and *in vivo* (Cooke et al., 1998, Gary et al., 1998).

A difference between yeast and mammalian systems is that PIKfyve may not be the sole PIPkIII in mammals. A recent study using the newly identified PIKfyve inhibitor YM201636 on NIH 3T3 cells only reduced PtdIns(3,5) P_2 levels by 85% (Jefferies et al., 2008) leaving an unexplained pool. No other kinase that phosphorylates PtdIns3P to PtdIns(3,5) P_2 has been identified in mammalian cells but it is likely that it would only contribute to a small amount of overall levels (Dove et al., 2009). Another possibility is that the result could just be because of an insensitive pool of PtdIns(3,5) P_2 that fails to be inhibited by YM201636; perhaps because its cellular

location might be inaccessible to lipid phosphatases (Dove et al., 2009). Further research is required in this area to clarify the result (Jefferies et al., 2008).

PIKfyve also appears to have additional ability compared to the yeast homolog; Fab1p exerts lipid kinase activity, however PIKfyve can also act as a protein kinase. It does this both via autophosphorylation, and in phosphorylating the Rab9 effector p40 (Ikonomov et al., 2003). Fab1p autophosphorylation has not been shown to date. PIKfyve is also able to generate PtdIns5P directly; through phosphorylation of PtdIns (Shisheva, 2001). Although Fab1p can also do this, it is a minor activity in yeast and may just be a biological artefact of *in vitro* assays.

1.14. Regulation of Fab1p

Although we do not formally know how Fab1p is regulated, i.e. by activation or by relief of constitutive inhibition, additional proteins have now been identified that are required for normal production of PtdIns(3,5) P_2 (Dove et al., 2002, Gary et al., 2002, Bonangelino et al., 2002, Bonangelino et al., 1997). Two are putative activators of Fab1p known as Vac7p and Vac14p, that appear to act independently to regulate the kinase activity of Fab1p and tightly control production of PtdIns(3,5) P_2 (Dove et al., 2002) whilst the third; Fig4p, appears to be an inositol lipid phosphatase.

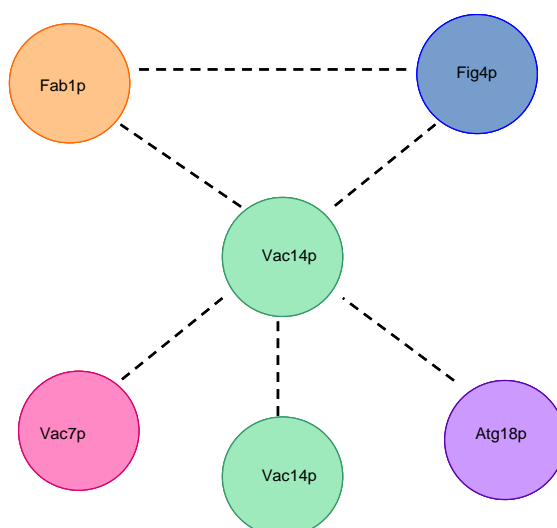
Vac7p seems to only be present in ascomycete fungi and no known mammalian homolog has been found (Bonangelino et al., 1997). Vac7p is a single pass trans-membrane protein, with a large C-terminal lumenal domain, whose sequence varies amongst closely related fungal species, possibly indicating that the protein folds in a way that is tolerant of mutation (Gary et al., 2002). This may mean that functional VAC7 homologs do exist in higher eukaryotes but that they will be difficult to identify

by conventional sequence analysis because a putative 'Vac7p protein fold' is being conserved rather than a primary amino-acid sequence (Gary et al., 2002).

Vac14p is a hydrophilic peripheral membrane protein that directly interacts with Fab1p and is conserved from yeast, through plants to mammals (Efe et al., 2007). It is predicted to be composed entirely of between 9 and 21 HEAT repeats (Jin et al., 2008). HEAT repeats consist of two antiparallel helices connected by a short loop and often appear in tandem or as multimers to generate surfaces for protein-protein interactions (Groves et al., 1999). Vac14p has been shown to interact with PIKfyve; the mammalian homolog of Fab1p. Over-expression of human Vac14p also leads to a slight increase in PtdIns(3,5) P_2 levels (Sbrissa et al., 2004). Indirect immunofluorescence experiments have shown that Fab1p, Vac7p and Vac14p all reside on the vacuolar membrane in yeast and that inactivation of any one of these three leads to cells that produce little or no PtdIns(3,5) P_2 , resulting in similar phenotypes. Recent research by the Weismann lab, on an *inglis* mouse mutant, containing a missense mutation of mVac14, elucidated how this multi-protein ternary complex regulates the levels of PtdIns(3,5) P_2 in mice (Jin et al., 2008). Other work in yeast also supports this model (Botelho et al., 2008). Co-immunoprecipitation experiments were used to determine that Vac14p acts as a scaffold onto which the regulatory units bind to form a complex. Vac14p interacts with itself, Fab1p, Fig4p, Atg18p and Vac7p, see Figure 1.8 (Jin et al., 2008). Fab1p-TAP also co-precipitates with Fig4p in the presence of Vac14p (Jin et al., 2008). Fab1p and Fig4p appear to bind to non-overlapping sites of Vac14p, which brings them into close proximity so they can share access to the same pool of PtdIns3P and PtdIns(3,5) P_2 (Jin et al., 2008). Vac14p is not only a general activator of Fab1p under normal conditions but also plays a critical role in the hyper-osmotic response of PtdIns(3,5) P_2 (Bonangelino

et al., 2002). When $\Delta vac14$ mutants are exposed to hyper-osmotic shock only a small amount of $PtdIns(3,5)P_2$ is observed, much lower than that of wild-type cells. Over expression of *FAB1* restores some synthesis of $PtdIns(3,5)P_2$ under basal conditions but fails to allow any elevation of $PtdIns(3,5)P_2$ induced in response to osmotic stress (Bonangelino et al., 2002).

Figure 1.8 Diagram of the multi protein $PtdIns(3,5)P_2$ regulatory complex.



Vac14p is present at the centre of the two complexes and act as a scaffold for the other components to interact on (Modified from Jin et al 2008)

In addition to the known phenotypes associated with *FAB1* knockout, mouse *vac14* and *fig4* knockouts have also been shown to suffer neurodegeneration; indeed the *fig4* locus is associated with a human neurodegenerative disease that resembles Charcot-Marie Tooth disease (CMT) (Chow et al., 2007, Zhang et al., 2007). Another recent report suggests that mutations that effect the generation of $PtdIns(3,5)P_2$ can result in both CMT and also amyotrophic lateral sclerosis (ALS) (Ferguson et al., 2009). Mice

with *FIG4* and *VAC14* mutations were shown to accumulate three proteins; LC3-11, p62 and LAMP-2 in both neurons and astrocytes. Cytoplasmic inclusion bodies containing ubiquitinated proteins and p62 were also found in areas of the brain that undergo degeneration, with formation and recycling of the autolysosome impaired (Ferguson et al., 2009). This work indicates a role for PtdIns(3,5) P_2 in autophagy in the mammalian central nervous system. It also suggests that disruption of the regulation of PtdIns(3,5) P_2 can lead to inclusion body disease (Ferguson et al., 2009).

1.15. Degradation of PtdIns(3,5) P_2

Fig4p is the PtdIns(3,5) P_2 specific 5-phosphatase (Rudge et al., 2004). Unexpectedly, Fig4p also appears to be required for basal PtdIns(3,5) P_2 synthesis, possibly because it is needed for proper localisation and function of Vac14p; $\Delta fig4$ mutants display very reduced PtdIns(3,5) P_2 synthesis in yeast, and mice after osmotic stress (Duex et al., 2006b, Duex et al., 2006a). This is likely to be because Fig4p is required for stability of Vac14p, at least in *S. cerevisiae*. It has also been suggested that Fig4p may activate Fab1p through dephosphorylation of Fab1p or Vac14p (Duex et al., 2006b), as PPI α phosphatases can, in certain cases, also act as protein phosphatases. An example is PTEN which resembles tyrosine phosphatases at the primary amino-acid sequence level, and can indeed attack artificial phosphotyrosine substrates such as *para*-nitrophenol phosphate *in vitro*, but in fact is likely to dephosphorylate PtdIns(3,4,5) P_3 *in vivo* (Cui et al., 1998). A protein phosphatase activity for Fig4p has not been directly demonstrated and remains speculation at the present time. Dephosphorylation of the PIKfyve autophosphorylation site has been shown to increase its kinase activity (Sbrissa et al., 2000) although point mutations of Fab1p, that would be predicted to prevent autophosphorylation, failed to have any effect on

activity of the yeast enzyme, suggesting that this mode of regulation may not be conserved. How PIKfyve might be dephosphorylated at the kinase domain is not clear.

The mammalian homolog of Fig4p is Sac3, which acts in the same way as its yeast counterpart. Again Sac3 forms a complex with mVac14p and associates with PIKfyve to increase levels of PtdIns(3,5) P_2 . Work from the Shisheva group suggests that mVac14 might control and prevent degradation of Sac3 (Ikononov et al., 2010). A mutation in Sac3 can lead to a neuropathy known as CMT4J because mVac14 can no longer prevent Sac3 being degraded and this results in a loss of basal synthesis of PtdIns(3,5) P_2 (Ikononov et al., 2010). Indeed the mutated Sac3 protein is found to be unstable and affected individuals are heterozygotes for the mutated missense allele and null allele. Levels of the protein found in tissues are only at 2% of wild-type levels, due to impaired interaction with mVac14 causing instability. It has been suggested that treatment which would increase levels to 10% would allow long term survival (Lenk et al., 2011). This implication in disease also provides further evidence of the importance of the Fig4p interaction with Vac14p.

Myotubularins (MTMs), in higher eukaryotes, can also degrade PtdIns(3,5) P_2 ; these enzymes belong to a family of ‘dual-specifically protein phosphatase-like’ PPI α phosphatases (Taylor et al., 2000). They can act to remove the D3 phosphate group from both PtdIns(3,5) P_2 and PtdIns3P. Naturally inactive versions of MTMs are able to heterodimerize with active phosphatases acting on PtdIns3P, they are then directed to PtdIns(3,5) P_2 and convert it to PtdIns5P (Dove et al., 2009, Lecompte et al., 2008). Inactivation of MTMs leads to increases in both PtdIns3P and PtdIns(3,5) P_2 with a decrease in levels of PtdIns5P (Nicot and Laporte, 2008, Lecompte et al., 2008). Catalytic sites of MTMs include the same CX₅R motif observed in both Fig4p and

PTEN (Robinson and Dixon, 2006). Again mutations in MTMs are inactivated in similar diseases as those associated with mutated *FIG4*, i.e. X-linked Myotubular Myopathy (XLMTM) and CMT disease (Nicot and Laporte, 2008, Zhang et al., 2007), Robinson et al 2008). A novel phosphoinositide phosphatase hJUMPY conserved through evolution, is similar to MTMs and also dephosphorylates PtdIns3P and PtdIns(3,5) P_2 . Disruptions of hJUMPYs function are also found in patients with centronuclear myopathy, a form of a severe congenital myopathy similar to XLMTM (Tosch et al., 2006). Understanding the regulation of PtdIns(3,5) P_2 is therefore crucial to unravelling many neurodegenerative diseases.

1.15.1 Negative Feedback regulation.

Atg18p, an effector that binds PtdIns(3,5) P_2 , has now been found to have a role in the regulation of PtdIns(3,5) P_2 levels. Efe et al (2007) hypothesised that Atg18p can act as a sensor of PtdIns(3,5) P_2 and continually cycles between the cytosol and limiting membrane of the vacuole in response to changes in phosphoinositide levels (Efe et al., 2007). Atg18p appears to act as an inhibitor of Fab1p, via a negative feedback loop, probably to regulate vacuolar morphology. When Atg18p is recruited by PtdIns(3,5) P_2 to the membrane, it associates with Vac7p, and a myosin-specific adapter; Vac17p (Efe et al., 2007). Atg18p may regulate activity of Fab1p through sequestration of the activator Vac7p. It is also known that Atg18p and Vac7p bind to overlapping sites on Vac14p, close to the site of Fab1p binding, presumably facilitating rapid activation or inactivation of Fab1p (Jin et al., 2008). The role of Vac17p is most probably in the retrograde membrane transport, from the vacuole to mediate cytoskeletal rearrangements for the process (Efe et al., 2007) and is likely downstream of Atg18p and Fab1p.

1.15.2 Svp3p/Art1p.

Svp3p was first identified in a screen along with Atg18p for mutants possessing a large unlobed vacuole and is a proposed component of the Fab1p pathway because of aberrant synthesis of PtdIns(3,5) P_2 ; levels of this lipid are 10 fold higher in $\Delta svp3$ cells than in wild-type cells (Dove, SK unpub).(Dove et al., 2004). Svp3p is encoded by the YOR322c locus in the *S. cerevisiae* genome and is also known as *ART1*, which is thought to function in endocytosis of plasma membrane proteins by recruiting the ubiquitin ligase Rsp5p, to its target (Lin et al., 2008). This is interesting as the ability of Rsp5p to ubiquitinate certain proteins is apparently dependent on PPI n , including PtdIns(3,5) P_2 . The exact role of Svp3p/Art1p has not been widely investigated to date and could be part of the Fab1p pathway; this is investigated in greater detail in Chapter 6.

1.16. Functional interactions of PtdIns(3,5) P_2 .

All phosphoinositides mediate cellular processes through binding to specific effector proteins. This allows an array of many different functions for each phosphoinositide. Separate pools of phosphoinositides carrying out specific functions with separate effector proteins have also been discovered such as in the case of PtdIns3P (Obara et al., 2008). Interaction of potential effectors with PtdIns(3,5) P_2 is not fully understood although it seems to be either through the PROPPIN domain e.g. the group of seven-bladed β -propellers such as Atg18p and Tup1p (Han and Emr, 2011) or an ENTH-domain such as in the EpsinR like proteins, Ent3p and Ent5p (Dove et al., 2009).

Although several effectors of PtdIns(3,5) P_2 have been identified, deletion of the genes encoding these effectors do not fully recapitulate the *fab1* mutant phenotype (Dove

and Johnson, 2007, Dove et al., 2004, Efe et al., 2007, Eugster et al., 2004, Krick et al., 2008). For example; there is no effector known to play a role in vacuole acidification or heat tolerance. This suggests that there are effectors left to find and novel roles for PtdIns(3,5) P_2 .

It is likely that, as for PtdIns3P, there is more than one distinct pool of PtdIns(3,5) P_2 ; each with a different function (Michell et al., 2006, Obara et al., 2006, Kihara et al., 2001).

1.16.1. Atg18p/Svp1p

Atg18p (also known as Svp1p) was first identified as an effector of PtdIns(3,5) P_2 in a screen for *S. cerevisiae* mutants with large $\Delta fab1$ like vacuoles (Dove et al., 2004).

WIPI-3/ WIPI-1 are the identified human homologs (Proikas-Cezanne et al., 2004, Barth et al., 2001). Homologs have also been identified in *Drosophila*, *Arabidopsis*, and *C. elegans*. The *ATG18* gene encodes a 500 amino acid protein on chromosome VI immediately adjacent to the *FAB1* gene; which produces a protein with a molecular weight of 55,102 Da. The sequence of *ATG18* contains seven WD-40 motifs near the centre of the gene, which are predicted to fold as a seven bladed- β propeller (Dove et al., 2004). This prediction is further supported by alignment to Tup1p a known β propeller (Dove et al., 2004) which has now also been shown to bind to PtdIns(3,5) P_2 (Han and Emr, 2011). Binding of Atg18p to PtdIns(3,5) P_2 was first shown through phosphoinositide ‘dot blots’, and quantitative approaches using GST-Atg18p found that specific binding to PtdIns(3,5) P_2 involved at least two interactions, that occur between the ionic head group and a basic amino acid cluster, and between hydrophobic parts of the lipid and a hydrophobic patch of Atg18p (Dove

et al., 2004). Mutation of part of the β -propeller sequence from 284-287 was shown to decrease affinity more than 40-fold. This mutant also loses the ability to correct the enlarged vacuole of a $\Delta atg18$ strain, indicating PtdIns(3,5) P_2 is crucial for Atg18p to function normally in vacuole membrane trafficking (Dove et al., 2004). Over expression of the mutated *atg18* in wild-type yeast resulted in a large unlobed vacuole, suggesting a dominant negative effect; possibly via sequestration of some component required for normal vacuole morphology (Dove et al., 2004). $\Delta atg18$ cells also possess a defect in membrane recycling from the vacuole, observed through an assay detecting trafficking of a modified alkaline phosphatase enzyme (Dove et al., 2004). When levels of PtdIns(3,5) P_2 were analysed from $\Delta atg18$ cells, they were found almost 10 times higher than wild-type, whereas levels of the other yeast phosphoinositides were normal (Dove et al., 2004). Atg18p has been shown to be localised in three different compartments, the PAS, vacuolar membrane and the endosomes (Krick et al., 2008). In all three locations a role in the biogenesis of transport vesicles is observed (Krick et al., 2008). Atg18p is now known to function in PtdIns(3,5) P_2 synthesis, probably as a sensor of phosphoinositide levels (Jin et al., 2008, Efe et al., 2007) and acts as an inhibitor of Fab1p (Efe et al., 2007). The main role for Atg18p as an effector of PtdIns(3,5) P_2 is in retrograde transport, probably from the vacuole membrane, and it is likely that it is required for membrane scission during this process as it does in autophagy and the Cvt pathways (Barth et al., 2001, Weisman, 2003). Atg18p is also strongly implicated in the control of autophagy, although this role may not require Fab1p or PtdIns(3,5) P_2 , at least in *S. cerevisiae*. Atg18p is also known to bind weakly to PtdIns3P *in vitro* (Stromhaug et al., 2004) and a recent paper shows that this phosphoinositide is essential for its full activity in both selective and non-selective autophagy (Obara et al., 2008). Atg18p also functions

in the selective Cvt-pathway to form vesicles as it does during autophagy (Barth et al., 2001).

1.16.2. Hsv1p/Atg21p and Hsv2p.

Hsv1p/Atg21p and Hsv2p (Homologous with Syp1) share many of the same structural characteristics as Atg18p (Barth et al., 2002); both Atg21p and Hsv2p are predicted to fold into seven bladed- β propellers (Krick et al., 2006, Krick et al., 2008) Both are shown to weakly bind PtdIns3P as well as strongly binding to PtdIns(3,5)P₂. However unlike Δ atg18 deletion of either gene does not result in large unlobed vacuoles.

Atg21p is only required for the Cvt –pathway and is not required for autophagy (Barth et al., 2002, Proikas-Cezanne et al., 2004). Hsv2p is largely uncharacterised and has no known function. A recent paper highlights the localisation of a pool of Atg18p, Atg21p and Hsv2p at the pre-vacuolar endosome, where they function in a PtdIns3P dependent manner (Krick et al., 2008). Over expression of Atg21p can cause CPY secretion, which is not observed with either Hsv2p or Atg18p, as this may disturb retromer function through competing to bind to PtdIns3P or Vps21p (Krick et al., 2008).

1.16.3 Tup1p and Cti6p.

The most recently identified effectors of PtdIns(3,5)P₂. Tup1p was identified through a BLAST search for proteins that share sequence similarity with Atg18p, as it contains a C-terminal β - propeller, which is crucial for its binding to PtdIns(3,5)P₂ (Han and Emr, 2011). Evidence suggests that PtdIns(3,5)P₂ can recruit Cti6p and the Cy8p-Tup1p complex to the late endosomal/ vacuole membrane and mediates the

formation of a Cti6-Cyc8-Tup1 complex which then can recruit the SAGA complex to the *GALI* promoter (Han and Emr, 2011).

1.16.4. Ent3p and Ent5p.

Both Ent3p and Ent5p contain epsin N-terminal homology (ENTH) domains (Friant et al., 2003). The ENTH domain is also known to bind phosphoinositides (Kay et al., 1999) and it is suggested that both Ent3p and Ent5p bind PtdIns(3,5) P_2 through this domain. PtdIns(3,5) P_2 and ubiquitin are necessary for proper sorting of cargos destined for the interior of the vacuole and are sorted into vesicles of the MVB. Ent3p and Ent5p are both required for protein sorting into the MVB. The ENTH domain is a membrane-interacting module found in proteins that have a role in the early stages of the endocytic pathway (De Camilli et al., 2002). Intracellular localisation of Ent3p and Ent5p to endosomes is dependent upon PtdIns(3,5) P_2 , discovered through fractionation assays and GFP tagging though some of this work is controversial as a number of labs have been unable to repeat it (Friant et al., 2003, Eugster et al., 2004). A temperature sensitive Ent3p, *ent3-1* was used to define a role for protein sorting at the MVB. Intracellular localisation of GFP-CPS and GFP-Phm5p was tested in *ent3-1* cells. At both 24°C and 37°C the constructs localised to the vacuolar membrane instead of being correctly localised the vacuole lumen. Previously $\Delta fab1$ cells were shown to be defective in the sorting of these two constructs (Odorizzi et al., 1998). Ent3p and Ent5p also have roles in the trafficking of Chs3p, and deletions in both of the genes can suppress a $\Delta chs6$ phenotype (Copic et al., 2007). This could be a key link to the Fab1p pathway, as similar effects are seen with a *FAB1* deletion. Unlike $\Delta fab1$ neither $\Delta ent3$ nor $\Delta ent5$ show enlarged unlobed vacuoles; in fact $\Delta ent3$ or $\Delta ent5$ cells have small and fragmented vacuoles (Friant et al., 2003, Eugster et al.,

2004). These mutants also have normal levels of PtdIns(3,5) P_2 and do not have defects in the synthesis of this phosphoinositide.

1.16.5. Vps24p.

Vps24p was first identified as a PtdIns(3,5) P_2 effector in 2003 (Whitley et al., 2003) through the use of mammalian cDNA phage libraries with synthetic biotinylated derivative of PtdIns(3,5) P_2 immobilised on beads. Vps24p is a class E member of the vacuolar protein-sorting mutants (Raymond et al., 1992, Babst et al., 1998). *S. cerevisiae* mutants with a deletion of Vps24p have the large swollen vacuole phenotype observed with $\Delta fab1$ cells. It has been suggested that many of the class E Vps proteins may interact with PtdIns(3,5) P_2 maybe in the form of a complex (Odorizzi et al., 1998). Vps24p unlike the other identified effectors does not contain a characteristic phosphoinositide binding domain, and it is unclear exactly how it binds PtdIns(3,5) P_2 . Through truncation experiments it was discovered that the N-terminus of mVps24 associates with class E compartments in a phosphoinositide dependent manner (Whitley et al., 2003). Vps24p is one of four subunits of the endosomal sorting complex required for transport III (ESCRT-III). It forms an ESCRT-III sub complex along with Did4p (Isakoff et al., 1998, Song et al., 2001). Both ESCRT-III and PtdIns(3,5) P_2 are involved in the sorting of transmembrane proteins into the MVB pathway (Raiborg et al., 2003, Shaw et al., 2003) and this is where a link between the two pathways may lie. The proposed model suggests PtdIns(3,5) P_2 production influences events co-ordinated by an assembled ESCRT-III complex (Whitley et al., 2003).

1.17. Roles of PtdIns(3,5) P_2 that lack effector proteins.

The above discussion on effectors highlights those processes for which an effector has been isolated. However, there remain a number of phenotypes/defects displayed by cells that lack PtdIns(3,5) P_2 that lack such molecular definition. These are discussed below.

1.17.1. PtdIns(3,5) P_2 in stress responses.

As previously mentioned, the levels of PtdIns(3,5) P_2 cellular levels increase dramatically in response to stress, in a transient manner. Therefore it is proposed that PtdIns(3,5) P_2 plays a major role in the response of cells to stress. The most obvious event to take place when cells are given a hyper-osmotic stress is the fragmentation of the yeast vacuole into smaller compartments; fragmentation is maintained for the length of time PtdIns(3,5) P_2 levels are raised. The reasons for this event and the machinery that control it are unclear; this is one of the focuses of this thesis and is discussed in greater detail in chapter 5.

Deletion of Fab1p or Vac14p leads to a large unlobed vacuole that can no-longer undergo fragmentation when a stress is applied. These mutants lack PtdIns(3,5) P_2 and it is likely that an effector protein(s) control this process but these remain to be identified. It has been shown that members of the Vacuolar V-ATPase are also components of the vacuolar fission machinery (Baars et al., 2007). Previous work has shown that both acidification of the vacuole and the presence of the V-ATPase are necessary for fragmentation during hyper-osmotic stress.

Hyper-osmotic stress induced vacuole fragmentation may also require the recently identified CORVET complex which is required for macro-fragmentation. This complex shares many of the same subunits as the HOPS complex which is responsible

for homotypic vacuole-vacuole fusion (Seals et al., 2000). Vps21p, which regulates CORVET, is also responsible for the controlling entry of proteins into the PVE (Baars et al., 2007). PtdIns(3,5) P_2 may therefore influence vacuolar fission and/or retrograde trafficking from the vacuole to the PVE, promoting HOPS-CORVET subunit exchange (Dove et al., 2009). Fab1p has also been linked with the CORVET machinery, as deletion of some CORVET subunits causes a mislocalisation of Atg18p, Atg21p and Hsv2p (Kane, 2005). Accumulation of PtdIns(3,5) P_2 also occurs in response to other stresses. The pathway can also be activated by heat and changes in pH; similar responses are observed but are less profound and occur at a slower rate (Dove and Johnson, 2007, Mollapour et al., 2006).

It also remains unclear how the PtdIns(3,5) P_2 signalling pathway interacts with the external environment to sense disruption of the milieu and acts to bring back internal homeostasis. This connection with the external environment may involve interaction with a specific effector protein that is yet to be identified (Dove et al., 2009). It has also been suggested that Fab1p itself may sense conformational changes in its partner proteins through its CCT domain during stress (Dove and Johnson, 2007, Michell et al., 2006).

1.17.2. Vacuolar acidification

Acidification is a defining feature of yeast vacuoles and mammalian lysosomes, and many of the functions of the vacuole require a low pH (Li and Kane, 2009). The Vacuolar ATPase controls acidification of the vacuole/lysosome, and is conserved amongst yeast and mammals (Li and Kane, 2009). ATP hydrolysis is coupled to proton transport from the cytosol to lumen. The yeast V-ATPase is regulated at the

level of assembly, through its two sectors. A similar mechanism is seen in lysosomes. A further level of regulation implicates the lipid composition of organelles (Li and Kane, 2009, Paroutis et al., 2004). The contents of the vacuole may also act as buffers to determine pH. For example polyphosphate, present in a very high concentration in the vacuole acts as such a buffer (Brett et al., 2006, Li and Kane, 2009).

Yeast cells lacking $\text{PtdIns}(3,5)P_2$ have a neutral vacuole (Nicot et al., 2006, Rusten et al., 2006). This defect is also observed in both *C. elegans* and *D. melanogaster* cells (Gary et al., 1998), but remains unreported in mice (Bonangelino et al., 2002, Dove et al., 2002). This may be due to an incomplete knockout of *FAB1* in some systems; even a small amount of $\text{PtdIns}(3,5)P_2$ can suppress this phenotype. Although the V-ATPase is linked to vacuole fragmentation as above, defects in vacuole acidification occur independently of vacuole enlargement (Dove et al., 2009). The unacidified vacuole in cells lacking $\text{PtdIns}(3,5)P_2$ is not due to the mis-localisation of the V-ATPase (Weisman et al., 1990, Starai et al., 2005). It is currently unknown how $\text{PtdIns}(3,5)P_2$ regulates vacuolar acidification and no effector proteins have been identified that are involved in this process. It is likely that a novel effector of $\text{PtdIns}(3,5)P_2$ could somehow directly or indirectly activate the V-ATPase (Dove et al., 2009).

1.17.3. Roles in autophagy

Recently Fab1p and ESCRT complexes have been shown to play roles in autophagy in higher eukaryotes (Rusten et al., 2007b, Rusten et al., 2007a). Autophagy is a process used by cells to recycle organelles, protein aggregates, and cytoplasmic constituents during nutrient limitation. Autophagy is a critical process in multicellular organisms and if inhibited can cause defects in development, starvation sensitivity,

the accumulation of protein aggregates, neuronal degradation, and eventually cell death. Atg18p has also been shown to be required for formation of autophagosomes during nutrient stress in most higher eukaryotes though this is likely in a PtdIns(3,5) P_2 independent but PtdIns3P dependent fashion. Autophagosomes are double membrane organelles that sequester cytoplasm containing items to be degraded and then fuse with endosomes or lysosomes where they are broken down and removed from the cell (Noda et al., 2002). The importance of the endosomal system in the regulation of autophagy and associated disease is not well known. But it has been shown in a recent report using *Drosophila melanogaster* that regulators of endosomal biogenesis play an important role in autophagy. Genetic and ultrastructural experiments were used to show that subunits of the endosomal sorting complex required for transport (ESCRT)-I, -II and -III, their regulatory ATPase Vps4p and also Fab1p, are all required for autophagy in *D. melanogaster*. Loss of ESCRT or Vps4p function leads to an accumulation of autophagosomes, which is probably due to inhibition of fusion with the endo-lysosomal system. Fab1p activity is necessary for the maturation of autolysosomes (Rusten et al., 2007b, Rusten et al., 2007a).

Another recent report implicates PtdIns(3,5) P_2 in the process of autophagy in mice (Ferguson et al., 2009). Results indicate that mutations in either *VAC14* or *FIG4*, lead to accumulation of several proteins in neurons and astrocytes, shown to be due to defective autophagy. Co-localisation studies indicate that this is due to the failure of recycling or formation of the autolysosome and they have proposed two models (Ferguson et al., 2009). It may be that PIKfyve is involved in autophagosome consumption rather than formation. Disruption of PIKfyve with siRNA means the late endosome/lysosome can no longer fuse with autophagosomes or MVBs (de Lartigue et al., 2009). It is likely that Atg18p, Atg21p and/or Hsv2p are the effectors

responsible for PtdIns(3,5) P_2 dependent autophagy, though this has yet to be formally investigated.

It may be that PtdIns(3,5) P_2 is not involved in the autophagic process in yeast cells because there is no actual lysosome, so maturation stops at the vacuole which is likely to be a modified late endosome and hence autolysosome formation is not observed or required because that compartment has been lost during evolution or exists only as a hybrid organelle fused with the late endosome. Hence autophagy in yeast is probably truncated and therefore PtdIns(3,5) P_2 independent.

1.17.4 PIKfyve regulation of ion channels.

A recent paper has suggested that during hyperosmotic stress in yeast, Ca^{2+} is released from the vacuole in a process requiring both PtdIns(3,5) P_2 and the mucolipin transient receptor potential (TRPML) channel (Dong et al., 2010). Like cells unable to synthesise PtdIns(3,5) P_2 , cells that lack TRPML have also been found to have many similar phenotypes, e.g. enlarged vacuoles and trafficking defects in the late endocytic pathway, although these are not as severe as in $\Delta fab1$ cells (Dong et al., 2010). The authors propose that TRPMLs are the connection between Ca^{2+} and PtdIns(3,5) P_2 , and changes of the lipid are used to regulate Ca^{2+} , which trigger membrane fusion and fission events. Indeed it has been shown that PtdIns(3,5) P_2 can bind TRPML1 (Dong et al., 2010).

PIKfyve has also been shown to regulate a Ca^{2+} channel; this time voltage gated. This however, is through sustained activation of glutamate receptors, which recruit PIKfyve to increase levels of PtdIns(3,5) P_2 around the calcium channel which seems

to target them for degradation at the lysosome (Tsuruta et al., 2009). This may explain some of the apparent links between $\text{PtdIns}(3,5)P_2$ and neuronal diseases.

The glutamate transporter EAAT4 can be regulated by PIKfyve (Alesutan et al., 2010, Klaus et al., 2009b, Gehring et al., 2009b, Klaus et al., 2009a). Activity of the transporter is stimulated by a signalling cascade involving SGK1, a kinase which can regulate channels and carriers by phosphorylation, and interference with ubiquitination (Alesutan et al., 2010). Previously SGK1 has been shown to phosphorylate PIKfyve, resulting in increased cell surface expression of EAAT4 (Seeböhm et al., 2007). PIKfyve, has also been observed in regulation of trafficking of the sodium glucose cotransporter SGLT1 and in the SGK1 mediated regulation of the creatine transporter SLC6A8 (Shojaiefard et al., 2007, Strutz-Seeböhm et al., 2007). SGK1 stimulation of PIKfyve is also required for the increased cell surface expression of the Ca^{2+} channel TRPV6 (Sopjani et al., 2009), and the chloride channel CLC-2 where PIKfyve both stimulates the channel and contributes to SGK1 dependent regulation of localisation (Klaus et al., 2009b). PIKfyve can also up-regulate CFTR the cystic fibrosis transmembrane conductive regulator, in a similar way (Gehring et al., 2009a). $\text{PtdIns}(3,5)P_2$ also regulates cardiac contractility through directly activating Ca^{2+} release and activation of the ryanodine receptor (Touchberry et al., 2010).

A role for PIKfyve in regulation of the insulin stimulated GLUT4 glucose transporter and phosphorylation of PIKfyve by protein kinase B (PKB) has also been recently identified (Berwick et al., 2004). Through use of YM201636, an inhibitor of PIKfyve catalysed $\text{PtdIns}(3,5)P_2$ synthesis, it has been shown that PIKfyve is involved in

glucose entry in adipocytes (Ikonomov et al., 2009b). In response to both insulin and osmotic stresses, PIKfyve becomes phosphorylated by PKB (Berwick et al., 2004). Data presented by the Tavarè group strongly suggests that PIKfyve is regulated by external phosphorylation, which increases activity of PIKfyve rather than decreases it (Berwick et al., 2004). This indicates that PIKfyve is able to control both the trafficking and activity of many mammalian channels in the early endocytic system. Such a function for Fab1p in *S. cerevisiae* so far remains un-investigated.

Other recent research has also defined a role for PIKfyve in the endosome to TGN trafficking of furin (de Lartigue et al., 2009), which has protease activity and may be responsible for the cleavage of the HIV envelope. Using yeast two hybrid and co-immunoprecipitation assays it was found that a novel splice variant of the Jip4 gene product JLP, is a kinesin adapter that links PIKfyve to microtubules in this trafficking pathway (Ikonomov et al., 2009a). Knockdown of PIKfyve also results in marked inhibition of HIV replication due to its roles in retroviral budding (Murray et al., 2005). Only low levels of PtdIns(3,5) P_2 may be required for many of these trafficking pathways, hence only pharmacological intervention may disrupt them (de Lartigue et al., 2009).

1.17.5. Exocytosis

PIKfyve has also been shown to have roles in exocytosis (Osborne et al., 2008). Regulated secretion of neurotransmitters and hormones depends on both protein-protein and protein-lipid interactions. Both PtdIns3P and PtdIns(4,5) P_2 have previously been shown to be required to prime the secretory apparatus in an ATP dependent manner before Ca^{2+} dependent secretion (Kong et al., 2006). Through the

use of YM201636, a selective inhibitor of PIKfyve activity and PIKfyve knock-down by siRNA, it was discovered that PIKfyve localises to a sub-population of secretory granules in chromaffin and PC12 cells (Osborne et al., 2008). When $\text{PtdIns}(3,5)P_2$ was down regulated, secretion of granule exocytosis was potentiated. When PIKfyve or Fab1p was over expressed, regulated secretion in PC12 cells was inhibited. A catalytically inactive PIKfyve mutant had no effect. The investigation demonstrates a new role for PIKfyve and Fab1p in regulated secretion (Osborne et al., 2008). A role for Fab1p will be investigated in the secretion of Chs3p, this will be discussed in more detail in Chapter 4.

1.18 Aims.

The above introduction highlights an emerging role for PIKfyve in the regulation of trafficking in the early endocytic system. The mechanism for this mode of regulation is unknown, as no effectors have been isolated that might be responsible. The aims of this thesis were as follows:

- To dissect novel $\text{PtdIns}(3,5)P_2$ dependent trafficking events in the early endocytic system.
- To examine the role of $\text{PtdIns}(3,5)P_2$ in the trafficking of retromer.
- To see if PIKfyve's control of recycling in mammalian cells was conserved in yeast, using the trafficking of Chs3p as a model.
- As part of this work, we also wanted to examine if Svp3p/Art1p interacted with this pathway, since this arrestin-like protein also both affects synthesis of $\text{PtdIns}(3,5)P_2$ and also regulates endocytosis.

- To examine possible proteins involved in the fragmentation of the yeast vacuole under hyperosmotic stress.

The study was carried out in *S. cerevisiae*, as the mammalian system is largely homologous, and much of the work on $\text{PtdIns}(3,5)P_2$ was originally conducted in yeast. *S. cerevisiae* also provides a convenient model system that can be genetically manipulated easily, making it a good choice in which to study trafficking events if the caveats about compartment identity, noted above, are accepted.

Chapter 2

Materials and Methods

2.1. MATERIALS

2.1.1. Plasmid and *S. cerevisiae* strains

Plasmids pUG23-*YIF1* and pUG34-*YIF1* were kind gifts from Dr D. Pearce (University of Rochester, NY, USA). Plasmid pGem-T-Easy was obtained from Invitrogen. The mCherry *PHO8* marker, was made by Dr E.Khaznajdi, by creating an N terminal fusion in pRS416 (Sikorski and Hieter, 1989). The pRS315-*APL2*, pYCplac111-*APL4* and pRS316-*STE3* plasmids, were kind gifts of Dr F. Cooke (UCL, London, UK). pRS313-*SOI1* was a gift from Prof R. Fuller (University of Michigan, USA). p*CHS3-GFP* was a kind gift from Prof R. Schekman (University of California, Berkley, USA).

pUG34 is a low copy centromeric yeast expression vector and was modified by Dr. Hegemann (Heinrich-Heine-Universität, Düsseldorf, Germany) so that GFP is expressed as an N-terminal fusion to any gene cloned into the multiple cloning site (Niedenthal *et al.*, 1996).

Plasmid pUG36 (YCp, *URA3*, *P_{MET25}-yEGFP3-MCS-T_{CYC1}*) (Niedenthal *et al.*, 1996) was used as a vector to express green fluorescent protein, (GFP) fusion proteins. This version of yEGFP does not contain the anti-dimerisation mutation. Proper cloning of an insert into the multiple cloning sites (MCS) of pUG36 allows the expression of yEGFP N-terminal fusion proteins under the control of methionine-regulated *MET25* promoter (Mumberg *et al.*, 1994).

Plasmid pGEX-6P-K1 was obtained from Dr Dove who modified the commercially available vector pGEX-6P-1 (G.E Biotech) by inserting sequences that encode a protein kinase A phosphorylation consensus motif between the GST and the protein of interest.

All cloning and sub-cloning was carried out in *E. coli* TOP10 competent cells, which were prepared in the lab, as described below. *E. coli* strains were grown in LB broth containing the appropriate antibiotics. Plasmids used, and those created in this study, are summarised in Table 2.1. BL21-star (DE3)-RIL cells were obtained from the Dove lab *E. coli* strain collection and were used to express GST (glutathione-S-transferase)-fusion proteins.

The *fab1::LEU2* allele was a kind gift from Dr D. Koshland (Carnegie Institution of Washington, Maryland, USA.) (Yamamoto et al., 1995). The *vps26::LEU2* allele was a kind gift of Dr M. Seaman (University of Cambridge, Cambridge Institute for Medical Research/Clinical Biochemistry, U.K). The yeast RFP marker strains BY4741 *CHC1::CHC1-RFP*, BY4741 *ANP1::ANP1-RFP*, BY4741 *COP1::COP1-RFP* and BY4741 *SNF7::SNF7-RFP* were kind gifts from Dr E. O'Shea (Harvard University, Massachusetts, USA)(Huh et al., 2003). The BJ3505 strain (*pep4::HIS3* allele) was a kind gift from Dr A. Mayer (Université de Lausanne, Switzerland). Dr G. Payne (UCLA Los Angeles, USA) kindly provided *apl2::TRP* and *apl4::TRP* alleles. The *sec22::HIS3* allele was kindly provided by Dr D.Schmitt (Max Planck Institute, Germany).

Wild-type and some yeast deletion strains, bearing the *kanMX4* deletion cassette in BY4741, BY4742 and BY4739 background (Brachmann et al., 1998) were obtained from EUROSCARF (Institute for Microbiology, Frankfurt, Germany). Other deletion

strains were either from the Dove Lab yeast strain collection, or were made in this study. The *S. cerevisiae* strains used in this study are summarised in Table 2.2.

All budding yeast strains were grown in standard Yeast extract- Peptone-Dextrose (YPD) or Synthetic Complete (SC) minimal media supplemented with the appropriate essential amino acids, prepared as described below.

Table 2.1: Plasmids used in this study

Plasmid name	E.coli resistance:	S.cerevisiae Marker	Source
pUG23	<i>amp^R</i>	<i>HIS3</i>	J. Hegemann
pUG34	<i>amp^R</i>	<i>HIS3</i>	J. Hegemann
pUG36	<i>amp^R</i>	<i>URA3</i>	J. Hegemann
p-Gem-T-Easy	<i>amp^R</i>	-	Invitrogen
p-Gem-T-Easy- <i>CHS6</i>	<i>amp^R</i>	-	This study
p-Gem-T-Easy- <i>CHS6::LYS2</i>	<i>amp^R</i>	-	This study
m.Cherry <i>PHO8</i>	<i>amp^R</i>	<i>URA3</i>	Dove Lab
pUG23- <i>YIF1</i>	<i>amp^R</i>	<i>HIS3</i>	D. Pearce
pUG34- <i>YIF1</i>	<i>amp^R</i>	<i>HIS3</i>	D. Pearce
pUG36- <i>YIF1</i>	<i>amp^R</i>	<i>URA3</i>	This study
pUG23- <i>MRL1</i>	<i>amp^R</i>	<i>HIS3</i>	This study
pUG34- <i>MRL1</i>	<i>amp^R</i>	<i>HIS3</i>	This study
pRS416- <i>PHM5-GFP</i>	<i>amp^R</i>	<i>URA3</i>	Dove Lab
pRS416- <i>UbPHM5-GFP</i>	<i>amp^R</i>	<i>URA3</i>	Dove Lab
pRS316- <i>STE3-GFP</i>	<i>amp^R</i>	<i>URA3</i>	F.Cooke
pAEM42	<i>amp^R</i>	<i>URA3</i>	Dove Lab
pAEM44	<i>amp^R</i>	<i>URA3</i>	Dove Lab
pUG36- <i>ATG18</i>	<i>amp^R</i>	<i>URA3</i>	Dove Lab
pYEp13 based yeast plasmid library	<i>amp^R</i>	<i>LEU2</i>	Dove Lab
pYCplacIII- <i>APL4</i>	<i>amp^R</i>	<i>LEU2</i>	F.Cooke
pRS315- <i>APL2</i>	<i>amp^R</i>	<i>LEU2</i>	F.Cooke
pRS313- <i>SOL1</i>	<i>amp^R</i>	<i>HIS3</i>	R. Fuller
pEGKT- <i>FAB1</i>	<i>amp^R</i>	<i>URA3</i>	Dove Lab
pEGKT- <i>FAB1^{Kinase dead}</i>	<i>amp^R</i>	<i>URA3</i>	Dove Lab
pEGKT- <i>FAB1^{FYVE}</i>	<i>amp^R</i>	<i>URA3</i>	Dove Lab
pEGKT- <i>FAB1^{CTT-like}</i>	<i>amp^R</i>	<i>URA3</i>	Dove Lab
pEGKT- <i>FAB1^{PIPKIII unique}</i>	<i>amp^R</i>	<i>URA3</i>	Dove Lab
pEGKT- <i>SpFAB1</i>	<i>amp^R</i>	<i>URA3</i>	Dove Lab

pEGKT- <i>PIKfyve</i>	<i>amp^R</i>	<i>URA3</i>	Dove Lab
pGEX6T11	<i>amp^R chp^R</i>	-	Dove Lab
pGEX6T1-VMA1	<i>amp^R chp^R</i>	-	This study
pGEX6T1-VMA2	<i>amp^R chp^R</i>	-	This study
pGEX6T1-VMA4	<i>amp^R chp^R</i>	-	This study
pGEX6T1-VMA5	<i>amp^R chp^R</i>	-	This study
pUG36-SVP3	<i>amp^R</i>	<i>URA3</i>	Dove Lab
pUG36-SVP3 ^{CT1}	<i>amp^R</i>	<i>URA3</i>	Dove Lab
pUG36-SVP3 ^{NT1}	<i>amp^R</i>	<i>URA3</i>	Dove Lab
pUG36-SVP3 ^{PA1A/PACA}	<i>amp^R</i>	<i>URA3</i>	This study
pUG36-SVP3 ^{K486R}	<i>amp^R</i>	<i>URA3</i>	This study
pRS313-VPS13 ^{E003K}	<i>amp^R</i>	<i>URA3</i>	This study

Table 2.2: *S. cerevisiae* strains used in this study

Strain	Genotype	Source
BY4742	<i>MATα his3Δ1 leu2Δ0 lys2Δ0 ura3Δ0</i>	Euroscarf
BY4741	<i>MATα his3Δ1 leu2Δ0 met15Δ0 ura3Δ0</i>	Euroscarf
BY4742 Δ <i>fab1</i>	<i>MATα his3Δ1 leu2Δ0 lys2Δ0 ura3Δ0 <i>fab1::kanMX4</i></i>	Euroscarf
BY4741 Δ <i>fab1</i>	<i>MATα his3Δ1 leu2Δ0 met15Δ0 ura3Δ0 <i>fab1::kanMX4</i></i>	Euroscarf
BY4742 Δ <i>vps29</i>	<i>MATα his3Δ1 leu2Δ0 lys2Δ0 ura3Δ0 <i>vps29::kanMX4</i></i>	Euroscarf
BY4742 Δ <i>btn2</i>	<i>MATα his3Δ1 leu2Δ0 lys2Δ0 ura3Δ0 <i>btn2::kanMX4</i></i>	Euroscarf
BY4742 Δ <i>apl2</i>	<i>MATα his3Δ1 leu2Δ0 lys2Δ0 ura3Δ0 <i>apl2::kanMX4</i></i>	Euroscarf
BY4742 Δ <i>apl4</i>	<i>MATα his3Δ1 leu2Δ0 lys2Δ0 ura3Δ0 <i>apl4::kanMX4</i></i>	Euroscarf
BY4742 Δ <i>chs6</i>	<i>MATα his3Δ1 leu2Δ0 lys2Δ0 ura3Δ0 <i>chs6::kanMX4</i></i>	Euroscarf
BY4742 Δ <i>fig4</i>	<i>MATα his3Δ1 leu2Δ0 lys2Δ0 ura3Δ0 <i>fig4::kanMX4</i></i>	Euroscarf
BY4742 Δ <i>svp1</i>	<i>MATα his3Δ1 leu2Δ0 lys2Δ0 ura3Δ0 <i>svp1::kanMX4</i></i>	Euroscarf
BY4742 Δ <i>svp3</i>	<i>MATα his3Δ1 leu2Δ0 lys2Δ0 ura3Δ0 <i>svp1::kanMX4</i></i>	Euroscarf
BY4742 Δ <i>vac7</i>	<i>MATα his3Δ1 leu2Δ0 lys2Δ0 ura3Δ0 <i>vac7::kanMX4</i></i>	Euroscarf
BY4742 Δ <i>vac14</i>	<i>MATα his3Δ1 leu2Δ0 lys2Δ0 ura3Δ0 <i>vac14::kanMX4</i></i>	Euroscarf
BY4742 Δ <i>hsv1</i>	<i>MATα his3Δ1 leu2Δ0 lys2Δ0 ura3Δ0 <i>hsv1::kanMX4</i></i>	Euroscarf
BY4742 Δ <i>hsv2</i>	<i>MATα his3Δ1 leu2Δ0 lys2Δ0 ura3Δ0 <i>hsv2::kanMX4</i></i>	Euroscarf
BY4742 Δ <i>doa4</i>	<i>MATα his3Δ1 leu2Δ0 lys2Δ0 ura3Δ0 <i>doa4::kanMX4</i></i>	Euroscarf
BY4742 Δ <i>pep12</i>	<i>MATα his3Δ1 leu2Δ0 lys2Δ0 ura3Δ0 <i>pep12::kanMX4</i></i>	Euroscarf
BY4742 Δ <i>vps4</i>	<i>MATα his3Δ1 leu2Δ0 lys2Δ0 ura3Δ0 <i>vps4::kanMX4</i></i>	Euroscarf
BY4742 Δ <i>vps13</i>	<i>MATα his3Δ1 leu2Δ0 lys2Δ0 ura3Δ0 <i>vps13::kanMX4</i></i>	Euroscarf
BY4742 Δ <i>lcl3</i>	<i>MATα his3Δ1 leu2Δ0 lys2Δ0 ura3Δ0 <i>lcl3::kanMX4</i></i>	Euroscarf
BY4742 Δ <i>gup1</i>	<i>MATα his3Δ1 leu2Δ0 lys2Δ0 ura3Δ0 <i>gup1::kanMX4</i></i>	Euroscarf
BY4742 Δ <i>scy1</i>	<i>MATα his3Δ1 leu2Δ0 lys2Δ0 ura3Δ0 <i>scy1::kanMX4</i></i>	Euroscarf
BY4742 Δ <i>ygl082w</i>	<i>MATα his3Δ1 leu2Δ0 lys2Δ0 ura3Δ0 <i>ygl082w::kanMX4</i></i>	Euroscarf
BY4742 Δ <i>fsk2</i>	<i>MATα his3Δ1 leu2Δ0 lys2Δ0 ura3Δ0 <i>fsk2::kanMX4</i></i>	Euroscarf
BY4742 Δ <i>gas1</i>	<i>MATα his3Δ1 leu2Δ0 lys2Δ0 ura3Δ0 <i>gas1::kanMX4</i></i>	Euroscarf
BY4739 Δ <i>vps8</i>	<i>MATα leu2Δ0 lys2Δ0 ura3Δ0 <i>vps8::kanMX4</i></i>	Euroscarf

BY4742 $\Delta vma1$	<i>MATa his3Δ1 leu2Δ0 lys2Δ0 ura3Δ0 vma1::kanMX4</i>	Euroscarf
BY4742 $\Delta vma2$	<i>MATa his3Δ1 leu2Δ0 lys2Δ0 ura3Δ0 vma2::kanMX4</i>	Euroscarf
BY4742 $\Delta vma3$	<i>MATa his3Δ1 leu2Δ0 lys2Δ0 ura3Δ0 vma3::kanMX4</i>	Euroscarf
BY4742 $\Delta vma4$	<i>MATa his3Δ1 leu2Δ0 lys2Δ0 ura3Δ0 vma4::kanMX4</i>	Euroscarf
BY4742 $\Delta vma7$	<i>MATa his3Δ1 leu2Δ0 lys2Δ0 ura3Δ0 vma7::kanMX4</i>	Euroscarf
BY4742 $\Delta vma8$	<i>MATa his3Δ1 leu2Δ0 lys2Δ0 ura3Δ0 vma8::kanMX4</i>	Euroscarf
BY4742 $\Delta vma9$	<i>MATa his3Δ1 leu2Δ0 lys2Δ0 ura3Δ0 vma9::kanMX4</i>	Euroscarf
BY4742 $\Delta vma10$	<i>MATa his3Δ1 leu2Δ0 lys2Δ0 ura3Δ0 vma10::kanMX4</i>	Euroscarf
BY4742 $\Delta vma11$	<i>MATa his3Δ1 leu2Δ0 lys2Δ0 ura3Δ0 vma11::kanMX4</i>	Euroscarf
BY4742 $\Delta stv1$	<i>MATa his3Δ1 leu2Δ0 lys2Δ0 ura3Δ0 stv1::kanMX4</i>	Euroscarf
BY4742 $\Delta vph1$	<i>MATa his3Δ1 leu2Δ0 lys2Δ0 ura3Δ0 vph1::kanMX4</i>	Euroscarf
BY4742 $\Delta vps3$	<i>MATa his3Δ1 leu2Δ0 lys2Δ0 ura3Δ0 vps3::kanMX4</i>	Euroscarf
BY4742 $\Delta vps8$	<i>MATa his3Δ1 leu2Δ0 lys2Δ0 ura3Δ0 vps8::kanMX4</i>	This study
BY4742 $\Delta pho81$	<i>MATa his3Δ1 leu2Δ0 lys2Δ0 ura3Δ0 pho81::kanMX4</i>	Euroscarf
BY4742 $\Delta pho85$	<i>MATa his3Δ1 leu2Δ0 lys2Δ0 ura3Δ0 pho85::kanMX4</i>	Euroscarf
MSY2629	<i>MATa leu2-3,112 ura3-52 his3-Δ200 trp1-Δ901 suc2-Δ9 lys2-801 vps26::LEU2 vps29::HIS3</i>	M. Seamen
BY4741 <i>CHC1-RFP</i>	<i>MATa his3Δ1 leu2Δ0 met15Δ0 ura3Δ0 <i>CHC1::CHC1-RFP::kanMX4</i></i>	E. O'Shea
BY4741 <i>COP1-RFP</i>	<i>MATa his3Δ1 leu2Δ0 met15Δ0 ura3Δ0 <i>COP1::COP1-RFP::kanMX4</i></i>	E. O'Shea
BY4741 <i>ANP1-RFP</i>	<i>MATa his3Δ1 leu2Δ0 met15Δ0 ura3Δ0 <i>ANP1::ANP1-RFP::kanMX4</i></i>	E. O'Shea
BY4741 <i>SNF7-RFP</i>	<i>MATa his3Δ1 leu2Δ0 met15Δ0 ura3Δ0 <i>SNF7::SNF7-RFP::kanMX4</i></i>	E. O'Shea
BY4741 <i>CHC1-RFP $\Delta fab1$</i>	<i>MATa his3Δ1 leu2Δ0 met15Δ0 ura3Δ0 <i>CHC1::CHC1-RFP::kanMX4 fab1::LEU2</i></i>	This study
BY4741 <i>COP1-RFP $\Delta fab1$</i>	<i>MATa his3Δ1 leu2Δ0 met15Δ0 ura3Δ0 <i>COP1::COP1-RFP::kanMX4 fab1::LEU2</i></i>	This study
BY4741 <i>ANP1-RFP $\Delta fab1$</i>	<i>MATa his3Δ1 leu2Δ0 met15Δ0 ura3Δ0 <i>ANP1::ANP1-RFP::kanMX4 fab1::LEU2</i></i>	This study
BY4741 <i>SNF7-RFP $\Delta fab1$</i>	<i>MATa his3Δ1 leu2Δ0 met15Δ0 ura3Δ0 <i>SNF7::SNF7-RFP::kanMX4 fab1::LEU2</i></i>	This study
BY4741 <i>CHC1-RFP $\Delta vps26$</i>	<i>MATa his3Δ1 leu2Δ0 met15Δ0 ura3Δ0 <i>CHC1::CHC1-RFP::kanMX4 vps26::LEU2</i></i>	This study
BY4741 <i>COP1-RFP $\Delta vps26$</i>	<i>MATa his3Δ1 leu2Δ0 met15Δ0 ura3Δ0 <i>COP1::COP1-RFP::kanMX4 vps26::LEU2</i></i>	This study
BY4741 <i>ANP1-RFP $\Delta vps26$</i>	<i>MATa his3Δ1 leu2Δ0 met15Δ0 ura3Δ0 <i>ANP1::ANP1-RFP::kanMX4 vps26::LEU2</i></i>	This study
BY4741 <i>SNF7-RFP $\Delta vps26$</i>	<i>MATa his3Δ1 leu2Δ0 met15Δ0 ura3Δ0 <i>SNF7::SNF7-RFP::kanMX4 vps26::LEU2</i></i>	This study
BY4741 <i>CHC1-RFP VPS10-GFP</i>	<i>MATa his3Δ1 leu2Δ0 met15Δ0 ura3Δ0 <i>CHC1::CHC1-RFP::kanMX4 VPS10-GFP::HIS3MX6</i></i>	This study
BY4741 <i>COP1-RFP VPS10-GFP</i>	<i>MATa his3Δ1 leu2Δ0 met15Δ0 ura3Δ0 <i>COP1::COP1-RFP::kanMX4 VPS10-GFP::HIS3MX6</i></i>	This study
BY4741 <i>ANP1-RFP VPS10-GFP</i>	<i>MATa his3Δ1 leu2Δ0 met15Δ0 ura3Δ0 <i>ANP1::ANP1-RFP::kanMX4 VPS10-GFP::HIS3MX6</i></i>	This study
BY4741 <i>SNF7-RFP VPS10-GFP</i>	<i>MATa his3Δ1 leu2Δ0 met15Δ0 ura3Δ0 <i>SNF7::SNF7-RFP::kanMX4 VPS10-GFP::HIS3MX6</i></i>	This study

BY4741 <i>CHC1-RFP VPS10-GFP Δfab1</i>	<i>MAT_a his3Δ1 leu2Δ0 met15Δ0 ura3Δ0 CHC1::CHC1-RFP::kanMX4 fab1::LEU2 VPS10-GFP::HIS3MX6</i>	This study
BY4741 <i>COP1-RFP VPS10-GFP Δfab1</i>	<i>MAT_a his3Δ1 leu2Δ0 met15Δ0 ura3Δ0 COP1::COP1-RFP::kanMX4 fab1::LEU2 VPS10-GFP::HIS3MX6</i>	This study
BY4741 <i>ANP1-RFP VPS10-GFP Δfab1</i>	<i>MAT_a his3Δ1 leu2Δ0 met15Δ0 ura3Δ0 ANP1::ANP1-RFP::kanMX4 fab1::LEU2 VPS10-GFP::HIS3MX6</i>	This study
BY4741 <i>SNF7-RFP VPS10-GFP Δfab1</i>	<i>MAT_a his3Δ1 leu2Δ0 met15Δ0 ura3Δ0 SNF7::SNF7-RFP::kanMX4 fab1::LEU2 VPS10-GFP::HIS3MX6</i>	This study
BY4741 <i>CHC1-RFP VPS10-GFP Δfab1</i>	<i>MAT_a his3Δ1 leu2Δ0 met15Δ0 ura3Δ0 CHC1::CHC1-RFP::kanMX4 vps26::LEU2 VPS10-GFP::HIS3MX6</i>	This study
BY4741 <i>COP1-RFP VPS10-GFP Δfab1</i>	<i>MAT_a his3Δ1 leu2Δ0 met15Δ0 ura3Δ0 COP1::COP1-RFP::kanMX4 vps26::LEU2 VPS10-GFP::HIS3MX6</i>	This study
BY4741 <i>ANP1-RFP VPS10-GFP Δfab1</i>	<i>MAT_a his3Δ1 leu2Δ0 met15Δ0 ura3Δ0 ANP1::ANP1-RFP::kanMX4 vps26::LEU2 VPS10-GFP::HIS3MX6</i>	This study
BY4741 <i>SNF7-RFP VPS10-GFP Δfab1</i>	<i>MAT_a his3Δ1 leu2Δ0 met15Δ0 ura3Δ0 SNF7::SNF7-RFP::kanMX4 vps26::LEU2 VPS10-GFP::HIS3MX6</i>	This study
BY4742 <i>VPS10-GFP</i>	<i>MAT_a his3Δ1 leu2Δ0 lys2Δ0 ura3Δ0 VPS10-GFP::HIS3MX6</i>	This study
BY4742 <i>VPS10-GFP Δvps29</i>	<i>MAT_a his3Δ1 leu2Δ0 lys2Δ0 ura3Δ0 vps29::kanMX4 VPS10-GFP::HIS3MX6</i>	This study
BY4742 <i>VPS10-GFP Δsvp1</i>	<i>MAT_a his3Δ1 leu2Δ0 lys2Δ0 ura3Δ0 svp1::kanMX4 VPS10-GFP::HIS3MX6</i>	This study
BY4742 <i>VPS10-GFP Δhsv1</i>	<i>MAT_a his3Δ1 leu2Δ0 lys2Δ0 ura3Δ0 hsv1::kanMX4 VPS10-GFP::HIS3MX6</i>	This study
BY4742 <i>VPS10-GFP Δhsv2</i>	<i>MAT_a his3Δ1 leu2Δ0 lys2Δ0 ura3Δ0 hsv2::kanMX4 VPS10-GFP::HIS3MX6</i>	This study
BY4742 <i>VPS10-GFP Δvac7</i>	<i>MAT_a his3Δ1 leu2Δ0 lys2Δ0 ura3Δ0 vac7::kanMX4 VPS10-GFP::HIS3MX6</i>	This study
BY4742 <i>VPS10-GFP Δvac14</i>	<i>MAT_a his3Δ1 leu2Δ0 lys2Δ0 ura3Δ0 vac14::kanMX4 VPS10-GFP::HIS3MX6</i>	This study
BY4742 <i>Δatg18 Δ atg21 Δhsv2</i>	<i>MAT_a ; his3Δ1; leu2Δ0; lys2Δ0; ura3Δ0 atg18:: kanMX4 atg21::LEU2 hsv2::HIS3</i>	Dove Lab
BY4742 <i>Δ atg18 Δ atg21</i>	<i>MAT_a ; his3Δ1; leu2Δ0; lys2Δ0; ura3Δ0 atg18:: kanMX4 atg21::LEU2</i>	This study
BY4742 <i>Δ atg21 Δhsv2</i>	<i>MAT_a ; his3Δ1; leu2Δ0; lys2Δ0; ura3Δ0 atg21::HIS3 hsv2::LEU2</i>	This study
BY4742 <i>Δ atg18 Δ atg21 VPS10-GFP</i>	<i>MAT_a ; his3Δ1; leu2Δ0; lys2Δ0; ura3Δ0 atg18:: kanMX4 atg21::LEU2 VPS10-GFP::HIS3MX6</i>	This study
BY4742 <i>Δ atg21 Δhsv2 VPS10-GFP</i>	<i>MAT_a ; his3Δ1; leu2Δ0; lys2Δ0; ura3Δ0 hsv2:: kanMX4 atg21::LEU2 VPS10-GFP::HIS3MX6</i>	This study
BY4742 <i>Δvps29 Δfab1 VPS10-GFP</i>	<i>MAT_a his3Δ1 leu2Δ0 lys2Δ0 ura3Δ0 vps29::kanMX4 fab1::LEU2 VPS10-GFP::HIS3MX6</i>	This study
SEY6210.1 <i>VPS5-GFP</i>	<i>MAT_a leu2-3,112 ura3-52 his3-Δ200 trp1-Δ901 suc2-Δ9 lys2-801 VPS5::VPS5-GFP</i>	S.Emr
SEY6210.1 <i>VPS5-GFP Δfab1</i>	<i>MAT_a leu2-3,112 ura3-52 his3-Δ200 trp1-Δ901 suc2-Δ9 lys2-801 VPS5::VPS5-GFP fab1::LEU2</i>	This study
SEY6210.1 <i>VPS5-GFP Δvac14</i>	<i>MAT_a leu2-3,112 ura3-52 his3-Δ200 trp1-Δ901 suc2-Δ9 lys2-801 VPS5::VPS5-GFP vac14::kanMX4</i>	This study
SEY6210.1 <i>VPS5-GFP Δvps26</i>	<i>MAT_a leu2-3,112 ura3-52 his3-Δ200 trp1-Δ901 suc2-Δ9 lys2-801 VPS5::VPS5-GFP vps26::LEU2</i>	This study
BY4742 <i>MRL1-GFP</i>	<i>MAT_a his3Δ1 leu2Δ0 lys2Δ0 ura3Δ0 MRL1-GFP::HIS3MX6</i>	This study
BY4742 <i>Δfab1 MRL1-GFP</i>	<i>MAT_a his3Δ1 leu2Δ0 lys2Δ0 ura3Δ0 fab1::kanMX4 MRL1-GFP::HIS3MX6</i>	This study
BY4742 <i>Δvps29 MRL1-GFP</i>	<i>MAT_a his3Δ1 leu2Δ0 lys2Δ0 ura3Δ0 vps29::kanMX4 MRL1-GFP::HIS3MX6</i>	This study
BJ3505	<i>MAT_a pep4::HIS3 prb1-Δ1.6R his3 lys2-208 trp1-Δ101 ura3-52 gal2 can</i>	A. Mayer
BY4741 <i>Δchs6</i>	<i>MAT_a his3Δ1 leu2Δ0 met15Δ0 ura3Δ0 chs6::kanMX4</i>	This study
YPH499 <i>Δchs6</i>	<i>MAT_a ura3-52 lys2-801 ade2-101 trp1-Δ63 his3-Δ200 leu2-Δ1 chs6::LYS2</i>	This study
<i>fab1-Its</i>	<i>MAT_a fab1-lade3 trp1 can1 cyh1 gal1</i>	D. Koshland

GPY1783-20D	<i>MATa ura3-52 leu2-3, 112 his3-Δ200 trp1-Δ901 lys2-801suc2-Δ9 GAL mel apl2Δ6::TRP1</i>	G. Payne
GPY2424.1	<i>MATa ura3-52 leu2-3, 112 his3-Δ200 trp1-Δ901 lys2-801suc2-Δ9 GAL mel apl4Δ::TRP1</i>	G. Payne
BY4742 <i>CHS3-GFP</i>	<i>MATa his3Δ1 leu2Δ0 lys2Δ0 ura3Δ0 CHS3-GFP::HIS3MX6</i>	This study
BY4742 <i>Δfab1 CHS3-GFP</i>	<i>MATa his3Δ1 leu2Δ0 lys2Δ0 ura3Δ0 fab1::kanMX4 CHS3-GFP::HIS3MX6</i>	This study
BY4742 <i>Δapl4 CHS3-GFP</i>	<i>MATa his3Δ1 leu2Δ0 lys2Δ0 ura3Δ0 apl4::kanMX4 CHS3-GFP::HIS3MX6</i>	This study
BY4742 <i>Δchs6 CHS3-GFP</i>	<i>MATa his3Δ1 leu2Δ0 lys2Δ0 ura3Δ0 chs6::kanMX4 CHS3-GFP::HIS3MX6</i>	This study
BY4742 <i>Δchs6</i>	<i>MATa his3Δ1 leu2Δ0 lys2Δ0 ura3Δ0 chs6::LYS2</i>	This study
BY4742 <i>Δfab1 Δchs6</i>	<i>MATa his3Δ1 leu2Δ0 lys2Δ0 ura3Δ0 fab1::kanMX4 chs6::LYS2</i>	This study
BY4742 <i>Δfab1 Δchs6 CHS3-GFP</i>	<i>MATa his3Δ1 leu2Δ0 lys2Δ0 ura3Δ0 fab1::kanMX4 chs6::LYS2 CHS3-GFP::HIS3MX6</i>	This study
BY4742 <i>Δapl4 Δchs6</i>	<i>MATa his3Δ1 leu2Δ0 lys2Δ0 ura3Δ0 apl4::kanMX4 chs6::LYS2</i>	This study
BY4742 <i>Δapl4 Δchs6CHS3-GFP</i>	<i>MATa his3Δ1 leu2Δ0 lys2Δ0 ura3Δ0 apl4::kanMX4 chs6::LYS2 CHS3-GFP::HIS3MX6</i>	This study
BY4742 <i>Δfab1 Δchs6</i>	<i>MATa his3Δ1 leu2Δ0 lys2Δ0 ura3Δ0 fab1::kanMX4 chs6::LYS2</i>	This study
BY4742 <i>Δfab1 Δchs6</i>	<i>MATa his3Δ1 leu2Δ0 lys2Δ0 ura3Δ0 fab1::LEU2 chs6::LYS2</i>	This study
BY4742 <i>Δapl4 Δchs6 Δfab1</i>	<i>MATa his3Δ1 leu2Δ0 lys2Δ0 ura3Δ0 apl4::kanMX4 chs6::LYS2 fab1::LEU2</i>	This study
BY4742 <i>Δatg21Δchs6</i>	<i>MATa his3Δ1 leu2Δ0 lys2Δ0 ura3Δ0 atg21::kanMX4 chs6::LYS2</i>	This study
BY4742 <i>Δhsv2 Δchs6</i>	<i>MATa his3Δ1 leu2Δ0 lys2Δ0 ura3Δ0 hsv2::kanMX4 chs6::LYS2</i>	This study
BY4742 <i>Δvac7 Δchs6</i>	<i>MATa his3Δ1 leu2Δ0 lys2Δ0 ura3Δ0 vac7::kanMX4 chs6::LYS2</i>	This study
BY4742 <i>Δvac14 Δchs6</i>	<i>MATa his3Δ1 leu2Δ0 lys2Δ0 ura3Δ0 vac14::kanMX4 chs6::LYS2</i>	This study
BY4742 <i>Δsvp3 Δchs6</i>	<i>MATa his3Δ1 leu2Δ0 lys2Δ0 ura3Δ0 svp3::kanMX4 chs6::LYS2</i>	This study
BY4742 <i>Δdoa4 Δchs6</i>	<i>MATa his3Δ1 leu2Δ0 lys2Δ0 ura3Δ0 doa4::kanMX4 chs6::LYS2</i>	This study
BY4741 <i>Δvps13 Δchs6</i>	<i>MATa his3Δ1 leu2Δ0 met15Δ0 ura3Δ0 vps13::kanMX4 chs6::LYS2</i>	This study
BY4742 <i>Δvps13 Δchs6</i>	<i>MATa his3Δ1 leu2Δ0 lys2Δ0 ura3Δ0 vps13::kanMX4 chs6::LYS2</i>	This study
BY4742 <i>Δlcl3 Δchs6</i>	<i>MATa his3Δ1 leu2Δ0 lys2Δ0 ura3Δ0 lcl3::kanMX4 chs6::LYS2</i>	This study
BY4742 <i>Δgup1 Δchs6</i>	<i>MATa his3Δ1 leu2Δ0 lys2Δ0 ura3Δ0 gup1::kanMX4 chs6::LYS2</i>	This study
BY4742 <i>Δscy1 Δchs6</i>	<i>MATa his3Δ1 leu2Δ0 lys2Δ0 ura3Δ0 scy1::kanMX4 chs6::LYS2</i>	This study
BY4742 <i>Δygl082w Δchs6</i>	<i>MATa his3Δ1 leu2Δ0 lys2Δ0 ura3Δ0 ygl082w::kanMX4 chs6::LYS2</i>	This study
BY4742 <i>Δfsk2 Δchs6</i>	<i>MATa his3Δ1 leu2Δ0 lys2Δ0 ura3Δ0 fsk2::kanMX4 chs6::LYS2</i>	This study
BY4742 <i>Δgas1 Δchs6</i>	<i>MATa his3Δ1 leu2Δ0 lys2Δ0 ura3Δ0 gas1::kanMX4 chs6::LYS2</i>	This study
BY4742 <i>Δapl2 Δchs6</i>	<i>MATa his3Δ1 leu2Δ0 lys2Δ0 ura3Δ0 apl2::kanMX4 chs6::LYS2</i>	This study
BY4742 <i>Δfab1 Δchs6 Δpep12</i>	<i>MATa his3Δ1 leu2Δ0 lys2Δ0 ura3Δ0 fab1::LEU2 chs6::LYS2 pep12::kanMX4</i>	This study
BY4742 <i>Δfab1 Δchs6 Δvps4</i>	<i>MATa his3Δ1 leu2Δ0 lys2Δ0 ura3Δ0 fab1::LEU2 chs6::LYS2 vps4::kanMX4</i>	This study
GPY2424.1Δchs6	<i>MATa ura3-52 leu2-3, 112 his3-Δ200 trp1-Δ901 lys2-801suc2-Δ9 GAL apl4Δ::TRP1 chs6::LYS2</i>	This study

GPY2424.1 Δ chs6 Δ pep12	MATa ura3-52 leu2-3, 112 his3- Δ 200 trp1- Δ 901 lys2-801suc2- Δ 9 GAL pep12::kanMX4 apl4 Δ ::TRP1	This study
GPY2424.1 Δ chs6 Δ vps4	MATa ura3-52 leu2-3, 112 his3- Δ 200 trp1- Δ 901 lys2-801suc2- Δ 9 GAL vps4::kanMX4 apl4 Δ ::TRP1 chs6::LYS2	This study
SUA1-3D	MATa ade2 Δ ade8his3 Δ 1 leu2 Δ 0 lys2 Δ 0 ura3 Δ trp1- Δ 0 sec22::HIS3	H.D.Schmitt
BY4742 Δ vma1 Δ pep4	MATa his3 Δ 1 leu2 Δ 0 lys2 Δ 0 ura3 Δ 0 vma1::kanMX4 pep4::HIS3	This study
BY4742 Δ vma2 Δ pep4	MATa his3 Δ 1 leu2 Δ 0 lys2 Δ 0 ura3 Δ 0 vma2::kanMX4 pep4::HIS3	This study
BY4742 Δ vma3 Δ pep4	MATa his3 Δ 1 leu2 Δ 0 lys2 Δ 0 ura3 Δ 0 vma3::kanMX4 pep4::HIS3	This study
BY4742 Δ vma4 Δ pep4	MATa his3 Δ 1 leu2 Δ 0 lys2 Δ 0 ura3 Δ 0 vma4::kanMX4 pep4::HIS3	This study
BY4742 Δ vma7 Δ pep4	MATa his3 Δ 1 leu2 Δ 0 lys2 Δ 0 ura3 Δ 0 vma7::kanMX4 pep4::HIS3	This study
BY4742 Δ vma8 Δ pep4	MATa his3 Δ 1 leu2 Δ 0 lys2 Δ 0 ura3 Δ 0 vma8::kanMX4 pep4::HIS3	This study
BY4742 Δ vma9 Δ pep4	MATa his3 Δ 1 leu2 Δ 0 lys2 Δ 0 ura3 Δ 0 vma9::kanMX4 pep4::HIS3	This study
BY4742 Δ vma10 Δ pep4	MATa his3 Δ 1 leu2 Δ 0 lys2 Δ 0 ura3 Δ 0 vma10::kanMX4 pep4::HIS3	This study
BY4742 Δ vma11 Δ pep4	MATa his3 Δ 1 leu2 Δ 0 lys2 Δ 0 ura3 Δ 0 vma11::kanMX4 pep4::HIS3	This study
BY4742 Δ stv1 Δ pep4	MATa his3 Δ 1 leu2 Δ 0 lys2 Δ 0 ura3 Δ 0 stv1::kanMX4 pep4::HIS3	This study
BY4742 Δ vph1 Δ pep4	MATa his3 Δ 1 leu2 Δ 0 lys2 Δ 0 ura3 Δ 0 vph1::kanMX4 pep4::HIS3	This study
BY4742 Δ pho81 Δ pep4	MATa his3 Δ 1 leu2 Δ 0 lys2 Δ 0 ura3 Δ 0 pho81::kanMX4 pep4::HIS3	This study
BY4742 Δ pho85 Δ pep4	MATa his3 Δ 1 leu2 Δ 0 lys2 Δ 0 ura3 Δ 0 pho85::kanMX4 pep4::HIS3	This study
BY4742 Δ vps3 Δ pep4	MATa his3 Δ 1 leu2 Δ 0 lys2 Δ 0 ura3 Δ 0 vps3::kanMX4 pep4::HIS3	This study
BY4742 Δ vps8 Δ pep4	MATa his3 Δ 1 leu2 Δ 0 lys2 Δ 0 ura3 Δ 0 vps8::kanMX4 pep4::HIS3	This study

2.1.2. Reagents for culture of *S. cerevisiae* and *E. coli*.

Bactopeptone, Bactoagar, yeast extract and yeast nitrogen base without amino acids were obtained from Difco Laboratories (Detroit, MI, USA).

2.1.3. Reagents for molecular biology.

Restriction enzymes (*Bam*HI, *Eco*RI, *Xho*I *Eco*RV, *Cla*I, *Xba*I, *Nru*I and *Ade*I), dNTPs, T4 DNA ligase, 1KB DNA ladder and Biotaq polymerase were obtained from New England Biolabs (Beverly, MA, USA). Expand proof-reading DNA polymerase; long template DNA polymerase and $\times 10$ reaction buffer were obtained from Roche (Nutley, NJ, USA). Oligonucleotides were synthesised by Alta Bioscience (Birmingham, UK) or MWG Biotech (Ebersberg, Germany). Qiagen II resin gel extraction kits, genomic DNA kit, mini and midi prep plasmid kits were obtained from Qiagen Ltd (Valencia, CA, USA). All other reagents were obtained from Sigma-Aldrich (St. Louis, MI, USA), and were of biotechnological grade or better.

2.1.4. Materials for Microscopy.

22 x 22 mm coverslips and prewashed slides were purchased from Fischer Scientific (Loughborough, UK). Non fluorescent emersion oil was purchased from Nikon Ltd (Melville, NY, USA). FM4-64 lipid dye, Fluorescent brightener 28, WGA-FITC and Poly L-lysine were obtained from Sigma-Aldrich (St.Louis, MI, USA).

2.1.5. Materials for high efficiency transformation of Yeast and *E. coli*

Polyethylene glycol (PEG), lithium acetate, single-stranded salmon testis DNA, Ampicillin, 10 x TXN salts, glucose and MgCl₂ were obtained from Sigma-Aldrich (St.Louis, MI, USA). Isopropyl β -D-1-thiogalactopyranoside (IPTG) and X-gal were obtained from Bio-Line (London, UK).

2.1.6. Media composition and solutions

All yeast media were autoclaved for 15 minutes at 121°C and cooled. Glucose was added to a final concentration of 2% (from a 40% w/v stock) prior to use.

Yeast extract Peptone Dextrose (YPD) (1L):

Glucose (2.0% w/v), Bactopeptone (2.0% w/v), Yeast extract (1.0% w/v), Adenine (100 mg), Uracil (100 mg)

Yeast extract Tryptone Dextrose (YTD) (1L):

Glucose (2.0% w/v), Bacto-tryptone (2.0% w/v), Yeast extract (1.0% w/v), Adenine (100 mg), Uracil (100 mg).

Rich media (pre sporulation)

Glucose (4.0% w/v), Bactopeptone (2.0% w/v), Bacto-tryptone (2.0% w/v) Yeast extract (2% w/v) Amino acid stock mix (0.2%)

Rich YEPA

Potassium acetate (2.0% w/v), Bactopeptone (2.0% w/v), Bacto-tryptone (2.0% w/v)

Yeast extract (2% w/v) Amino acid stock mix (0.2%)

SPM sporulation media

Potassium acetate (0.3% w/v), Raffinose (0.1% w/v), Essential amino acids (20mg each)

Luria Broth (LB) (1L):

Tryptone (1.0% w/v), Yeast Extract (0.5% w/v), NaCl (1.0% w/v)

LB + 100 µg/ml Ampicillin (1L):

LB, Ampicillin (100 µg/ml)

To prepare agar plates for YPD, YTD or LB media, Bacto agar (2.0% w/v) was added prior to autoclaving. Media was cooled to 50°C and then glucose and/or antibiotics were added.

Amino acid (AA) mix stock:

Adenine (2 g), Arginine (2 g), Tyrosine (30 mg), Isoleucine (2g), Phenylalanine (2.06 g), Glutamic acid (2 g), Aspartic acid (2 g), Valine (2 g), Threonine (2 g), Serine (2 g), Glycine (2 g), Proline (2 g), Alanine (2 g). Powder was milled in powder mill for 1 minute and then stored at 4°C in sealed bottles.

Synthetic Complete (SC) (1L):

Glucose (2.0% w/v), Yeast Nitrogen Base without Amino Acids & Ammonium

Sulphate (1.7 g), Ammonium Sulphate (5 g), AA stock mix (2g), 100 mg leucine, lysine, tryptophan, histidine, methionine, uracil; pH 5.7

For selective SC medium, the corresponding amino acid was omitted. For example, to make SC-His, 100mg Histidine was left out.

In order to make SC plates, the pH was adjusted to 5.7 prior to the addition of Bacto agar (2.0% w/v). Media was then autoclaved, cooled and glucose (2% w/v final) added.

SOC medium (1L):

Tryptone (2.0% w/v), Yeast Extract (0.5% w/v), NaCl (0.05% w/v), KCl (2.5 mM), adjust pH to 7 with NaOH. After autoclaving and immediately prior to use, sterile solutions of MgCl₂ (10 µM) and Glucose (20 µM) were added.

2.2. METHODS

2.3. High efficiency transformation of yeast.

The following method was adapted from *Methods in Yeast Genetics* (Adam, A., Goccschling, D. E., Kaiser, C. A., and Sterns, T., eds), Cold Springs Harbour Laboratory Manual [1997].

Cells were subcultured at 5×10^6 cells/ml in YPD+2.0% glucose medium (50ml), and were grown at 25°C to 2×10^7 cells/ml. Cells were collected, resuspended in H₂O (25ml), and centrifuged at 1000g for 5 minutes at 25°C. Cell were again collected, resuspended in 1ml of 100mM lithium acetate (LiAc) and transferred to a 1.5ml Eppendorf tube. The cell suspension was centrifuged at 2000g for 1 minute and the

supernatant removed. Single-stranded salmon testis DNA 2mg/ml (carrier DNA) was boiled for 7 minutes and chilled on ice. The cell pellet was resuspended with a mixture of; 240µl PEG (50% w/v), 36µl LiAc (1.0 M), 50µl boiled carrier DNA and 25µl ddH₂O containing plasmid or construct DNA (0.1-10µg). The resulting mixture was vortexed for 1 minute, incubated for 20 minutes at 30°C, and then heat-shocked for 20 minutes at 42°C. Cells were collected by centrifugation at 3000g for 1 minute. The supernatant was discarded and the cells gently washed with 1ml of ddH₂O, centrifuging as above. The resulting pellet was resuspended in ddH₂O (150µl), plated on selective agar plates and incubated at 25°C for three days.

2.4. Extraction of Genomic DNA from *S. cerevisiae*.

Genomic DNA was extracted from Yeast strains using the Gentra Puregene Yeast/Bact. Kit from Qiagen. The following method is from Gentra Puregene Handbook, second edition, Qiagen, p47- 48, 09/2007.

Cells were subcultured at 5×10^6 cells/ml in YPD+2.0% glucose medium (50 ml), and were grown at 25°C to 1×10^8 cells/ml. 1ml of the cell suspension was transferred to a 1.5ml Eppendorf tube on ice, and centrifuged for 5 seconds at 16000g to collect cells. Cells were resuspended in 300µl of cell suspension solution (part of kit), 1.5µl of Lytic enzyme solution was added, then incubated at 37°C for 30 minutes. Cells were collected by centrifugation at 16000g for 1 minute and the supernatant discarded. Cells were resuspended in 300µl of cell lysis solution, and then 100µl of protein precipitation solution was added. The sample was vortexed, then centrifuged at 16000g to form a pellet of precipitated proteins. The supernatant was transferred to a fresh tube containing 300µl of isopropanol, was mixed by inversion and centrifuged

for 1 minute to pellet DNA. The supernatant was discarded and the pellet washed with 300 µl of 70% ethanol. The supernatant was removed, and pellet air dried for 10 minutes, before being resuspended in 50µl of DNA hydration solution. 1.5µl of RNase A solution was added, and the sample mixed. To dissolve the DNA, sample was incubated at 37°C for 30 minutes, then at 65°C for 1 hour.

2.5 Changing the mating type of *S. cerevisiae* cells.

In order to change the mating type of *S. cerevisiae* strains, two haploid strains were mated to create a diploid. This was then sporulated (to divide and form spores) and the tetrad (the four spores that separate after mating) dissected to create haploid cells of interest.

2.5.1 Mating of haploid cells to form a diploid.

Two haploid strains of opposite mating type, were grown to 1×10^7 cells/ml. Equal amounts of each strain were mixed, and incubated at 30°C for 3 hours. Diploid cells were selected by plating onto selective SC plates that would only permit growth of a diploid cell because of amino-acid deficiencies.

2.5.2 Sporulation.

A diploid colony was sub-cultured to 1×10^7 cells/ml in rich pre sporulation media at 30°C overnight, and was then used to inoculate rich YEPA (20ml). Cells were incubated at 30°C for 4 hours, then collected by centrifugation at 2000g for 5 minutes, and washed twice with ddH₂O. The cells were resuspended in SPM (20ml) in a 250ml conical flask, and incubated at 30°C 220rpm for 3-5 days until asci (wall bound structure containing four spores) developed.

2.5.3 Tetrad dissection.

50µl of the sporulation mixture (containing asci) was incubated with 5µl of zymolyase (dissolved in sorbitol) for 5 minutes. A loop full was used to inoculate the start position on a YTD plate. A singer MSM MKIII micromanipulator, (Singer Instrument Co Ltd. Watchet, Somerset, UK) was used to dissect the tetrad. A four spore tetrad was picked up from the inoculation strip then deposited at position A1. The needle was used to separate the ascospores; the remaining three spores were moved to position B1, where another spore was deposited. The next spore was deposited at C1 and the final spore deposited at D1. This process was repeated to fill the plate. The plate was incubated at 25°C for 3 days and then replica plated onto various SC and drug containing plates to genotype each spore.

Mating type was discovered by performing test matings with known haploids, to look for the formation of a diploid.

2.6. Preparation of competent *E. coli* cells.

LB medium (10ml) was inoculated with an appropriate *E. coli* strain, and incubated overnight at 37°C. 1ml of culture was used to inoculate super comp media (BIO101 Carlsbad, CA, USA Formulation is proprietary, and therefore not defined further) (100ml) and was grown at 37°C in a 2 litre flask to an OD of A₆₆₀ ~0.8. Cells were collected through centrifugation at 4000g for 15 minutes at 4°C. Cells were then resuspended in ice-cold 1 x TXN salts (30ml) and incubated on ice overnight. Cell suspensions were centrifuged at 3000g 4°C for 15 minutes and were then resuspended

in 1x TXN salts + glycerol (20% v:w final) (5ml). Cells were incubated at 4°C for 1 hour, before being aliquoted and stored at -80°C.

2.7. Transformation of competent *E. coli* cells.

Plasmid DNA (0.1-10µg) was added to an aliquot of competent *E. coli* cells (100µl), incubated on ice for 15 minutes and heat shocked at 42°C for 45 seconds. Ice cold SOC medium (1.0 ml) was added to the cell suspension, mixed gently and incubated at 37°C for 30 minutes. Cells were collected through centrifugation at 8000g for 1 minute, and were then resuspended in LB medium (100µl). Sample was plated onto a LB + 100µg/ml amp plate and incubated at 37°C overnight.

For blue white selection of pGem-T-Easy, *E. coli* transformations were carried out as above and plated onto LB + 100µg/ml amp agar plate + IPTG + X-Gal.

2.8. Purification of plasmids from *E. coli*.

2.8.1 Mini-prep.

Single colonies were picked from agar plates, resuspended in LB+100µg/ml amp (5ml) and were grown at 37°C, 220rpm for 12-16 hours. *E. coli* was harvested by centrifugation at 8000g for 3 minutes at 25°C. The Qia-prep spin mini-prep kit and protocol was then followed.

2.8.2 Midi preps

A starter culture was inoculated using a single colony off a fresh plate into LB+100µg/ml amp (5ml). This was then used to inoculate LB+100µg/ml amp (50ml),

and was grown at 37°C 220 rpm for 12-16 hours. *E. coli* cells were harvested by centrifugation at 6000g 4°C for 15 minutes. The Qiagen anion exchange midi-prep protocol and Qiagen tip-100 were then used to complete the plasmid extraction.

2.8.3 Boiling preps

Single colonies were picked from agar plates, resuspended in LB+100µg/ml amp (5ml) and were grown at 37°C, 220rpm for 12-16 hours. *E. coli* cells were harvested by centrifuging at 16000g, 25°C for 2 minutes. Each pellet was resuspended in 110µl of STETL (8% Sucrose, 5% Triton X100, 50mM EDTA, pH 8.0, 50mM Tris, pH 8.0, 1 mg/ml lysozyme) and was incubated at room temperature for 15 minutes. Samples were boiled for 40 seconds and centrifuged at 16000g for 20 minutes. The pellet was removed and 110µl of 100% isopropanol added to the supernatant. The samples were centrifuged at 16000g for 20 minutes and supernatant discarded. Pellet was washed with 70% ethanol and centrifuged at 16000g for 1 minute, supernatant was removed and pellet air dried for 15 minutes. The pellet was resuspended in 40µl of 10mM Tris-HCl with 20µg/ml RNaseA and incubated at 55 °C for 10 minutes.

2.9 Extraction of plasmids from *S. cerevisiae*.

Plasmids were extracted by a method adapted from a protocol by Julia Sidorova and Linda Breeden from Hoffman and Winston, *Gene*, 1987, Vol. 57: 267-272.

Fresh colonies of yeast were resuspended in yeast lysis buffer (100mM NaCl, 10mM Tris-HCl pH8.0, 1mM EDTA, 0.1% SDS) (20µl). Acid washed glass beads (200µl) and 1:1 (v/v) Phenol:chloroform (20µl) were added to each sample in a 1.5ml Eppendorf tube. Samples were vortexed for 5 minutes and then centrifuged at 16000g

for 5 minutes. The aqueous layer was moved to a fresh tube and centrifuged at 16000g for 5 minutes. The aqueous layer (10µl) was used for TOP10 *E. coli* transformation as above.

2.10 Polymerase chain reaction (PCR)

All PCRs were prepared on ice, and performed with Expand High Fidelity PCR system unless indicated. Reactions were carried out in a TECHNE TC-3000 (Staffordshire, UK) thermal block cycler. 'Master mix 1' (50µl) contained Deoxyribonucleotide mix (25mM stock), upstream primer (300nM), downstream primer (300nM), and target DNA. 'Master mix 2' (50µl) contained, 10x buffer with MgCl₂ (10µl), and Expand enzyme (1µl). Each master mix was mixed, then 'master mix 2' was added to 'master mix 1' mixed well, and aliquoted (50µl), the volume the thermal cycler profile was calibrated for. The general cycling profile was as follows:

94°C	94°C	T _{MI} -5°C	68°C	94°C	T _M -5°C	68°C	68°C	4°C
3 minute	1 minute	1 minute	1 minute/kb +1 minute	1 minute	1 minute	1 minute/kb +1 minute	20 minutes	To store
1cycle	5 cycles			20 cycles			1cycle	1cycle

T_{MI} indicates T_M of the initial matching region only.

2.11. Purification and concentration of DNA after PCR.

DNA was purified by gel extraction for use in cloning. The Qiagen gel extraction spin kit and protocol was followed.

Ethanol precipitation was carried out to concentrate construct DNA after PCR amplification. DNA was precipitated by adding two volumes of ice cold 100% ethanol and one tenth volume of 0.3M sodium acetate. Samples were mixed well and incubated at -20°C for 1 hour. Samples were centrifuged at 16000g, 4°C for 40 minutes, supernatant was removed and pellet washed with 70% ethanol. DNA was pelleted by centrifugation at 16000g, 4°C for 20 minutes, supernatant was discarded and pellet air dried for 10-15 minutes. The pellet was resuspended in 10mM Tris-HCl, pH 8.5.

2.12. Plasmid construction and GFP tagging of proteins.

2.12.1. VPS10-GFP, CHS3-GFP and MRL1-GFP

Constructs were generated via the short-flanking homology approach (Longtine et al., 1998). One step-PCR was used to modify the chromosomal genes and introduce a green fluorescent protein tag that was expressed under the target genes own promoter. Plasmid pFa6A-GFP(S65T)-HIS3MX6 was used as a template for each of the PCR reactions. Oligonucleotides were designed that had 5' ends that corresponded to the desired target gene sequences and 3' ends that annealed to and allowed amplification of the selectable marker gene and the GFP tag. The gene specific sequences of the sense oligonucleotide were chosen to end just upstream of the stop codon to preserve the reading frame of the tag, those of the anti-sense oligonucleotide were chosen to end just downstream of the stop codon. The specific oligonucleotides and conditions are as follows:

Vps10p 5'-CTCTGCCTTATTTTCCTTGTAGTTC -3' 5'-

CCCATCACAACTGGCCAT TTAT - 3'. Vps10p-GFP genomic DNA was used as a template. The reactions were conducted by denaturing at 94°C for 3 minutes, followed by 5 cycles with denaturing at 94°C for 1 minute, annealing at 49°C for 1 minute and extension at 68°C for 10 minutes. This was followed by 20 cycles with denaturing at 94°C for 1 minute, annealing at 58°C for 1 minute, and extension at 68°C for 10 minutes, and a final extension step at 68°C for 20 minutes. A PCR product of around 8.0 Kb was produced.

Mrl1p 5'-

AACAGAAAGCGACCACCCAACCTTTGGCTGATAATAGCGTACGGATCCC
CGGGTTAATTAA -3' 5'-

GCATAAATATATCTACTGCATTGTATTTTGAACGTACAA AGTATGCAT
TGTGAATTCGA GCTCGTTTAAAC -3'

The reactions were conducted by denaturing at 94°C for 4 minutes, followed by 10 cycles with denaturing at 94°C for 1 minute, annealing at 55°C for 1 minute and extension at 72°C for 3 minutes. This was followed by 20 cycles with denaturing at 94°C for 1 minute, annealing at 65°C for 1 minute, and extension at 72°C for 3 minutes, followed by a final extension step at 72°C for 10 minutes. A PCR product of around 2.6Kb was produced.

Chs3p 5'-

ATATTCTCAATCGGAAGGAGGAAAGTGACTCCTTCGTTGCAGCGATC
CCCGGGTTAATTAA -3' 5'- CACACAACCATATATCAACTTGTAAGTATCAC
AGTAAAAATATTTTCATACTGTGAATTCGAGCTCGTTTAAAC -3'

reactions were conducted by denaturing at 94°C for 4 minutes, followed by 10 cycles with denaturing at 94°C for 1 minute, annealing at 55°C for 1 minute and extension at 72°C for 5 minutes. This was followed by 20 cycles with denaturing at 94°C for 1 minute, annealing at 65°C for 1 minute, and extension at 72°C for 5 minutes, followed by an additional extension step at 72°C for 10 minutes. A PCR product of around 2.8Kb was produced.

After PCR tagging with GFP, the fragments were gel purified using the Qiagen kit and transformed into *S. cerevisiae* as above.

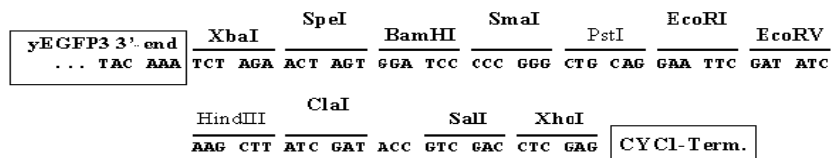
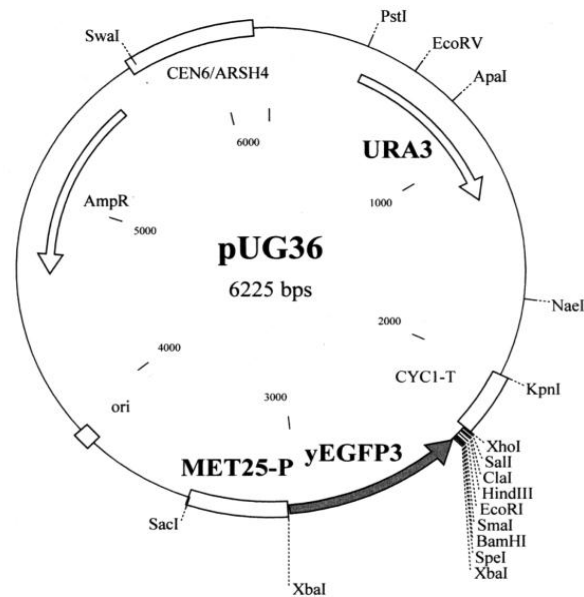
2.12.2. pUG36-*YIF1*

pUG36-*YIF1* was constructed by PCR amplification of the *YIF1* ORF from yeast genomic DNA, using sense and antisense oligonucleotides integrating *EcoRI* and *XhoI* restriction sites respectively, 5'-TTTGGGAATTCATGTCTTATAATCCGTACGCATATGC-3' and 5'-TTTTTCTCGAGTCAACCCATTAACCACATTAGACAA-3'. The reactions were conducted by denaturing at 94°C for 2 minutes, followed by 5 cycles with denaturing at 94°C for 1 minute, annealing at 50°C for 1 minute and extension at 68°C for 4 minutes. This was followed by 20 additional cycles denaturing at 94°C for 1 minute, annealing at 58°C for 1 minute and extension at 68°C for 4 minutes and a final extension step at 68°C for 20 minutes. The resulting products of around 1Kb were purified using Qiagen gel purification kit.

Plasmid pUG36-*YIF1* was created by ligation of a ~1.0 kb PCR fragment encoding the entire *YIF1* ORF, digested with *EcoRI* and *XhoI* into the *EcoRI* and *XhoI* sites of pUG36. The ligated plasmid was transformed into *E. coli*. Correct clones were identified by performing mini-preps and diagnostic restriction enzyme digests. A

mid-prep of the correct clone was performed and sent for sequencing to confirm integration.

Fig 2.1: pUG36 map



2.12.3. pUG23-*MRL1* and pUG34-*MRL1*.

pUG23-*MRL1* contained *MRL1* tagged at the C terminus with GFP. pUG34-*MRL1* contained *MRL1* N terminally tagged with GFP. Both plasmids were created in similar ways. The entire *MRL1* ORF was amplified by PCR using the following sense oligonucleotide to introduce a *Bam*H1 restriction site: Oligo A 5'-TGTTGTGGATCC

ATGTTGAAACGATCATCTCTAA-3, and an anti sense oligonucleotide to introduce a *SalI* restriction site, either incorporating the stop codon: oligo B 5'-GTGTTT GTCGACTTATACGCTATTATCAGCCAAA -3' or without stop codon, Oligo C 5'-TGTTTGTCGACTACGCTATTATCAGCCAAAGTT-3'. Oligo A and C were used for integration into pUG23 and oligos A and B for integration into pUG34. The reactions were conducted by denaturing at 94°C for 2 minutes, followed by 5 cycles with denaturing at 94°C for 1 minute, annealing at 45.7°C for 1 minute and extension at 68°C for 3 minutes. This was followed by 20 additional cycles, denaturing at 94°C for 1 minute, annealing at 58°C for 1 minute and extension at 68°C for 3 minutes and a final extension step at 68°C for 20 minutes. The resulting products were purified using Qiaex II resin.

Plasmids pUG34-*MRL1* and pUG23-*MRL1* were created by ligation of the appropriate ~1.2 kb PCR fragment, encoding the entire *MRL1* ORF with or without stop codon, digested with *Bam*HI and *Sal*I into the *Bam*HI and *Sal*I sites of pUG34 or pUG23. Plasmids were transformed into *E. coli*, mini-preps and restriction enzyme digests were performed to confirm correct integration. The plasmid was then sequenced to confirm.

2.12.4. Construction of pGEX6PK-1 VMA1, pGEX6Pk-1 VMA2, pGEX6Pk-1 VMA4 and pGEX6Pk-1 VMA5.

Plasmid pGEX6T1-*VMA1* was constructed by amplification of the whole *VMA1* ORF from BY4742 genomic DNA, using sense and antisense oligonucleotides integrating *Bam*HI and *Xho*I restriction sites respectively, 5'-TTATTGGATCCATGGCTGG TGCAATTGAAAAC -3' and 5'-CCTCGAGTTAATCGGTAGATTCAGCAAA TCTT -3'. The reactions were conducted by denaturing at 94°C for 2 minutes,

followed by 5 cycles with denaturing at 94°C for 1 minute, annealing at 48.9°C for 1 min and extension at 68°C for 4 min. This was followed by 20 additional cycles denaturing at 94°C for 1 minute, annealing at 57°C for 1 minute and extension at 68°C for 4 minutes and a final extension step at 68°C for 20 minutes. The resulting product of ~ 3.25 Kb was purified using Qiagen gel purification kit. The purified gene fragment was digested with *Bam*HI and *Xho*I and inserted into the *Bam*HI and *Xho*I sites of digested pGEX6pK1 digested. The ligated plasmid was transformed into *E. coli*. Midi-preps and restriction enzyme digests were performed to identify a correct clone. This was then further verified by sequencing.

Plasmid pGEX6T1-*VMA2* was constructed by amplification of the whole *VMA2* ORF from BY4742 genomic DNA, using sense and antisense oligonucleotides integrating *Bam*HI and *Xho*I restriction sites respectively, 5' - TGGATCCATGGTTTTGTCT GATAAGGAGTTGT -3' and 5' - TCTCGAGTTAGATTAGAGATTCTTCT TGGCTG -3'. The PCR was conducted by denaturing at 94°C for 2 minutes, followed by 5 cycles with denaturing at 94°C for 1 minute, annealing at 50°C for 1 minute and extension at 68°C for 2 minutes. This was followed by 20 additional cycles denaturing at 94°C for 1 minute, annealing at 57°C for 1 minute and extension at 68°C for 2 minutes and a final extension step at 68°C for 20 minutes. The resulting product of ~1.55 Kb was purified using Qiagen gel purification kit. The purified gene fragment was digested with *Bam*HI and *Xho*I and inserted into the *Bam*HI and *Xho*I sites of digested pGEX6T1. The ligated plasmid was transformed into *E. coli*. Midi-preps and a restriction enzyme digest were performed to identify a correct clone. This was then further verified by sequencing.

Plasmid pGEX6T1-*VMA4* was constructed by amplification of the whole *VMA4* ORF from BY4742 genomic DNA using sense and antisense oligonucleotides integrating *Bam*HI and *Xho*I restriction sites respectively, 5'- TTTTGGATCCATGTCC TCCGCTATTACTGCT -3' and 5'- TTTTCTCGAGTCAATCAAAGAACT TTCTTGTCTTGG -3'. The reactions were conducted by denaturing at 94°C for 2 minutes, followed by 5 cycles with denaturing at 94°C for 1 minute, annealing at 50°C for 1 minute and extension at 68°C for 1.5 minutes. This was followed by 20 additional cycles denaturing at 94°C for 1 minute, annealing at 58°C for 1 minute and extension at 68°C for 1.5 minutes and a final extension step at 68°C for 20 minutes. The resulting product of ~0.7 Kb was purified using Qiagen gel purification kit. The purified gene fragment was digested with *Bam*HI and *Xho*I and inserted into the *Bam*HI and *Xho*I sites of digested pGEX6T1. The ligated plasmid was transformed into *E. coli*. Midi-preps and a restriction enzyme digest were performed to identify a correct clone. This was then further verified by sequencing. Plasmid pGEX6T1-*VMA5* was constructed by amplification of the whole of the *VMA5* ORF from BY4742 genomic DNA, using sense and antisense oligonucleotides integrating *Bam*HI and *Xho*I restriction sites respectively, 5'- TTTTGGATCCATGGCTACTGCGTTATAT ACTG -3' and 5'- CTCGAGTTATAAATTGATTATATACATCACAAATGG -3'. The reactions were conducted by denaturing at 94°C for 2 minutes, followed by 5 cycles with denaturing at 94°C for 1 minute, annealing at 48°C for 1 minute and extension at 68°C for 2 minutes. This was followed by 20 additional cycles denaturing at 94°C for 1 minute, annealing at 54.5°C for 1 minute and extension at 68°C for 2 minutes and a final extension step at 68°C for 20 minutes. The resulting product of ~1.2 Kb was purified using Qiagen gel purification kit. The purified gene fragment

was digested with *Bam*HI and *Xho*I and inserted into the *Bam*HI and *Xho*I sites of digested pGEX6T1. The ligated plasmid was transformed into *E. coli*. Midi-preps and restriction enzyme digests were performed to identify a correct clone. This was then further verified by sequencing.

2.12.5 Creation of pUG36-SVP3, pUG36-SVP3^{CT1}, pUG36-SVP3^{NT1} pUG36-SVP3^{K486R} and pUG36-SVP3^{PPIY/PPCY to PAIA/PACA}.

pUG36-SVP3, pUG36-SVP3^{CT1} and pUG36-SVP3^{NT1} were previously made by Dr Stephen Dove and Gavin McNee (Birmingham Uk.) They created the plasmids as follows:

pUG36-SVP3 was made by PCR amplifying the full length SVP3 ORF (YOR322c) from wild-type genomic DNA using the Expand polymerase and the following oligonucleotides 5'-TTTCCAAGCTTATGGCATT TCACGTCTTACA-3' and 5'-TTTTTCTCGAGCTACTGGGTTATTCTATTGGA-3' which incorporated HindIII and XhoI restriction sites 5' and 3' of the ORF respectively. The resulting 2.4kB fragment was gel purified and digested with Hind III and Xho I. It was then ligated with pUG36 plasmid that had been similarly digested. The resulting ligation mixture was transformed into competent TOP10 *E.coli* and recombinant plasmids identified by digesting 5mg amounts of plasmid DNA with the same two enzymes. This yielded the plasmid pUG36-SVP3, that was analysed by DNA sequencing, to ensure that the PCR amplification had introduced no errors into the YOR322c ORF.

pUG36-SVP3^{CT1} was made by digesting the pUG36-SVP3 plasmid with the enzyme EcoRI and gel purifying the resulting fragments. The large 7.4 kB fragment, comprising the entire sequence of plasmid pUG36 ligated to a 1.1kB fragment of the SVP3 ORF, constituting the most 3' third of the gene, was then self ligated to produce

a construct that would express the C-terminal most third of Svp3p expressed as a N-terminal GFP tagged protein in *S. cerevisiae*. This ligation was transformed, analysed and sequenced according to standard procedures and designated pUG36-SVP3^{CT1}.

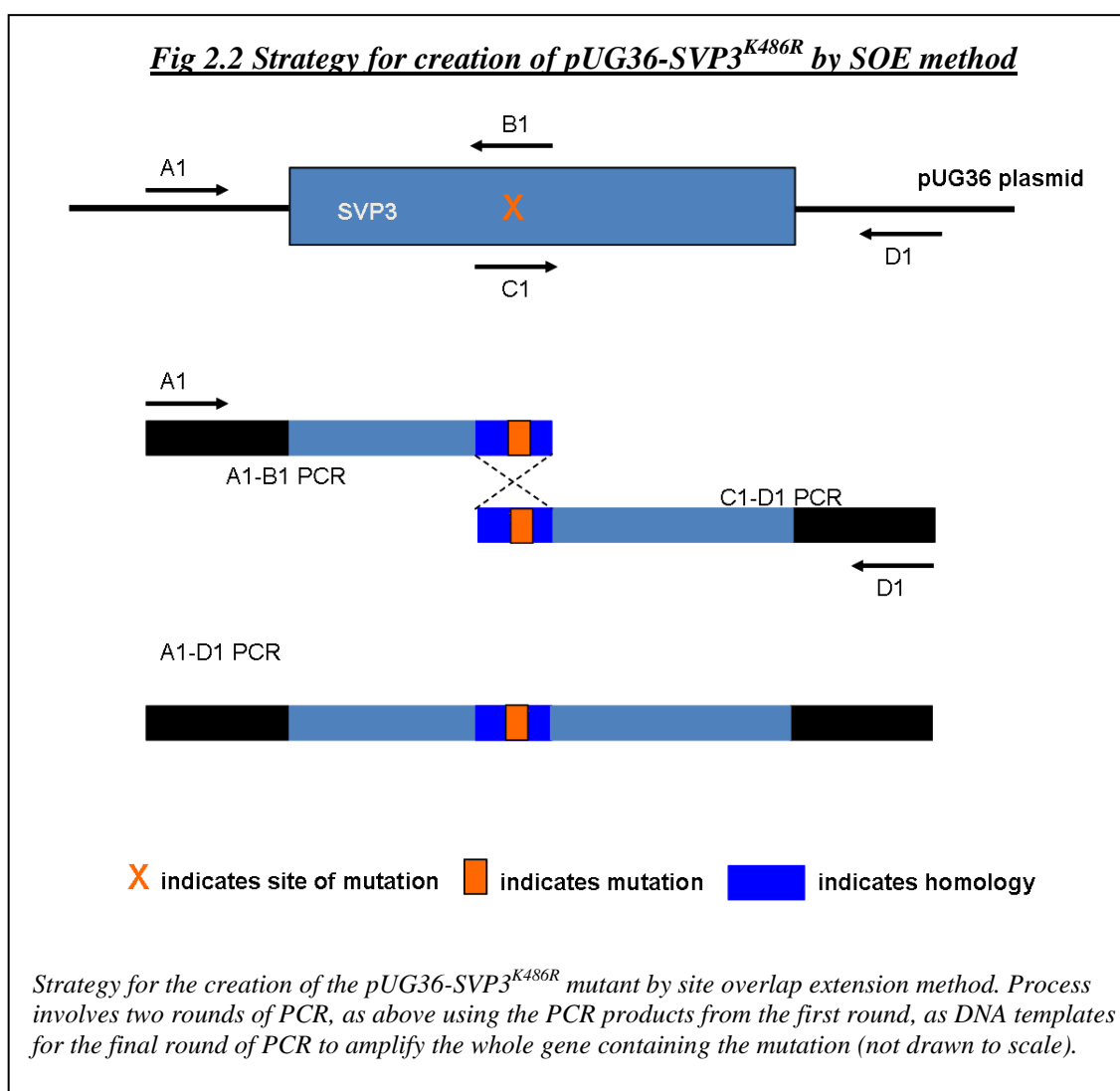
pUG36-SVP3^{NT1} was made by digesting the pUG36-SVP3 plasmid with the enzyme BamHI. the resulting 1.6 kB fragment, comprising the 5' two-thirds of the *SVP3* ORF, was gel purified, and ligated with BamHI digested pUG36 to yield a construct that would express the N-terminal two thirds of the SVP3/YOR322c ORF as an N-terminal GFP fusion when transformed into *E.coli*. This construct was recovered, identified and sequenced according to standard practise and designated pUG36-SVP3^{NT1}.

pUG36-SVP3^{K486R} and pUG36-SVP3^{PPIY/PPCY to PAIA/PACA} were created by serial overlap extension (SOE), a method adapted from *Molecular Cloning: A laboratory manual, third edition*. (Sambrook J & Russell DW., eds), Cold Spring Harbour Laboratory Press, Cold Spring Harbour, New York, USA, 2001, Volume 2: 13.36.

Four oligonucleotides were used to introduce a site-specific mutation by overlap extension (See Figure 2.2). The primers B and C were used to amplify the DNA and introduce the specific mutation site. Primers A and D bound to the pUG36 plasmid at either side of the *SVP3* ORF, allowing amplification of the whole gene.

Two sets of primers were used in two separate amplification reactions using pUG36-SVP3, to amplify over-lapping DNA fragments (Fragments AB and CD) containing the mutations required. The fragments were purified using the Qiagen gel extraction

kit, and were used as a template for a third PCR. The overlapping fragments were mixed, denatured and annealed to generate heteroduplexes, which were extended and amplified into full-length DNA using primers A and D, which bound to the extremes of the two initial fragments. The full length fragment was purified and digested through the qiagen gel extraction kit and was then digested with *XhoI* and *HindIII* and cloned back into pUG36.



The following oligonucleotides were used for the pUG36-SVP3^{PAIA/PACA} and pUG36-SVP3^{K486R} mutations:

pUG36-SOEA1- 5'-GTGTGTGTGTCTTGTACCAGACAACCATTACTTAT -3'

pUG36-SOED1- 5'-GTTTGTGTTTTGTTTGATTAAAGTTGGGTAACGCCAGG -3'

PAIA/PACA_B1-5'-TATAGAGAGCTCG**GC**ACATG**CT**GGCGAGAGCAACT
CGACATCTTGG**GA**ATGG**C**AGGAACTTCTTC-3

PAIA/PACA_C1-5' -GAAGAAGTTCCT**G**CCATT**G**CCCAAGATGTCGAGTTGC
TCTCGCCA**G**CATGT**G**CCGAGCTCTCTATA -3'

K486R_B1- 5' - GTCAAATCGGTT**C**TCCATCCACTCTT -3'

K486R_C1- 5' -AAGAGTGGATGG**A**AACCGATTTTGAC -3'

*Red indicates nucleotide base change.

The PCR reaction conditions were as follows:

SVP3^{PACA/PAIA} AB and CD PCRs - Both reactions were conducted by denaturing at 94°C for 2 minutes, followed by 5 cycles with denaturing at 94°C for 1 minute, annealing at 50.85°C for 1 minute and extension at 68°C for 3 minutes. This was followed by 20 additional cycles denaturing at 94°C for 1 minute, annealing at 59.0°C for 1 minute and extension at 68°C for 3 minutes, and a final extension step at 68°C for 20 minutes. The resulting AB product was ~1.9 Kb and the CD product ~0.9Kb.

SVP3^{PACA/PAIA} AD PCR - The reaction was conducted by denaturing at 94°C for 2 minutes, followed by 25 cycles with denaturing at 94°C for 1 minute, annealing at 54°C for 1 minutes and extension at 68°C for 5 minutes with a final extension step at 68°C for 20 minutes. The resulting product was ~2.9 Kb.

SVP3^{K486R} AB PCR - The reaction was conducted by denaturing at 94°C for 2 minutes, followed by 5 cycles with denaturing at 94°C for 1 minute, annealing at 51°C for 1 minute and extension at 68°C for 3 minutes. This was followed by 20 additional cycles, denaturing at 94°C for 1 minute, annealing at 55°C for 1 minute and extension at 68°C for 3 minutes, with a final extension step at 68°C for 20 minutes. The resulting product was ~1.6kb.

SVP3^{K486R} CD PCR - The reaction was conducted by denaturing at 94°C for 2 minutes, followed by 5 cycles with denaturing at 94°C for 1 minute, annealing at 50°C for 1 minute and extension at 68°C for 3 minutes. This was followed by 20 additional cycles denaturing at 94°C for 1 minute, annealing at 55°C for 1 minute and extension at 68°C for 3 minutes and a final extension step of 68°C for 20 minutes. The resulting product was around 1.3kb.

SVP3 K486R AD PCR - The reaction was conducted by denaturing at 94°C for 2 minutes, followed by 25 cycles with denaturing at 94°C for 1 minute, annealing at 54.0°C for 1 minute and extension at 68°C for 5 minutes, and a final extension step at 68°C for 20 minutes. The resulting product was ~2.8kb.

2.12.6 Creation of *VPS13*^{E003K}

The pRS313-*VPS13*^{E003K} plasmid was created by SOE as above. A 1.02kb fragment of DNA was excised from pRS313-*VPS13* by digesting the plasmid with restriction enzymes *Nru*I and *Age*I. Two rounds of PCR reaction were carried out. AB and CD fragments were amplified by PCR reactions using pRS313-*VPS13* as a template and the following oligonucleotides:

VPS13 E003K A1 5'-GATGGTAGAACCTTGTCTGACTACAACATCC -3'

VPS13 E003K B1 5'-GCCTAGCAATCGGTTTAGCAAATTAGCAGC
TAAAGACTTTAACATTTAACTGT TCTTAATTTTCCT -3'

VPS13 E003K C1 5'-AGGAAAATTAAGAACAGTTAAATGTTAAAGTCTTTAG
CTGCTAATTTGCTAAACCGA TTGCTAGGC -3'

VPS13 E003K D1 5'- GAGCTAGCTGTTGGTGTGGGTGAGTCTT -3'

AB and CD PCRs - The reaction was conducted by denaturing at 94°C for 2 minutes, followed by 25 cycles with denaturing at 94°C for 1 minute, annealing at 59°C for 1 minute and extension at 68°C for 2 minutes, and a final extension step at 68°C for 20 minutes. The resulting AB product was ~750bp and CD product was ~1.3Kb.

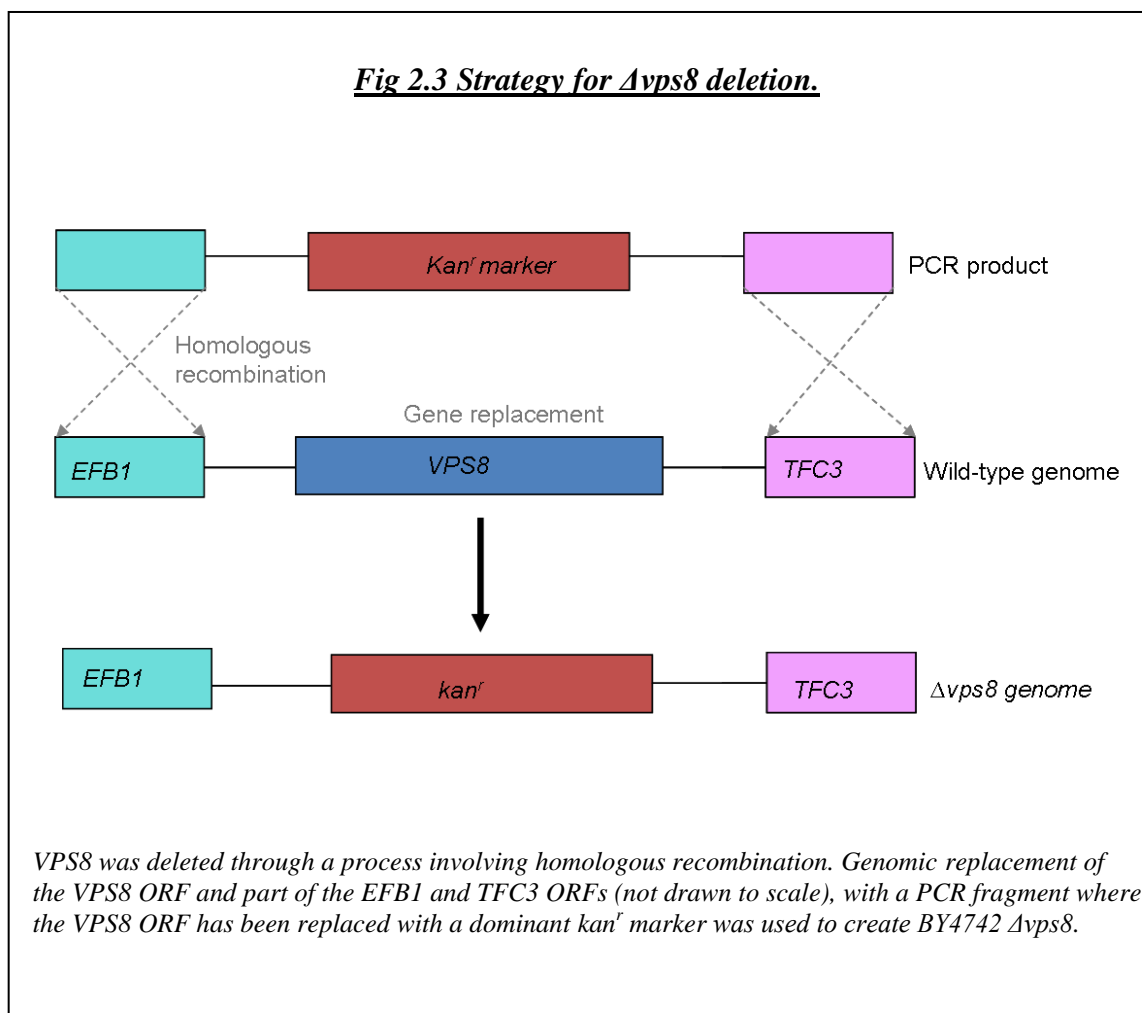
The gel purified products from the above PCRs were used as templates to amplify the whole AD fragment, which incorporated sequence upstream and downstream of the *AgeI* and *NruI* restriction enzyme sites.

AD PCR - The reaction was conducted by denaturing at 94°C for 2 minutes, followed by 25 cycles with denaturing at 94°C for 1 minute, annealing at 59°C for 1 minute and extension at 68°C for 3 minutes, and a final extension step at 68°C for 20 minutes. The resulting product was ~2.0kb.

The AD PCR product was gel purified and digested with *AgeI* and *NruI* restriction enzymes overnight. This produced a 1.02kb fragment which was gel purified and ligated into the digested pRS313-*VPS13* plasmid. A correct plasmid was confirmed by transformation into *E. coli*, mini preps, diagnostic restriction enzyme digests and sequencing.

2.13. Transfer of deletions

2.13.1 BY4742 $\Delta vps8::kanMX4$



Genomic DNA was prepared from BY4739 $vps8::kanMX4$ cells as above. This was used as a template to amplify the complete *VPS8* ORF and N- and C-terminal regions of the ORFs from flanking genes. PCR amplification using the sense and antisense oligonucleotides 5'-CTACCGATATTGCTGCTATGC-3' and 5'-TGATGGCTATTGGGTCAATCATA-3', resulted in the generation of a PCR fragment (~2.8 kb). The reactions were conducted by denaturing at 94°C for 3 minutes, followed by 25 cycles

with denaturing at 94°C for 1 minute, annealing at 49.8°C for 1 minute and extension at 68°C for 4 minutes. This was followed by an additional extension step at 68°C for 20 minutes. The resulting products were purified using Qiagen spin gel extraction kit.

The ~2.8 kb PCR fragment containing the putative *VPS8* ORF replaced by the dominant *kan^r* marker was transformed into BY4742 wild-type cells. Kanamycin-resistant colonies were selected by growth on G418-containing agar plates and these colonies were re-streaked on G418-containing agar plates to further select the *kan^r* marker. Replacement of the *VPS8* ORF with the *kan^r* marker was confirmed through colony PCR using the kanamycin-resistant colonies and resulted in the generation of a fragment ~3.0 kb in size if correct.

2.13.2 $\Delta atg21::LEU2$

Deletion was transferred using the method above. Genomic DNA was prepared from a BY4742 $\Delta atg18::KAN \Delta atg21::LEU2 \Delta hsv2::HIS3$ strain and the following sense and anti-sense oligonucleotides used. 5'-TCGGAACAGTCACAT TCACAC-3' and 5'-GAAGCCT TGGTATAGGAGATG -3'

2.13.3 $\Delta fab1::LEU2$

Mutation was deleted as above using *fab1::LEU2* genomic DNA and the following sense and anti-sense oligonucleotides, 5'-ATGCACCTGAAATAGCACCAACAGG TACGC-3' 5'-GGGTCGATTATTGAGTTGCTGATTACCTCC-3'

2.13.4 $\Delta vps26::LEU2$

Mutation was deleted as above using genomic DNA from MSY2629, and the following sense and anti-sense oligonucleotides, 5'-AGGAAGAGCCAGAATCA GATA-3', 5'-ATCTACCGATTCTACCGAAC-3'

2.13.5 $\Delta vac14::kanMX4$

Deletion was transferred using the method above. Genomic DNA was prepared from BY4742 $\Delta vac14::kanMX4$ and the following sense and anti-sense oligonucleotides used, 5'-ACCGACTTATCTCGATGAGCT-3' 5'-GCCATTAATACGCAGATCC GT-3'

2.13.6 $\Delta vps13::kanMX4$

Mutation was deleted as above using genomic DNA from BY4742 $\Delta vps13::kanMX4$ and the following sense and anti-sense oligonucleotides, 5'-GCCATACCCTTCTTC GTCACC-3' 5'-CACCTTGTCTTGAGGTTGAGGG-3'

2.13.7 $\Delta pep4::HIS3$

Mutation was deleted as above using BJ3505 genomic DNA and the following sense and anti-sense oligonucleotides, 5'-CGGTAAGTTTATCGCAATCAC-3' 5'-ACGA TGAAGTTGATCGTACAG -3'

2.13.8 $\Delta pep12::kanMX4$

Mutation was deleted as above using genomic DNA from BY4742 $\Delta pep12::kanMX4$ and the following sense and anti-sense oligonucleotides, 5'-TTCCCTTTCTCACAC AGTGGC-3' 5'-GCCTACGTGTTATTCGGGAAC-3'

2.13.9 $\Delta vps4::kanMX4$

Mutation was deleted as above using genomic DNA from BY4742 $\Delta vps4::kanMX4$ and the following sense and anti-sense oligonucleotides, 5'-AATCTCCGACTGA GGATTCGG -3' 5'- GGTGGCGAAACCGAAATTGTC -3'

2.13.10 $\Delta sec22::HIS3$

Mutation was deleted as above using genomic DNA from SUA1-3D and the following sense and anti-sense oligonucleotides, 5'-GCTCAATTAGAGGACGA CTCTAAC -3' 5'- GGTGGAATCGAGGACACTAAC -3'.

2.14. Creation of BY4742 $\Delta chs6::LYS2$

Genomic DNA was prepared from BY4742 cells as above and used as a template to amplify the complete *CHS6* ORF, and N- and C-terminal regions of the flanking ORFs. The following sense and antisense oligonucleotides were used, 5'- GCGGCTA CAAATAGTCAATTCC -3' and 5'- AGCTAATGGAGACTGTGAACC -3', and resulted in the generation of a PCR fragment ~3.2Kb. The reactions were conducted by denaturing at 94°C for 3 minutes, followed by 25 cycles with denaturing at 94°C

for 1 minute, annealing at 50°C for 1 minute and extension at 68°C for 4 minutes. This was followed by an additional extension step at 68°C for 20 minutes. The resulting products were purified using Qiagen spin gel extraction kit. *LYS2* was PCR amplified using *fabI-1(ts)* genomic DNA as a template and the following oligonucleotides 5'- TTTTCTCTAGAACGCCAGCTGATTACAGTTC-3' and 5'- TTTTATCGATAG CAGTTGCTTTCTCCTATGG-3'. This resulted in the generation of a PCR fragment (~6.0kb) which introduced the restriction sites *XbaI* and *ClaI*. The PCR reactions was conducted by denaturing at 94°C for 3 minutes, followed by 5 cycles with denaturing at 94°C for 1 minute, annealing at 50°C for 1 minute and extension at 68°C for 7 minutes, followed by 20 cycles with denaturing at 94°C for 1 minute, annealing at 55°C for 1 minute and extension at 68°C for 7 minutes. This was followed by an additional extension step at 68°C for 20 minutes. TA cloning was used to ligate the *CHS6* and *LYS2* fragments into p-Gem-T-Easy plasmid using T4 DNA ligase, and incubation overnight at 4°C. The plasmids were transformed into Top10 *E. coli* and blue/white colonies used to select correct clones. Minipreps were digested with *XbaI* and *ClaI* in a double digest reaction overnight to release the *LYS2* fragment.

The middle section of *CHS6* (~1.3kb) was excised and the resulting p-Gem-T-Easy plasmid with *CHS6* flanking genes either side, purified through gel extraction. The sticky ended *LYS2* was also purified, through gel extraction. The resulting purified fragments were then ligated with T4 DNA ligase at 15°C for 5 hours, and transformed into *E.coli*. Mini preps were used to identify correct plasmids through size, and PCR. Sequencing was used to confirm integration.

The resulting plasmid was then used as a template for PCR to amplify the *chs6::LYS2* construct using the original *CHS6* oligonucleotides. This was then transformed into a range of BY4742 strains to create $\Delta chs6::LYS$ through homologous recombination.

Colonies exhibiting lysine prototrophy were selected by growth on SC-LYS agar plates, and were re-streaked on SC-LYS agar plates to further select the *LYS2* marker. Replacement of the *CHS6* ORF with the *LYS2* marker was confirmed through PCR amplification of *CHS6* using genomic DNA prepared from the Lysine producing colonies and the generation of a fragment ~6.0 kb in size compared to the wild-type of ~3.0 kb.

2.15. DNA Sequencing

DNA sequencing was performed by a service run at the functional Genomics and Proteomics unit at the University of Birmingham (Birmingham, UK). A reaction mix (10µl) was prepared for each template to be sequenced, as follows: template (100 ~ 500ng), primer (3.2pmol), and ddH₂O added to total volume. The Genomics facility then added a Terminator Reaction Mix to each primer/DNA mix supplied, to give a final volume of 20µl. The reaction mixes were amplified via PCR and the resulting chain-termination reaction resolved using an ABI sequencing device that separated the dye labelled fragments by capillary electrophoresis. The sequencing data was then analyzed in Chromas (version 1.45). Sequences were compared to wild-type *S. cerevisiae* sequences available by performing a BLAST search on the *Sachromyces* genome database website.

2.16. Visualisation of GFP and RFP tagged proteins.

Yeast strains were grown to a density of 2×10^6 - 1×10^7 cells/ml in SC-Ura-Met + 2.0% glu medium (the promoter in pUG36 is methionine-regulated) at 25°C with

shaking. Cells were centrifuged at 200g and resuspended in non-fluorescent media (5mg/ml (NH₄)₂SO₄, 2% glucose, pH 5.7) and visualised on a Nikon Eclipse E600 Microscope as live wet mounts, sometimes attached to poly-L-lysine coated cover slips. The projector used was a Nikon Plan Apo (100×/1.40 oil DIC H). A XF100-3 filter cube (Omega Optical) was used to visualise GFP. Strains expressing DsRed,mCherry-tagged proteins or FM4-64 were visualised with an XF1074-XF2016-XF309-NQ960 filter cube (Omega Optical). Strains stained with Fluorescent Brightener 28 (Calcofluor) were visualised with a DAPI filter cube (Omega Optical). Images were acquired with an ORCA digital camera (Hamamatsu, Japan) and coloured in Simple PCI (C*Imaging Systems). All images were cropped and contrast/brightness adjusted as a whole unit in Photoshop 6.0.

2.17. Co-localisation of RFP and GFP tagged proteins.

Images of cells expressing both GFP and RFP tagged proteins were captured, false coloured and viewed as both separate and merged images. The total numbers of dots for GFP were counted, and then the number of RFP dots that co-localised to the same position also counted. The total numbers of RFP dots were also counted and then the total number of GFP dots the co-localised to the same position counted. This resulted in the generation of two percentages for GFP and RFP co-localisations. A number of random co-localisations were also conducted, this was performed by marking the same number of random dots on a DIC picture and then seeing if these co localised with the RFP or GFP dots, in order to calculate random co-localisation. Cells without obvious expression of **both** GFP and RFP were not included in the analysis. Some attempt was also made to remove from the analysis any dots that co-localised when

the shape of the RFP and GFP labelled compartments were obviously very different. At least one hundred cells were counted for each compartment.

2.18. FM4-64 staining of vacuoles.

Adapted from a method developed by Vida and Emr (Vida and Emr, 1995). 100µg FM4-64 was made up in DMSO (10.3µl) to a concentration of 16mM and stored at -80 °C.

Yeast strains were subcultured to 1×10^5 cells/ml in YPD + 2.0% glu medium and were grown at 25°C to around 1×10^7 cells/ml. 10 ml of the cell culture was collected by centrifugation at 200g at 25°C for 5 minutes, resuspended in ddH₂O (200µl) and transferred to a 1.5ml Eppendorf tube, and centrifuged as above. Cells were resuspended in YPD + 2.0% glucose (200µl), and FM4-64 (0.5µl) added to a final concentration of 40µM. Cells were then incubated at 25°C, 200 rpm for 15 minutes. Cells were collected as described previously and washed twice with YPD + 2.0% glu (400 µl). Cells were resuspended in 400µl of YPD + 2.0% glucose and chased for 1 hour at 25°C 200 rpm, before being visualised.

2.19 Hyper osmotic stress.

After treatment with FM4-64, cells were subjected to a hyperosmotic stress. Microscope buffer containing 0.4M NaCl was used to resuspend cells prior to microscopy. Cells were incubated for 10 minutes in the solution prior to taking pictures.

2.20 WGA-FITC staining of bud scars

Staining of bud scars was performed by a method adapted from (Chen et al., 2003).

Yeast strains were subcultured at 1×10^5 cells/ml in YPD + 2.0% glu and were grown at 25°C to around 1×10^7 cells/ml. Cell number was counted using a haemocytometer, and density adjusted to give 1×10^7 cells/ml in a Eppendorf tube. Cells were centrifuged for 3 minutes at 200g and media removed. The pellet was resuspended in PBS (Phosphate buffered saline) (1ml), and 6µl of 2mg/ml WGA-FITC added to give a final concentration of 12µg/ml. Cells were stained in the dark for 1.5 hours at room temperature. Cells were washed twice with PBS, with centrifugation at 200g for 3 minutes.

2.21 Calcofluor staining of bud scars

Adapted from *Methods in Yeast Genetics* (Adam, A., Goccschling, D. E., Kaiser, C. A., and Sterns, T., eds), Cold Springs Harbour Laboratory Manual [1997].

1mg/ml stock of Fluorescent Brightener 28 (Calcofluor) was prepared with ddH₂O and stored in the dark at -20°C. Yeast strains were subcultured to 1×10^5 cells/ml in YPD+2.0% glu and were grown at 25°C to around 1×10^7 cells/ml. 1ml of the cell culture was centrifuged at 200g for 2 minutes, media removed and pellet resuspended in YPD without glucose, and incubated for three hours at 25°C. To stain, calcofluor stock solution was added, to a final concentration of 100µg/ml. Cultures were incubated at room temperature for 10 minutes, and washed twice with ddH₂O, with centrifugation at 200g.

2.22 Calcofluor resistance spot dilutions

Yeast strains were subcultured to 1×10^5 cells/ml in appropriate SC+2.0% glu medium, and were grown at 25°C to around 1×10^7 cells/ml. Cell densities were counted using an improved Neubauer haemocytometer and adjusted to 1×10^7 cells/ml, 5µl samples of 5 fold or 10 fold spot dilutions were pipetted onto YTD+200ng/ml Fluorescent Brightener 28 + 2.0% glu and a control of YTD +2.0% glucose (unless indicated otherwise). Plates were grown at 25°C for at least two days.

2.23 Calcofluor resistance replica plating.

EMS mutagenised cells were diluted to give 200 colonies per plate and were spread onto YTD + 2% glu plates. Colonies were allowed to grow at 25°C for three days and then replica plated using velvet onto another YTD + 2% glu plate and a YTD + 2% glu + 600 µg/ml Fluorescent Brightener 28 + 20µg/ml Phloxine B plate. The two plates were allowed to grow at 25°C for 2 days. Colonies that appeared to not be growing on the YTD + 2% glucose + 600 µg/ml Fluorescent Brightener 28 + 20µg/ml Phloxine B plate but were growing on the YTD + 2% glucose plate were picked out and restreaked onto an additional YTD + 2% glucose plate. This plate was immediately replica plated onto a YTD + 2% glucose + 500 µg/ml calcofluor white + 20µg/ml Phloxine B plate to confirm the original result.

2.24 EMS mutagenesis.

BY4742 $\Delta chs6$ was subcultured to 1×10^5 cells/ml in YEPD +200µg/ml G418 +2.0% glu medium and was grown at 25°C to around 1×10^8 cells/ml. The cell density was

determined using an improved Neubauer haemocytometer and adjusted to 1×10^8 cells/ml. The cells were collected by centrifugation for 5 minutes at 3000g, the pellet was then washed twice with 0.1M sodium phosphate buffer NaH_2PO_4 pH 7.0 (5ml). Cells were centrifuged as above and resuspended in 0.1M sodium phosphate buffer (1.7ml). In a fume hood EMS (ethyl methanesulfonate) (50 μ l) was added, cells were incubated with shaking at 30°C for 40 minutes. After this time around 40% of cells were killed. An excess of sterile 5% sodium thiosulfate was added to stop the mutagenesis reaction. The cells were spun down at 1000g for 5 minutes and resuspended in ddH₂O (9ml). The cell suspension was then diluted to give around 200 colonies, and plated onto YTD with incubation at 25°C for three days. To find out kill rate, a control reaction without EMS addition was carried out, cells from both samples were plated and colony production compared.

2.25 Flow cytometry data collection and FACS sorts.

This work was carried out in collaboration with Dr Tim Overton (Chemical engineering, University of Birmingham, Birmingham UK). Data was collected on a BD FACS Aria Cell-sorter. For each data set at least 10000 events were sampled. For calcofluor staining the UV laser (351 to 364 nm) was used. For WGA-FITC the Hoescht laser (248 nm) was used. Sort boundary gates were defined by comparing single mutant and double mutant data, as indicated in the relevant results chapter.

2.26 Expression of GST-Vma1p, GST-Vma2p, GST-Vma4p and GST-Vma5p

pGEX6T1-VMA1, pGEX6T1-VMA2, pGEX6T1-VMA4 and pGEX6T1-VMA5 were transformed into BL21 competent *E. coli* cells. To purify GST-Vma1p, GST-Vma2p, GST-Vma4p and GST-Vma5p, the BL21 strains were diluted to an A_{600} of 0.1-0.2 in LB+100 μgml^{-1} ampicillin+ 50 μgml^{-1} chloramphenicol (1.0L), grown to an A_{600} of 0.6-0.8 (~2.5 hours) and induced with IPTG at a final concentration of 1mM (4-5 hours). After incubation at 30°C for 5 hours the cells were collected (centrifugation at 10000g for 15 min at 4°C) and 'washed' in 40 ml ice-cold breakage buffer (40ml) (100 mM HEPES KOH pH7.5, 150mM NaCl, 1mM PMSF). Cells were resuspended in ice cold breakage buffer containing bacterial protease inhibitor cocktail and 4 mgml^{-1} lysozyme (40ml). All subsequent procedures were carried out at 4°C. The *E. coli* cells were lysed by incubation on ice for 1 hour. This was followed by the addition of 10% (v:v) Triton X-100 (4.5ml), and incubation with gentle swirling for 30 minutes. Protease inhibitors were then added and incubated as above. The Glutathione-Sepharose 4B resin was prepared by resuspending 1ml of a 75% slurry in breakage buffer + protease inhibitors+ 1% Triton X-100 (10ml). This was end-to-end mixed for 30 min and the resin was washed twice in the same buffer with centrifugation at 500g for 5minutes. The cell debris was pelleted at 10000g for 20 minutes and then further centrifuged to pellet the triton insoluble debris at 25000rpm for 20 minutes. The supernatant was filtered through a 0.45 μM filter. The filtrate was added to the 1ml of pre-swollen and washed Glutathione-Sepharose beads in a 50ml tube and were end-to-end mixed for 1 hour at 4°C. Beads were pelleted at 500g for 5 minutes at 4°C. The beads were washed twice with ice-cold breakage buffer +0.1% Triton X-100+ protease inhibitors (50ml). The beads were then washed twice with ice cold breakage buffer + protease inhibitors (50ml) and centrifuging to collect the

beads. The beads were resuspended in ice cold washing buffer (5ml)(100mM Hepes KOH pH7.5, 300 mM NaCl, bacterial protease inhibitors) and transferred to a 10 ml Econo-Pac column and the beads allowed to settle. The column was washed with again with washing buffer. GST-tagged proteins were eluted in ice cold elution buffer (3ml)(50mM Tris pH8.5, 150mM NaCl, 1mM PMSF) containing 20mM Glutathione (flow rate 0.5 ml/min). 0.5 ml fractions were collected and protein concentration was quantified using Bradford's reagent and the manufacture's protocol (modified from Bradford [1976]). Fractions containing protein were stored at -20°C.

Chapter 3

Fab1p and Retromer

3.1 Introduction.

The 1980s saw the isolation of the generic machinery that eukaryotic cells use to sort cargo in the endocytic system (Banta et al., 1988). Genetic screens using chemical mutagenesis of *S. cerevisiae*, identified mutant cells that aberrantly secreted the vacuolar hydrolase carboxypeptidase Y (CPY) (Robinson et al., 1988). The subsequent identification and characterisation of these vacuolar (*VPS*) genes is one of the cornerstones upon which our current understanding of endosomal trafficking is built (Robinson et al., 1988, Banta et al., 1988).

These studies showed that soluble protein cargoes such as CPY are normally directed to the correct compartment via interaction with membrane bound “cargo receptors”.

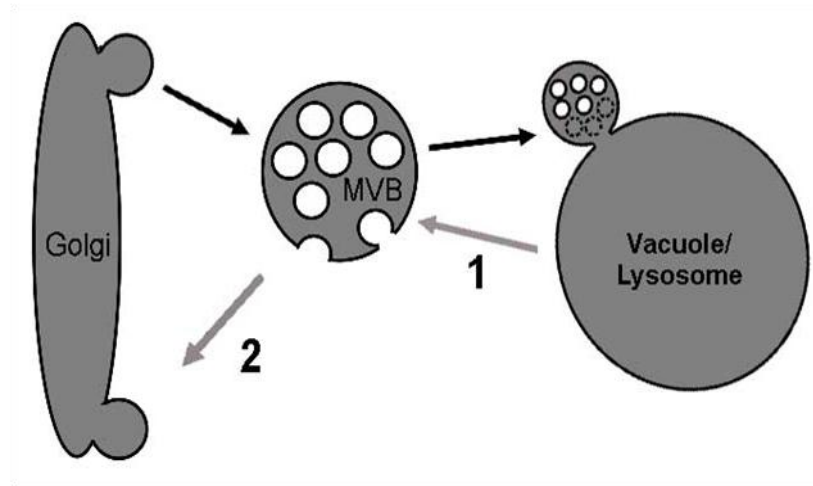
The receptor for CPY was identified as Vps10p, a 177 kD type I protein that has homologs in animal cells known as Sortillins (Cooper and Stevens, 1996, Rutherford et al., 2006) or analogs known as mannose-6-phosphate receptors. CPY was the first identified cargo of this pathway, and has been the focus of research in the area.

However, it is now known that receptors for other vacuolar hydrolases including proteinase A (PrA) Pep4p and amino-peptidase Y (Marcusson et al., 1994, Cooper and Stevens, 1996) also cycle in the same fashion.

Correct trafficking of Vps10p is essential for sorting of CPY to the vacuole. Cells that lack Vps10p secrete around 90% of newly synthesised CPY (Cooper and Stevens,

1996, Marcusson et al., 1994, Jorgensen et al., 1999). Vps10p has been identified as a receptor for CPY (Marcusson et al., 1994). *VPS10* encodes a large 177kDa type I trans-membrane protein. Research has shown that during anterograde (forward) trafficking, CPY bound Vps10p exits the Trans Golgi network (TGN) in clathrin coated vesicles and fuses with the pre-vacuolar endosome (PVE) (Cooper and Stevens, 1996, Rutherford et al., 2006). Once at the PVE, Vps10p and CPY dissociate, probably due to the low pH of the endocytic compartment. This leaves Vps10p free to be recycled back to the TGN, a process which involves a novel protein coat (comprising a complex of proteins) known as retromer (Seaman et al., 1998). The recycling or retrograde step in this process is very important because failure to retrieve Vps10p from the PVE leads to degradation of the cargo receptor, when the PVE matures and fuses with the lysosome like vacuole (Cooper and Stevens, 1996). This results in the secretion of CPY to the cell surface, because nascent Vps10p cannot be generated quickly enough. CPY is secreted because this is the default pathway for the trafficking of soluble proteins in yeast (Cooper and Stevens, 1996). The cytosolic domain of Vps10p is known to be required for trafficking (Cooper and Stevens, 1996, Cereghino et al., 1995), it contains two aromatic based signals YSSL and FYVF (Bowers and Stevens, 2005). Ligand and cargo binding takes place in the luminal portion of Vps10p in a specific region named domain 2 (Jorgensen et al., 1999). Over expression of Vth2p, a glycoprotein with similarity to Vps10p, can partially suppress secretion of CPY in a $\Delta vps10$ mutant (Cooper and Stevens, 1996).

Figure 3.1; *PtdIns(3,5)P₂* dependent membrane trafficking.

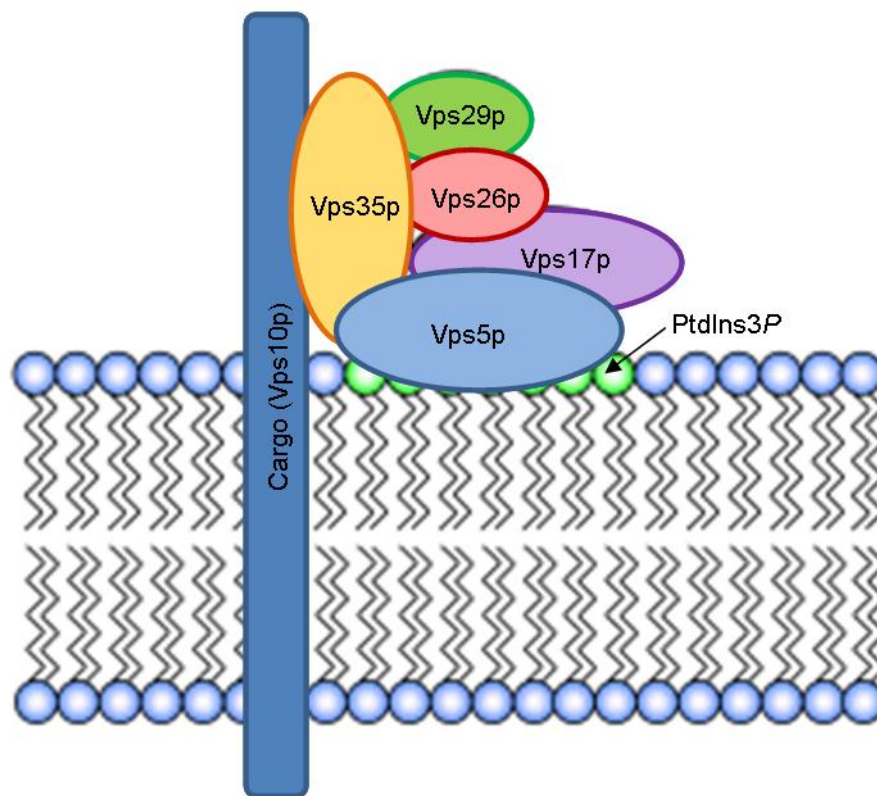


PtdIns(3,5)P₂ is required for at least 3 different trafficking steps; in yeast, it regulates vacuole to late endosome/MVB trafficking (Bryant et al 1997; pathway 1) and also the sorting of some proteins into the internal vesicles of the MVB (Odorizzi et al 1998). In mammalian cells, *PtdIns(3,5)P₂* may also mediate the retromer pathway (pathway 2); i.e. late and/or early endosome to Golgi trafficking (Rutherford et al 2007).

The retromer complex is conserved between *S. cerevisiae* and mammalian cells. The yeast complex is composed of five proteins, Vps35p, Vps29p, Vps26p, Vps17p and Vps5p. The proteins are able to form a protein coat, which tubulates *PtdIns3P* containing membranes when added to them *in vitro* (Seaman, 2005). Vps17p and Vps5p are sorting nexins, which the cargo selective complex comprising Vps26p, Vps29p and Vps35p associate onto (Seaman, 2005). Mammalian versions of this complex have been identified and their structures characterised (Hierro et al., 2007, Bonifacino and Hurley, 2008). SNX1 and SNX2 seem to be the mammalian equivalents of Vps5p and Vps17p respectively, although some doubt surrounds Vps17p, and SNX5 and SNX6 may in fact be its functional equivalents (Wassmer et

al., 2007). A model where retromer couples membrane deformation with cargo sorting has been suggested (Cullen, 2008).

Figure 3.2 Diagram of the yeast retromer coat complex



Individual proteins form a complex on the phospholipid bi-layer to act as a coat to recycle the transmembrane protein Vps10p (Adapted from an image on the Cullen lab website)

Recycling of cargo receptors like Vps10p in yeast and the mannose-6-phosphate receptor (M6R) in mammalian cells is dependent on at least one lipid. PtdIns3P is a phosphoinositide required for the function of the retromer complex (Cozier et al., 2002). PtdIns3P is known to be required for recycling because two essential

components of the retromer complex are members of the sorting nexin family of proteins (Seaman, 2005, Horazdovsky et al., 1997). It has also recently been shown that these sorting nexins can bind to $\text{PtdIns}(3,5)P_2$ (Catimel et al., 2008). Sorting nexins appear to be involved in both retromer dependent and independent retrieval of cargo receptors from endosomes to the TGN (Hettema et al., 2003). All sorting nexins contain a $\text{PtdIns}3P$ binding motif known as a PX domain that is required for their association with the endosomal membrane (Cozier et al., 2002, Carlton et al., 2004). Hence $\text{PtdIns}3P$ is required for the correct localisation of sorting nexins and formation and function of the retromer coat complex. $\text{PtdIns}3P$ has also previously been shown to be required for Vps10p recycling due to Vps15p; a protein kinase that recruits Vps34p to a membrane complex to sort proteins in both the Golgi to endosome and endosome to Golgi transport pathways (Burda et al., 2002, Stack et al., 1995).

$\text{PtdIns}(3,5)P_2$ has recently been implicated in the retrieval of cargo receptors from endosomes in some systems. It was demonstrated that PIKfyve (the mammalian homolog of Fab1p; the $\text{PtdIns}3P5$ -kinase) has a role in regulation of endosome to trans-Golgi network retrograde transport, since the M6R is mislocalised when PIKfyve is silenced via siRNA (Rutherford et al., 2006). The disruption of $\text{PtdIns}(3,5)P_2$ synthesis by use of a kinase dead PIKfyve also resulted in mis-sorting of the M6R in mice (Ikononov et al., 2003, Murray et al., 2005, Zhang et al., 2007). This has led to speculation that one of the primary defects in cells unable to synthesise $\text{PtdIns}(3,5)P_2$ is a failure of retrograde endosome to TGN trafficking (Rutherford et al., 2006). The evidence is somewhat conflicting as studies in other systems including *C.elegans* and *D. melanogaster* have not reported this effect (Nicot et al., 2006, Rusten et al., 2006). Also the use of YM201636, the recently discovered small molecule inhibitor of PIKfyve that inhibits $\text{PtdIns}(3,5)P_2$ synthesis, also failed to

show mis-sorting of M6R raising the possibility that this defect is an indirect phenotype of cells that lack PtdIns(3,5) P_2 (Jefferies et al., 2008).

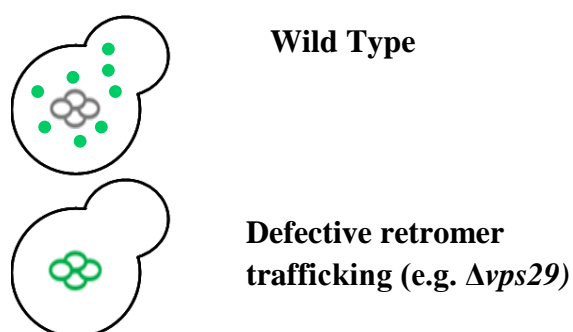
Due to conflicting data this chapter seeks to examine the role Fab1p and PtdIns(3,5) P_2 in the endosome to TGN recycling of several cargos in *S. cerevisiae*, as this is the system in which Fab1p, PtdIns(3,5) P_2 and retromer are best characterised and offers a convenient model system.

3.2 Generation of an assay to assess retromer function.

Vps10p has previously been used as a marker for the integrity of the endosome to TGN retrieval pathway known as retromer (Seaman et al., 1997). However in previous studies aberrant Vps10p trafficking was assayed using antibodies and SDS-PAGE analysis to detect vacuole protease mediated cleavage of Vps10p.

It was decided that a Vps10-GFP probe may offer a more convenient marker, allowing a fluorescence microscopy assay to be performed. A strain was constructed bearing a *VPS10* gene fused to GFP at its C terminus so expression was from the *VPS10* native promoter at the normal chromosomal locus. In wild-type cells where retromer is functioning, the Vps10-GFP should appear as small dot like punctuate structures throughout the cell, which represent the pre-vacuolar endosomes. In retromer inactivated cells e.g. $\Delta vps29$, the Vps10-GFP localisation would change dramatically and become directed to the vacuole membrane, as Vps10p can no-longer be recycled back to the Golgi complex via the retromer coat.

Figure 3.3 Cartoon of Vps10-GFP assay.



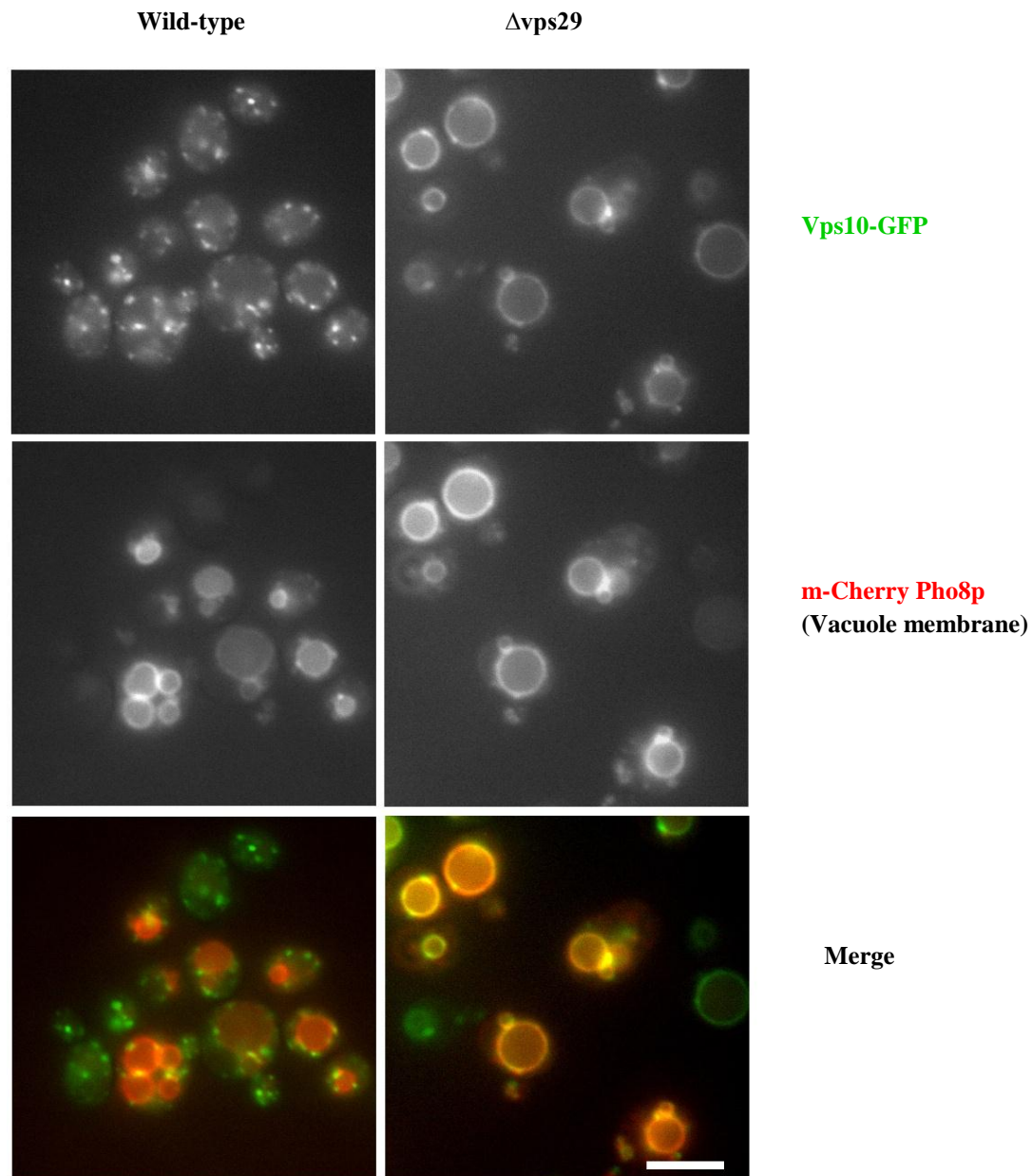
In Wild-type cells the Vps10-GFP tagged construct appears as punctae throughout the cell. Whereas in a cell where retromer trafficking is no longer functioning, Vps10-GFP cannot recycle back to repeat the process and is visualised on the vacuole membrane, where it builds up and is eventually degraded.

3.3 Sub-cellular localisation of Vps10-GFP

To confirm that Vps10p recycling is truly retromer dependent, a $\Delta vps29$ mutant expressing both a vacuole marker (mCherry-Pho8p) and Vps10-GFP was constructed. Cells that possess a retromer defect cannot recycle Vps10p back to the Golgi and hence the GFP signal should appear on the vacuole. Indeed, Vps10-GFP co-localises with the RFP marker for the vacuole as shown in Figure 3.4 when *VPS29*, a component of retromer is deleted. As expected in wild-type cells Vps10-GFP can be visualised as punctae throughout the cell.

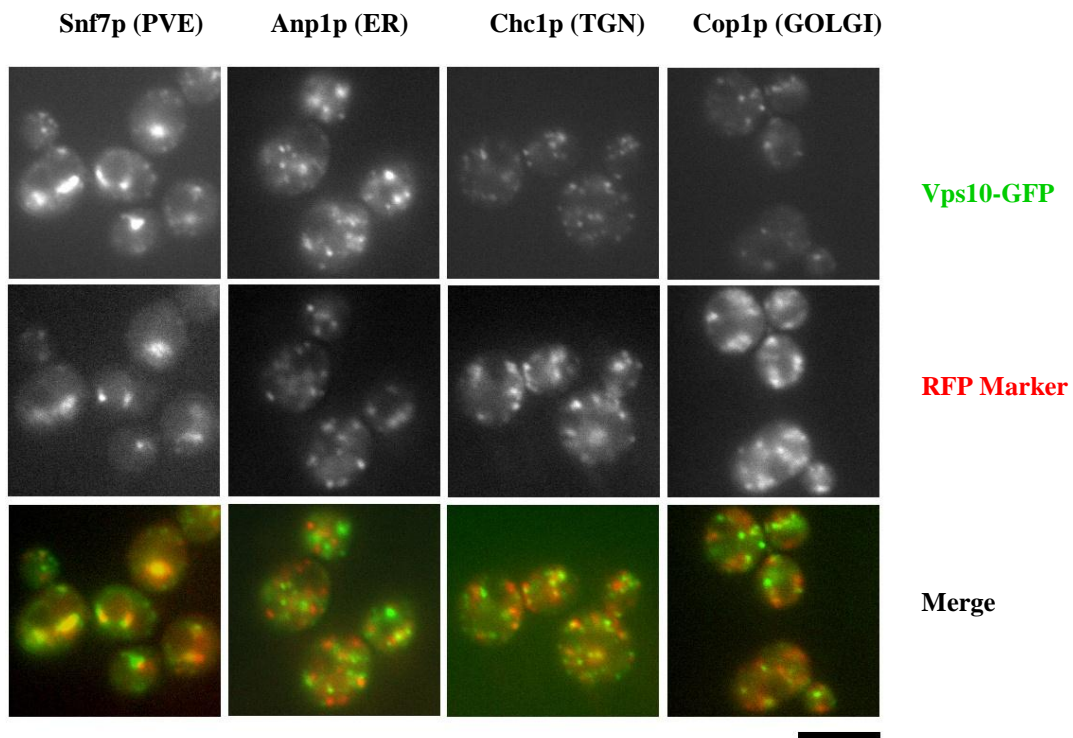
Since re-distribution to the vacuole is not the only potential defect that could be induced in Vps10p trafficking, it was decided to closely define the nature of the punctate compartment that is the wild-type steady-state localisation of Vps10p. To identify the compartments Vps10p localised to in Wild-type cells, Vps10-GFP was co-expressed with a series of RFP tagged proteins that are known residents of various compartments in yeast and act as good markers for those organelles (Huh et al., 2003). Figure 3.5 shows the results of these co-localisations.

Figure 3.4 Localisation of Vps10-GFP in a wild-type and retromer deficient strain.



Vps10-GFP is a reliable marker for retromer function. mCherry-Pho8p is used as a marker for the vacuole. Shown above are fluorescence images of logarithmic phase cultures ($5 \times 10^6 - 1 \times 10^7$ cells/ml) of wild-type (left -hand columns) and $\Delta vps29$ (right hand columns) cells transformed with VPS10-GFP (top panels) and mCherry-Pho8p (middle panels). The bottom panel shows a merge of both red and green images for co-localisation study. Both strains were cultured in SC-His-Ura+2% glu medium and grown at 25°C. These images are representative of three replicate cultures. Scale bar represents 5μM.

Figure 3.5 Co-localisations of Vps10-GFP with RFP-markers in wild-type cells.



63.5% ±3.1***	8.5% ±4.8	8.3% ±1.4	12.5% ±3.2	GFP co-localisation
6.7% ±2.9	8.3% ±3.2	4.5% ±1.7	8.1% ±2.3	Random GFP co-localisation
56.8% ±5.6	0.2% ±6.8	3.8% ±3.2	4.4% ±2.1	Adjusted GFP co-localisation
72.7% ±7.2***	11.7% ±3.9	11.5% ±0.8	13.6% ±2.9	RFP co-localisation
4.5% ±1.6	6.1% ±3.0	4.0% ±2.0	11.0% ±0.7	Random RFP co-localisation
68.2% ±12.9	5.6% ±4.4	7.5% ±3.2	2.6% ±3.3	Adjusted RFP co-localisation

[Significantly different from random co-localiation: *** $P < 0.001$, N/S not indicated]

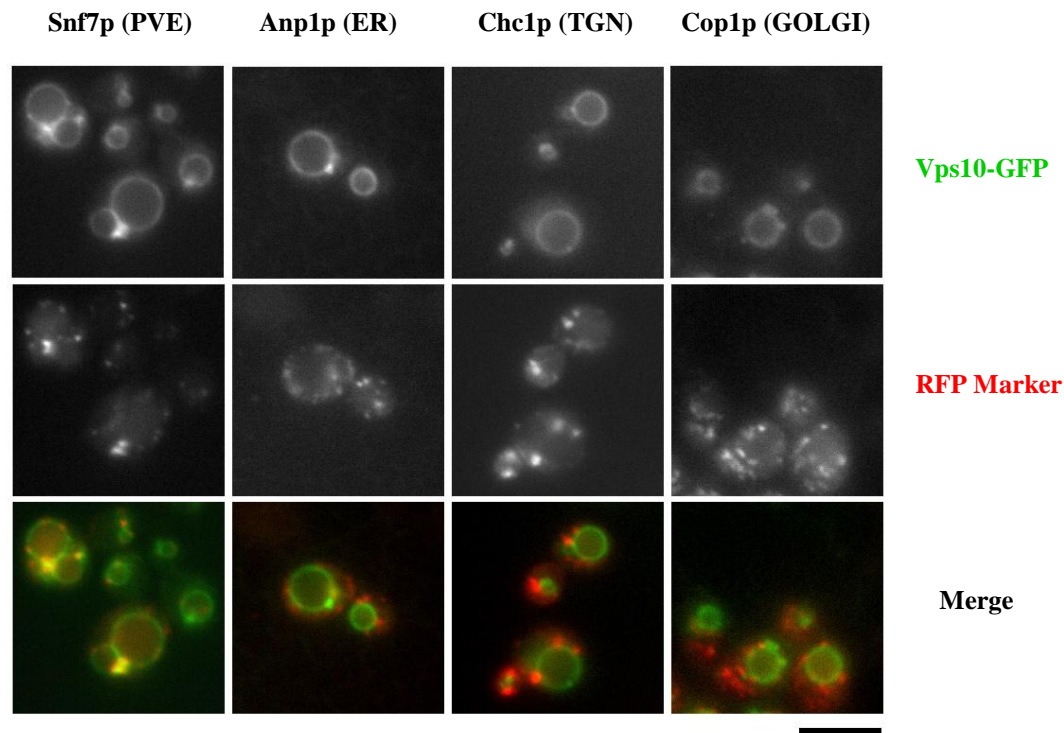
In wild-type cells Vps10-GFP co-localises with Snf7p, a marker for the endocytic compartment. Shown above are fluorescence images of logarithmic phase cultures ($5 \times 10^6 - 1 \times 10^7$ cells/ml) of BY4741 wild-type cells containing various RFP tagged proteins acting as markers (middle panels) transformed with VPS10-GFP (top panels). The bottom panel shows a merge of both red and green images for co-localisation. Strains were cultured in SC-His+2% glu medium and grown at 25°C. Images are representative of three replicate cultures and scale bar represents 5µM.

The data shows that Vps10-GFP significantly co-localises with the Snf7-RFP positive compartment which is the pre-vacuolar endosome (PVE), but not with Anp1-RFP, Chc1-RFP or Cop1-RFP that mark the ER, TGN and Golgi respectively. Careful

quantification of merged images shows that most Vps10-GFP co-localises with the Snf7p-RFP marker in around 60% of spots, suggesting a late endosomal steady-state localisation for Vps10p. The other compartments showed co-localisation of less than 5% when adjusted for random co-localisation events. Note that this result suggests that Vps10-GFP spends much (40%) of its lifetime in a compartment that is not defined or labelled by any of the RFP-markers that we have available.

The experiments were replicated for a retromer deficient strain bearing a deletion of *VPS26*, another component of retromer. In contrast almost all of the Vps10-GFP is vacuolar not punctate, with only a minor pool still present in the Snf7-RFP positive compartment, although this is probably due to the compartment size as the random co-localisation result suggests. A small amount of co-localisation, similar to that of wild-type is seen with the other RFP markers (Figure 3.6). The only significant colocalisation seen is with the Anp1 positive compartment which marks the ER. This data demonstrates that Vps10-GFP is a reliable marker for endosome to TGN recycling and is not substantially mis-localised as a result of the GFP-tag. It also demonstrates that Vps10p is unable to recycle when a different component of retromer is deleted.

Figure 3.6 Co-localisation of Vps10-GFP with RFP markers in a retromer mutant strain.



12.6 % \pm 7.4	13.6% \pm 9.2	10.3% \pm 1.9	12.8% \pm 7.8	GFP co-localisation
20.1% \pm 11.8	4.9% \pm 1.6	6.8% \pm 6.0	6.0% \pm 6.2	Random GFP co-localisation
-7.5% \pm 5.6	8.7% \pm10.8*	3.5% \pm 2.2	6.8% \pm 3.4	Adjusted GFP co-localisation
14.1% \pm 8.3	6.4% \pm 3.0	3.8% \pm 0.5	5.0% \pm 3.4	RFP co-localisation
16.8% \pm 9.7	12.5% \pm 4.6	10.3% \pm 5.4	9.8% \pm 4.7	Random RFP co-localisation
-2.7% \pm 1.6	-6.1% \pm5.3*	-6.5% \pm 5.5	-4.8% \pm 2.6	Adjusted RFP co-localisation

[Significantly different from random co-localiation: $0.01 < *P < 0.05$, N/S not indicated]

In retromer deficient cells Vps10-GFP is seen as a ring on the vacuole membrane. Shown above are fluorescence images of logarithmic phase cultures ($5 \times 10^6 - 1 \times 10^7$ cells/ml) of $\Delta vps26$ cells containing various RFP tagged proteins acting as markers (middle panels) transformed with VPS10-GFP (top panels). The bottom panel shows a merge of both red and green images for co-localisation. Strains were cultured in SC-His+2% glu medium and grown at 25°C. These images are representative of three replicate cultures. Scale bar represents 5 μ M.

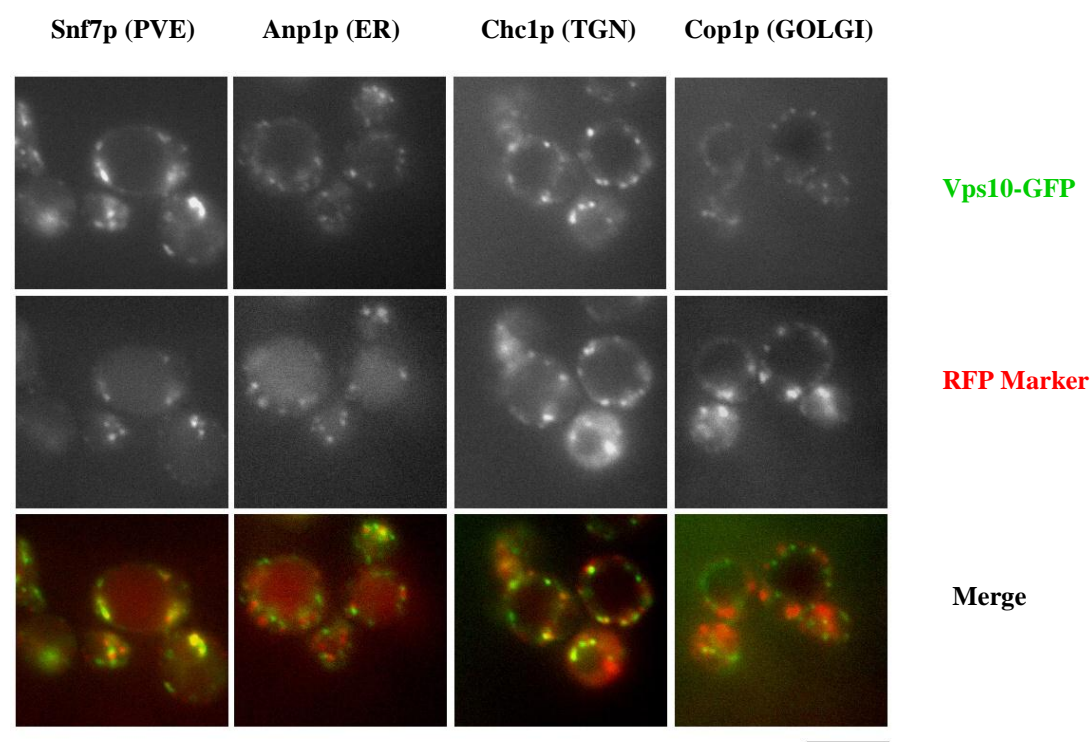
3.4 PtdIns (3,5) P_2 is not involved in retromer mediated recycling

This work set the basis to investigate whether PtdIns(3,5) P_2 is required for endosome to TGN recycling. The *FAB1* gene encodes the sole known PtdIns3P 5-kinase in yeast and once deleted results in complete loss of PtdIns(3,5) P_2 synthesis (Gary et al., 1998, Cooke et al., 1998). This makes $\Delta fab1$ cells a good background in which to study PtdIns(3,5) P_2 function. Cells with a deleted *FAB1* gene were examined for Vps10-GFP mis-localisation. Figure 3.7 shows that despite the characteristic huge swelling of the vacuole seen in $\Delta fab1$ cells, Vps10-GFP recycling appears to be unaffected as significant co-localisation is observed between Snf7-RFP and Vps10-GFP, in dot like structures. There is no observation of vacuolar Vps10-GFP in the $\Delta fab1$ strain, indicating that endosome to TGN recycling is indistinguishable from wild-type in the absence of Fab1p and PtdIns(3,5) P_2 and therefore Vps10p recycling via retromer is unaffected in a $\Delta fab1$ strain (see Figure 3.7)

In order to ensure that Vps10-GFP trafficking was not aberrant in some fashion in $\Delta fab1$ cells, the distribution of Vps10-GFP against the other membrane markers was also determined. The data show that, whilst there is a slightly greater co-localisation of Vps10p with Cop1-RFP and Chc1-RFP than wild-type cells this is not significant. The percentage of Vps10-GFP that displays this co-localisation is relatively minor especially when it is considered that the cytoplasm makes up a much smaller percentage of a $\Delta fab1$ cell due to its enlarged vacuole. This result again further suggests that localisation of Vps10p is not different in the absence of Fab1p and implies that retromer function is completely independent of PtdIns(3,5) P_2 in yeast.

To confirm that Snf7-RFP is a functional marker a strain which contained Fur4-GFP and Snf7-RFP was constructed. Localisation was not affected and this confirmed that Snf7 was functional (data not shown).

Figure 3.7 Co-localisation of Vps10-GFP and RFP markers in a $\Delta fab1$ strain.



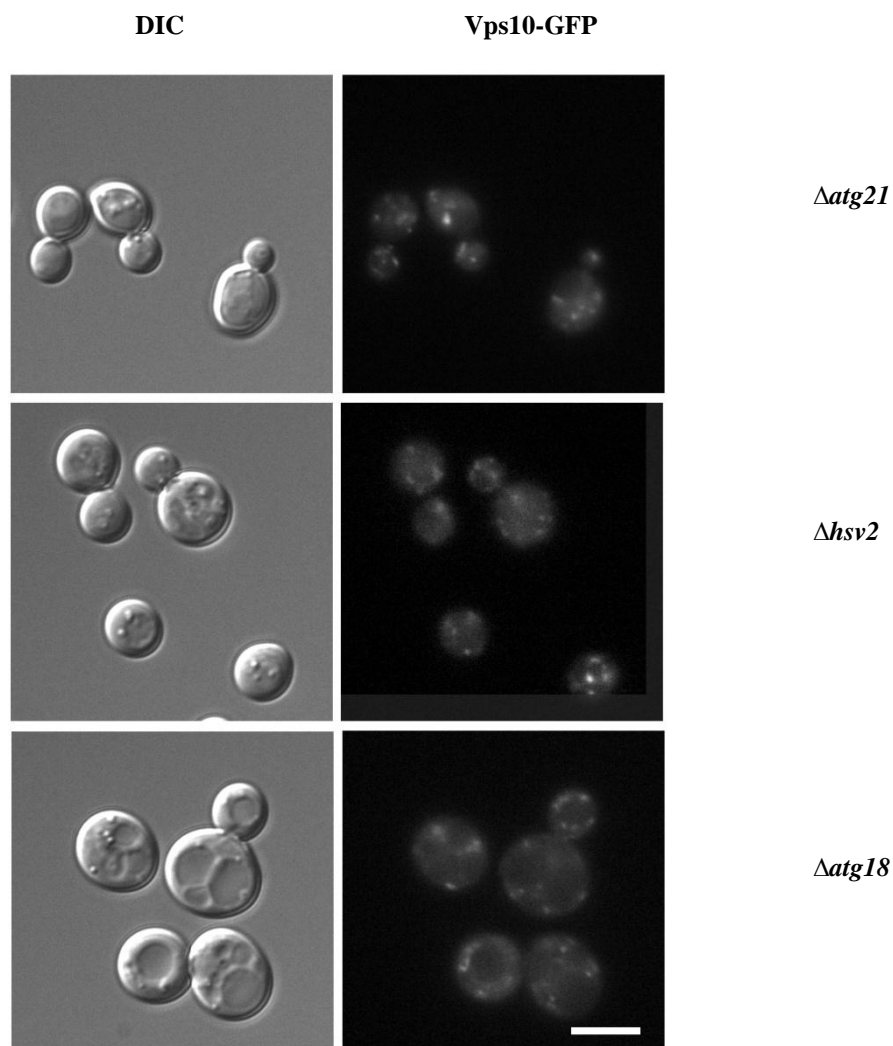
72.6% \pm 2.8	7.7% \pm 1.4	14.1% \pm 5.4	18.3% \pm 3.7	GFP co-localisation
5.9% \pm 1.7	7.8% \pm 2.5	7.4% \pm 2.5	9.5% \pm 2.1	Random GFP co-localisation
66.7% \pm11.0***	-0.1% \pm 1.8	6.7% \pm 4.0	8.8% \pm 5.3	Adjusted GFP co-localisation
81.2% \pm 7.4	9.0% \pm 3.0	13.2% \pm 4.5	22.7% \pm 3.3	RFP co-localisation
5.3% \pm 0.4	7.8% \pm 2.1	16.3% \pm 3.4	12.4% \pm 6.5	Random RFP co-localisation
75.9% \pm16.0***	-1.2% \pm 0.9	-3.1% \pm 2.0	10.3% \pm 2.4	Adjusted RFP co-localisation

[Significantly different from random co-localisation: *** $P < 0.001$, N/S not indicated]

Vps10-GFP appears to co localise with Snf7p-RFP; a marker for the endosome. Shown above are fluorescence images of logarithmic phase cultures ($5 \times 10^6 - 1 \times 10^7$ cells/ml) of $\Delta fab1$ cells containing various RFP tagged proteins acting as markers (middle panels) transformed with VPS10-GFP (top panels) The bottom panel shows a merge of both red and green images for co-localisation. Strains were cultured in SC-His+2% glu medium and grown at 25°C. These images are representative of three replicate cultures. Scale bar represents 5 μ M.

To check whether the recycling Vps10p is dependent on downstream effectors of PtdIns(3,5)P₂ or whether an indirect role may exist, Vps10-GFP localisation was investigated in strains bearing a deletion of proteins that are proposed effectors of PtdIns(3,5)P₂; $\Delta atg18$, $\Delta atg21$ and $\Delta hsv2$

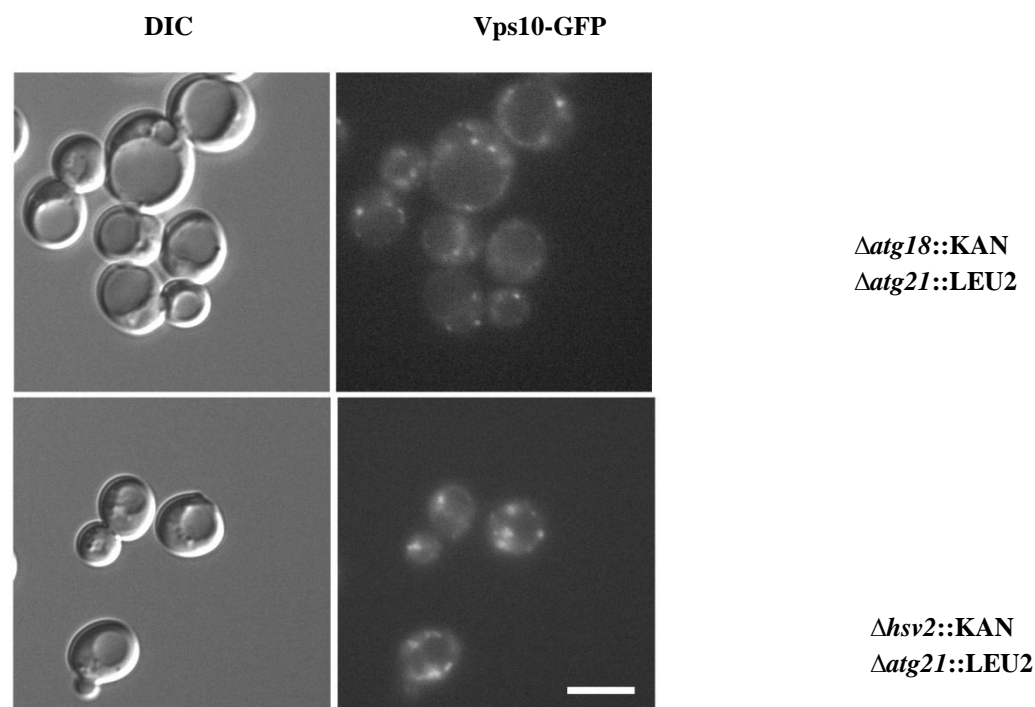
Figure 3.8 VPS10-GFP localisation in effectors of PtdIns(3,5)P₂.



In all deletion strains of potential PtdIns(3,5)P₂ effectors, VPS10-GFP appears as punctae throughout the cell. Shown above are fluorescence images of logarithmic phase cultures ($5 \times 10^6 - 1 \times 10^7$ cells/ml) of $\Delta atg21$ (top panel), $\Delta hsv2$ (middle panel) and $\Delta atg18$ (bottom panel) transformed with Vps10-GFP. All strains were cultured in SC-His+2% glu medium and grown at 25°C. The left-hand columns show low light DIC images. The right-hand columns show the GFP localisation of Vps10-GFP visualised as punctae. These images are representative of three replicate cultures. Scale bar represents 5 μ M.

The results obtained in Figure 3.8 suggest that trafficking of Vps10-GFP is still correct and unaffected, when any of the genes that encode potential PtdIns(3,5) P_2 effectors are deleted. The Vps10-GFP is not seen on the vacuole membrane, as in a strain with a true retromer defect. A subtle observation is that there are fewer Vps10-GFP punctae present in the $\Delta atg21$ and $\Delta hsv2$ strains. This may be due to the close homology between the proteins, allowing compensation for loss of function when one is deleted. Vps10-GFP trafficking may be dependent upon both genes. Deletion of just one protein may allow enough recycling of Vps10-GFP to take place, to still visualise it as punctae. It may be that to interrupt Vps10p recycling both components need to be deleted. To investigate whether this was the case double mutants containing either $\Delta atg21\Delta hsv2$ or $\Delta atg18\Delta atg21$ were made, results are shown in Figure 3.9.

Figure 3.9 VPS10-GFP localisation in double mutants of PtdIns(3,5) P_2 effectors.



VPS10-GFP is visualised as punctae throughout the cell in double mutants of PtdIns(3,5) P_2 effectors. Shown above are fluorescence images of logarithmic phase cultures ($5 \times 10^6 - 1 \times 10^7$ cells/ml) of $\Delta atg18::KAN \Delta atg21::LEU2$ (top panel) and $\Delta hsv2::KAN \Delta atg21::LEU2$ (bottom panel) transformed with VPS10-GFP. Both strains were cultured in SC-His-Leu+2% glu medium and grown at 25°C. The left-hand columns shows low light DIC images. The right-hand columns show the GFP localisation of VPS10-GFP. These images are representative of three replicate cultures. Scale bar represents 5 μM .

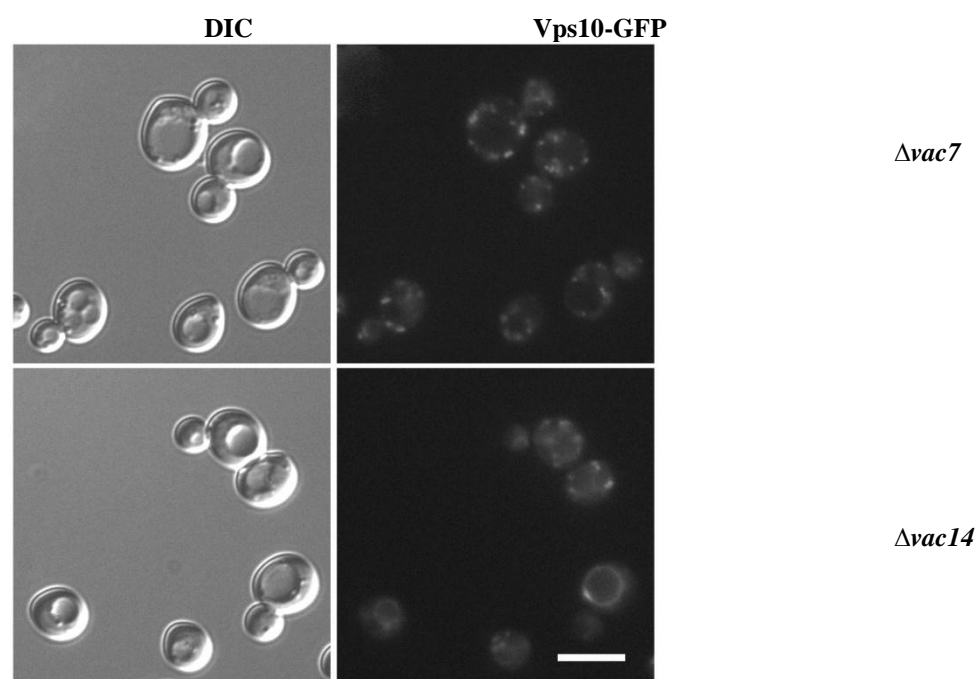
From the data in Figure 3.9 it seems that retromer is still able to recycle Vps10-GFP, even in strains lacking two potential effectors of PtdIns(3,5) P_2 . Vps10-GFP can still be seen as punctae inside the cell and not visualised as a ring on the vacuole. Neither Atg18p, Atg21p nor Hsv2p seem to play a role in Vps10p recycling.

There is a possibility that it is not Fab1p that plays a role in Vps10p recycling but one of its activators, therefore what happens in strains bearing a deletion of two proteins which are necessary to make PtdIns(3,5) P_2 , was investigated. During production of PtdIns(3,5) P_2 Vac14p acts as a scaffold on which Fab1p and other accessory proteins form a complex in order to activate Fab1p. Vac7p is also involved in production of yeast PtdIns(3,5) P_2 but no mammalian homolog has been found to date. $\Delta vac14$ and $\Delta vac7$ strains both have reduced levels of PtdIns(3,5) P_2 however unlike $\Delta fab1$, they do possess some of the lipid.

The results obtained for activators of Fab1p (Figure 3.10) seem to suggest that Vac7p plays no role in Vps10-GFP recycling. There is still punctae present throughout the cell as observed in the wild-type strain, indicating that Vps10-GFP is correctly being recycled via retromer. The large vacuole of $\Delta vac7$, similar to that visualised in $\Delta fab1$ strain makes the punctae closer together and appear slightly on the vacuole, but the dots are present in the neck and daughter cell indicating that retromer is still functioning. The $\Delta vac14$ strain provides more interest; in the majority of the cells Vps10-GFP punctae is seen throughout. However, in approximately 40% of cells Vps10-GFP is aberrantly localised to form a clear circle on the vacuolar membrane. In these cells it can clearly be seen that Vps10-GFP is not being trafficked correctly, the ring is continuous and not composed of punctae fused together. In a population of cells there is always some diversity visualised from cell to cell but this phenotype was

not observed in any of the other strains examined. This indicates that mis-trafficking of Vps10-GFP in $\Delta vac14$ is likely to be a true phenotype and not an artefact.

Figure 3.10 Localisation of VPS10-GFP in activators of *Fab1p*; *Vac7p* and *Vac14p*.



	<i>Percentage of cells with punctae VPS10-GFP</i>	<i>Percentage of cells with vacuole VPS10-GFP</i>
$\Delta vac14$	$61.5\% \pm 3.3^{***}$	$38.5\% \pm 3.2^{***}$
$\Delta vps29$	$0\% \pm 0^{***}$	$100\% \pm 0^{***}$
<i>Wild-type</i>	$100\% \pm 0$	$0\% \pm 0$

[Significantly different from wild type values: $***P < 0.001$,] Vps10-GFP is visualised as punctae in both activators of *Fab1p*. In the $\Delta vac14$ mutant, VPS10-GFP can additionally be seen on the vacuole membrane. Shown above are fluorescence images of logarithmic phase cultures ($5 \times 10^6 - 1 \times 10^7$ cells/ml) of $\Delta vac7$ (top panel) and $\Delta vac14$ (bottom panel) transformed with Vps10-GFP. Both strains were cultured in SC-His +2% glu medium and grown at 25°C. The left-hand columns show low light DIC images. The right-hand columns show the GFP localisation of Vps10-GFP visualised as punctae. These images are representative of three replicate cultures. Scale bar represents 5μM.

By calculating the percentage of cells that show Vps10-GFP as a ring on the vacuole it emerges that 38% of $\Delta vac14$ cells are unable to recycle Vps10-GFP in a retromer

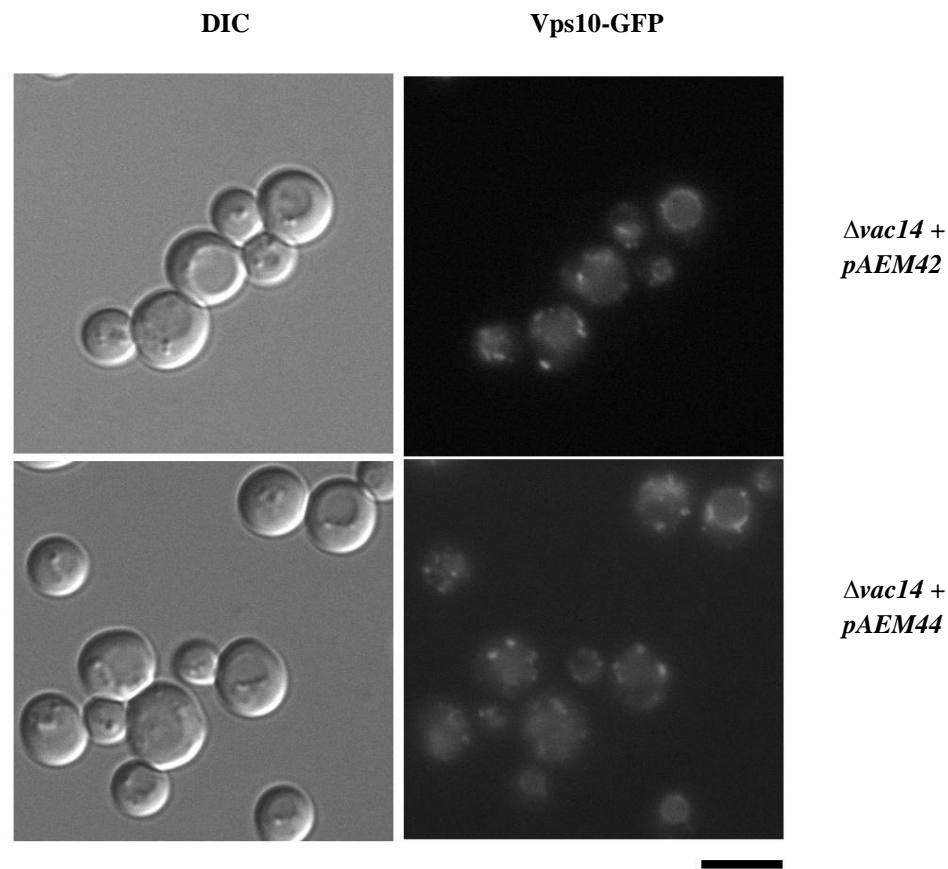
dependent manner. The phenotype is not as striking as that seen in a cell possessing a deletion of *VPS29*, where 100% of cells have defective recycling of Vps10-GFP.

Therefore Vac14p is not absolutely essential for retromer dependent recycling.

To further study the role of Vac14p in retromer dependent Vps10p recycling, rescue of $\Delta vac14$ with two plasmids was carried out. pAEM42 is a URA based plasmid with C terminal expressed Vac14p. pAEM44 possess N terminal expressed Vac14p.

As seen in Figure 3.11 addition of either pAEM42 or pAEM44 plasmids expressing Vac14p should rescue the $\Delta vac14$ *Vps10-GFP* strain, and allow correct recycling of Vps10p via the retromer complex. In both strains some Vps10-GFP does still appear on the vacuole, and values are not significantly different when compared to $\Delta vac14VPS10-GFP$ cells. Upon further investigation it appears that both *VAC14* constructs do not offer a full rescue of the $\Delta vac14$ strain in many other situations. This is potentially because the *VAC14* gene on these plasmids may lack essential regulatory elements upstream or downstream of this gene.

Figure 3.11 Localisation of VPS10-GFP in $\Delta vac14$ strains with a plasmid rescue of VAC14.



	<i>Punctae</i>	<i>Vacuole</i>
<i>$\Delta vac14 + pAEM42$</i>	$72.2\% \pm 3.5$	$27.7\% \pm 2.1$
<i>$\Delta vac14 + pAEM44$</i>	$63.7\% \pm 6.1$	$36.2\% \pm 4.27$

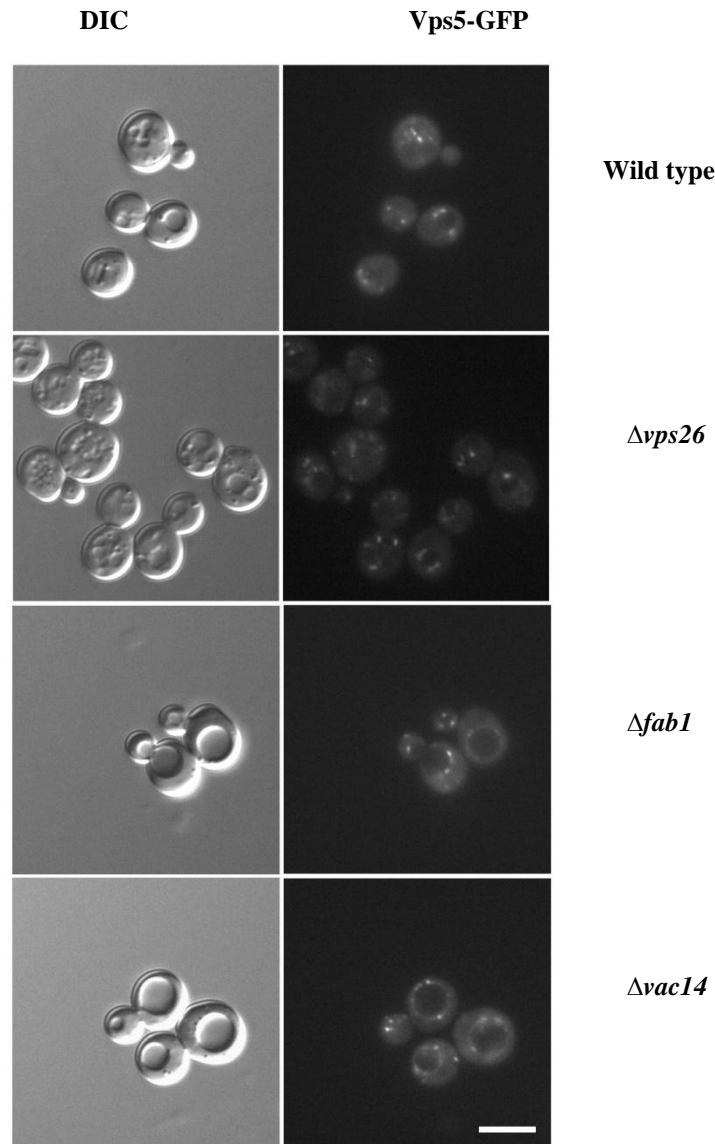
[There was no significant difference between the above and $\Delta vac14$ VPS10-GFP values]

Vps10-GFP is visualised as both punctae and on the vacuole membrane in both strains. Shown above are fluorescence images of logarithmic phase cultures ($5 \times 10^6 - 1 \times 10^7$ cells/ml) of $\Delta vac14$ transformed with VPS10-GFP and either pAEM42 (top panel) and $\Delta vac14 + pAEM44$ (bottom panel). Both strains were cultured in SC-His-Ura +2% glu medium and grown at 25°C. The left-hand columns show low light DIC images. The right-hand columns show the GFP localisation of Vps10-GFP. These images are representative of three replicate cultures. Scale bar represents 5 μ m.

To further investigate the phenotype observed in the $\Delta vac14$ strain the localisation of other components of retromer was investigated. A Vps5-GFP construct, a kind gift from Prof Emr, was used to see whether any other retromer components were

mislocalised in a $\Delta vac14$ strain. Vps5-GFP was constructed by endogenously tagging *VPS5* with GFP and expression was under the native promoter

Figure 3.12 Vps5-GFP localisation.

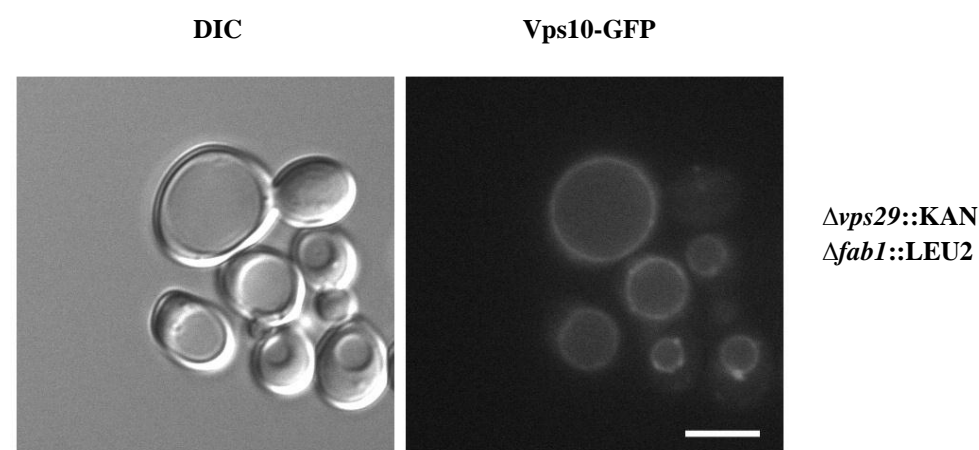


*Vps5-GFP can be visualised as punctae throughout all strains. Additionally it can be observed on the vacuole membrane in cells deficient in *PtdIns(3,5)P₂*. Shown above are fluorescence images of logarithmic phase cultures ($5 \times 10^6 - 1 \times 10^7$ cells/ml) of wild-type (top panel), $\Delta vps26$ (second panel) $\Delta fab1$ (third panel) and $\Delta vac14$ (bottom panel) cells with integrated chromosomally tagged *Vps5-GFP*. The left-hand column shows low light DIC images. The right-hand column shows the GFP localisation of *Vps5-GFP*. These images are representative of three replicate cultures. All strains were cultured in SC-His+2% glu medium and grown at 25°C. Scale bar represents 5μM.*

As shown in Figure 3.12, in a retromer deficient strain Vps5-GFP can be seen on the vacuole membrane and as punctae. In wild-type cells, Vps5-GFP is visualised as punctae throughout the cytoplasm. However in both $\Delta fab1$ and $\Delta vac14$ strains, Vps5-GFP can be seen as a ring on the vacuole. A reason for this may be due to an increased amount of PtdIns3P on the vacuole membrane in the absence of PtdIns(3,5)P₂, forcing Vps5p to bind inappropriately.

As a further control to the Vps10-GFP work, a double retromer mutant was constructed that contained a deletion of a retromer component *VPS29* and also *FAB1*. Therefore the strain produced no PtdIns(3,5)P₂ and retromer should be unable to recycle. Figure 3.13 shows that no changes in the localisation of Vps10-GFP are seen, therefore it seems that Fab1p on its own does not play a role in the retrograde trafficking of Vps10p in *S.cerevisiae*.

Figure 3.13 Vps10-GFP double mutant localisation



Vps10-GFP can be visualised on the vacuole membrane in a retromer and PtdIns(3,5)P₂ deficient strain. Shown above are fluorescence images of logarithmic phase cultures ($5 \times 10^6 - 1 \times 10^7$ cells/ml) of $\Delta vps29::KAN \Delta fab1::LEU2$ transformed with Vps10-GFP. The left-hand column shows low light DIC images. The right column shows the GFP localisation of Vps10-GFP on the vacuole membrane. These images are representative of three replicate cultures. Scale bar represents 5 μ M.

In order to confirm the Vps10p results, the localisation of two other cargos of the endosome to TGN machinery were examined.

3.5 Yif1p another mode of retrograde trafficking.

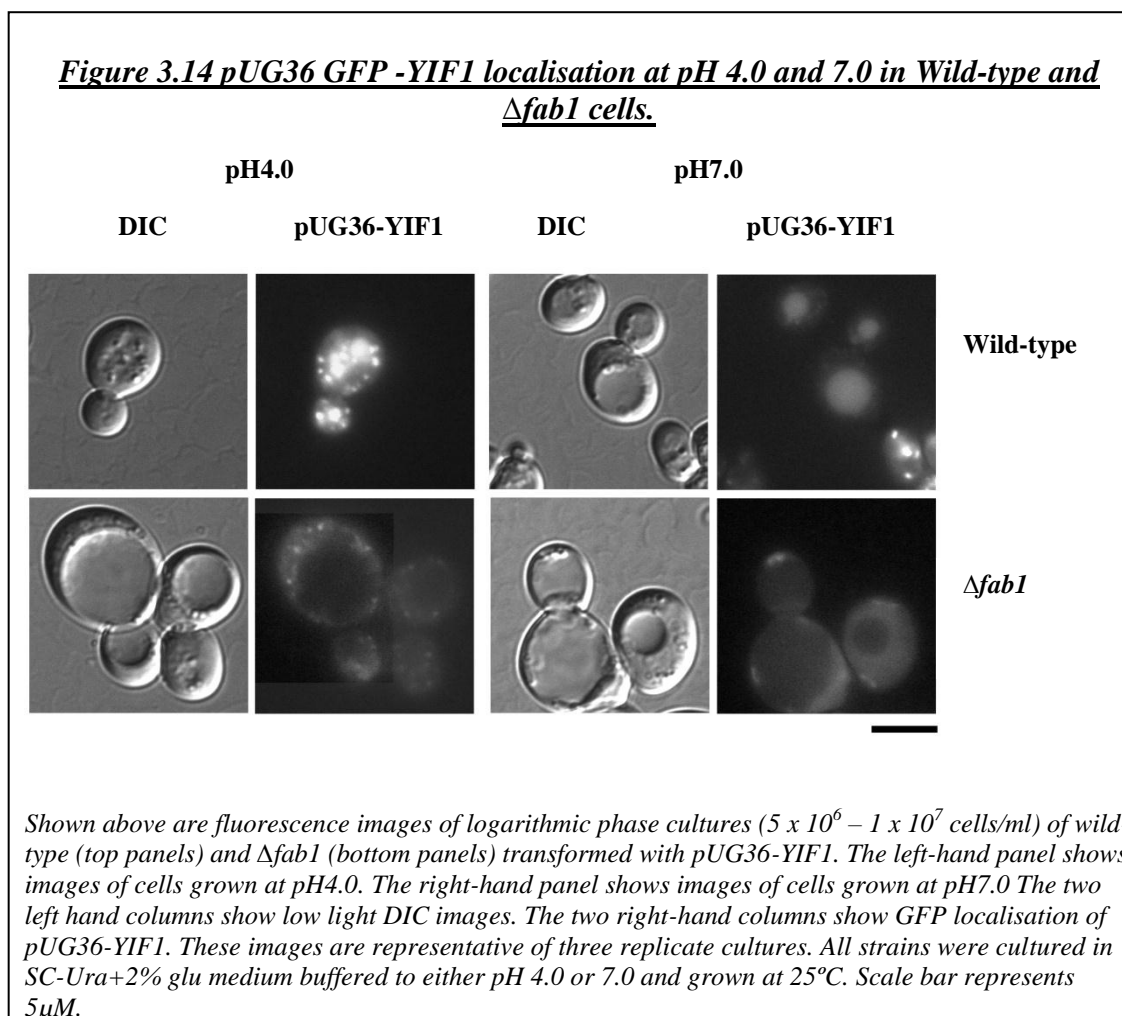
Yif1p is a Golgi localised multispan membrane protein that is reported to cycle via the endosome, back to the Golgi in a retromer and Btn2p dependent fashion. Deletion of *YIF1* causes a block in ER to Golgi transport (Matern et al., 2000). Localisation of Yif1-GFP is reported to be disrupted in both $\Delta btn2$ cells and in mutants of members of the retromer complex including $\Delta vps26$ and $\Delta snx4$. Instead of being seen as GFP punctae throughout the cell, it becomes trapped inside the vacuole (Kama et al., 2007) where it is degraded.

3.6 Localisation of YIF1-GFP

In retromer or $\Delta btn2$ cells Yif1p was reported to enter the MVB pathway and end up inside the vacuole (Kama et al., 2007). To examine if $\Delta fab1$ mutants caused mislocalisation of Yif1p, a pUG36-Yif1 plasmid was created and transformed into wild-type, $\Delta fab1$, $\Delta vps29$ and $\Delta btn2$ strains to see the localisation of N-terminally GFP tagged Yif1p. However, contrary to the published report, the construct was already mislocalised in wild-type cells; it is already inside the vacuole, whereas the reported true steady-state localisation of this protein is known to be the mid-Golgi. Oddly, when the exact construct described in the original paper on Yif1p recycling, was obtained, in our hands, this construct was also vacuolar and not localised to the Golgi. This suggested that the original description of Yif1p trafficking was incorrect

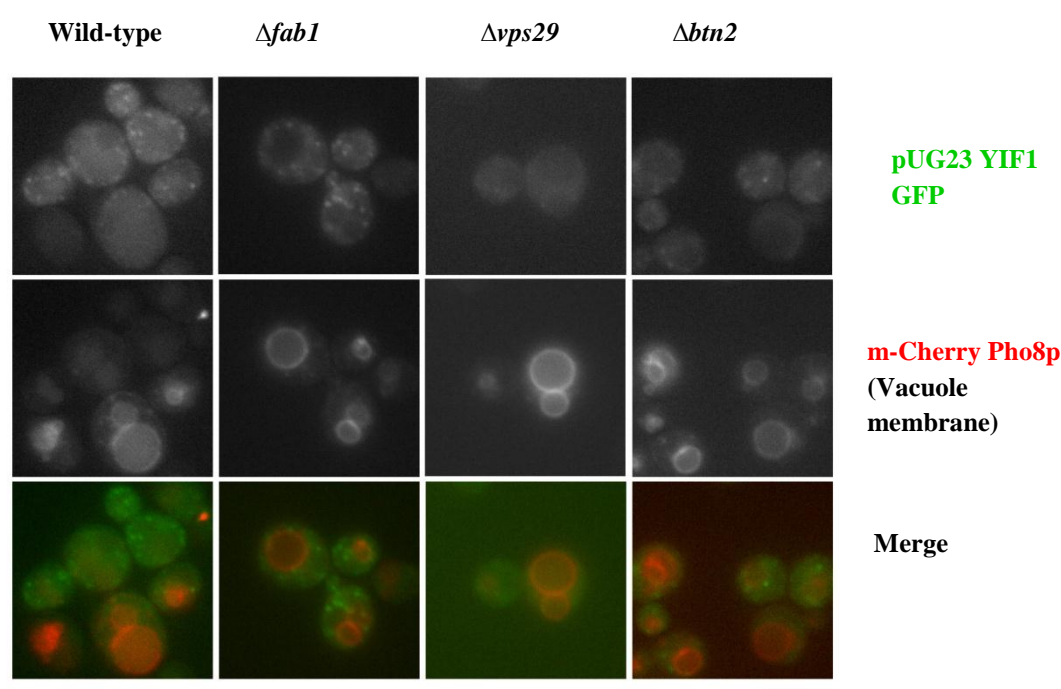
or not consistent between different strains. The observed mislocalisation of Yif1p could be induced by the GFP tag as has been seen in yeast before. (Tsien, 1998)

Discussions with another researcher, Dr Pearce (University of Rochester, NY; USA) who has worked on Yif1p extensively, revealed that the localisation of Yif1p may be dependent upon pH. To investigate this, media was buffered to a pH of 4.0 and 7.0 and cells were grown overnight before microscopy. As shown in Figure 3.14, buffered media does not seem to make a difference to the localisation of Yif1p so both constructs were deemed unusable.



A gift of pUG23-Yif1p from Dr Pearce allowed the Yif1p work to be continued. The plasmid recieved bears a C-terminally tagged Yif1p, that earlier work had shown was stable. Again the same strains were transformed with the construct, and a marker for the vacuole (mCherry-Pho8p), so it could be established more easily whether Yif1p-GFP is mislocalised.

Figure 3.15 pUG23 Yif1-GFP and mCherry-Pho8p visualised in various strains.

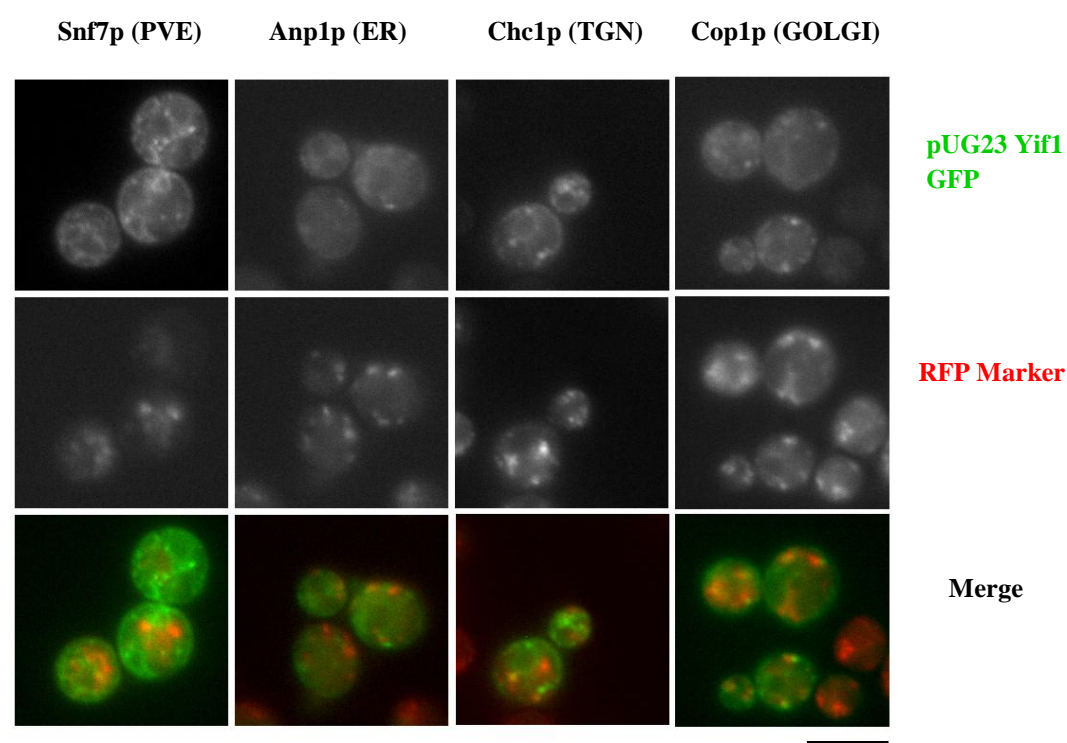


YIF1 was tagged at the C terminal with GFP in a pUG23 plasmid and could be observed as punctae in all strains although somewhat faintly. mCherry-Pho8p is a marker for the vacuole, if trafficking of yif1 is not correctly working the Yif1-GFP should be seen in the vacuole. Shown above are fluorescence images of logarithmic phase cultures ($5 \times 10^6 - 1 \times 10^7$ cells/ml) of Wild-type (first column), $\Delta fab1$ (second column), $\Delta vps29$ (third column) and $\Delta btn2$ (fourth column) transformed with VPS10-GFP (top panels) and mCherry-Pho8p (middle panels) the bottom panel shows a merge of both red and green images for co-localisation. Both strains were cultured in SC-His-Ura+2% glu medium and grown at 25°C. These images are representative of three replicate cultures. Scale bar represents 5μM.

As shown in Figure 3.15 the pUG23-YIF1 construct was expressed weakly, and images show faint punctate compartments, as expected in wild-type cells. Oddly, deletion of *BTN2* did not affect Yif1p-GFP trafficking, suggesting that the original

description of this protein's recycling could be artefactual (Kama et al., 2007). To observe whether a small difference in localisation of the punctae could be observed, the set of RFP markers used previously for the Vps10p work were utilised to define the exact compartment to which Yif1p localises.

Figure 3.16 pUG23-Yif1 localisation in Wild-type cells containing the RFP markers *Snf7p*, *Anp1p*, *Chc1p* and *Cop1p*.



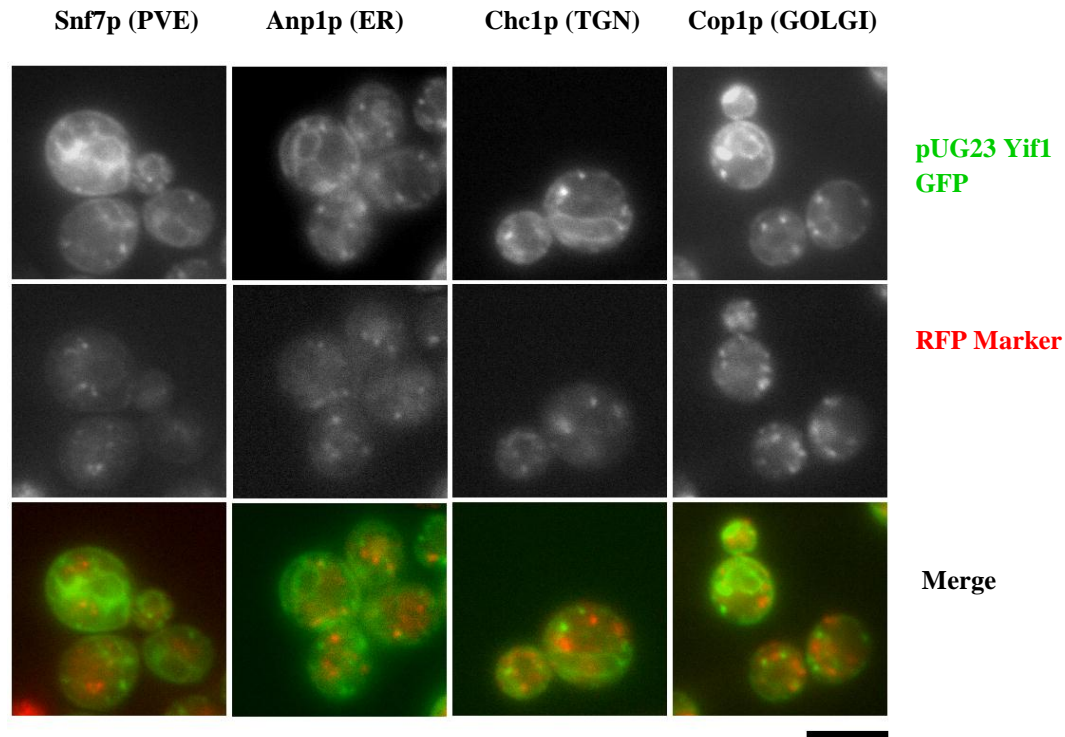
8.7% \pm 6.6	15.0% \pm 8.8	7.0% \pm 0.4	28.1% \pm 4.4	GFP co-localisation
22.4% \pm 9.4	14.5% \pm 1.3	10.6% \pm 8.8	9.4% \pm 13.3	Random GFP co-localisation
-13.7% \pm 8.0	0.5% \pm 10.1	-3.6% \pm 9.2	18.7% \pm 8.8	Adjusted GFP co-localisation
8.7% \pm 6.6	18.8% \pm 3.7	9.2% \pm 5.4	25.0% \pm 3.6	RFP co-localisation
14.5% \pm 10.3	12.4% \pm 3.6	8.4% \pm 6.2	34.4% \pm 4.4	Random RFP co-localisation
-5.8% \pm 13.6	6.4% \pm 0.1	0.8% \pm 11.6	-9.4% \pm 7.9	Adjusted RFP co-localisation

[There was no significant difference between co-localisation and random co-localisation values]

Yif1-GFP can be visualised as punctae. Shown above are fluorescence images of logarithmic phase cultures ($5 \times 10^6 - 1 \times 10^7$ cells/ml) of wild-type cells containing various RFP tagged proteins acting as markers (middle panels) transformed with pUG23YIF1-GFP (top panels). The bottom panel shows a merge of both red and green images for co-localisation. Strains were cultured in SC-His+2% glu medium and grown at 25°C. These images are representative of three replicate cultures. Scale bar represents 5 μ M.

As seen in Figure 3.16 it is hard to clearly define the compartment YIF1-GFP is localised to in the Wild-type strain and there is no significant co-localisation with any marker. Vps26p was used as a retromer control because a *vps26::LEU2* allele was available. In this strain there appears to be significant co-localisation with the Cop1p positive compartment which marks the Golgi. There do seem to be additional punctae that do not co-localise with any of the examined compartments, so this may mean that Yif1p is localised to another compartment as well (as seen in Figure 3.17). It also looks like Yif1-GFP is localised on the vacuole membrane.

Figure 3.17 pUG23-YIF1 localisation in $\Delta vps26$ cells containing the RFP markers Snf7p, Anp1p Chc1p and Cop1p.

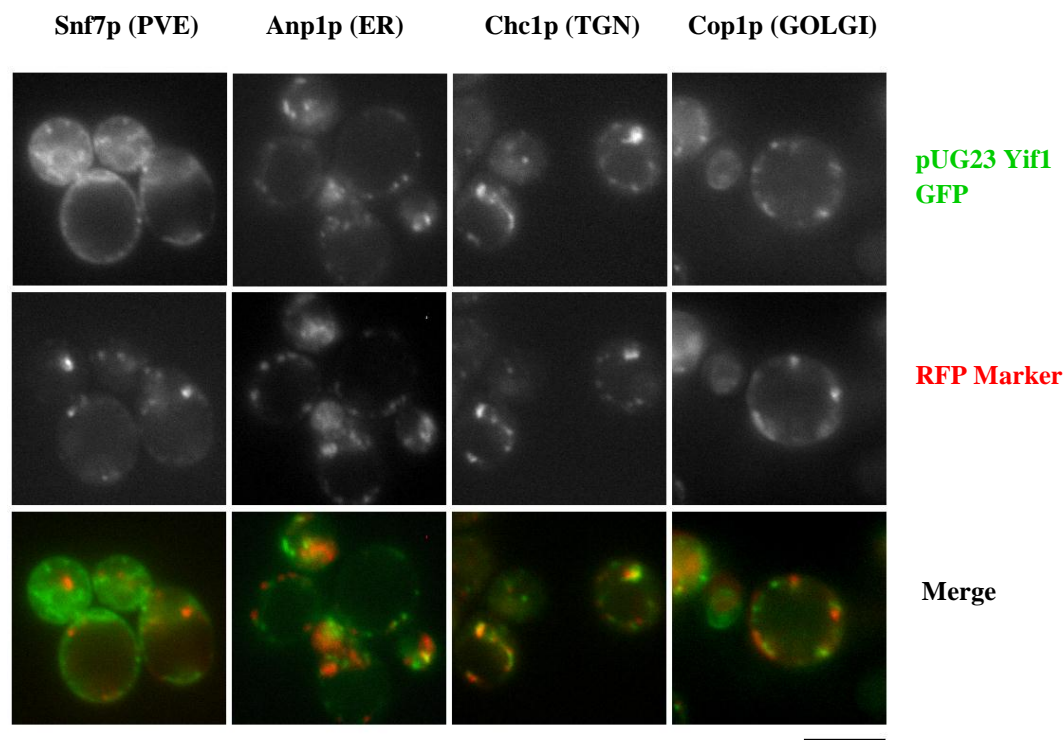


0.0% \pm 0.0	3.3% \pm 3.9	2.9% \pm 1.0	28.1% \pm 1.2	GFP co-localisation
6.9% \pm 1.8	8.9% \pm 1.5	3.3% \pm 4.7	12.1% \pm 3.4	Random GFP co-localisation
-6.9% \pm 1.76	-5.6% \pm 2.3	-0.4% \pm 1.5	16.% \pm 8.0	Adjusted GFP co-localisation
0.0% \pm 0.0	2.2% \pm 2.6	6.7% \pm 2.4%	32.2% \pm7.0***	RFP co-localisation
0.0% \pm 0.0	10.6% \pm 5.0	3.2% \pm 4.6	5.9% \pm 2.4	Random RFP co-localisation
0.0% \pm 0.0	-8.4% \pm 1.5	3.5% \pm 3.8	26.3% \pm 2.9	Adjusted RFP co-localisation

[Significantly different from random co-localiation: *** $P < 0.001$, N/S not indicated]

Yif1-GFP is visualised as punctae. Shown above are fluorescence images of logarithmic phase cultures ($5 \times 10^6 - 1 \times 10^7$ cells/ml) of $\Delta vps26$ cells containing various RFP tagged proteins acting as markers (middle panels) transformed with pUG23YIF1-GFP (top panels) and various RFP markers (middle panels). The bottom panel shows a merge of both red and green images for co-localisation. Strains were cultured in SC-His+2% glu medium and grown at 25°C. These images are representative of three replicate cultures. Scale bar represents 5 μ M

Figure 3.18 pUG23-YIF1 localisation in $\Delta fab1$ cells containing the RFP markers Snf7p, Anp1p Chc1p and Cop1p.



6.4% \pm 2.5	7.6% \pm 4.3%	49.4% \pm 9.4*	40.0% \pm 11.8*	GFP co-localisation
7.9% \pm 12.1	10.2% \pm 10.3%	14.4% \pm 6.5	13.3% \pm 9.4	Random GFP co-localisation
-1.5% \pm 6.3	-2.6% \pm 12.2	35.0% \pm 9.4	26.7% \pm 6.8	Adjusted GFP co-localisation
9.0% \pm 6.5	6.9% \pm 5.3	38.3% \pm 12.4	46.5% \pm 8.5*	RFP co-localisation
2.9% \pm 1.1	15.1% \pm 9.1%	8.3% \pm 8.8	14.8% \pm 5.0	Random RFP co-localisation
6.1% \pm 10.4	-8.2% \pm 6.0	30.0% \pm 8.4%	31.7% \pm 9.4	Adjusted RFP co-localisation

[Significantly different from random co-localiation: $0.01 < *P < 0.05$, N/S not indicated]

Yif1-GFP is visualised as punctae. Shown above are fluorescence images of logarithmic phase cultures ($5 \times 10^6 - 1 \times 10^7$ cells/ml) of $\Delta fab1$ cells containing various RFP tagged proteins acting as markers (middle panels) transformed with pUG23YIF1-GFP (top panels). The bottom panel shows a merge of both red and green images for co-localisation. Strains were cultured in SC-His+2% glu medium and grown at 25°C. These images are representative of three replicate cultures. Scale bar represents 5 μ M.

The $\Delta fab1$ strain appears to have some significant co-localisation with the Cop1p and Chc1p positive compartments (Figure 3.18). This difference in Yif1p trafficking in the $\Delta fab1$ strain is not observed in the retromer deficient strain, suggesting that this phenotype is not due to a deficiency in retromer trafficking. The random co-localisations suggest that the difference in co-localisation is not due to the compartment sizes as when random co-localisation is taken into account, a difference is still observed. This effect may be due to the Cop1p and Chc1p compartments overlapping in a $\Delta fab1$ cell because they mark the Golgi and TGN respectively. The colocalisation with the Cop1p positive compartment is not as significant as in the retromer deficient strain. This data suggests that Yif1p trafficking, if it even does recycle, is not retromer or Fab1p-dependent and hence neither Yif1p nor Vps10p require PtdIns(3,5) P_2 to recycle. This strongly suggests that retromer function does not require PtdIns(3,5) P_2 and that the results from animals either represent a difference between fungi and animals or else that the data from animals are misleading.

3.7 Mr11p a homolog of the mammalian mannose-6-phosphate receptors.

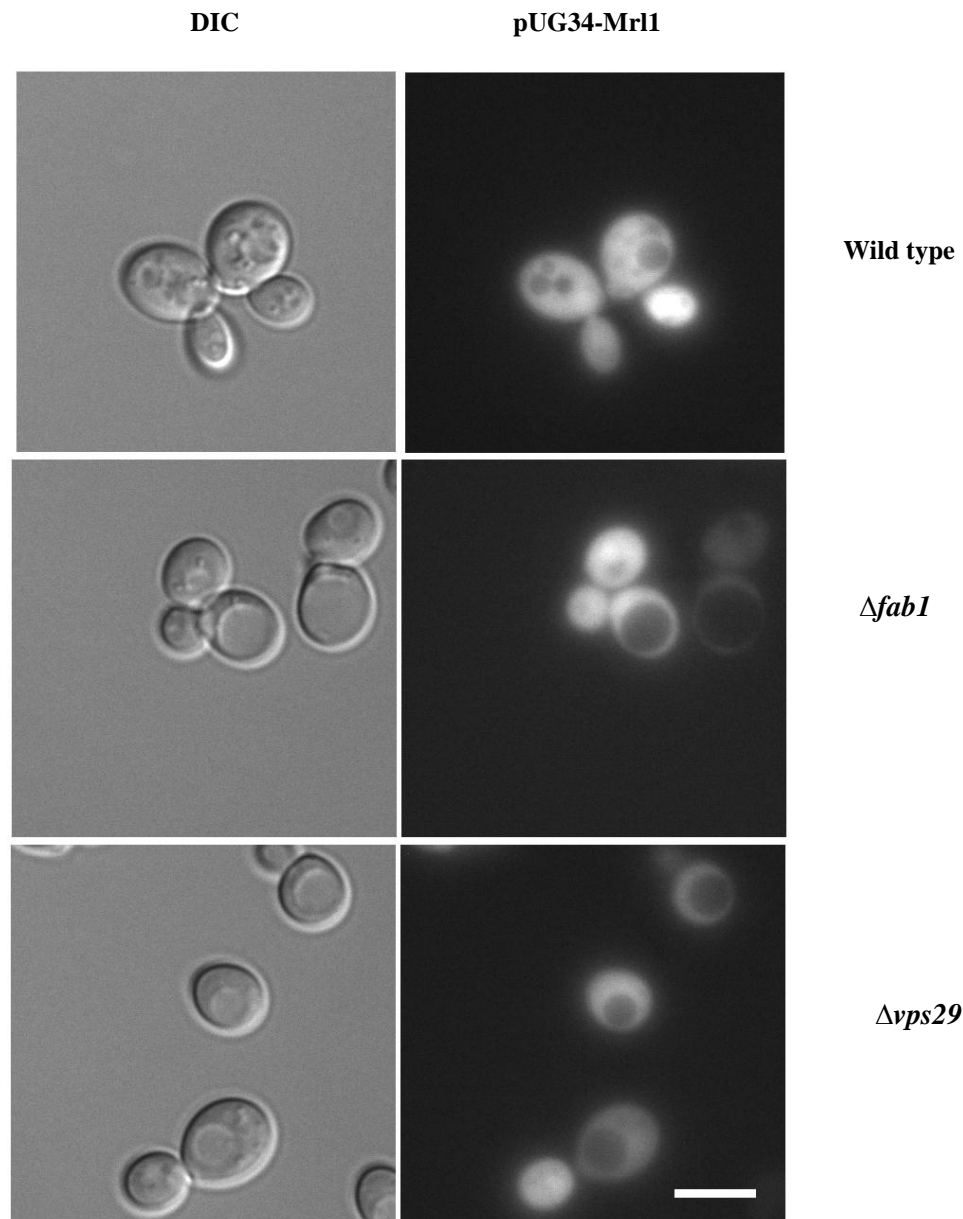
Mr11p is a yeast protein identified in 2001 which shares homology to cation dependent mammalian mannose-6-phosphate receptors (Whyte and Munro, 2001). This raises the possibility that Mr11p may also be a cargo receptor and recycle in a retromer dependent manner. In mammalian cells soluble hydrolases of the lysosomes are marked for delivery to the organelle by addition of mannose-6-phosphate to their N-glycans. This is recognised by two mannose 6-phosphate receptors in the TGN and who then deliver the hydrolases to the late endosome (Whyte and Munro, 2001).

S.cerevisiae vacuolar hydrolases do not have this feature and *VPS10* encodes the sorting receptor that cycles between the Golgi and late endosome. However Vps10p is unrelated to the mammalian mannose 6-phosphate receptors. Mr11p is not a widely researched protein but it cycles as Vps10p does from the Golgi to the PVE. Although there is currently no evidence for direct binding of vacuolar hydrolases to Mr11p, it is possible it does play a role in their sorting (Bowers and Stevens, 2005). Mr11p is a candidate for the transport of PrA and PrB which are transported along the same pathway as CPY. Mr11p is encoded by the ORF YPR079w and is predicted to encode a protein of 381 amino acids with a single transmembrane domain and a cleaved signal peptide. Closely related proteins are found in both *S. pombe* and the fungus *Botrytis cinerea* (Bowers and Stevens, 2005). A role for PtdIns(3,5) P_2 in the cycling of Mr11p was investigated, by making several constructs that allow expression of this protein as a GFP-fusion.

3.8 Localisation of Mr11p

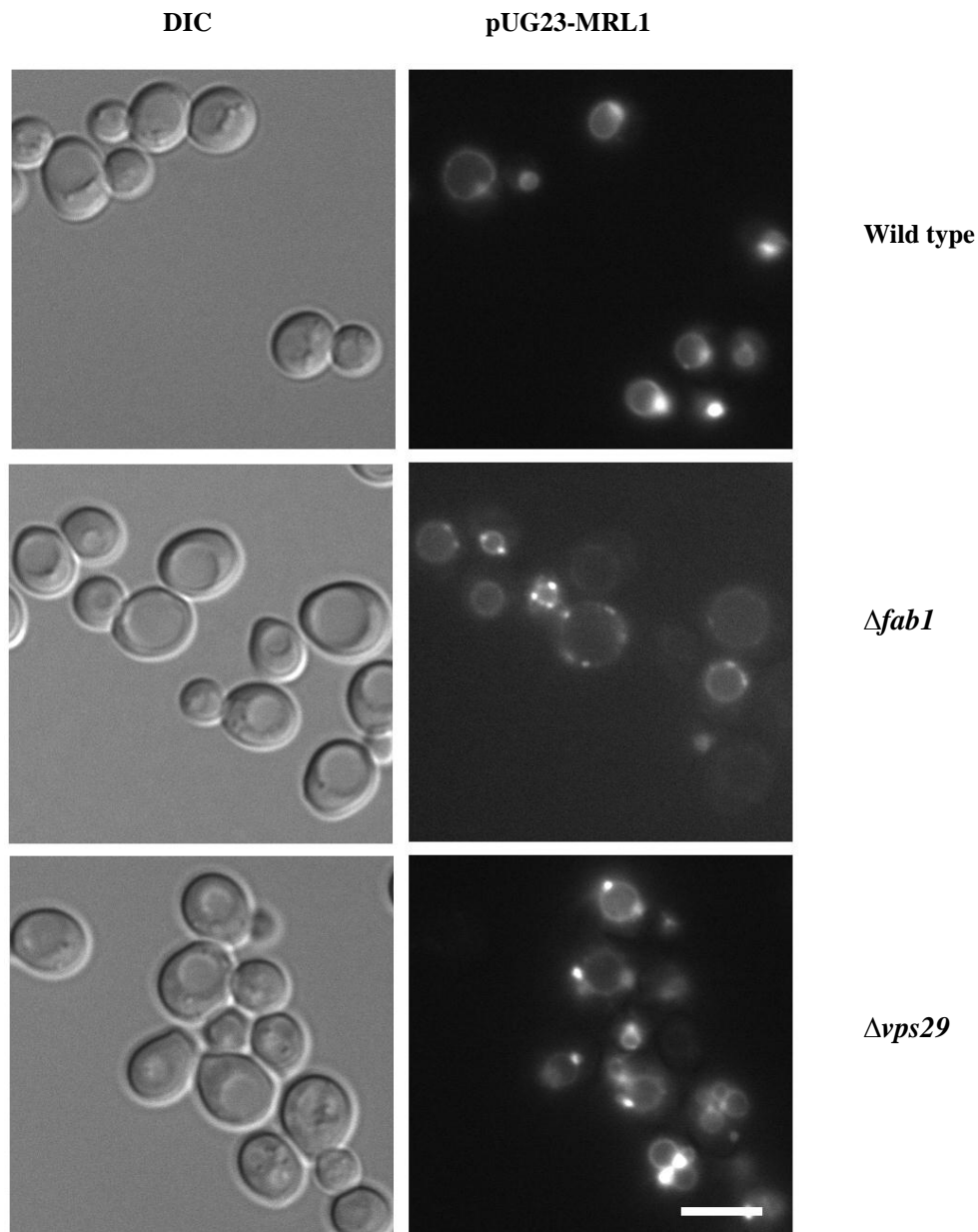
Mr11p has been previously shown to co-localise with Vps10p, but to date has not been shown to recycle via the retromer pathway. A pUG34 MRL1-GFP plasmid was made with the GFP located at the N-terminal and expressed under a Met25 promoter. As shown in Figure 3.19 it appears that the N terminal construct was not correctly trafficked and the GFP signal appeared throughout the cell in the cytoplasm. This is probably due to the transmembrane domain of Mr11p and the N terminus of the protein being situated inside the lumen, therefore the signal could not be observed correctly. A C-terminal GFP tagged plasmid was also made, so Mr11p would not be over expressed.

Figure 3.19 Localisation of pUG34 Mrl1



*pUG34-Mrl1GFP can be visualised throughout the cellular cytoplasm in all strains. Shown above are fluorescence images of logarithmic phase cultures ($5 \times 10^6 - 1 \times 10^7$ cells/ml) of wild-type (top panel), *Δfab1* (middle panel) and *Δvps29* (bottom panel) transformed with pUG34 Mrl1-GFP. The left-hand column shows low light DIC images. The right-hand column shows the GFP localisation of N terminal GFP tagged Mrl1p. These images are representative of three replicate cultures. All strains were cultured in SC-His+2% glu medium and grown at 25°C. Scale bar represents 5μM.*

Figure 3.20 pUG23 MRL1 (C-terminal plasmid GFP tagged) localisation



pUG23-Mrl1GFP can be visualised on the vacuole membrane in all strains. Shown above are fluorescence images of logarithmic phase cultures ($5 \times 10^6 - 1 \times 10^7$ cells/ml) of wild-type (top panel), $\Delta fab1$ (middle panel) and $\Delta vps29$ (bottom panel) transformed with pUG23 Mrl1-GFP. The left-hand column shows low light DIC images. The right-hand column shows the GFP localisation of C terminal GFP tagged Mrl1p. These images are representative of three replicate cultures. All strains were cultured in SC-His+2% glu medium and grown at 25°C. Scale bar represents 5μM.

In the C terminal plasmid construct, Mrl1-GFP appeared to be on the vacuole membrane in all strains examined (See Figure 3.20). No clear difference could easily

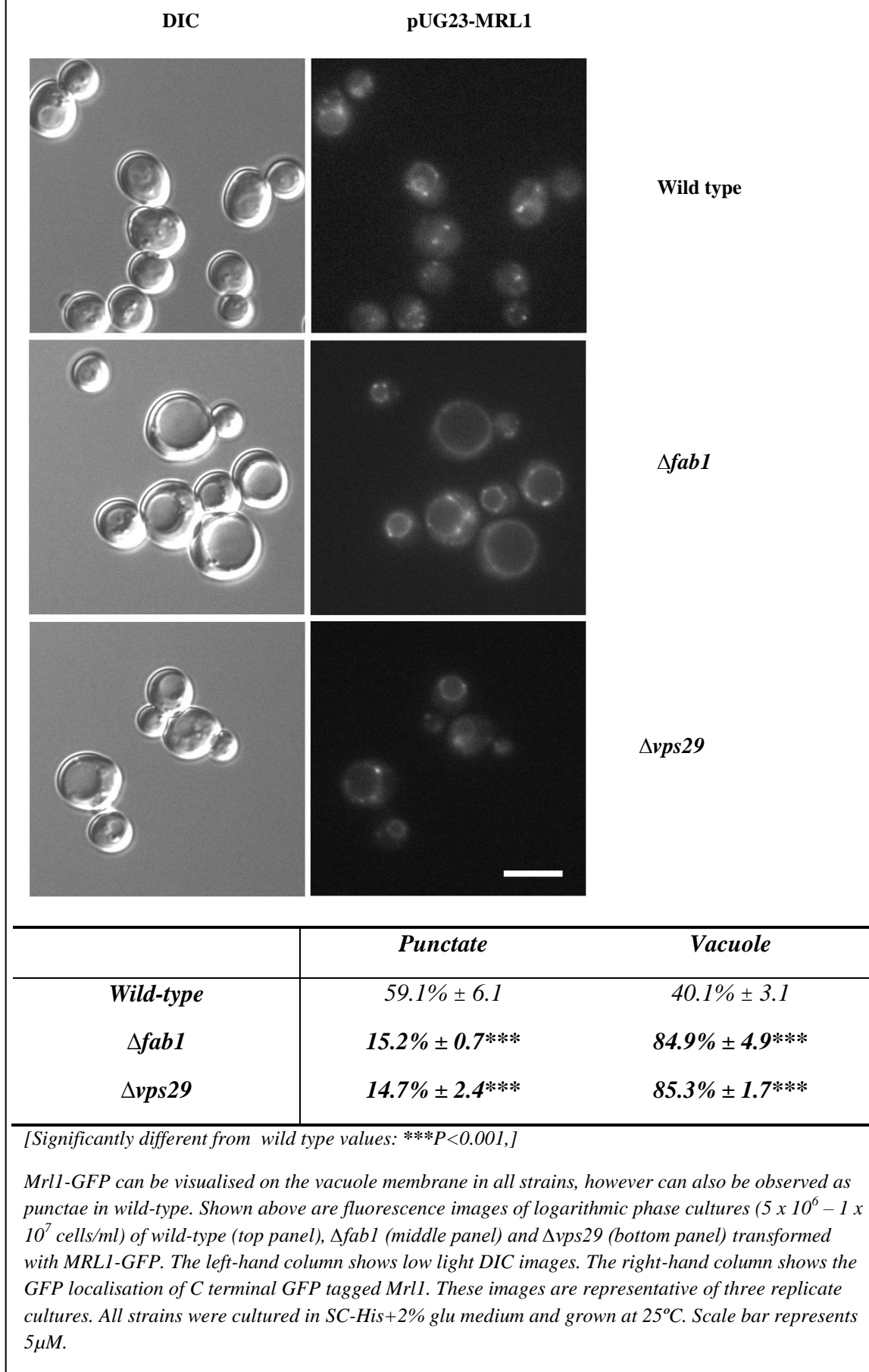
be observed between any of the strains. If more time was available GFP could have been inserted elsewhere in the gene but due to restriction site locations this couldn't quickly be done so due to time constraints this work was abandoned.

At the same time a construct with GFP fusion of *MRL1* at the C-terminus was created, using the Longtine homology approach. In this case Mr11-GFP was expressed constitutively under the control of the endogenous promoter. The results in Figure 3.21 indicate that Fab1p and PtdIns(3,5) P_2 may play a role in the trafficking of Mr11p.

As seen in Figure 3.21, in the $\Delta vps29$ strain in around 85% of cells, the Mr11-GFP construct appears on the vacuole membrane with a few bright punctae coming off of the vacuole and in some cases in the cytoplasm. It is likely that this is because Mr11p is not being trafficked correctly, maybe due to retromer dysfunction. The wild-type strain appears to have both punctate (~60%) and vacuolar (~40%) Mr11-GFP localisation. The $\Delta fab1$ strain has signal on the vacuole membrane in virtually every cell; sometimes small dot like structures can be seen on the vacuole but this occurs less than in wild-type cells. Levels of vacuolar Mr11-GFP are almost at the levels seen in the retromer deficient strain. This suggests that deletion of *FAB1* creates a defect in Mr11p trafficking and leads to its mis-localisation on the vacuole membrane.

The Mr11p work suggests that there may be a role for Fab1p or PtdIns(3,5) P_2 in the trafficking of some cargoes who recycle via retromer.

Figure 3.21 Mr11-GFP endogenously tagged fusion protein localisation



3.9 Discussion

The results obtained from this chapter of experiments indicate that retromer mediated trafficking of Vps10p and Yif1p does not appear to be affected by Fab1p. Vac14p does however appear to play a role in the trafficking of Vps10p, but without further work it is hard to envisage a mechanism. The results show that deletion of *VAC14* does not lead to a total defect in Vps10p localisation and so it may be that some Vps10p can still be recycled and that this enough for us to observe some normal localisation. The results rule out the possibility that retromer trafficking is absolutely dependent on PtdIns(3,5) P_2 , at least in yeast, because a single knockout of *FAB1*, creating a cell with no PtdIns(3,5) P_2 has no effect on localisation of Vps10p nor Yif1p. It may be that PtdIns(3,5) P_2 is playing an accessory role and it is not the phosphoinositide itself that is required for retromer mediated trafficking but part of the activation complex. Vac14p is composed of HEAT motifs and acts as a scaffold for a complex essential for PtdIns(3,5) P_2 production, so maybe it plays a similar scaffolding role during retromer trafficking. A yeast two hybrid analysis to see if there is interaction between Vac14p and the retromer complex may be a way to further dissect this process.

The findings also suggest that Yif1p may not recycle in the way that has been postulated; in our hands such recycling is neither PtdIns(3,5) P_2 nor retromer dependent. It would be interesting to see if Vac14p plays a role in trafficking of this construct.

Intriguing results have been obtained for one of the Mr11p constructs and suggests that PtdIns(3,5) P_2 does play a role in the trafficking of this cargo receptor. Localisation of Mr11p in a $\Delta fab1$ strain is clearly aberrant and similar to that observed in a retromer

deficient strain; this suggests that Mr11p is recycled in a retromer dependent fashion, as deletion of a retromer component results in mislocalisation of Mr11p to the vacuole membrane. To establish a role for PtdIns(3,5) P_2 in the trafficking of Mr11p, further experiments need to be performed. A rescue of the $\Delta fab1$ strain with different *FAB1* constructs would indicate whether or not the process is dependent upon the lipid. Expression of Mr11p and dot blots could be performed to see if direct interaction with PtdIns(3,5) P_2 takes place. A role for Vac14p could also be investigated.

Several studies where PIKfyve function was inhibited via siRNA mediated knock-down or via over expression of a dominant negative PIKfyve strongly suggested that one function of PtdIns(3,5) P_2 might be to regulate endosome to TGN sorting of membrane proteins such as the Vps10p-like sortillins and M6R (Ikononov et al., 2003, Rutherford et al., 2006). The differences observed between the mammalian and *S. cerevisiae* systems may also be due to the fact that Fab1p is a lipid kinase whereas PIKfyve also has protein kinase activity (Sbrissa et al., 2000, Ikononov et al., 2003). Indeed it has been suggested that PIKfyve can phosphorylate p40, a Rab9 effector that is implicated in retromer function (Sbrissa et al., 2005, Ikononov et al., 2003). Since p40 and Rab9 are essential for endosome to TGN recycling in animal cells (Murray et al., 2005) but are absent from yeast, this may explain why there is a difference between these two groups of organisms; we have been unable to demonstrate Fab1p auto-phosphorylation indicating that the yeast enzyme may not express protein-kinase activity. Indeed, mutation of the site in Fab1p that would be predicted to autophosphorylate if Fab1p is also a protein kinase resulted in no substantial difference in Fab1p-activity, suggesting that Fab1p and PIKfyve are not identical in this respect (Duex et al., 2006b). Perhaps this is the reason for the divergent functions of these enzymes. The differences between yeast and animals may also reflect the fact

that sorting nexins in yeast do not bind $\text{PtdIns}(3,5)P_2$ as they are reported to in animal cells. This work shows a key difference between mammalian and yeast systems that has previously been unreported

There is no exact M6R homologue in yeast, so it may be that the result observed in mammalian cells may be a different trafficking event not observed in yeast. Vps10p is not a homologue for M6R, but Mr11p does share a region of homology to cation dependent M6R (Whyte and Munro, 2001). The results do indicate that Mr11p trafficking is disrupted in cells lacking $\text{PtdIns}(3,5)P_2$. This suggests that Vps10p trafficking of CPY is a different event in yeast to that in mammalian cells and utilises different machinery.

The exact nature of the apparent endosome to TGN sorting defect observed in some $\text{PtdIns}(3,5)P_2$ deficient cells has not been defined and therefore it is difficult to know if the effect is direct, which may explain the Vac14p result. Currently no $\text{PtdIns}(3,5)P_2$ effector has been identified that might explain the requirement for $\text{PtdIns}(3,5)P_2$ in the retrograde trafficking step although both sorting nexin1 and an Atg18p like protein, known as WIPI, have been proposed (Jeffries et al., 2004, Carlton et al., 2004). Sorting nexin1 can bind $\text{PtdIns}(3,5)P_2$ through a FYVE domain although it has a much higher affinity for $\text{PtdIns}3P$ even in *in vitro* binding assay whilst the lipid binding specificity of WIPI is in doubt because it resembles Atg18p; a protein that is known to be a true effector of $\text{PtdIns}(3,5)P_2$ in yeast, yet WIPI is reported to bind $\text{PtdIns}3P$ *in vitro*. It would be interesting to see if Δatg18 has an effect on the trafficking of Mr11p.

Alternatively the apparent endosome to TGN recycling defect that is variably observed when PIKfyve is ablated may be a secondary consequence of perturbation of

a genuine PtdIns(3,5) P_2 dependent process further upstream and hence an artefact of chronic loss of PtdIns(3,5) P_2 . Studies conducted in lower organisms such as *C. Elegans* and also a new study of mammalian cells using a specific PIKfyve inhibitor have failed to show any such role for PtdIns(3,5) P_2 in this process (Jefferies et al., 2008, Rusten et al., 2006, Nicot et al., 2006).

Chapter 4

PtdIns(3,5) P_2 in the early endosomal system?

4.1 Introduction

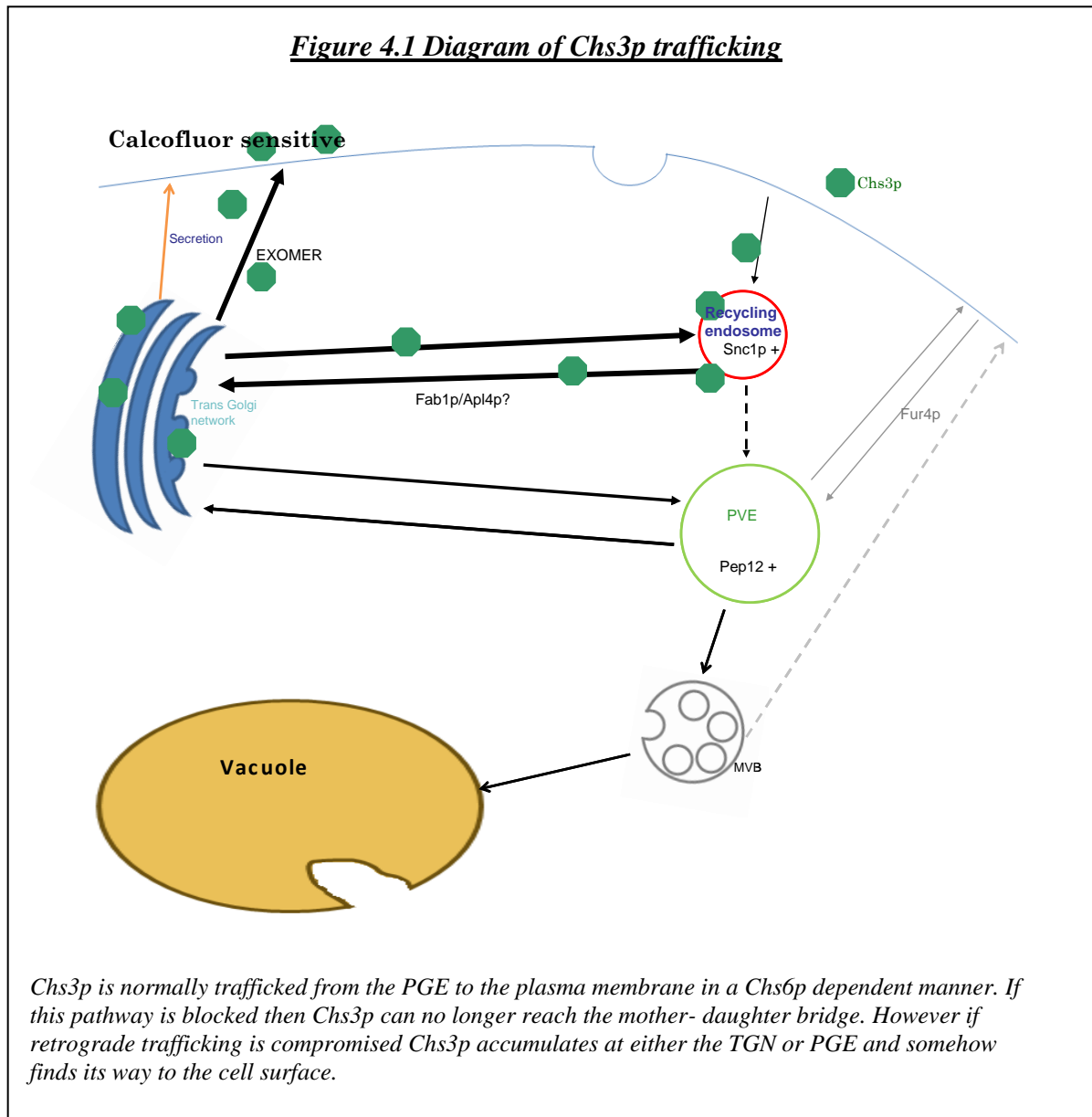
Evidence has recently emerged pointing to a role for PtdIns(3,5) P_2 in the regulation of the early endocytic system in mammalian cells. The mammalian homolog of Fab1p; PIKfyve has been shown to control a multitude of ion channels ranging from the chloride CLC-2 (Klaus et al 2009a), the calcium TRPV6 channel (Sopjani et al 2010), Sodium coupled glutamate EAAT3 transporter (Klaus et al 2009b) and ryanodine receptor trafficking. This makes a role for Fab1p in the early endocytic system likely; even though these functions of PIKfyve could be lipid kinase independent.

Also, since the retromer phenotype observed in animal cells may be an indirect effect of losing PtdIns(3,5) P_2 , one of the compartments linked to the mammalian early endosome might have trafficking regulated by Fab1p.

It was therefore decided to see if Fab1p or PtdIns(3,5) P_2 has any role in the retrograde trafficking between the recycling endosome and the TGN in the yeast *S. cerevisiae*.

Due to the problem of compartment identity between mammalian and yeast systems, it is hard to identify equivalent organelles. The compartment most likely to be the recycling endosome in yeast, is the Snc1p (t-SNARE) positive compartment. This compartment underlies the yeast plasma membrane, and appears to have no direct trafficking route to the cell surface. Cargo must first pass through the Golgi, so the compartment is sometimes named the Post Golgi endosome (PGE) (See Figure 4.1).

FM4-64 is endocytosed and appears in this compartment at early time points, providing evidence it is either an early or recycling endosome (Dove et al., 2009).



When *S. cerevisiae* cells grow and divide, they do so by budding from the mother cell. A daughter cell is initiated as a bud from the mother cell, when the latter attains a critical size and DNA replication has occurred. Genetic information and organelles are shared between the two cells in a process that requires the mother cell wall to

weaken, so cytoplasm can be allowed into the new daughter cell that is bound by a new cell wall, in a process requiring specific proteins and membrane receptors (Feldmann, 2005). The daughter cell grows and eventually ‘buds off’ and separates from the mother cell. During this process the polysaccharide chitin is deposited at the mother daughter cell junction, forming a ring. This ring is retained at the surface of the mother cell after separation and is known as a bud scar. The number of bud scars present can give an indication of cellular ‘age’ and how many budding events have occurred (Feldmann, 2005).

The process of chitin disposition requires an integral membrane enzyme; chitin synthase 3 (Chs3p) (Bulawa, 1993). Chs3p is responsible for around 90% of the total cellular chitin. Chitin is not only deposited at the mother-daughter neck junction but is also present in the walls of *S. cerevisiae* (Bulawa, 1993). During the G₁ phase of the cell cycle Chs3p builds a ring of chitin at the junction between mother and daughter cell, in a process requiring septins.

When visualised, Chs3p is localised to both the plasma membrane and internal ‘punctate’ structures. These internal punctae co-localise with the TGN and early endosome markers (Chaung et al., 1996, Ziman et al., 1996, Valdivia et al., 2002) and have been termed ‘chitosomes’. Chitosomes are suggested to represent an internal pool of Chs3p, ready for trafficking to the plasma membrane during times of cellular stress such as heat shock, and in a cell cycle dependent manner. Chs3p is only found in the daughter cell during G₁, at all other phases it can be seen in the chitosomes (Chuang and Schekman, 1996).

To gain access to the mother-daughter cell bridge Chs3p transits from the internal chitosomes via the TGN and endosomal system. Two proteins have been identified as being required to sort selected cargo proteins into secretory vesicles; Chs5p and Chs6p, (Trautwein et al., 2006, Ortiz and Novick, 2006). Deletion of either Chs5p or Chs6p causes disruption of localisation of Chs3p to the incipient bud site at the onset of bud emergence. Redistribution of Chs3p upon heat stress is also hindered (Ziman et al., 1998, Valdivia and Schekman, 2003, Ruiz-Herrera et al., 2006).

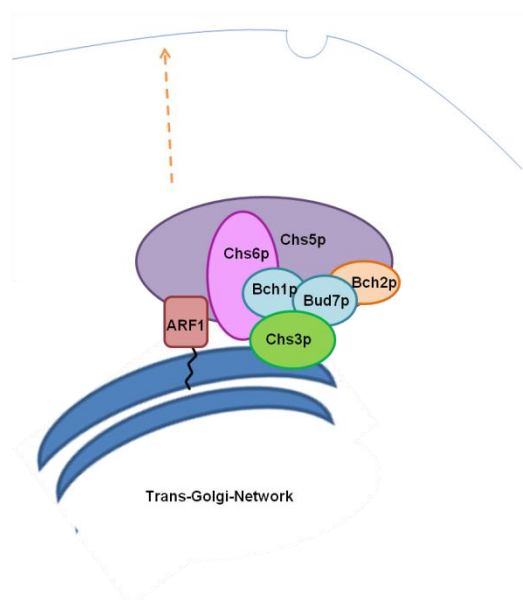
Research in 2006 discovered a large novel coat complex of around 1 MD, known as exomer (Wang et al., 2006). The complex transiently interacts with Chs3p and is necessary for its correct trafficking. Exomer is comprised of Chs5p, Chs6p and three Chs6 paralogues: Bch1p, Bud7 and Bch2p. Every component is critical for the association of Chs3p with exomer (Sanchatjate and Schekman, 2006). Chs5p and Chs6p have non-redundant roles in the complex, deletion of either gene causes a large reduction in the amount of Chs3p bound to the remaining coat. Whereas the roles of Bch1p and Bud7p seem to be somewhat overlapping, as deletion of both genes is required in order to impede Chs3p binding to exomer (Sanchatjate and Schekman, 2006). Chs5p is required for structural integrity of the complex and may act as a scaffold on which the other subunits assemble. It is also essential for the transport of other cargos to the cell surface; such as Fus1p (Santos and Snyder, 2003). Chs5p is recruited to the TGN surface *in vivo* in a GTP dependent process by Arf1p (Wang et al., 2006).

Regulatory proteins control the formation of transport carriers at the TGN by modulating lipid composition, and other proteins such as FAPPs (four phosphate

adapter proteins), which are able to bind PPIs and associate with the TGN through interaction with Arf1p (Godi et al., 2004). Arf1p-GTP may act to tether Chs5p to the membrane as it does for coatmer in Cop1p vesicle formation and adapter proteins (AP-1 and AP-2) do for clathrin coated vesicles (Wang et al., 2006). Acidic phospholipids have been shown to stimulate coat recruitment and assembly on artificial membranes; recombinant Chs5p interacts with Chs6p and with a variety of acidic phospholipids (Wang et al., 2006)

Several other proteins are essential for the regulation of Chs3p transport to the cell surface. Chs7p is a chaperone that controls export of Chs3p from the endoplasmic reticulum (Trilla et al., 1999). Chs4p is needed to activate and link Chs3p to the septins at the mother-daughter bridge (Bulawa, 1993).

Figure 4.2 Cartoon of how an Exomer complex might form.



The exact way the Exomer complex forms is not known. It is likely that Chs5p acts as a scaffold for the other components to form onto. Arf1-GTP is required for interaction with the TGN. Chs6p, Bch1p and Bud7p are required for Chs3p interaction.

Interrupted transport of Chs3p when either *CHS6* or *CHS5* are deleted has been reported to be restored when any subunit of the clathrin AP-1 complex is also inactivated (Valdivia et al., 2002). It has also been suggested that clathrin and AP-1 mediate the cycling of Chs3p between the TGN and the early endosome, and that the pathway serves to retain an underlying Chs5p and Chs6p independent route of Chs3p traffic to the cell surface (Sanchatjate and Schekman, 2006). The normal purpose of this division of Chs3p between the TGN and the early endosome may be to maintain Chs3p in the internal chitosomes that are required when cells are stressed or in G1 (Sanchatjate and Schekman, 2006).

Research by the Cooke group in 2006 presented evidence that Fab1p and AP-1 are required for the trafficking of ubiquitinated cargos from the TGN to the vacuole lumen (Phelan et al., 2006). Biochemical analysis shows all components of the AP-1 complex, when deleted, have compromised PtdIns(3,5) P_2 synthesis and any trafficking defects of $\Delta apl2$ and $\Delta apl4$ can be recovered by Fab1p over-expression (Phelan et al., 2006).

Calcofluor white, can be use to visualise chitin rings, deposited at the neck of the mother-daughter cell during replication (Manheit et al., 1984). In a $\Delta chs6$ strain, calcofluor white staining is diffuse. This is because chitin can no longer reach the mother-daughter junction correctly, and chitin rings are absent (Valdivia et al., 2002). Wild-type cells lacking a component of the AP-1 complex, and $\Delta fab1$ strains all appear to have normal calcofluor white staining. Here, bud scars from previous daughter cells are observed. Intriguingly, when an additional deletion of an AP-1 subunit, is added to a $\Delta chs6$ strain, the bud scars are reported to be restored. The same phenotype is also reported to be observed when an additional Fab1p deletion is added to the $\Delta chs6$ strain (Phelan et al., 2006, Valdivia et al., 2002). This suggests

that Fab1p, as well as AP-1, may mediate the internal recycling of Chs3p that occurs in wild-type cells but becomes much more exaggerated when Chs6p is inactivated.

Research has also implicated Ent3p and Ent5p, two putative effectors of PtdIns(3,5) P_2 in this process. Deletion of both Ent3p and Ent5p together, can reverse the calcofluor resistance observed in a $\Delta chs6$ strain (Copic et al., 2007). Several studies have linked Ent3p, Ent5p and PtdIns(3,5) P_2 in the regulation of Chs3p trafficking, to and from the cell surface (Phelan et al., 2006) Ent3p and Ent5p have also been implicated in intracellular retention of Chs3p, they have previously been shown to bind clathrin, AP-1 and Gga2p (Dove et al., 2009, Seaman, 2005, Costaguta et al., 2006).

4.2 Aim

The aim of this work was to use the endocytic trafficking of Chs3p in yeast, in order to identify additional components of the pathway influenced by Fab1p and PtdIns(3,5) P_2 . Another aim was to establish what this pathway actually is. In order to find additional components of the pathway, a screen was devised. A secondary screen to identify potential mutants with Fab1p like ‘co-phenotypes’ was also developed. This was calculated to allow discovery of the machinery involved in this pathway and shed light on the role of PIKfyve and PtdIns(3,5) P_2 in the early endosomal system.

4.3 Chs3-GFP localisation

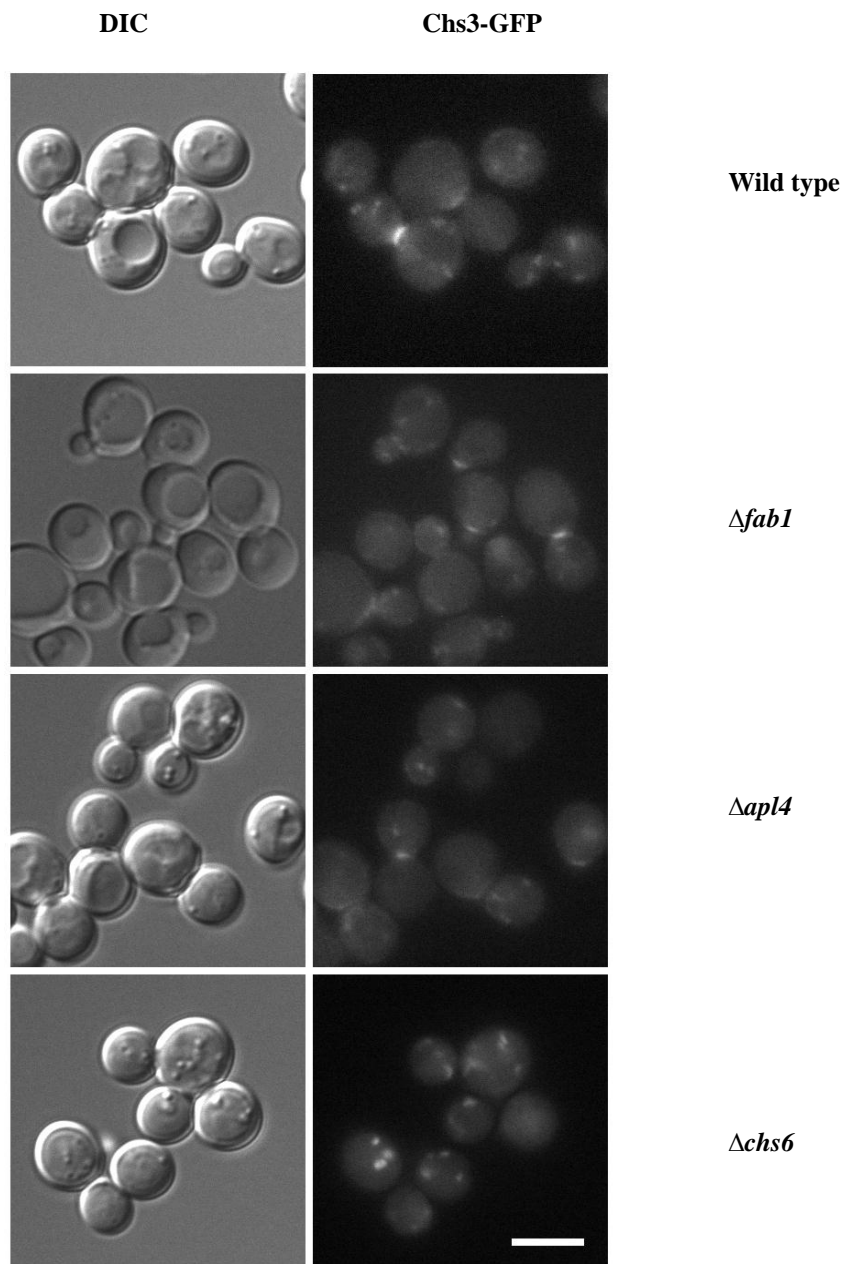
To verify localisation of Chs3p a Chs3-GFP construct was made using the Longtine short flanking homology approach as detailed in Chapter 2. The construct also allowed investigation into whether Fab1p or any AP-1 subunit plays a role in the localisation of Chs3p in a $\Delta chs6$ strain. Chs3p-GFP was expressed under the

endogenous promoter, so trafficking defects would not be due to over expression; though mislocalisation due to GFP was still possible.

As shown in Figure 4.3. Chs3-GFP localisation is disrupted in a $\Delta chs6$ strain. In wild-type, $\Delta apl4$ and $\Delta fab1$ strains, Chs3-GFP can be localised on the mother-daughter bridge of budding cells. This is observed in around 60% of wild-type cells. In a $\Delta chs6$ strain Chs3-GFP is no longer seen on the bridge as often (around 7%), and is present mostly as internal punctate vesicles. It appears that without Chs6p, Chs3p can no longer reach the bridge of the mother/daughter bud. This is likely due to exomer no longer functioning to transport Chs3p to the cell surface, without Chs6p.

To investigate whether Fab1p or Apl4p (a subunit of the AP-1 complex) have a role in trafficking Chs3p, double mutants with an additional mutation of *CHS6* were constructed and examined (Figure 4.4).

Figure 4.3 Localisation of Chs3-GFP in single deletion mutant strains.

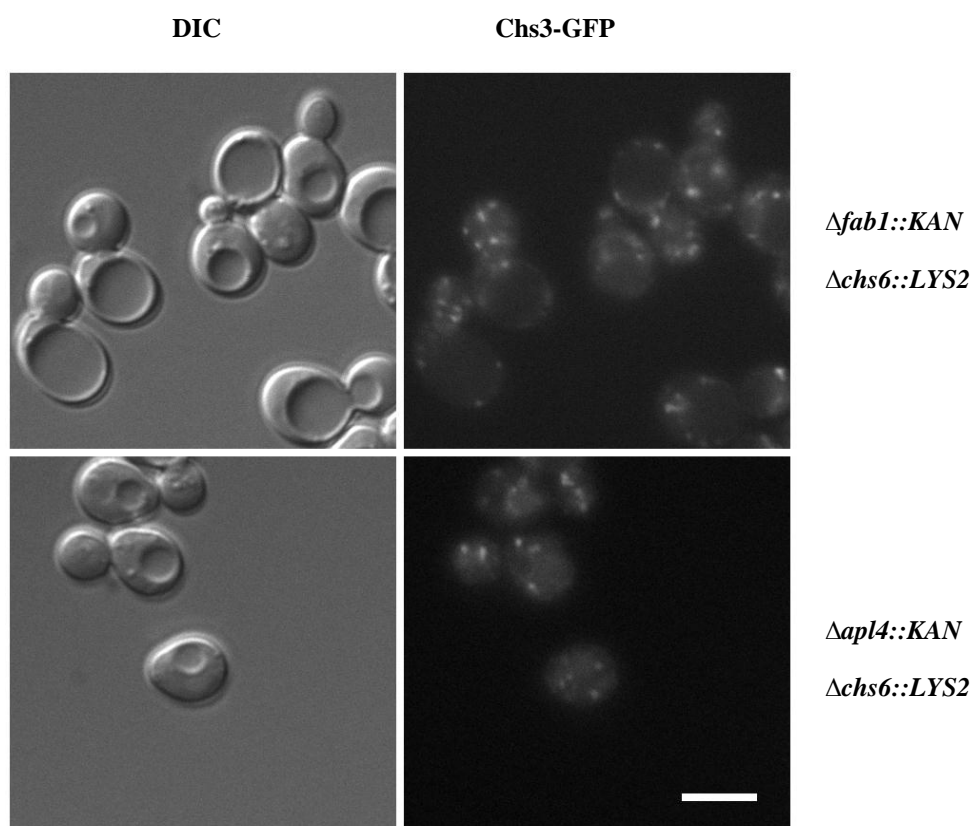


Strain	Percentage of cells with Chs3-GFP on bridge
Wild-type	60.6% \pm 5.2
$\Delta chs6$	7.2% \pm 2.4***

[Significantly different from wild type values: *** $P < 0.001$.]

Chs3-GFP is seen in punctae in all single mutant stains. Shown above are fluorescence images of logarithmic phase cultures ($5 \times 10^6 - 1 \times 10^7$ cells/ml) of wild-type (top panel), $\Delta fab1$ (second panel), $\Delta apl4$ (third panel) and $\Delta chs6$ (bottom panel) transformed with Chs3-GFP. The left-hand column shows low light DIC images. The right-hand column shows the GFP localisation of C terminal GFP tagged Chs3p. These images are representative of three replicate cultures. All strains were cultured in SC-His+2% glu medium and grown at 25°C. Scale bar represents 5 μ M.

Figure 4.4 Chs3-GFP localisation in double mutants



Strain	Percentage of cells with Chs3-GFP on bridge	Average number of punctae per cell
$\Delta chs6$	7.2% \pm 2.4	2.7 \pm 0.9
$\Delta fab1 \Delta chs6$	12.5% \pm 4.2	4.7 \pm 1.1
$\Delta apl4 \Delta chs6$	8.9% \pm 1.7	3.7 \pm 0.7

[No significant difference with $\Delta chs6$ values was observed]

Chs3-GFP is seen in punctae in both double mutant stains, and is not observed on the bridge between mother and daughter cell. Shown above are fluorescence images of logarithmic phase cultures (5×10^6 – 1×10^7 cells/ml) of $\Delta fab1 \Delta chs6$ (top panel) and $\Delta apl4 \Delta chs6$ (bottom panel) transformed with Chs3-GFP. The left-hand column shows low light DIC images. The right-hand column shows the GFP localisation of C terminal GFP tagged Chs3p. These images are representative of three replicate cultures. All strains were cultured in SC-His+2% glu medium and grown at 25°C. Scale bar represents 5 μ M.

The results demonstrate that the additional deletion of *FAB1* in a $\Delta chs6$ strain does not significantly alter the localisation of Chs3-GFP.

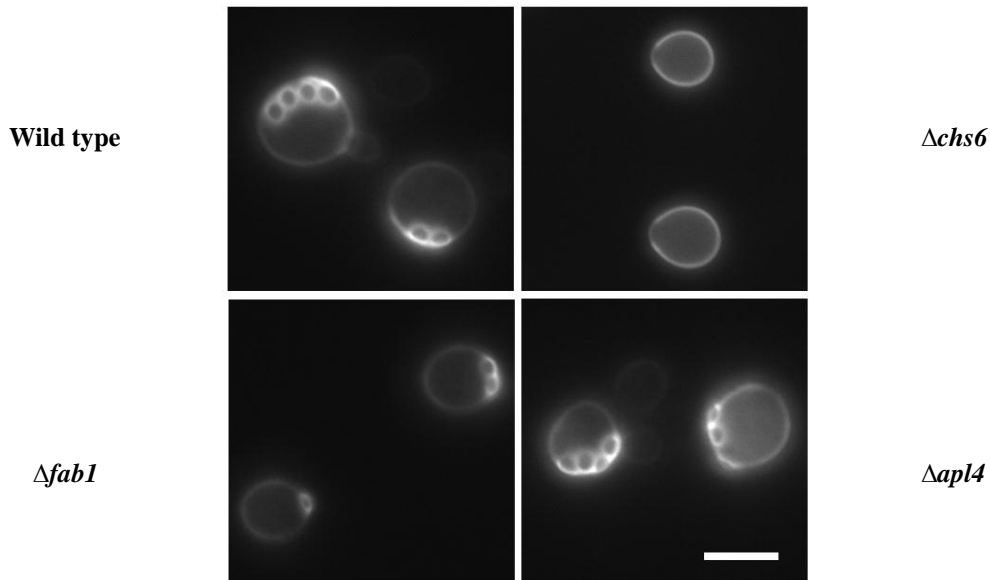
4.4 Calcofluor staining.

Calcofluor white is a non-specific flurochrome, that can be used to stain polysaccharides and has long been used as a fluorescence signal to visualise chitin and cellulose (Harrington and Raper, 1968). Calcofluor white can be used to visualise the bud scars which are rich in chitin, and remain on mother cells following budding. Haploid cells only bud from one position so the bud scars should stem from the same region of the cell. Calcofluor was therefore used to observe bud scars in a variety of strains. The literature reports that bud scars can no longer be observed in a $\Delta chs6$ strain, because chitin cannot reach the mother-daughter bridge, due to disruption of Chs3p transport.

As shown in Figure 4.5, bud scars of previous daughter cells can be observed in a wild-type strain. These are visualised as clear rings at one end of the cell. A $\Delta chs6$ mutant no-longer shares this phenotype. Staining can still be seen on the wall of the cell, as this contains other polysaccharides that calcofluor will also bind. A small amount of chitin will also still be present, as its synthesis is due to other chitin synthases. A small gap in calcofluor staining of the cell wall can be seen in the $\Delta chs6$ strain where bud scars would normally be present. This represents the lack of chitin that would normally build up at the mother-daughter bridge. Bud scars can also be seen in single deletion mutants of *FAB1* and *APL4*. The bud scars in these strains are not significantly different to those in wild-type. This means that correct trafficking of chitin to the mother daughter bridge is occurring during budding in these strains, this is not surprising since no studies implicate Fab1p function in control of exomer.

Figure 4.5 Calcofluor staining of bud scars in Wild-type and single deletion mutants.

Calcofluor staining



<i>Strain</i>	<i>Percentage of cells with bud scars</i>
<i>Wild type</i>	94.6% ±2.1
<i>Δchs6</i>	16.1% ±1.4 ***
<i>Δfab1</i>	92.7% ±4.5
<i>Δapl4</i>	89.8% ±5.4

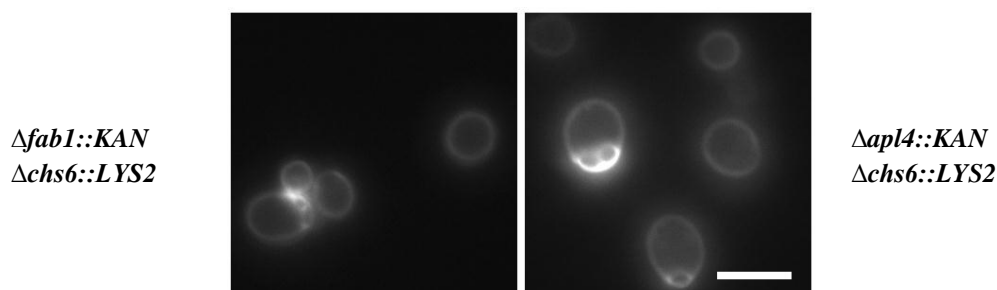
[Significantly different from wild type values: *** $P < 0.001$, N/S not indicate]

Bud scars can be visualised by staining cells with calcofluor. Bud scars are seen in all strains except Δchs6. Shown above are fluorescence images of logarithmic phase cultures ($5 \times 10^6 - 1 \times 10^7$ cells/ml) of wild-type (top left), Δchs6(top right), Δfab1 (bottom left) and Δapl4 (bottom right) stained with calcofluor white for 10 minutes. The images show calcofluor staining visualised using a DAPI filter. These images are representative of three replicate cultures. All strains were cultured in SC-YETD+2% glu medium and grown at 25°C. Scale bar represents 5μM.

To investigate whether an additional deletion of *FAB1* or *APL4* in a *Δchs6* strain can also bring back bud scars, staining of double mutants with calcofluor was also conducted.

Figure 4.6 Calcofluor staining of bud scars in $\Delta chs6$ double mutants

Calcofluor staining



Strain	Percentage of cells with bud scars.
$\Delta chs6$	16.1% \pm 1.4
$\Delta fab1 \Delta chs6$	49.4% \pm 5.2***
$\Delta apl4 \Delta chs6$	48.8% \pm 6.0***

[Significantly different from $\Delta chs6$ values: *** $P < 0.001$,]

Deletion of either *FAB1* or *APL4* can bring back the presence of bud scars in a $\Delta chs6$ strain. Shown above are fluorescence images of logarithmic phase cultures ($5 \times 10^6 - 1 \times 10^7$ cells/ml) of $\Delta fab1::KAN \Delta chs6::LYS2$ (left hand panel) and $\Delta apl4::KAN \Delta chs6::LYS2$ (right hand panel) stained with calcofluor white for 10 minutes. The images show calcofluor staining visualised using a DAPI filter. These images are representative of three replicate cultures. All strains were cultured in SC-Lys+2% glu medium and grown at 25°C. Scale bar represents 5 μ M.

As seen in Figure 4.6 when both *APL4* (a subunit of the AP-1 complex) and *CHS6* are deleted, then bud scars are observed in just under 50% of cells. The same result is observed if a *FAB1* deletion is added to the $\Delta chs6$ strain. Therefore, when *APL4* and *FAB1* are deleted chitin is again able to traffic to the cell surface in some manner. This is possibly due to build up of Chs3p at the TGN or PGE, because Fab1p and AP-1 appear to act in an ill-defined trafficking step between the PGE and the Golgi. This build up of Chs3p may allow this protein to find a new route to the cell surface via bulk secretion or via a novel route from the PGE. Once Chs3p is able to access the cell surface chitin is again present at the bridge between mother and daughter cells, overriding the $\Delta chs6$ phenotype. However, the occurrence of bud scars is still less

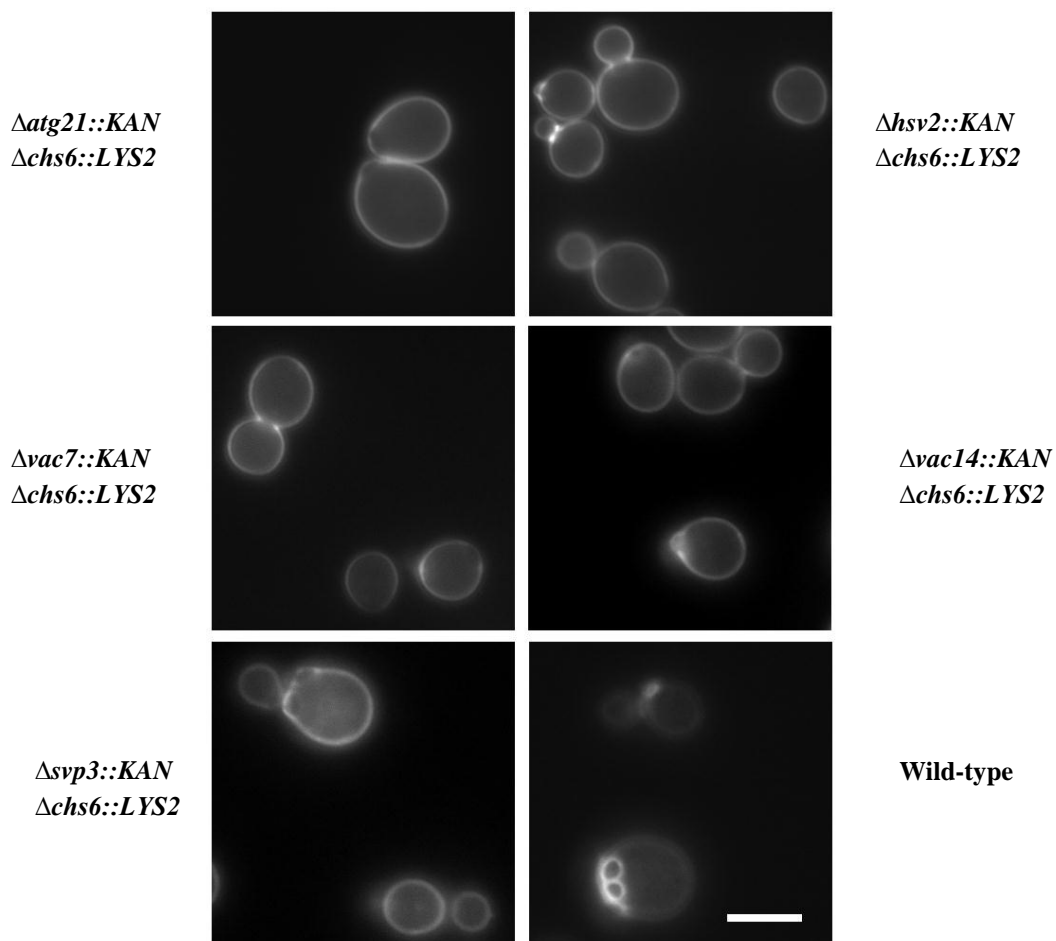
than seen in wild-type cells (Figure 4.5), suggesting that this pathway does not allow as much Chs3p to reach the cell surface as is normally the case.

To further investigate this result, several other double mutants were made, combining $\Delta chs6$ with deletions of other known genes in the Fab1p pathway. The double mutants were stained with calcofluor to see if they could reverse the $\Delta chs6$ phenotype and allow the visualisation of bud scars from previous divisions.

Figure 4.7 shows the results of calcofluor staining in a variety of double mutants, all possessing deletion of *CHS6*. The $\Delta chs6 \Delta vac7$ strain does not have any visible bud scars, although a greater amount of calcofluor staining may be observed at the bridge between mother and daughter cell. An additional deletion of *VAC14* seems to have a bigger effect on calcofluor staining and a small number of bud scars can be observed. These however are not as obvious or as prominent as in the $\Delta fab1 \Delta chs6$ or $\Delta apl4 \Delta chs6$ strains, suggesting only a partial restoration in this process; consistent with the fact that inactivation of *VAC14* leaves some PtdIns(3,5) P_2 present in the cell (Bonangelino et al., 2002). The $\Delta hsv2 \Delta chs6$ strain seems to have staining similar to that of the $\Delta vac7 \Delta chs6$ strain with a greater intensity of calcofluor being observed at the bridge, however no bud scars are seen. The $\Delta atg21 \Delta chs6$ strain serves as a nice control; here calcofluor staining appears as it did in a single *CHS6* knockout strain with no increased staining or bud scars. This suggests that it is likely that neither Vac7p, Atg21p nor Hsv2p play a role in the cycling of Chs3p between the PGE and TGN.

Figure 4.7 Calcofluor staining of bud scars in Δ chs6 double mutants

Calcofluor staining



<i>Strain</i>	<i>Percentage of cells with bud scars.</i>
Δ chs6	16.1% \pm 1.4
Wild type	94.6% \pm 2.1
Δ atg21 Δ chs6	15.4% \pm 2.6
Δ hsv2 Δ chs6	19.1% \pm 3.5
Δ vac7 Δ chs6	18.3% \pm 3.2
Δ vac14 Δ chs6	29.7% \pm4.2*
Δ svp3 Δ chs6	17.2% \pm 2.3

[Significantly different from $\Delta chs6$ values: $0.01 < *P < 0.05$, N/S not indicated]

Shown above are fluorescence images of logarithmic phase cultures ($5 \times 10^6 - 1 \times 10^7$ cells/ml) of various $\Delta chs6::LYS2$ double mutants (left hand panel) and wild-type (bottom right panel) for comparison stained with calcofluor white for 10 minutes. The images show calcofluor staining visualised using a DAPI filter. These images are representative of three replicate cultures. All strains were cultured in SC-Lys+2% glu medium and grown at 25°C. Scale bar represents 5 μ M.

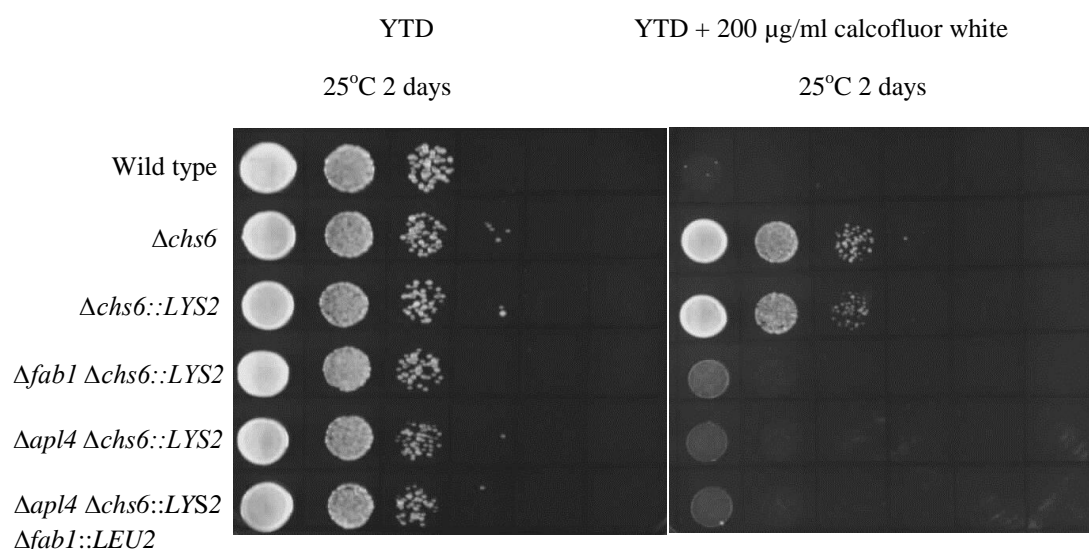
4.5 Calcofluor resistance.

It has previously been shown that when calcofluor is added to *S. cerevisiae* growth media either in liquid culture or plates, it is toxic and shows antifungal activity (Roncero et al., 1988). Calcofluor works by binding to microfibrils of cellulose and chitin and as a result of this interaction β -glucan chains cannot co-crystallise and form microfibrils. Chitin is one of the main structural polysaccharides in the fungal cell wall and abnormal deposition may cause lysis and weakening of the wall (Roncero et al., 1988). Because of this activity *S. cerevisiae* cells are sensitive to calcofluor and cannot grow in/on media which contains the compound. The $\Delta chs6$ strain has a defect in chitin disposition; because of this, the levels of chitin present in the cell wall are much lower than are present in wild-type (Sanchatjate and Schekman, 2006). This can be measured because $\Delta chs6$ strains are resistant to calcofluor and can still grow on/in media with it present. This calcofluor resistant phenotype is also observed for other strains with deletion of proteins involved in the chitin synthase III pathway as cellular chitin levels are reduced, therefore decreasing the target for the fluorophore (Harrington and Raper, 1968).

An assay was developed to assess whether any of the double mutant strains made, and stained above also showed sensitivity to calcofluor. A variety of concentrations of calcofluor in YETD pates were tested to verify the best concentration. It was found that 200 μ g/ml of calcofluor was sufficient to allow growth of a $\Delta chs6$ strain and stop

growth of a wild-type strain. This allowed the other mutants to be assayed. It should be noted that calcofluor was found to produce unreliable results in YEPD medium. This may be due to the composition of peptone. Peptone is produced by digestion of animal milk or meat by proteolytic enzymes, which produces small peptides but also many other compounds such as fat, metals, salts and vitamins, which may inhibit calcofluor action. YETD containing tryptone was found to be a much better medium to use. The peptides present in tryptone are longer and produced only from milk. Calcofluor also appears to be quite unstable in plates and has a short lifetime, resulting in experiments that are only reproducible when media containing calcofluor is freshly made.

Figure 4.8 10X spot dilution of $\Delta chs6$ mutants



Various strains were grown to exponential phase till about $\sim 1 \times 10^7$ cells/ml in YPD + 2% glu for wild-type cells or SC-LYS+2% glu for double mutants. Dilution assay was carried out as described in methodology section. Cells were serially diluted ten-fold then grown on YTD+2% glu agar plates or on the same plate but with 200µg/ml calcofluor white at 25°C for 2 days. Data represents three independent experiments.

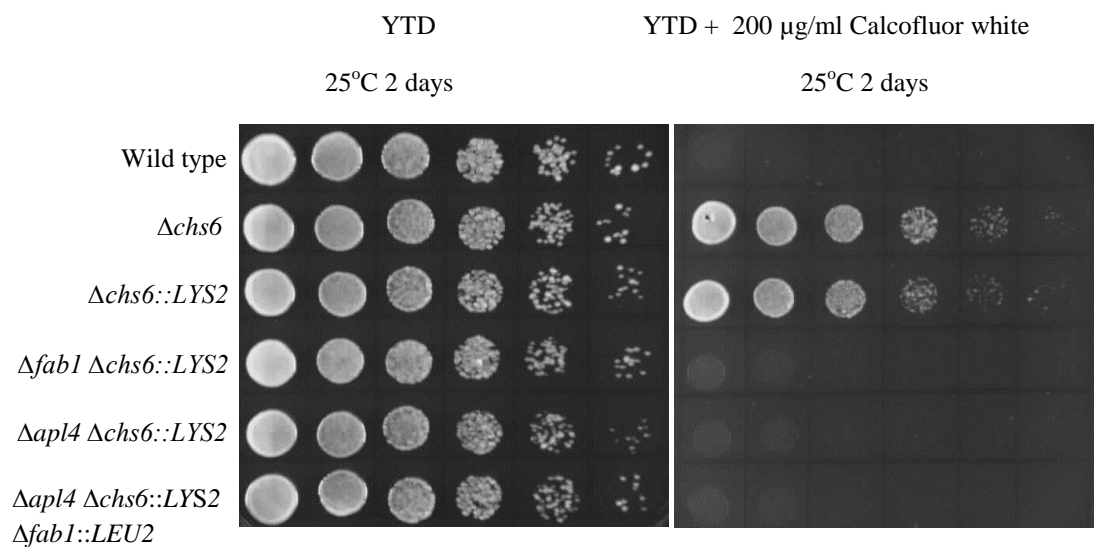
A ten-fold serial spot dilution from a starting culture of 1×10^7 cells/ml was prepared for each of the above strains. A BY4742 *chs6::LYS2* strain was made as a control to verify that any reduction in calcofluor resistance wasn't construct specific and was in fact a true phenotype associated with *CHS6* deletion. The wild-type strain shows high calcofluor sensitivity when grown at 25°C for two days, and hardly any growth is observed compared to the control plate. The two strains possessing a deletion of the *CHS6* gene showed resistance to calcofluor, although growth was slightly reduced from the control YEPD plate. Both the $\Delta fab1\Delta chs6$ and $\Delta apl4\Delta chs6$ strains showed reduced growth on the calcofluor plate, demonstrating that they are reversing the $\Delta chs6$ resistance and have raised levels of chitin in their cell walls. The additional deletion of either *FAB1* or *APL4* is therefore somehow allowing some transport of Chs3p back to the cell surface and allowing chitin to form during budding. Levels of sensitivity however are not brought back to that of wild-type, suggesting this route is not as efficient. To investigate if Apl4p and Fab1p are indeed on the same pathway, a triple mutant was made, with simultaneous inactivations of Fab1p, Apl4p and Chs6p. It is hard to tell whether $\Delta fab1$ and $\Delta apl4$ are having an additive effect and whether the triple mutant is reducing calcofluor resistance further using the standard protocol. To see if a lower dilution factor would yield clearer results, a 5-fold serial spot dilution plate was completed.

It appears from these results that the calcofluor resistance is decreased in both the double and triple mutants to almost wild-type levels. Hardly any growth is seen on the calcofluor plate apart from that of the two $\Delta chs6$ mutants. Some variability is seen between calcofluor plates made at different times, and once stored the properties of calcofluor appear reduced. The above result comes from a freshly made plate and it

appears that an additional deletion of *FAB1* or *APL4* in a $\Delta chs6$ strain can induce calcofluor sensitivity.

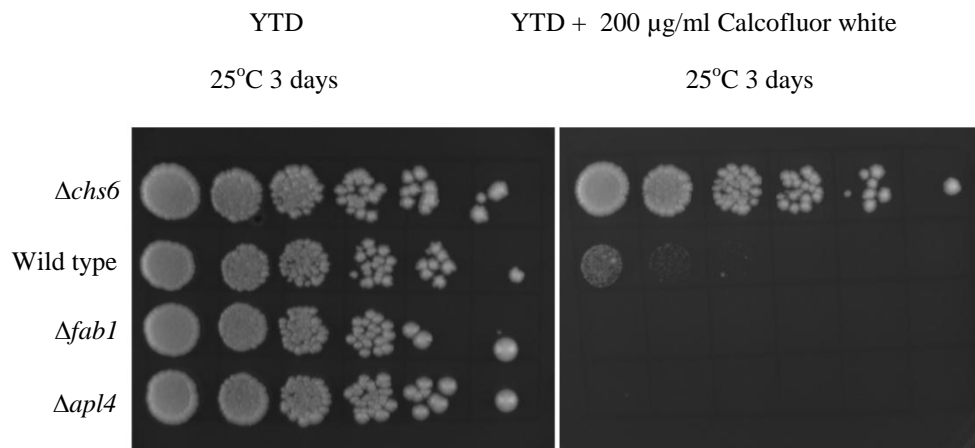
In order to confirm that neither the $\Delta fab1$ or $\Delta apl4$ strains have defects in this pathway spot dilutions of the single mutants were also carried out.

Figure 4.9 5X spot dilution of $\Delta chs6$ mutants



Various strains were grown to exponential phase till about $\sim 1 \times 10^7$ cells/ml in YPD + 2% glu for wild-type cells or SC-LYS+2% glu for double mutants. Dilution assay was carried out as described in methodology section. Cells were serially diluted five-fold then grown on YTD+2% glu agar plates or on the same plate but with 200µg/ml calcofluor white at 25°C for 2 days. Data represents three independent experiments.

Figure 4.10 5X spot dilution mutants



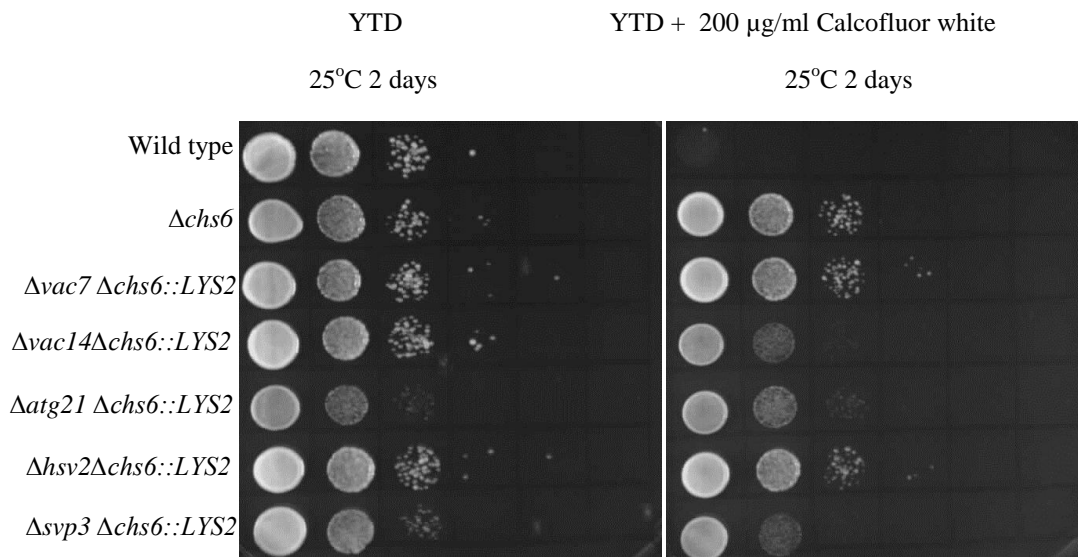
Various strains were grown to exponential phase till about $\sim 1 \times 10^7$ cells/ml in YPD + 2% glu with added G418 for mutants. Dilution assay was carried out as described in methodology section. Cells were serially diluted five-fold then grown on YTD+2% glu agar plates or on the same plate but with 200µg/ml calcofluor white at 25°C for 2 days. Data represents three independent experiments.

As shown in Figure 4.10 *Δchs6* cells are calcofluor resistant as previously shown.

Wild-type strains and mutants with a single *Δfab1* or *Δapl4* deletion appear to be calcofluor sensitive. This is because in these strains the exomer complex is functioning and chitin is being deposited as it should be, during the cell cycle.

The calcofluor resistance of the other *Δchs6* double mutants examined for bud scars above, was also investigated in order to fully see any role, if any they had in the trafficking of Chs3p.

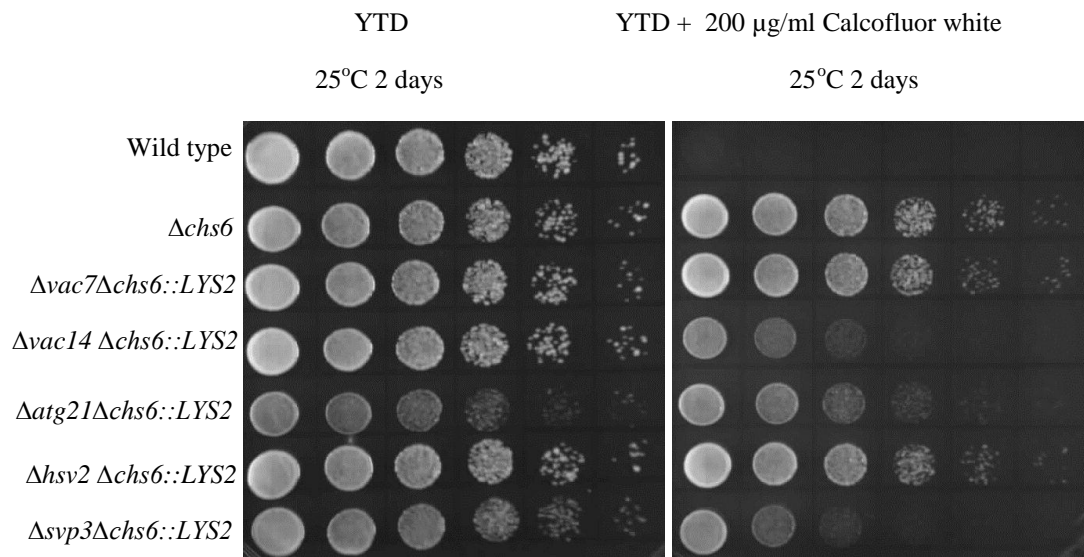
Figure 4.11 10X spot dilution of $\Delta chs6$ double mutants.



Various strains were grown to exponential phase till about $\sim 1 \times 10^7$ cells/ml in YPD + 2% glu for wild-type cells or SC-LYS+2% glu for double mutants. Dilution assay was carried out as described in methodology section. Cells were serially diluted ten-fold then grown on YTD+2% glu agar plates or on the same plate but with 200 μ g/ml calcofluor white at 25°C for 2 days. Data represents three independent experiments.

The 10-fold spot dilution plate as shown in Figure 4.11 with wild-type used as a control shows the $\Delta chs6$ strain is still resistant to calcofluor. The $\Delta vac7 \Delta chs6$, $\Delta hsv2 \Delta chs6$ and $\Delta atg21 \Delta chs6$ strains do not appear to have reduced calcofluor resistance, which agrees with the bud scars observed microscopically. However a small increase in calcofluor sensitivity is seen in the $\Delta vac14 \Delta chs6$ and $\Delta svp3 \Delta chs6$ strains. The growth of these strains on the calcofluor plate is however increases when compared to the wild-type control. Only a reduction in calcofluor resistance is seen and sensitivity has not been brought back to the levels seen in $\Delta fab1 \Delta chs6$ or $\Delta apl4 \Delta chs6$ double mutants. A 5 fold spot dilution plate was carried out to get clearer results.

Figure 4.12 5X spot dilution of $\Delta chs6$ double mutants.

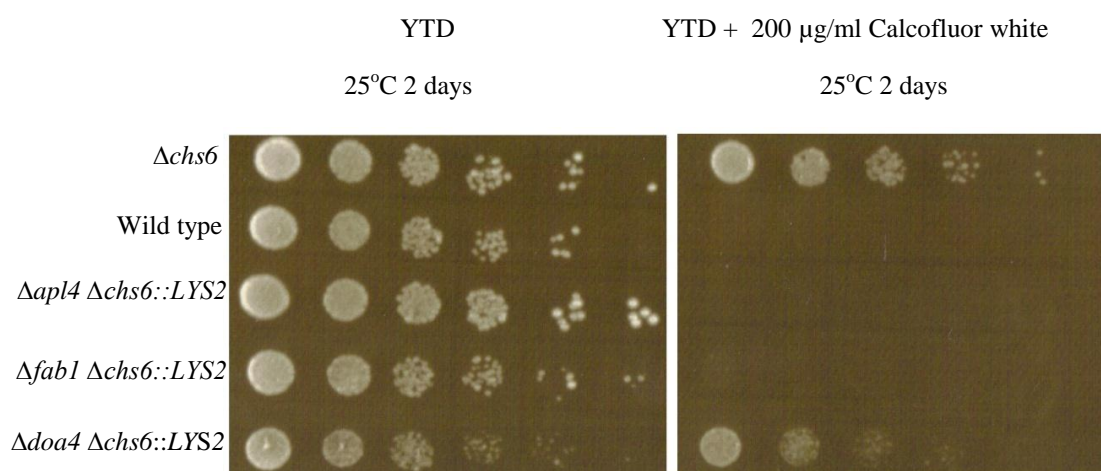


Various strains were grown to exponential phase till about $\sim 1 \times 10^7$ cells/ml in YPD + 2% glu for wild-type cells or SC-LYS+2% glu for double mutants. Dilution assay was carried out as described in methodology section. Cells were serially diluted five-fold then grown on YTD+2% glu agar plates or on the same plate but with 200 μ g/ml calcofluor white at 25°C for 2 days. Data represents three independent experiments.

The wild-type control is calcofluor sensitive and no growth is observed on the test plate. In agreement with the previous results of the 10-fold spot dilution plate, no decrease in calcofluor resistance is observed for the $\Delta vac7\Delta chs6$, $\Delta hsv2\Delta chs6$ and $\Delta atg21\Delta chs6$ strains. Interestingly growth of the $\Delta vac14\Delta chs6$ and $\Delta svp3\Delta chs6$ strains does seem to be calcofluor sensitive, growth is not reduced to the level seen in the wild-type or in the *apl4* or *fab1* mutant strains but the deletions appear to be having a clear effect and may partially contribute to the Fab1p/AP-1 trafficking pathway.

The role of Doa4p a ubiquitin ligase was also examined by making a double mutant, as this might be what connects this phenotype of $\Delta fab1$ cells to other Fab1p associated phenotypes such as defects in MVB sorting.

Figure 4.13 5X spot dilution of $\Delta doa4\Delta chs6$ mutant



Various strains were grown to exponential phase till about $\sim 1 \times 10^7$ cells/ml in YPD + 2% glu for wild-type cells or SC-LYS+2% glu for double mutants. Dilution assay was carried out as described in methodology section. Cells were serially diluted five-fold then grown on YTD+2% glu agar plates or on the same plate but with 200µg/ml calcofluor white at 25°C for 2 days. Data represents three independent experiments.

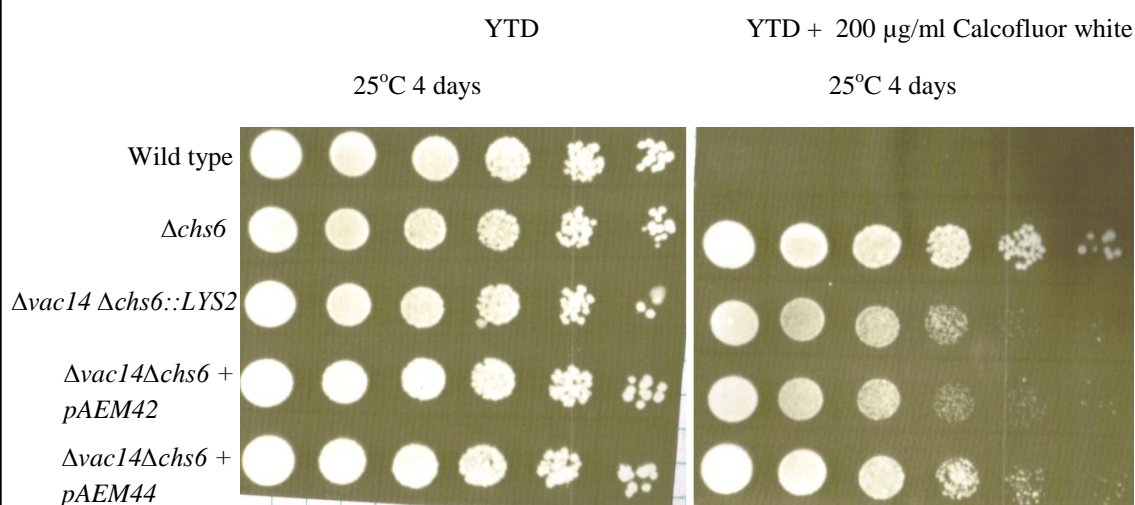
As shown above the additional deletion of *DOA4* does not appear to reverse the calcofluor resistance of a $\Delta chs6$ mutant. This result makes a role for ubiquitin in the trafficking of Chs3p unlikely.

To investigate the role of Vac14p in the Chs3p pathway further, the $\Delta vac14\Delta chs6$ was rescued by adding back *VAC14* expressed in a plasmid. Two constructs were available pAEM42 and pAEM44, both were used.

As shown in Figure 4.14 the $\Delta vac14 \Delta chs6$ double mutant appears to show reduced calcofluor sensitivity even when grown for a number of days at 25 °C. As a control the wild-type strain shows no growth. The pAEM42 plasmid does not appear to rescue the $\Delta vac14 \Delta chs6$ double mutant and exhibits the same amount of growth as the double mutant, on the calcofluor plate. The pAEM44 plasmid appears to increase growth on the test plate slightly. These results are consistent with Vac14p being part

of the same pathway that influences Chs3p trafficking as Fab1p. It also provides evidence that the plasmids may not fully rescue a *VAC14* deletion as previously observed in Chapter 3.

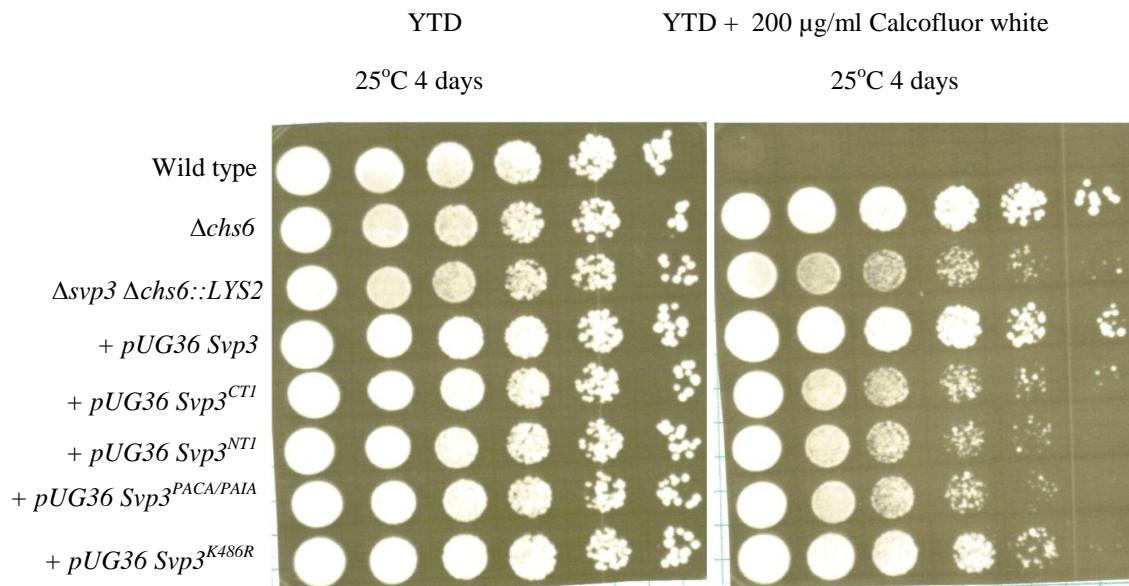
Figure 4.14 5X spot dilution of $\Delta vac14 \Delta chs6$ double mutant rescue.



Various strains were grown to exponential phase till about $\sim 1 \times 10^7$ cells/ml in YPD + 2% glu for wild-type cells or SC-Lys+2% glu for $\Delta vac14 \Delta chs6$ and additionally –Ura for strains with additional plasmid's. $\Delta vac14 \Delta chs6$ was transformed with the *pAEM42* or *pAEM44* plasmid. Dilution assay was carried out as described in methodology section. Cells were serially diluted five-fold then grown on YTD+2% glu agar plates or on the same plate but with 200µg/ml calcofluor white at 25°C for 4 days. Data represents three independent experiments.

In order to further investigate the role of Svp3p in this pathway, new constructs were made. It was discovered that heat shock can cause a $\Delta svp3$ mutant to revert, because of its temperature sensitivity. The original strain as observed in Figures 4.10 and 4.11 had been made using heat shock, so the mutant was re-made adding the *SVP3* deletion in last. The strain was also rescued with various *SVP3* plasmid constructs.

Figure 4.15 5X spot dilution of $\Delta svp3 \Delta chs6$ double mutant rescue.



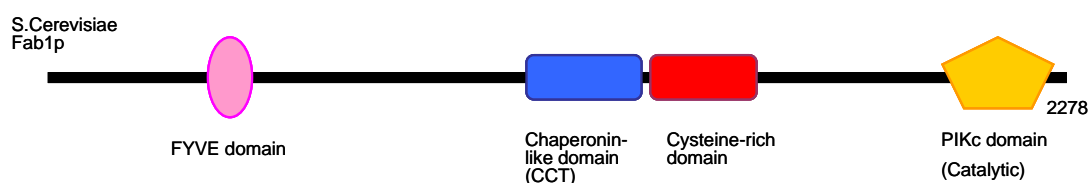
Various strains were grown to exponential phase till about $\sim 1 \times 10^7$ cells/ml in YPD + 2% glu for wild-type cells or SC-Lys+2% glu for $\Delta svp3 \Delta chs6$ and additionally –Ura for strains with additional plasmid's. $\Delta svp3 \Delta chs6$ was transformed with various Svp3 plasmids. Dilution assay was carried out as described in methodology section. Cells were serially diluted five-fold then grown on YTD+2% glu agar plates or on the same plate but with 200μg/ml calcofluor white at 25°C for 4 days. Data represents three independent experiments.

As shown in Figure 4.15 it appears that Svp3p does not in fact play a major role in Chs3p trafficking. It appears the previous results were probably due to a revertant strain. Although the $\Delta svp3 \Delta chs6$ double mutant does show slightly reduced growth on the calcofluor plate this is no where near as reduced as seen in the *fab1*, *apl4* or *vac14* $\Delta chs6$ double mutants, and in fact on the control plate reduced growth is also seen. Consistent with this, the pUG36 SVP3 plasmid can rescue the double mutant. The other mutant plasmids containing various portions of SVP3 (detailed in chapter 6) do not appear to rescue.

4.6 Calcofluor sensitivity of $\Delta chs6\Delta fab1$ is $PtdIns(3,5)P_2$ dependent

To test whether the rescue of calcofluor sensitivity in a $\Delta chs6\Delta fab1$ strain is dependent upon the Fab1p protein, part of the protein, or whether it is in fact lipid dependent a series of Fab1p expression plasmids were transformed into the $\Delta chs6\Delta fab1$ strain to see if they could rescue the calcofluor sensitivity phenotype. All the constructs were expressed under a galactose inducible promoter in the pEGKT vector.

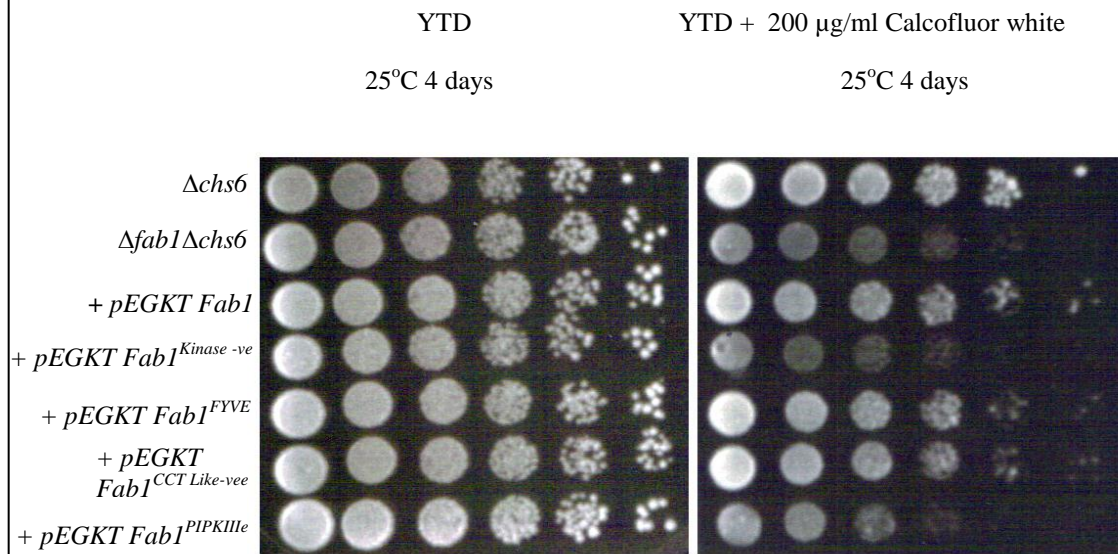
Figure 4.16 diagram of fab1p domains.



Fab1p contains various domains that were mutated. Fab1p mutated in its FYVE domain in conserved Cys residues, loses its ability to bind $PtdIns3P$. Mutation in the PIPKinase domain yields a catalytically inactive protein, unable to make $PtdIns(3,5)P_2$. The CCT-like domain was mutated in a conserved central Gly residue. The PIPKIII-unique mutant contains mutations in conserved Cys residues in the region of the protein.

As a control the plasmid pEGKT–Fab1 was used as this contains the whole ORF. A kinase dead version of *FAB1* was used to see if the process was lipid dependent as this plasmid lacks the ability to make $PtdIns(3,5)P_2$. Other controls with deletions of the following domains were also used: FYVE deleted so it can no longer bind $PtdIns3P$; CCT-like domain ablated; and PIPkIII unique Cysteine rich domain ablated.

Figure 4.17 5X spot dilution of $\Delta fab1 \Delta chs6$ double mutant rescue.

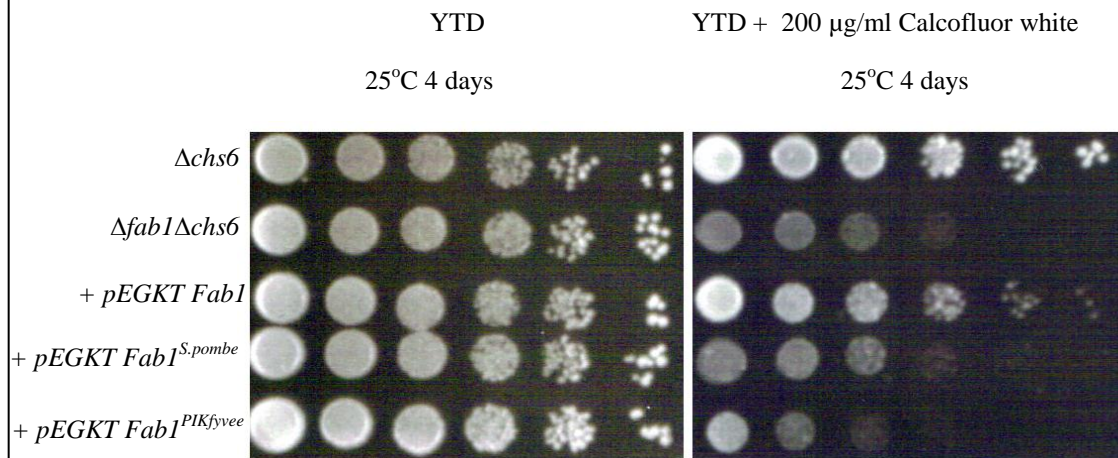


Various strains were grown to exponential phase till about $\sim 1 \times 10^7$ cells/ml in SC-Lys+2% glu for $\Delta fab1 \Delta chs6$ and additionally –Ura for strains with additional plasmids. $\Delta fab1 \Delta chs6$ was transformed with various *Fab1p* plasmids. Dilution assay was carried out as described in methodology section. Cells were serially diluted five-fold then grown on YTD+2% glu agar plates or on the same plate but with 200µg/ calcofluor white at 25°C for 4 days. Data represents three independent experiments.

From the results shown in Figure 4.17 it appears that the process *Fab1p* is involved in is dependent upon $\text{PtdIns}(3,5)\text{P}_2$. The *FAB1* construct lacking the kinase domain is unable to rescue the calcofluor sensitivity defect of $\Delta fab1 \Delta chs6$. Full length *FAB1* is able to rescue the double mutant strain as expected. Deletion of the PIPKIII domain makes a difference which again we would expect if the process relies on the lipid rather than the protein. Deletion of the CCT like and FYVE domains do not seem to make a difference, therefore it is likely these are not crucial for the process.

To see if the process could be complemented by other homologs of *FAB1*, plasmids containing an *S. pombe FAB1* and the mammalian homolog PIKfyve were also used. Bud scars were also examined for the same rescues carried out in this section and the results agreed with what is observed in the spot dilutions (Data not shown)

Figure 4.18 5X spot dilution of $\Delta fab1 \Delta chs6$ double mutant rescue.



Various strains were grown to exponential phase till about $\sim 1 \times 10^7$ cells/ml in SC-Lys+2% glu for $\Delta fab1 \Delta chs6$ and additionally –Ura for strains with additional plasmids. $\Delta fab1 \Delta chs6$ was transformed with various *Fab1p* plasmids. Dilution assay was carried out as described in methodology section. Cells were serially diluted five-fold then grown on YTD+2% glu agar plates or on the same plate but with 200µg/ml calcofluor white at 25°C for 4 days. Data represents three independent experiments.

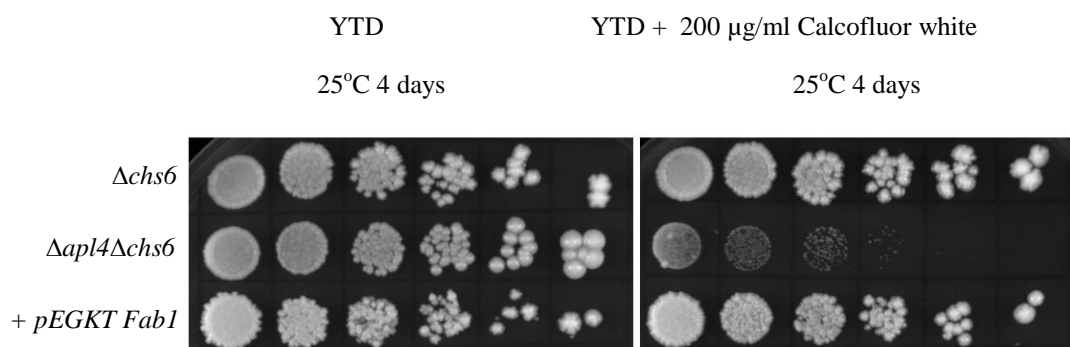
The results shown in Figure 4.18 indicate that both the *S. pombe* and PIKfyve versions of *FAB1* are not able to rescue the calcofluor sensitivity observed in the $\Delta fab1 \Delta chs6$ strain. The constructs, although expressed do not rescue the strains like wild-type *S. cerevisiae FAB1*, suggesting that the constructs are not properly regulated due to an inability to interact with *S. cerevisiae* proteins.

4.7 Fab1p and Apl4p are in the same pathway and perform the same role?

A question arose as to whether Fab1p and Apl4p were in fact carrying out the same role, in the same pathway or whether they were in the same pathway but were responsible for different jobs. To test this, *FAB1* plasmids as used above were transformed into a $\Delta apl4 \Delta chs6$ strain. If the proteins were in the same pathway, but

with different roles, over expression of *FAB1* should rescue the calcofluor sensitive phenotype and bring back calcofluor resistance.

Figure 4.19 5X spot dilution of $\Delta apl4 \Delta chs6$ double mutant rescue.



Various strains were grown to exponential phase till about $\sim 1 \times 10^7$ cells/ml in SC-Lys+2% glu for $\Delta apl4 \Delta chs6$ and additionally –Ura for strains with additional plasmids. $\Delta apl4 \Delta chs6$ was transformed with various *Fab1p* plasmids. Dilution assay was carried out as described in methodology section. Cells were serially diluted five-fold then grown on YTD+2% glu agar plates or on the same plate but with 200µg/ml calcofluor white at 25°C for 4 days. Data represents three independent experiments.

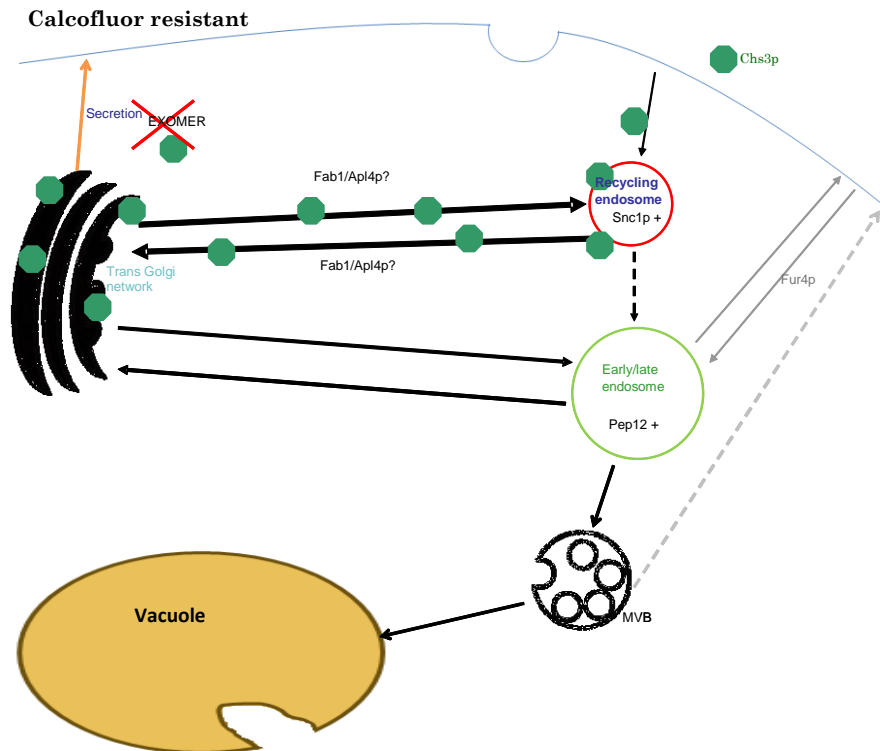
From Figure 4.19 it appears that the pEGKT-Fab1 plasmid can rescue the $\Delta apl4 \Delta chs6$ double mutant. One explanation for this is that Fab1p and Apl4p are in the same pathway. Over-expression of *FAB1* is able to rescue a $\Delta apl4$ strain, which may mean that the role of Apl4p can be compensated for, by Fab1p when it is over expressed. Another explanation is that Fab1p is downstream of Apl4p, an insight supported by earlier work (Phelan et al., 2006).

4.8 An alternative route for Chs3p to the cell surface.

The results above and the literature suggest that when *APL4* or *FAB1* are deleted in a $\Delta chs6$ background some Chs3p is still able to reach the cell surface. Schekman and colleagues have suggested that when exomer is inactivated, such as in a $\Delta chs6$ strain,

Chs3p just cycles continually from the TGN to the recycling endosome and this cycling is sufficient to prevent Chs3p from gaining access to the cell surface. It is only when an additional pathway, from the recycling endosome to the TGN is disrupted, that build up of Chs3p may occur in one of these compartments. This build up apparently allows some of the Chs3p to escape and leak back to the cell surface non-specifically (Valdivia et al., 2002). This hypothesis further suggests that Fab1p and AP-1 control just such an internal cycling pathway, between the PGE and the TGN but do not tell us in which direction this pathway acts. On one hand, it seems more likely that Fab1p controls the TGN to PGE step, because there is no known route from the PGE to the cell surface. Inactivation of the TGN to PGE step would lead to build-up of Chs3p in the TGN; a compartment which is constantly sending material to the cell surface, whereas inactivation of the PGE to TGN step would lead to build-up of Chs3p in the PGE; a compartment from which there appears to be no route to the plasma membrane. Having said this, the above argument is based the limited information we possess at present, as the PGE has been the subject of very few studies.

Figure 4.20 Diagram of disruption of exomer.

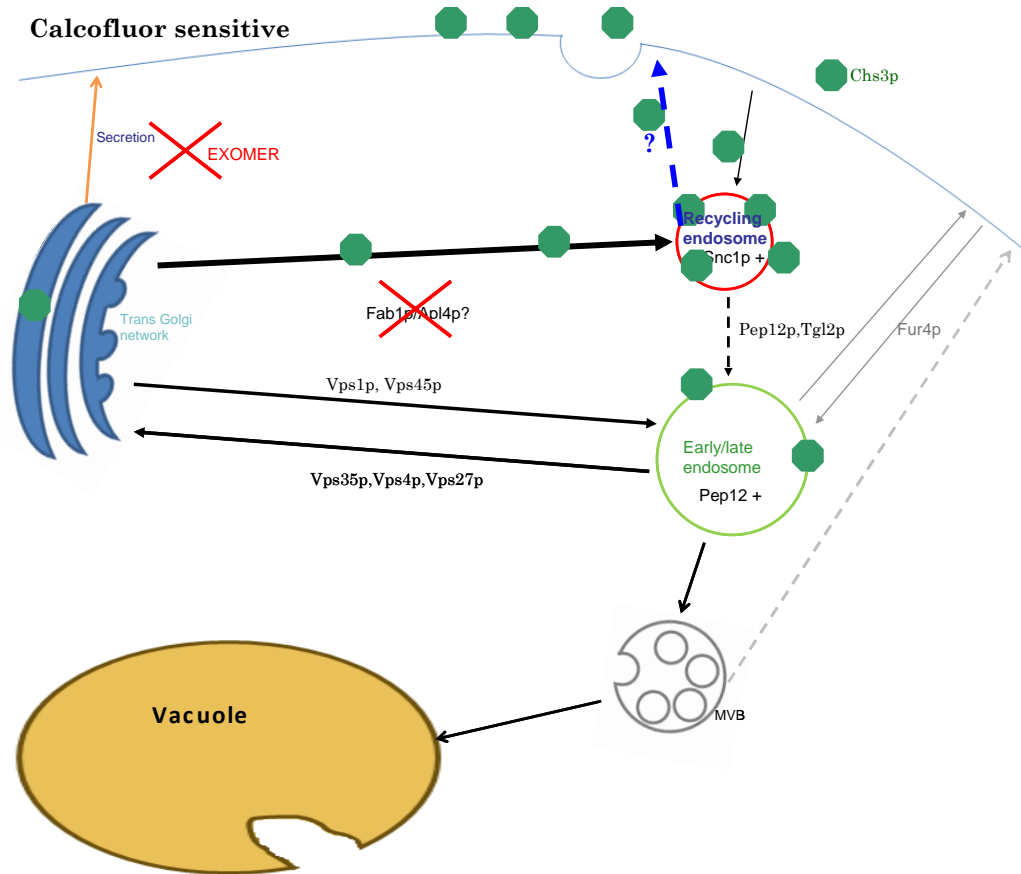


When exomer is not working such as in $\Delta chs6$ cells, Chs3p can no longer reach the cell surface and is instead cycled between the recycling endosome and TGN via a pathway that is controlled by Fab1p and the AP-1 complex.

What we wanted to know is does Chs3p then reach the cell surface by default or non-specific secretion from the TGN or does it reach the cell surface via another route? In order to discover if Fab1p was taking a known route a series of triple mutants were made to see if calcofluor resistance could be brought back in either a $\Delta fab1\Delta chs6$ or $\Delta apl4\Delta chs6$ strain.

If *VPS4* is deleted then Chs3p cannot take an alternative route to the TGN from the early/late endosome as shown in Figure 4.21. From the TGN Chs3p may be transported to the cell surface via mass secretion. Therefore a *VPS4* mutation was combined with the double mutants to see if Chs3p is transported from the early/late endosome to the TGN.

Figure 4.21 Diagram of disruption of exomer and retrograde pathway.

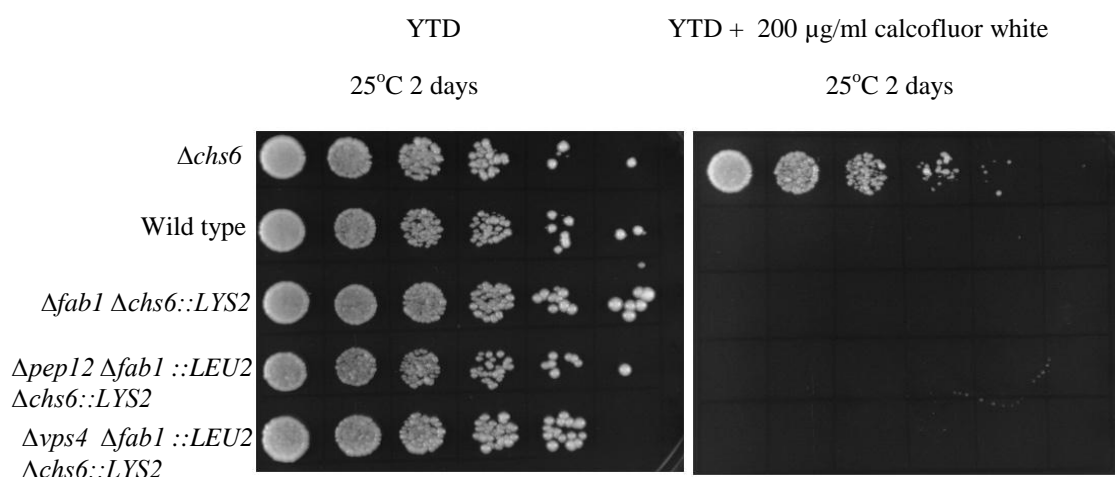


When exomer and the retrograde pathway from the recycling endosome and TGN controlled by Fab1p and the AP-1 complex is not working, such as in $\Delta fab1 \Delta chs6$ cells, Chs3p builds up at the recycling endosome and finds an alternative route to the plasma membrane.

An additional deletion of *PEP12* was also made in the double mutants, as when this gene is disrupted proteins are unable to be transported into the early endosome. This would indicate whether Chs3p finds a new route to the cell surface via the early/late endosome. To see if Chs3p reaches the cell surface by default or non specific secretion an additional triple mutant would need to be made. Unfortunately the only alleles of classical secretion mutants that are viable are the temperature sensitive

versions. Because *fab1* mutants also exhibit temperature sensitive growth, such alleles cannot be used to answer this question.

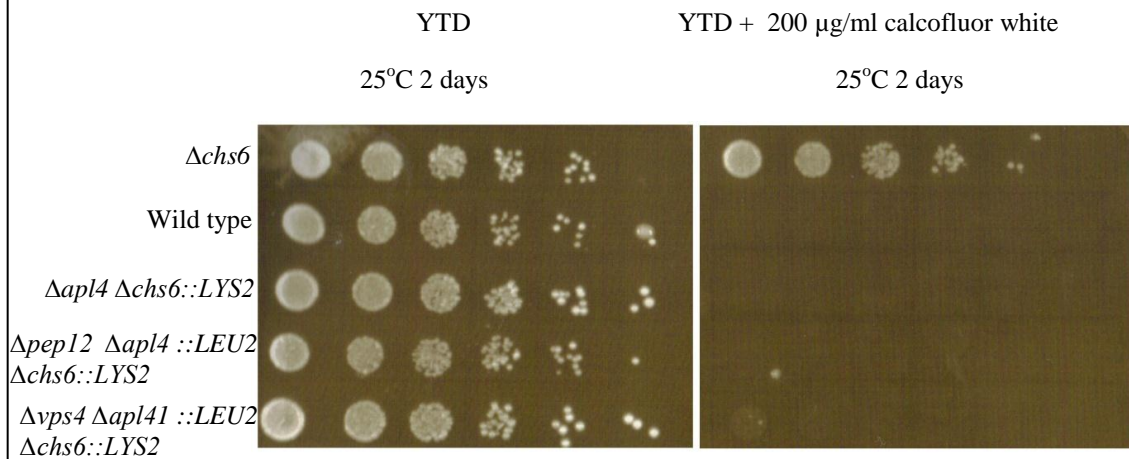
Figure 4.22 5X $\Delta fab1$ triple mutant spot dilution.



Various strains were grown to exponential phase till about $\sim 1 \times 10^7$ cells/ml in YPD + 2% glu for wild-type cells or SC-LYS+2% glu for double mutants. Dilution assay was carried out as described in methodology section. Cells were serially diluted five-fold then grown on YTD+2% glu agar plates or on the same plate but with 200 μ g/ml calcofluor white at 25°C for 2 days. Data represents three independent experiments.

As shown in Figures 4.22 and 4.23, additional deletion of either *VPS4* or *PEP12* does not bring back calcofluor resistance in either double mutant. This raises the possibility that Chs3p is not using either of these pathways to reach the cell surface. It is likely a novel route from the recycling endosome is used by Chs3p to leak back to the cell surface. Alternatively it may be that the triple mutants are so sick, they are increasingly drug sensitive. A further experiment to discover this would be to measure the amount of chitin in the cell walls of the triple mutants.

Figure 4.23 5X $\Delta apl4$ triple mutant spot dilution.



Various strains were grown to exponential phase till about $\sim 1 \times 10^7$ cells/ml in YPD + 2% glu for wild-type cells or SC-LYS+2% glu for double mutants. Dilution assay was carried out as described in methodology section. Cells were serially diluted five-fold then grown on YTD+2% glu agar plates or on the same plate but with 200 μ g/ml calcofluor white at 25°C for 2 days. Data represents three independent experiments.

4.9 Mutagenesis

Having established a role for Fab1p in the trafficking of Chs3p, a screen was devised to identify potential effectors of Fab1p, or more of the machinery that Fab1p acts with in this system. The logic for this is simple; if inactivation of Fab1p and AP-1 causes $\Delta chs6$ cells to become calcofluor sensitive again, then inactivation of other components of the same pathway should also result in restoration of calcofluor sensitivity. A classical mutagenesis approach was adopted in order to create mutations in a BY4742 $\Delta chs6$ strain. EMS was used to create random point mutations. For the mutagenesis reaction to work best, around 60% cell survival was required. The incubation period with EMS required to achieve this was found, by experiment, to be ~40 minutes. In order to select mutants that contained a mutation which brought back calcofluor sensitivity, mutants were plated both onto standard YEPD and replica plating using velvet onto the following media; YETD + 500 μ g calcofluor + 20 μ g/ml

Phloxine B. The concentration of calcofluor had previously been arrived at by using a range of calcofluor concentrations to discover one that allowed $\Delta chs6$ cells to grow, but not the double mutants. Essentially, the screen was looking for mutants that grew normally on the YEPD plate but died on the calcofluor plate. Phloxine B was added to the calcofluor plates because it is a vital stain which allows colonies that are mainly composed of dead cells to be identified. Dead colonies accumulate the dye and appear dark pink, whereas, live colonies appear white/light pink. As a secondary screen, all mutants identified as calcofluor sensitive were spot diluted onto calcofluor plates as above, to confirm their sensitivity, as this seems to be the most reliable test for mutants with defects in the Chs3p pathway.

4.9.2 Spot dilutions

Mutants were isolated and spot dilutions were carried out, using the same method as in section 4.5 and detailed in Chapter 2. For each of the mutants identified above, spot dilutions were carried out, to see whether in fact they were calcofluor sensitive. From spot diluting 72 mutants initially identified, it appeared that 26 did in fact show calcofluor sensitivity on re-test. These mutants were then used as the basis for further screens to characterise the mutations and see if they possessed any other Fab1p-like co-phenotypes.

The process of identifying these mutants was very lengthy, as the majority of initial plates examined contained no colonies which appeared to lose calcofluor resistance. A novel method using flow cytometry was therefore developed to make the initial screening process more efficient.

4.10 FACS sorting of strains

Flow cytometry can be used as a powerful method to sort groups of cells exhibiting a particular phenotype. It has previously been used to sort yeast cells into different groups on the basis of age, by calculating the number of bud scars present. It has also been used to isolate yeast mutants defective in localisation of vacuolar dyes (Zheng et al 1998). During FACS, a stream of cells is passed through a beam of light. Detectors are present and calculate the forward, side scatter and fluorescence. This data is then used to form a graph with a point for each 'event' or cell. Thousands of events can be captured in seconds. The aim of this work was to develop a FACS based assay that allowed sorting of the EMS mutagenised $\Delta chs6$ cells to identify mutants that had brought back bud scars and sensitivity to calcofluor white, or to enrich for calcofluor sensitive mutants. It also served as another way to characterise potential mutants that may be part of the Fab1p pathway because the FACS profile of any strain, after staining with calcofluor, is very distinctive. The FACS work was carried out in conjunction with Dr Tim Overton, Chemical Engineering, University of Birmingham UK.

In order to see if FACS could be used for this work, wild-type strain and $\Delta chs6$ strains needed to be examined to see if any difference could be observed in bud scar staining. The double mutants $\Delta fab1\Delta chs6$ and $\Delta apl4\Delta chs6$ could then be examined to see if their FACS profile became more like wild-type. Two different stains were used for this work; calcofluor white as previously used for microscopy and WGA-FITC that had previously been used for previous FACS work on yeast bud scars, because of its much narrower excitation and emission spectra.

4.10.1 Characterisation of the strains

Yeast cells were stained with calcofluor as previously described for microscopy and WGA-FITC as described in Chapter 2. Yeast strains were grown to late exponential phase, stained both ways and 10,000 events captured each time for single budded cells of each of the following strains; $\Delta fab1$, $\Delta chs6$, $\Delta fab1\Delta chs6$, $\Delta apl4\Delta chs6$. A $\Delta fab1$ strain was used as a control because a *FAB1* mutation makes the vacuoles of yeast cells larger and this could affect the scatter results. The sort graphs indicated that calcofluor appears to be better for distinguishing between the strains.

Table 4.1. Mean fluorescence data for the four different strains.

Strain	Hoechst blue mean for calcofluor stained cells (Population P2 single cells)	FITC-A mean for WGA-FITC stained cells (Population P2 single cells)
$\Delta fab1$ (bud scars)	414 \pm 62***	4589 \pm 172
$\Delta chs6$ (no bud scars)	165 \pm 28	2305 \pm 157
$\Delta fab1\Delta chs6$	378 \pm 44***	3854 \pm 168
$\Delta apl4\Delta chs6$	318 \pm 47***	2179 \pm 162

[Significantly different from $\Delta chs6$ values: *** $P < 0.001$, NS not shown]

The $\Delta fab1$ single mutant strain seemed to have the greatest calcofluor fluorescence which is as expected because it contains wild-type levels of bud scars and does not contain a defect in Chs3p transport. The lowest calcofluor fluorescence is seen in the

Δchs6 strain, which again agrees with previous results, as although there are no bud scars, fluorescence of the cell wall is still seen. The double mutants appear to lie in the middle of the two controls, which suggests they are bringing back some bud scars but do not completely return the levels to normal amounts. This is consistent with what is observed microscopically and the proposal that Chs3p ‘leaks’ back to the cell surface in the double mutants. Looking at just single cells (population P2), the levels seen in the double mutants seem to be close to the *Δfab1* control suggesting that the double mutants do bring back bud scars, and that they can be identified through flow cytometry. It is better to look at just single cell population as having budding cells will naturally increase the variable fluorescence because there is almost double the amount of cell wall present.

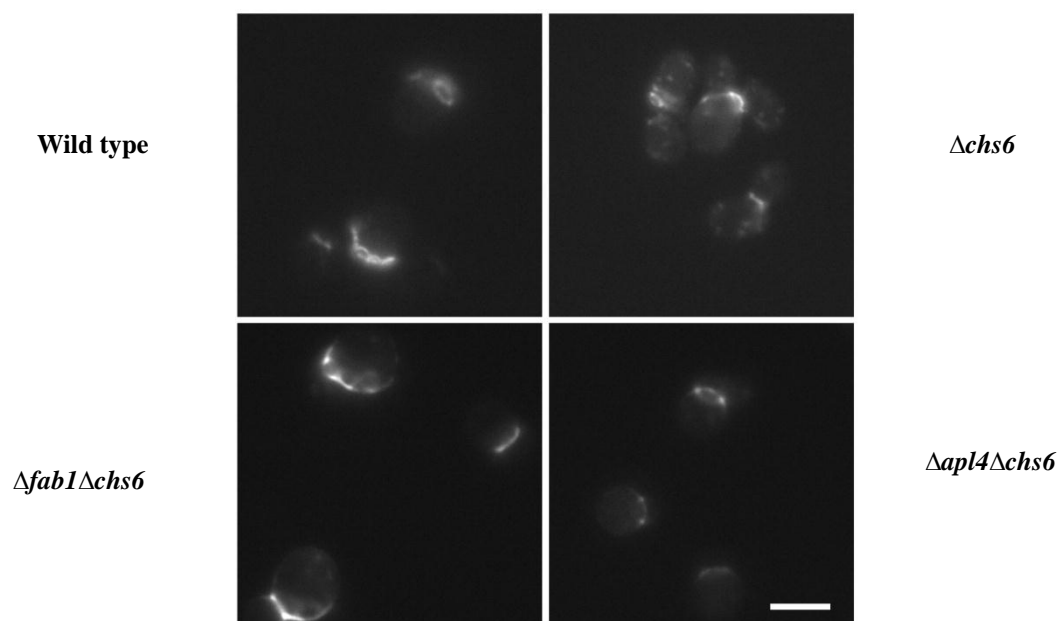
To find out why the WGA-FITC staining didn’t appear to work as well as calcofluor WGA stained cells were examined microscopically.

As shown in Figure 4.24 WGA-FITC stains bud scars in wild-type, and double mutant strains, although these are not as easy to see as staining with calcofluor. In *Δchs6* cells, diffuse staining is observed and in some cases small punctate like structures. The population, as with calcofluor staining, is not homogenous and some bud scars are still seen.

Figure 4.25 shown below shows *Δchs6* cells double stained with both calcofluor white and WGA-FITC.

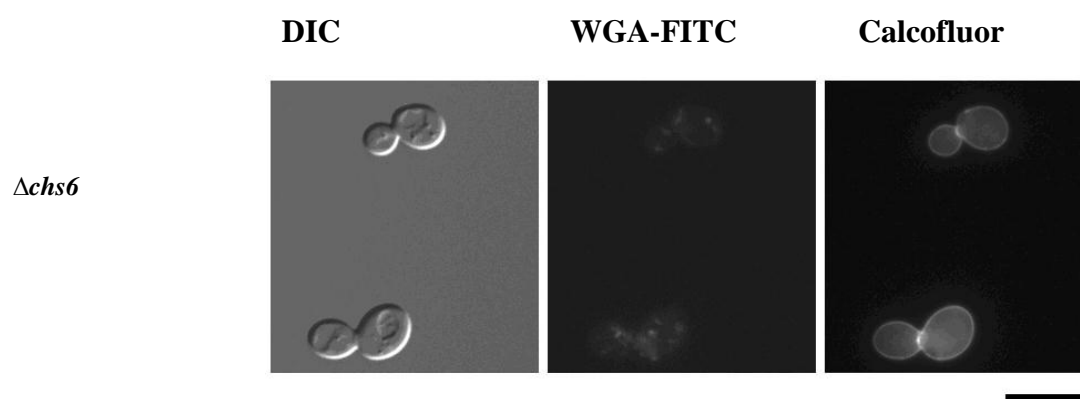
Figure 4.24 WGA-FITC staining of bud scars in wild-type and double deletion mutants.

Calcofluor staining



Bud scars can be visualised by staining cells with WGA-FITC. Shown above are fluorescence images of logarithmic phase cultures ($5 \times 10^6 - 1 \times 10^7$ cells/ml) of wild-type (top left), $\Delta chs6$ (top right), $\Delta fab1$ (bottom left) and $\Delta apl4$ (bottom right) stained with WGA-FITC. The images show staining visualised using a GFP filter. These images are representative of three replicate cultures. All strains were cultured in SC-YETD+2% glu medium and grown at 25°C. Scale bar represents 5 μ M.

Figure 4.25 WGA-FITC and calcofluor white stained $\Delta chs6$ cells



Staining of $\Delta chs6$ cells with both WGA-FITC and calcofluor. Shown above are fluorescence images of logarithmic phase cultures ($5 \times 10^6 - 1 \times 10^7$ cells/ml) Images are representative of three replicate cultures. All strains were cultured in SC-YETD+2% glu medium and grown at 25°C. Scale bar represents 5 μ M

Some cells in the population stained with WGA-FITC seem to contain small structures which may distort the FACS results. The WGA stain co-localises with calcofluor white on the bud scars of the few cells which contain them. On other cells where WGA is observed in smaller punctate structures, localisation with calcofluor is not seen, suggesting this is a difference between the stains (Data not shown).

Incubating cells with WGA-FITC for an extra 15 minutes and washing three times seems to improve the staining of cells and reduce the amount of background observed, but it appears that calcofluor is a better stain for FACS analysis. It may be that differences are observed because of the specificities of each dye; calcofluor can also bind to other polysaccharides.

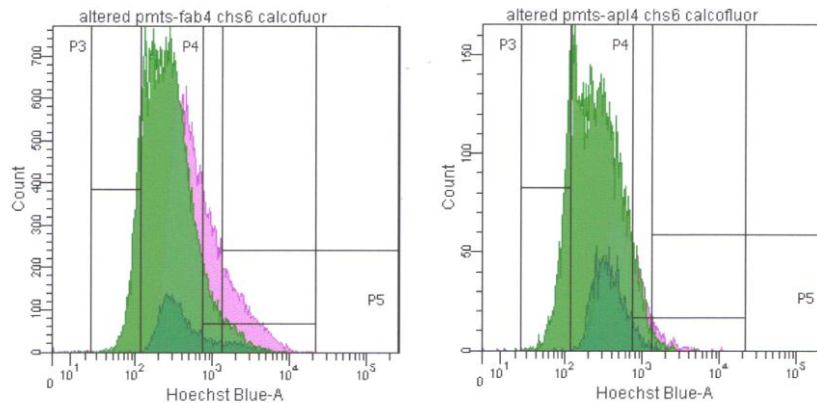
4.10.2 Sort 1 of low and high fluorescence population of the $\Delta fab1\Delta chs6$ strain.

The $\Delta fab1\Delta chs6$ strain produced an interesting fluorescence graph for the calcofluor staining, where there seem to be two separate peaks; this was also apparently the case for the other double mutant, although not quite as distinctly.

To investigate the result as seen in Figure 4.26 a sort was taken of the low fluorescence population and the high fluorescence population to be examined microscopically (Figure 4.27).

As shown in Figure 4.27, it appears that the low fluorescence population does not contain cells with bud scars. All of the cells examined from the high fluorescence population clearly had one or more bud scars present; this is intriguing as previous microscope experiments had indicated that the bud scars were present in only a subset of cells in any population and this result confirms it.

Figure 4.26. Fluorescence profiles of $\Delta fab1\Delta chs6$ and $\Delta apl4\Delta chs6$.

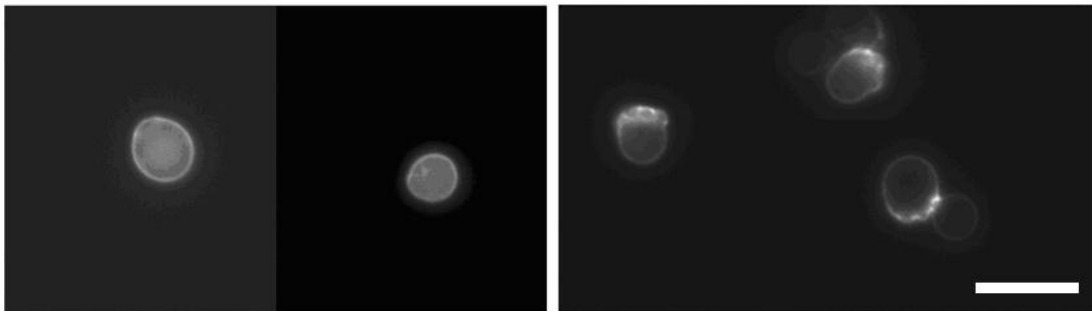


Samples were stained with calcofluor, graph represents 10000 events.

Figure 4.27. Microscopy of sorted $\Delta fab1\Delta chs6$ cells.

Low fluorescence sort

High fluorescence sort

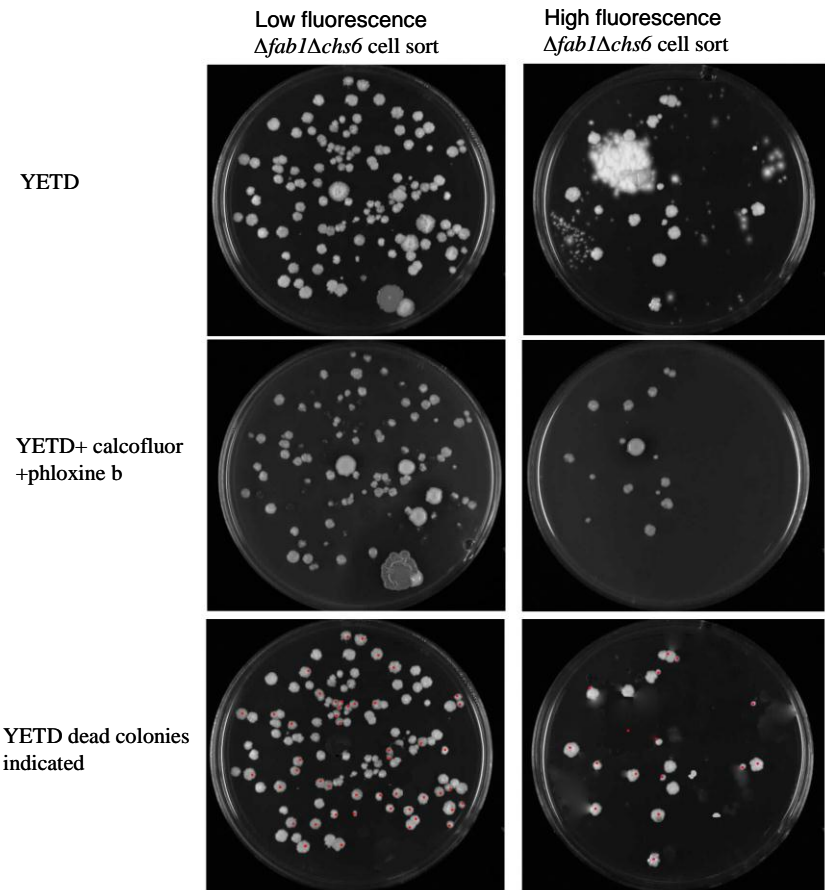


Calcofluor staining of $\Delta fab1\Delta chs6$ cells sorted for both high and low fluorescence. with both WGA-FITC and calcofluor. Shown above are fluorescence images of logarithmic phase cultures ($5 \times 10^6 - 1 \times 10^7$ cells/ml) Images are representative of three replicate cultures. All strains were cultured in SC-YETD+2% glu medium and grown at 25°C. Scale bar represents 5 μ M

To see if either of the populations showed differences in sensitivity to calcofluor, a growth test was also performed. Cell suspensions used for microscopy were diluted to get around 200 colonies per plate. After growth on a YETD plate for two days at 25°C the plates were replica plated using velvet onto new plates containing 500µg/ml calcofluor white and 20µg/ml Phloxine B. Plates were again grown for 2 days at 25°C (See Figure 4.19). Contamination seemed to be present; probably due to the buffer used for FACS.

For the high fluorescence sort, around 30% could grow on the calcofluor media which means, 70% showed the calcofluor sensitivity expected of a $\Delta fab1\Delta chs6$ strain. In the low fluorescence sort around 60% of the colonies could grow on calcofluor media meaning 40% of colonies showed calcofluor sensitivity. So there is a significant difference between the two sorts, but the data suggests that the calcofluor is killing even resistant cells when they are plated as single cells. If more time was available experiments could have been performed to optimise the calcofluor concentration, especially for this assay.

Figure 4.28. Replica plating of both low and high fluorescence sorts of $\Delta fab1\Delta chs6$ cells



Medium	Low fluorescence sort	High fluorescence sort
	Percentage of colonies that are alive	
YETD	100% ±0	100% ±0
YETD+Calcofluor+Phloxine b	59.7% ±5.3***	27.2% ±4.6***

[Significant difference between high and low fluorescence sort at ****P*<0.001,]

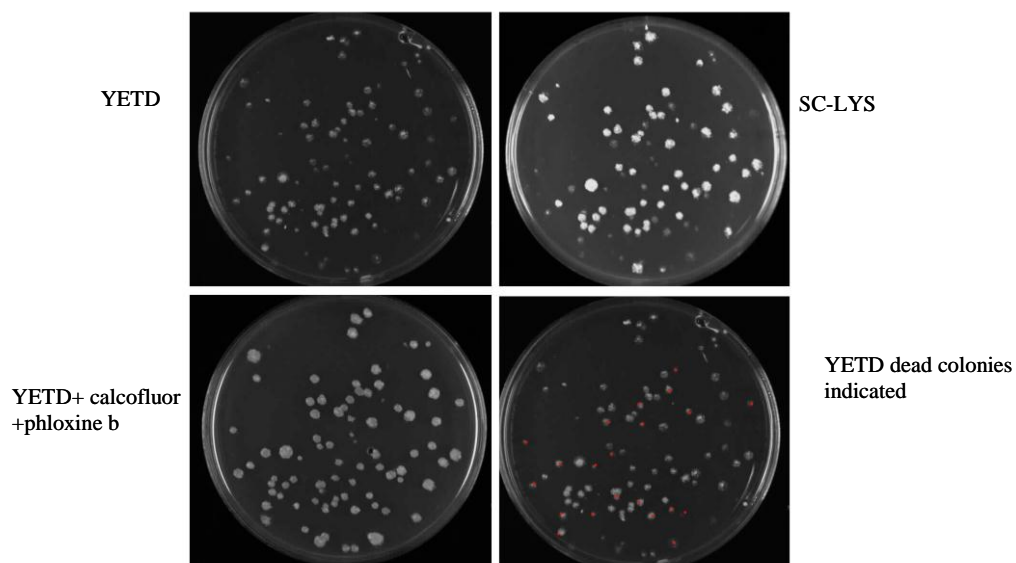
Replica plating of both low (left hand columns) and high fluorescence sort (right hand column) of $\Delta fab1\Delta chs6$ cells. The first panels show original colonies on YETD plates. The middle panel shows growth on calcofluor plates. The bottom panels are of the original YETD plates that have been adjusted in Photoshop to remove contamination red dots to indicate colonies that are calcofluor sensitive.

Sort 2 Sorting double mutants from a mixture.

Sort 2 was designed to see if FACS could be used to sort potential double mutants which bring back bud scars from the EMS mutagenised cell culture. To see if this would work $\Delta chs6::KAN$ and $\Delta apl4 \Delta chs6::LYS2$ calcofluor stained strains were mixed to give a 1% population of double mutants. The sample was run on the FACS machine and a gate was drawn around the resulting graph, to select cells with high fluorescence; this was, as expected, approximately 0.1% of the population. The graphs for the double mutant and $\Delta chs6$ samples were used to help define the gate for cells to be sorted. Approximately 51% of the sorted cells survived the process of being plated onto YETD and were alive after being grown at 25 °C for three days. The plate was then replica plated onto YETD+ 500µg/ml calcofluor white + 20µg/ml Phloxine B, to see how many of the colonies were actually double mutants and resistant to calcofluor. Replica plating was also carried out onto SC-Lys media to select the $\Delta apl4 \Delta chs6::LYS2$ double mutants.

From Figure 4.29 it can be seen that approximately 22.3% of colonies failed to grow on SC-LYS and are therefore $\Delta chs6::KAN$ colonies. This means that around 77% of sorted colonies are in fact $\Delta apl4::KAN \Delta chs6::LYS$ cells. If the mixture had been plated without any form of sorting, out of 100 cells only 1 colony would be expected to grow. It appears that the sorting worked very well to enrich the number of double mutants present. This represents a good method in order to sort mutagenised $\Delta chs6$ cells that have bud scars. This meant the screen could be performed more efficiently.

Figure 4.29. Replica plating sorts from mixture. of $\Delta apl4::KAN\Delta chs6::LYS$ and $\Delta chs6::KAN$ cell sorted to get just $\Delta apl4::KAN\Delta chs6::LYS$ cells



<i>Medium</i>	<i>Percentage of alive colonies</i>
<i>YETD</i>	<i>100% ± 0</i>
<i>YETD+ Calcofluor+ Phloxine b</i>	<i>80.2% ± 9.7</i>
<i>SC-LYS</i>	<i>77.7% ± 6.1</i>

Replica plating sort from mixture of $\Delta apl4::KAN\Delta chs6::LYS$ and $\Delta chs6$ cell sorted to get just $\Delta apl4::KAN\Delta chs6::LYS$ cells Red dots indicate colonies that do not contain the LYS marker and therefore cannot grow on SC-LYS so are $\Delta chs6$ colonies.

4.11 Characterisation of the EMS mutants.

From the initial plate based screen (numbered with the prefix 1) twenty six mutant colonies were identified that revert the $\Delta chs6$ strain calcofluor resistance back to sensitivity. A further thirty five colonies were identified by FACS (numbered with the prefix 2).

To characterise the mutants, and see if it was likely any of them were involved in the Fab1p pathway, a number of secondary screens were initiated. The DIC light phase image was examined to determine the morphology of the cells, with particular attention paid to mutants with abnormal vacuoles, as aberrations in this compartment are characteristic of mutants in components of the Fab1p pathway. Calcofluor staining was also conducted to see if bud scars had been restored, localisation of Chs3-GFP (clones in group one) was also examined. For results of these experiments please see appendix 1 and 2.

The mutants were also spot diluted onto YETD plates containing 0.9M NaCl and incubated at 25°C to see if the clones were salt resistant. A characteristic of *FAB1* mutant cells is temperature sensitivity, so the mutants were also tested to see if they exhibited this ‘co-phenotype’. To test temperature sensitivity a YETD spot dilution was also incubated at 37°C.

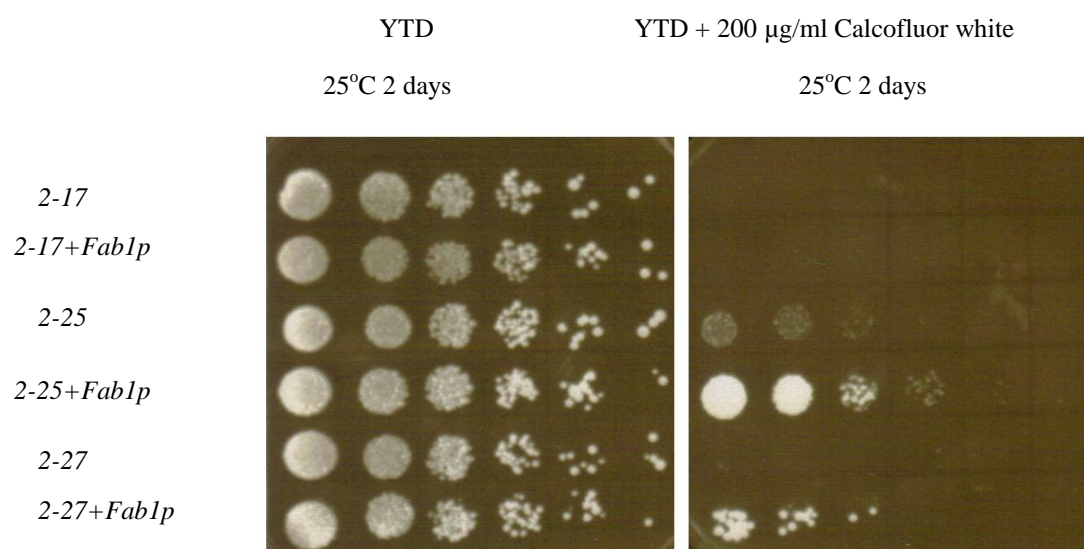
As a further test for Fab1p phenotypes, the mutants were also screened for defects in MVB sorting. This was performed by visualising two constructs, Phm5-GFP and ubiquitinated Phm5-GFP. Cells in which Fab1p or AP-1 have been inactivated, display a defect in MVB sorting, and do not correctly target Phm5p to the vacuole lumen. In these cells Phm5-GFP is visualised as a ring on the vacuole membrane. However UbPhm5-GFP can be correctly targeted to the vacuole lumen in $\Delta fab1$ cells, as the construct expresses Phm5-GFP as an in frame, N-terminal fusion with a single ubiquitin. We reasoned that because Phm5p and Chs3p mislocalisation both occur in *fab1* and *apl4* cells, they might also in novel mutants as well.

4.12 Rescue of large vacuole bearing EMS mutants by Fab1p overexpression.

From the microscope data gathered in section 4.11 it could be seen that some of the clones had a large vacuolated phenotype similar to that of a $\Delta fab1$ strain; some also possessed a temperature sensitive growth defect. To test whether these clones contained a mutation in the *FAB1* gene, a plasmid that expressed *FAB1*: pEGKT – *FAB1* was placed into each of the strains. This plasmid is under the control of a galactose inducible promoter. Spot dilutions were carried out onto media containing 200µg calcofluor and galactose as a carbon source. This tested whether the introduction of the *FAB1* plasmid had reversed the phenotype of the EMS mutants and brought back calcofluor resistance.

From the results it could be seen that none of the group 1 mutants tested (1-2, 1-4, 1-5, 1-13, 1-16, 1-20, 1-21, 1-22, 1-23 and 1-24) could be rescued and made calcofluor resistant again by the addition of the full length *FAB1* gene.

Figure 4.30 5X spot dilution of pEGKT *Fab1* rescues



Various strains were grown to exponential phase till about $\sim 1 \times 10^7$ cells/ml in YPD + G418. Each mutant had been transformed with pEGKT *Fab1*. Dilution assay was carried out as described in methodology section. Cells were serially diluted ten-fold then grown on YTD+2% glu agar plates or on the same plate but with 200µg/ml calcofluor white at 25°C for 2 days. Data represents three independent experiments.

As shown in Figure 4.30 it appears that mutants 2-25 and 2-27 can be rescued by addition of *FAB1*. However, the ‘rescue’ of 2-25 is more dubious as the growth of 2-25 on calcofluor plates is already more than expected. The change in growth observed for 2-27 however is large and it appears it is truly being rescued. Mutants 2-13, 2-14, 2-15, 2-31 and 2-34 were also tested but showed no difference in growth. The screen was performed to try and isolate additional components of the pathway influenced by *Fab1p* and *PtdIns(3,5)P₂*. *FAB1* over expression is an important experiment, as those mutants who *FAB1* can rescue are likely to be in the same pathway.

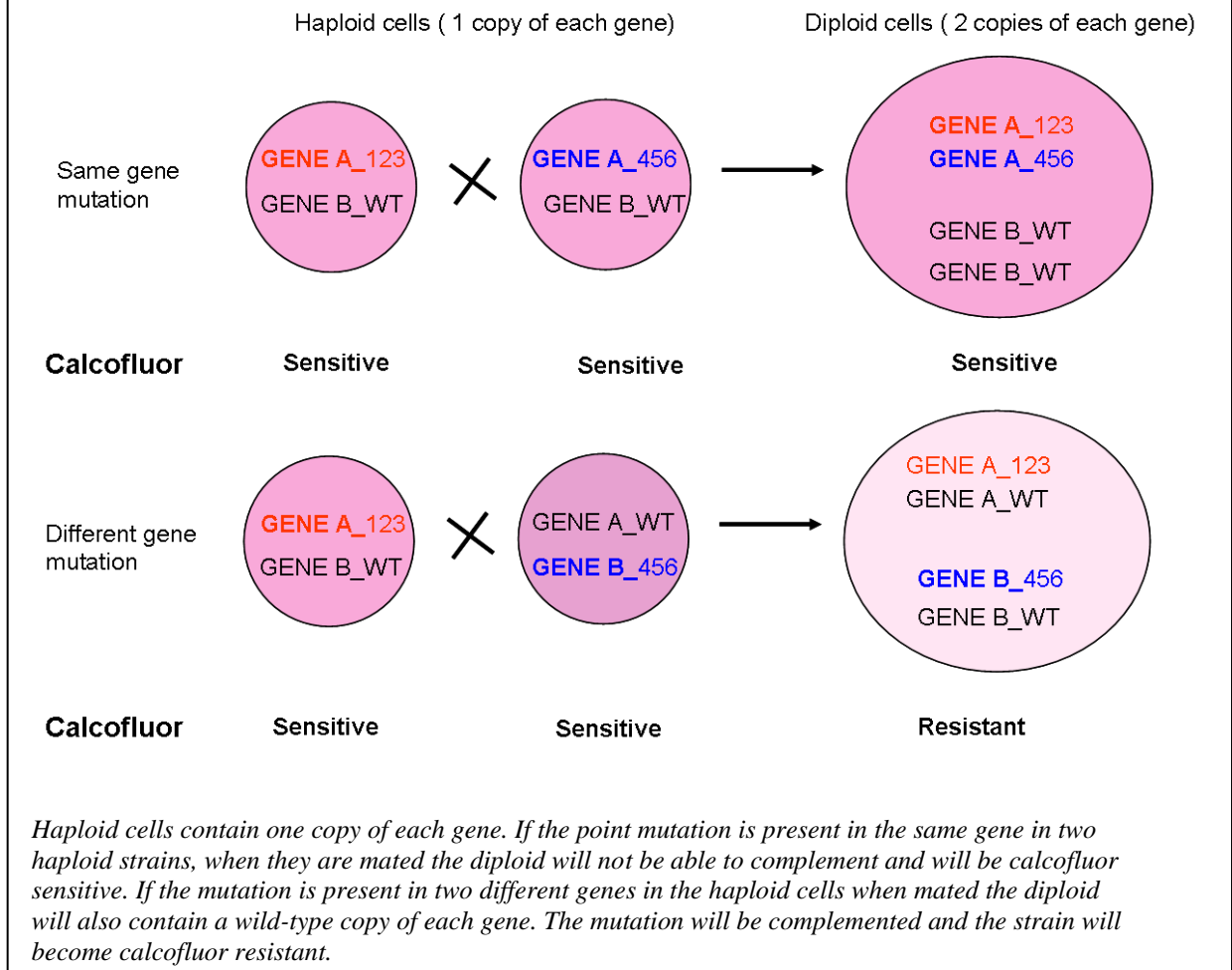
4.13 Complementation analysis.

To discover whether the mutants identified represent mutations in different genes or just different mutations in the same gene, yeast complementation analysis was used.

When two haploid *S. cerevisiae* strains are mated together they will form a diploid. If the two haploid strains contain a deletion in the same gene that is bringing back calcofluor sensitivity, the mutations will not be able to complement in the diploid, and the diploid will still be calcofluor sensitive. If the two strains contain mutations in different genes, complementation can occur because the cell will contain one unmutated copy of each gene, so the diploid will be calcofluor resistant. One caveat is that the above assumes that gene-dosage has no effect in the system under study; however, Chs3p trafficking does not appear subject to gene dosage for those components that are known. A diagram of this system is shown in Figure 4.31.

To be able to mate each of the clones with each other, the mating type of the cells needed to be changed. In laboratory strains of *S. cerevisiae*, two mating types are present; a and α , and each strain is 'locked' into one of these types because of inactivation of the HO locus. The gene product of HO is usually responsible for random mating type switching in wild yeast. In order to mate, one haploid strain needs to be a and the other α (Sherman, 2002).

Figure 4.31 Cartoon of complementation



The EMS mutagenesis was carried out in the BY4742 $\Delta chs6$ background and therefore all mutants isolated were α type. To change the mutants to the \underline{a} mating type, the mutant strains were backcrossed with a BY4741 $\Delta chs6$ strain; this also had the secondary effect of cleaning up the genetic background since chemical mutagenesis often introduces more than one mutation into each cell, and sporulation is an excellent way to remove unlinked mutations that are on different chromosomes (or even on the same chromosomes because of chiasmata). In order to select a haploid strain which contained the desired mutation, and was $\Delta chs6$ and \underline{a} type, sporulation and tetrad dissection were carried out. When a diploid is starved under certain conditions it will

sporulate and form a tetrad of four haploids, which can be separated and analysed by replica plating, to discover the haploid cell with the desired auxotrophic markers and the phenotype of interest. In order to uncover the colony which had the mutation of interest, tetrad plates were replica plated onto G418 to select $\Delta chs6$, onto calcofluor plates to select the mutation as the colony will still be calcofluor sensitive and then onto SC-Lys and SC-Met to select for markers which are required to select for diploids. In order to test for mating type, test matings were conducted with known mating types, to see if diploids would form; diploids will only form if opposite mating types were present.

Once the mating type of the mutants had been changed, each mutant was crossed with the other mutants to form a diploid. The diploid was then tested for complementation, by plating onto a calcofluor plate.

It appears that all of the mutations tested are able to complement each other and therefore the screen is likely to represent 61 distinct complementation groups. This high number of distinct complementation groups suggests that the screen was not saturated and that multiple processes and pathways can lead to loss of calcofluor resistance in yeast. Many of the ways to become calcofluor sensitive may have nothing to do with Chs3p trafficking and might include inactivation of drug transporters or defects in the cell wall; these processes are known to result in non-specific drug sensitivity from previous screens.

As a test for dominant negative mutations, all the haploid mutants were mated with BY4741 $\Delta chs6$ cells. If any strain possessed a dominant negative mutation this cross would remain calcofluor sensitive. None of the strains showed this phenotype so no dominant negative mutants were isolated.

In order to discover which gene had been mutated in each of the clones identified, a plasmid library was used to rescue the mutation. A pYEp13 based library was used which contains fragments of the whole yeast genome inserted into a *LEU2* based plasmid. The library was made by partially digesting yeast genomic DNA with *Bam**HI* and covers the genome approximately 5 times.

When the library is transformed into the mutant strains, the plasmid containing the gene that is mutated in the strains will be able to complement the mutation. The plasmid can be isolated by plating transformants onto Sc-Leu plates to select for yeast which have taken up the plasmid, and then onto plates containing 600µg/ml calcofluor white and 20µg/ml Phloxine B. The colonies containing plasmids which have complemented should now be able to grow on the calcofluor plates. This method proved to be problematic as some of the strains are not as calcofluor resistant as others, so when replica plated onto calcofluor plates many of the colonies still grew. This is because a colony of cells can grow on calcofluor plates more easily than if you spot dilute because larger numbers of cells often 'shield' some members of the colony from the full effects of any drug or treatment, resulting in many 'false positives'. If more time was available a way to overcome this would have been to keep replica plating onto media that does not select for the plasmid but does for calcofluor resistance (e.g. plates with calcofluor). Eventually the colonies which are not resistant due to complementation from the plasmid will lose this episome as there is no selective pressure to keep the gene encoded by the plasmid in the genome. Thus when these mutants are replica plated back onto Sc-Leu plates eventually only a small number of colonies should remain whose plasmids can be extracted and transformed back into the original strain to see if they do in fact rescue.

When a plasmid was isolated that did indeed restore calcofluor resistance it was sequenced to get the start and end of the insert. The sequencing results were then BLAST searched on the Sacchromyces Genome Database and the insert contained thereby delineated. This usually resulted in identification of a piece of genomic DNA encoding 3 or 4 genes because the average insert size in this library is around 15 kb. Potential candidates were then further examined, by creation of double deletions of each potential gene with $\Delta chs6$.

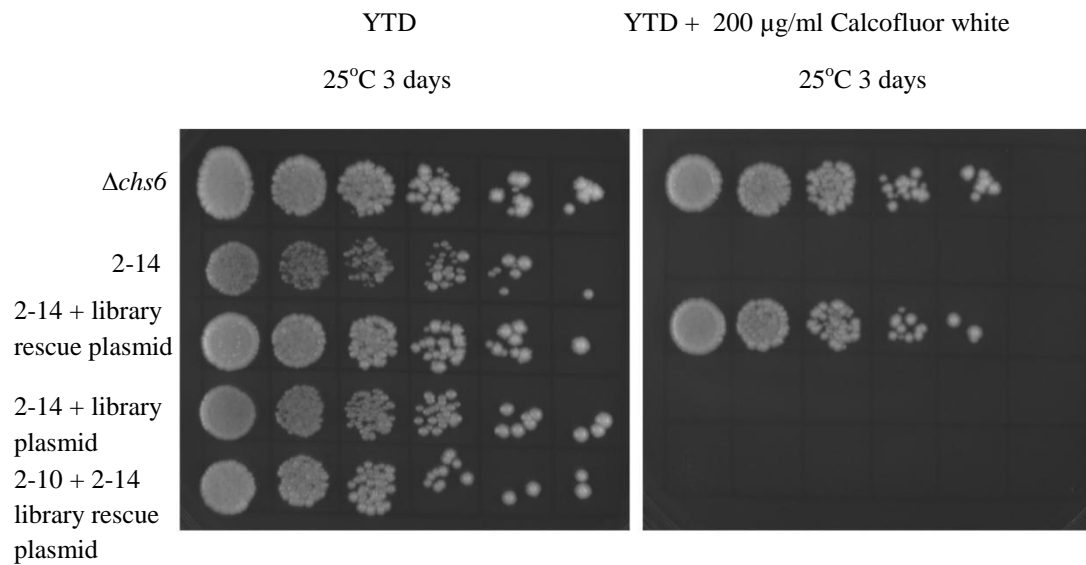
Due to the lengthy process of identifying genes it was only possible to confirm the nature of mutations in four of my strains.

4.14 Mutant 2-14 is *APL2*

Through the process described above, mutant 2-14, sorted in the FACS screen was identified.

As shown in Figure 4.32, the plasmid that appeared to rescue mutant 2-14, does indeed allow the strain to grow on calcofluor containing plates. The plasmid however does not rescue another mutant, so the rescue observed is the result of specific complementation. To make sure the insert is what is conferring resistance, another library plasmid was transformed into mutant 2-14; as shown this does not restore calcofluor resistance.

Figure 4.32 5X spot dilution of 2-14 rescues.



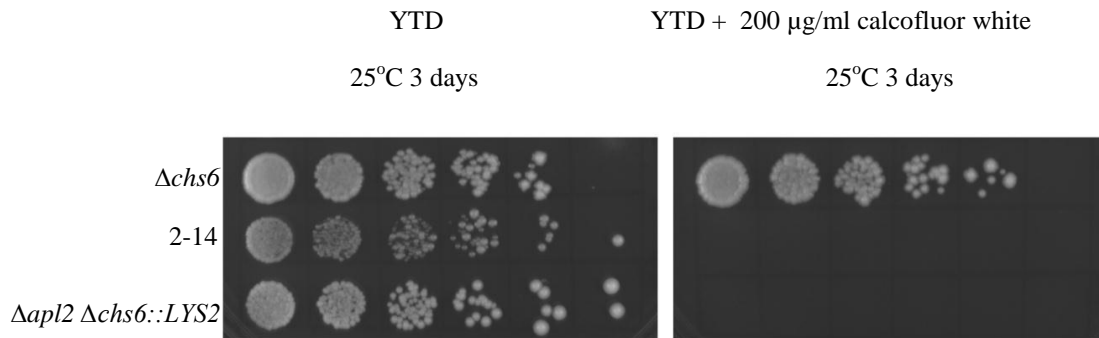
Various strains were grown to exponential phase till about $\sim 1 \times 10^7$ cells/ml in YPD + 2% glu + G418 or SC-LYS+2% glu for double mutants. Dilution assay was carried out as described in methodology section. 2-14 was transformed with the plasmid from the library that rescued the strain. This plasmid was also transformed into mutant 2-10. Another library plasmid was transformed into 2-14 to serve as a control. Cells were serially diluted five-fold then grown on YTD+2% glu agar plates or on the same plate but with 200µg/ml calcofluor white at 25°C for 3 days. Data represents three independent experiments.

The plasmid was sequenced and *APL2* was contained in the insert. Apl2p is a beta adaptin and a large subunit, of the AP-1 complex, like Apl4p. Like the other members of the AP-1 complex *APL2* has previously been shown to have a role in this pathway. A $\Delta apl2\Delta chs6$ double mutant was made to see if it does in fact have calcofluor sensitivity.

As shown in Figure 4.33 the $\Delta apl2\Delta chs6$ double mutant, like 2-14 is unable to grow on media supplemented with calcofluor. *APL2* possess the same phenotype as *FAB1*, in that when deleted in addition to $\Delta chs6$ it is able to bring back calcofluor sensitivity. To confirm that 2-14 did contain a mutation in *APL2*, 2-14 was mated with $\Delta apl2\Delta chs6$, and the resulting diploid was calcofluor sensitive, showing that the mutation could not be complemented. This suggests 2-14 possesses a mutation in the

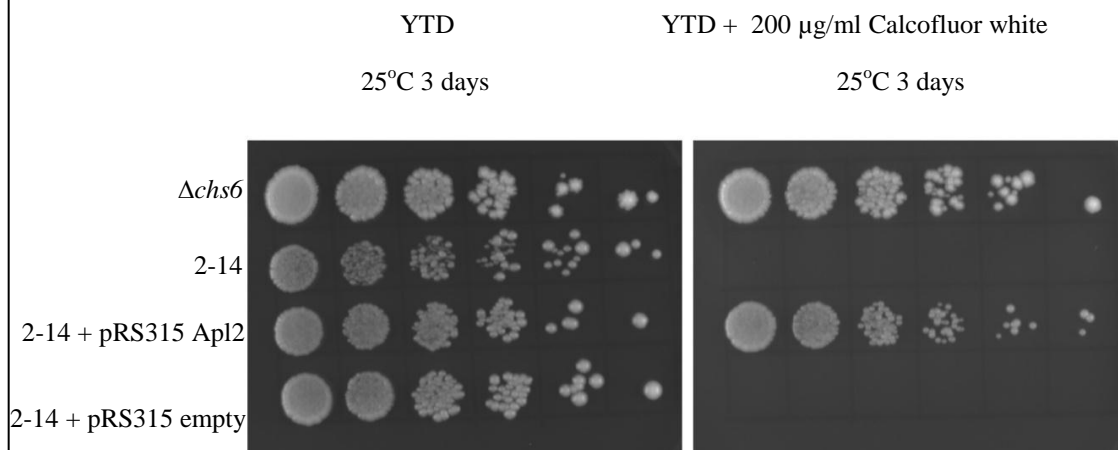
APL2 gene. Therefore *APL2* should be able to rescue 2-14, in order to verify this pRS315-*APL2* plasmid was transformed into 2-14.

Figure 4.33 5X spot dilution of 2-14.



Various strains were grown to exponential phase till about $\sim 1 \times 10^7$ cells/ml in YPD + 2% glu + G418 or SC-LYS+2% glu for double mutants. Dilution assay was carried out as described in methodology section. Cells were serially diluted five-fold then grown on YTD+2% glu agar plates or on the same plate but with 200µg/ml calcofluor white at 25°C for 3 days. Data represents three independent experiments.

Figure 4.34 5X spot dilution of 2-14 *Apl2p* rescue.



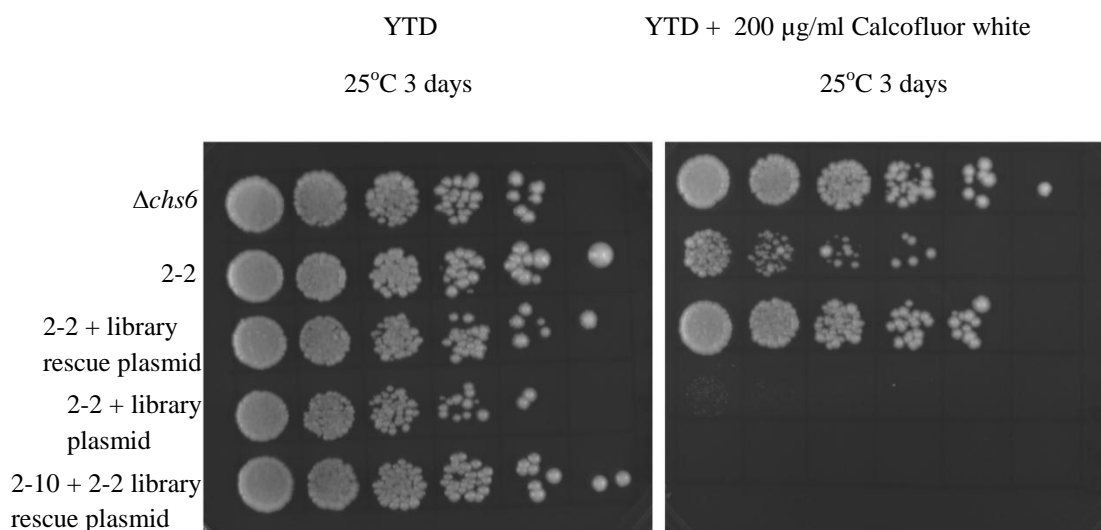
Various strains were grown to exponential phase till about $\sim 1 \times 10^7$ cells/ml in YPD + 2% glu + G418 or SC-LYS+2% glu for double mutants. Dilution assay was carried out as described in methodology section. 2-14 was transformed with pRS315*Apl2*, or the empty vector. Cells were serially diluted five-fold then grown on YTD+2% glu agar plates or on the same plate but with 200µg/ml calcofluor white at 25°C for 3 days. Data represents three independent experiments.

As shown in Figure 4.34 *APL2* expressed in pRS315 can rescue the calcofluor sensitivity of 2-14, this is further proof that 2-14 contains a mutated *APL2*. Any good screen should isolate both known and unknown components of the pathway examined. Identification of *APL2* as one of the mutants helps to validate the screen, because a known component has been isolated. This indicates the screen should be well placed to identify novel members of the trafficking pathway.

4.15 Mutant 2-2 is *GUP1*.

A library plasmid as shown in Figure 4.35 was identified that only rescued mutant 2-2.

Figure 4.35 5X spot dilution of 2-2 rescues.



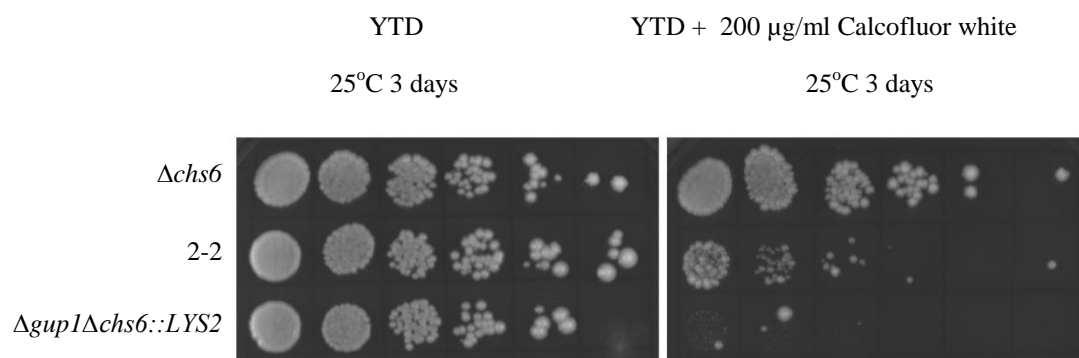
Various strains were grown to exponential phase till about $\sim 1 \times 10^7$ cells/ml in YPD + 2% glu + G418 or SC-LYS+2% glu for double mutants. Dilution assay was carried out as described in methodology section. 2-2 was transformed with the plasmid from the library that rescued the strain. This plasmid was also transformed into mutant 2-10. Another library plasmid was transformed into 2-2 to serve as a control. Cells were serially diluted five-fold then grown on YTD+2% glu agar plates or on the same plate but with 200µg/ml calcofluor white at 25°C for 3 days. Data represents three independent experiments.

The plasmid isolated from the yeast library, is only able to rescue the 2-2 strain.

Another library plasmid is unable to rescue the mutant. This indicates that the insert is specifically complementing the mutation in strain 2-2.

When sequenced, the insert contained a region of DNA including genes *LCL3*, *GUP1*, *SCY 1* and *YGL082W*. Known functions of the genes were looked at and double mutants with deletions of each gene combined with $\Delta chs6$ were made. These double mutants were spot diluted and mated back with 2-2. The results indicated that the gene mutated in 2-2 is *GUP1*, as shown in Figure 4.35. When 2-2 was mated with the other double mutants complementation occurred and the diploids were calcofluor resistant. When mated with the $\Delta gup1 \Delta chs6$ double mutant the diploid remained calcofluor sensitive.

Figure 4.36 5X spot dilution of 2-2.



Various strains were grown to exponential phase till about $\sim 1 \times 10^7$ cells/ml in YPD + 2% glu + G418 or SC-LYS+2% glu for double mutants. Dilution assay was carried out as described in methodology section. Cells were serially diluted five-fold then grown on YTD+2% glu agar plates or on the same plate but with 200µg/ml calcofluor white at 25°C for 3 days. Data represents three independent experiments.

Both the mutant 2-2 and $\Delta gup1 \Delta chs6$ appear to have reduced calcofluor resistance.

The calcofluor resistance of the $\Delta gup1 \Delta chs6$ double mutant is less than 2-2 which

suggests that complete knockout of the gene causes more disruption in the process than the point mutation present in 2-2.

From sequencing the *GUP1* gene from 2-2 genomic DNA, it appears that the mutation in this gene is E238K. This mutation obviously partially inactivates Gup1p.

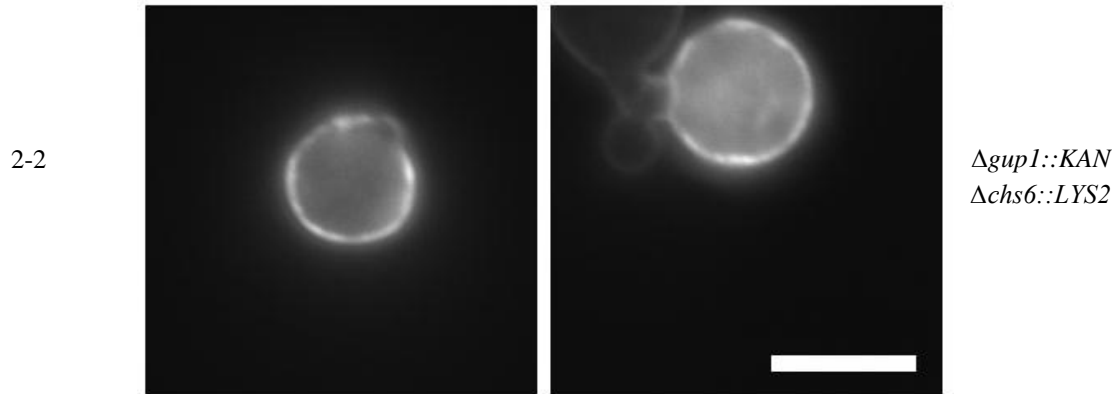
Figure 4.37 Sequence line up of Wild-type and mutated Gup1p

Query	1	MSLISILSPLITSEGLDSRIKPSPKKDASTTTKPSLWKTTEFKFYIIAFLVVVPLMFYAG	60
Gup1p	1	MSLISILSPLITSEGLDSRIKPSPKKDASTTTKPSLWKTTEFKFYIIAFLVVVPLMFYAG	60
Query	61	LQASSPENPNYARYERLLSQGWLFGRKVDNSDSQYRFFRDNFALLSVLMLVHTSIKRIVL	120
Gup1p	61	LQASSPENPNYARYERLLSQGWLFGRKVDNSDSQYRFFRDNFALLSVLMLVHTSIKRIVL	120
Query	121	YSTNITKLRFDLIFGLIFLVAAHGVNSIRILAHMLILYIAIAHVLKNFRRIATISIIWIYGI	180
Gup1p	121	YSTNITKLRFDLIFGLIFLVAAHGVNSIRILAHMLILYIAIAHVLKNFRRIATISIIWIYGI	180
Query	181	STLFINDNFRAYPFGNICSFLSPLDHWYRGIIPRWDVFFNFTLLRVLSYNLDFLERWKNL	240
Gup1p	181	STLFINDNFRAYPFGNICSFLSPLDHWYRGIIPRWDVFFNFTLLRVLSYNLDFLERWENL	240
Query	241	QKKKSPSYESKEAKSAILLNERARLTAAHPIQDYSLMNYIAYVTYTPFIAGPIITFNDY	300
Gup1p	241	QKKKSPSYESKEAKSAILLNERARLTAAHPIQDYSLMNYIAYVTYTPFIAGPIITFNDY	300
Query	301	VYQSKHTLPSINFKFIFYAVRFVIALLSMEFILHFLHVVAISKTKAWENDTPFQISMIG	360
Gup1p	301	VYQSKHTLPSINFKFIFYAVRFVIALLSMEFILHFLHVVAISKTKAWENDTPFQISMIG	360
Query	361	LFNLNIIWLKLLIPWRLFRLWALLDGDIDTPENMIRCVDNNYSSLAFWRAWHRSYNKWVVR	420
Gup1p	361	LFNLNIIWLKLLIPWRLFRLWALLDGDIDTPENMIRCVDNNYSSLAFWRAWHRSYNKWVVR	420
Query	421	YIYIPLGGSKNRVLTSLAVFSFVAIWHDIELKLLWGWLIVLFLPEIFATQIFSHYTDA	480
Gup1p	421	YIYIPLGGSKNRVLTSLAVFSFVAIWHDIELKLLWGWLIVLFLPEIFATQIFSHYTDA	480
Query	481	VWYRHVCAVGAVFNIWMMIANLFGFCLGSDGTKKLLSDMFCTVSGFKFVILASVSLFIA	540
Gup1p	481	VWYRHVCAVGAVFNIWMMIANLFGFCLGSDGTKKLLSDMFCTVSGFKFVILASVSLFIA	540
Query	541	VQIMFEIREEEKRHGIYLC	560
Gup1p	541	VQIMFEIREEEKRHGIYLC	560

Gup1p is predicted to have 10 trans-membrane domains and it blasts to the MBOAT family of membrane-bound O-acyltransferases.

Figure 4.38 Calcofluor staining of 2-2 and $\Delta gup1\Delta chs6$.

Calcofluor staining

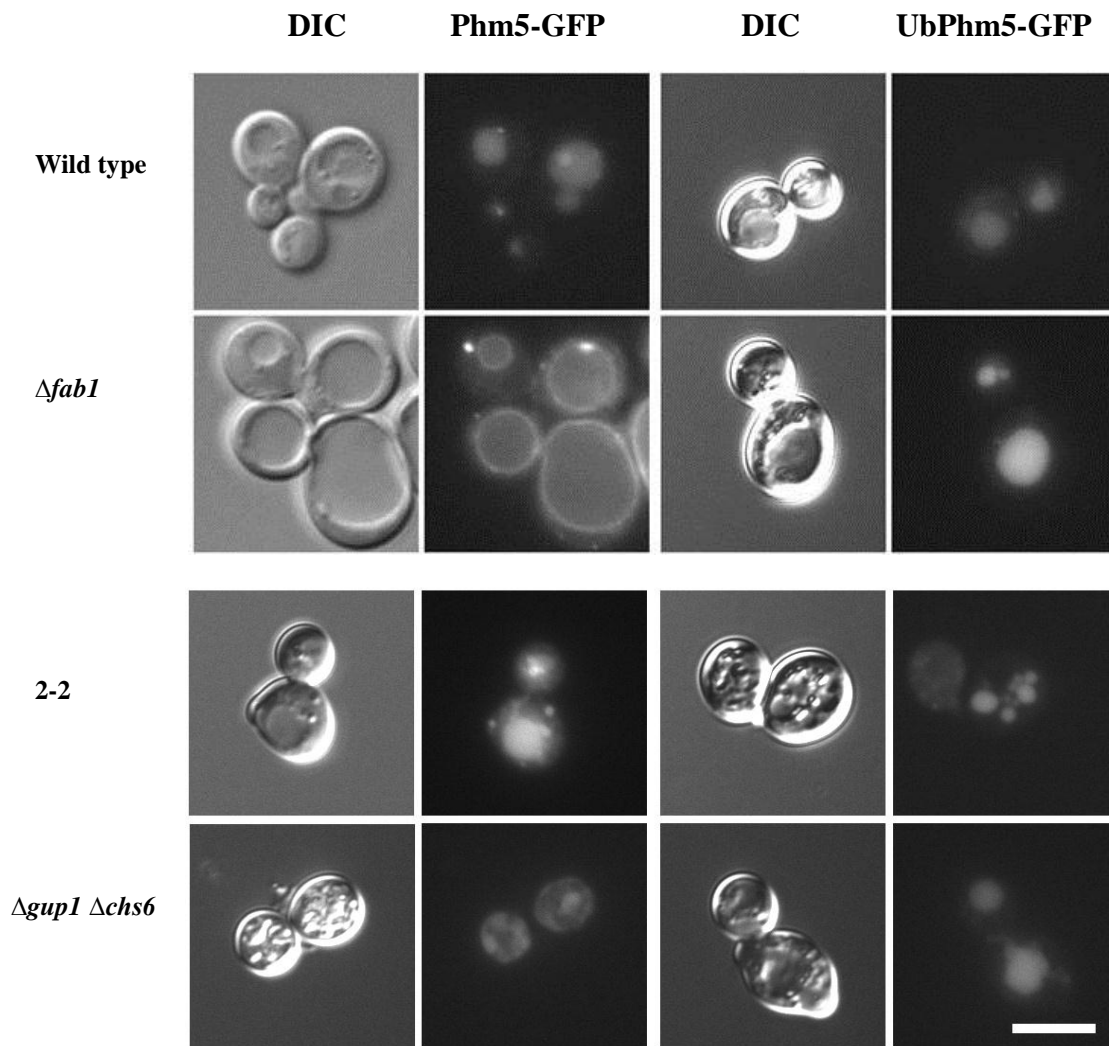


Shown above are fluorescence images of logarithmic phase cultures ($5 \times 10^6 - 1 \times 10^7$ cells/ml) of 2-2 (left hand panel) and $\Delta gup1::KAN \Delta chs6::LYS2$ (right hand panel) stained with calcofluor white for 10 minutes. The images show calcofluor staining visualised using a DAPI filter. These images are representative of three replicate cultures. All strains were cultured in SC-Lys+2% glu medium and grown at 25°C. Scale bar represents 5 μM .

As shown in Figure 4.38 bud scars are hard to visualise in both the 2-2 mutant and the $\Delta gup1 \Delta chs6$ double mutant. This suggests that these mutants are not allowing Chs3p to reach the cell surface. This makes it unlikely that Gup1p is on a specific pathway that controls trafficking of Chs3p and increases the likelihood that the calcofluor sensitivity result is as a consequence of a more general drug hyper-sensitivity of $\Delta gup1$.

To see if Gup1p may be involved with the Fab1p pathway or share any phenotypes several assays were performed in order to see if MVB sorting was working normally. The localisation of Phm5p and Ste3p were examined for defects.

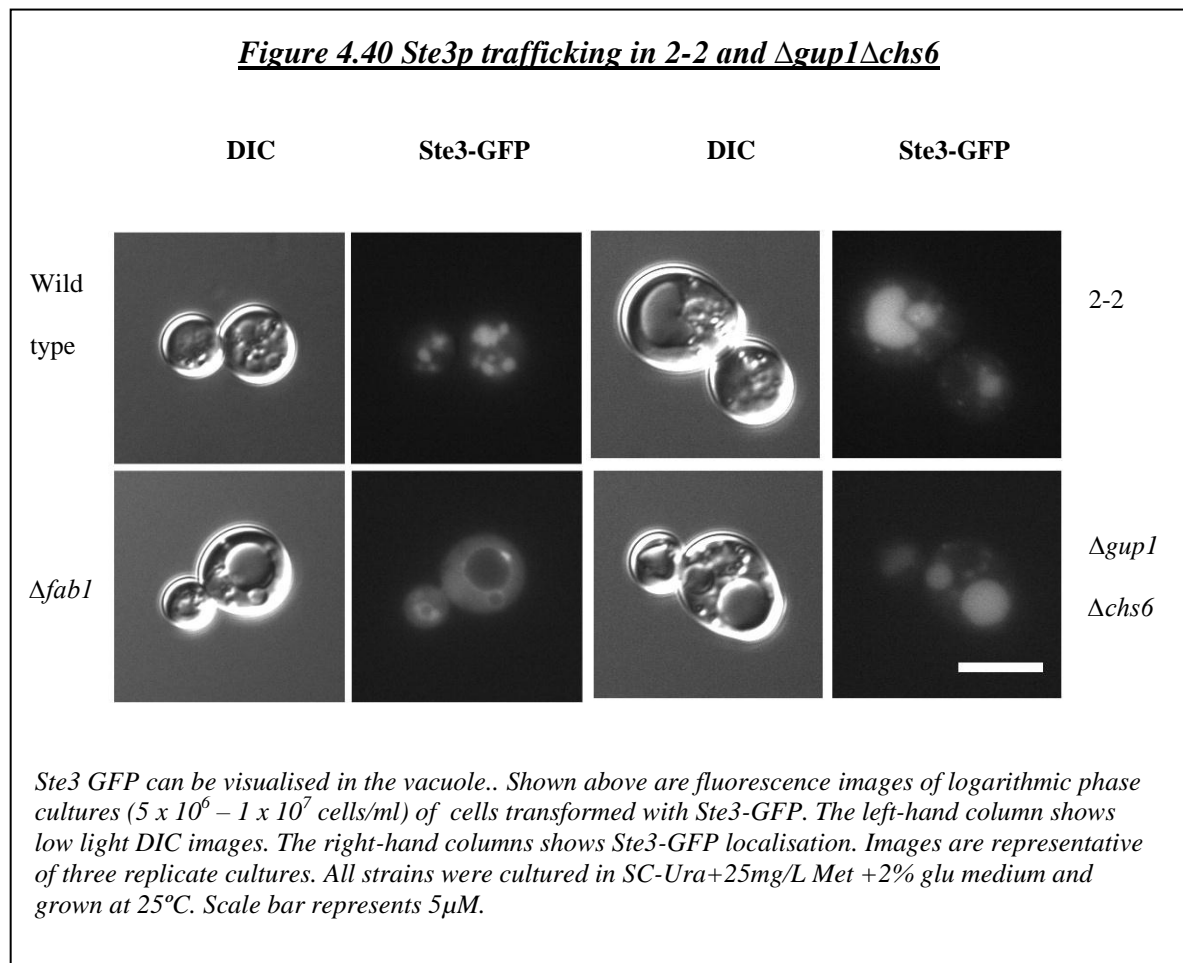
Figure 4.39 Phm5p trafficking in 2-2 and $\Delta gup1\Delta chs6$



Both Phm5 GFP and UbPhm5 GFP can be visualised in the vacuole.. Shown above are fluorescence images of logarithmic phase cultures ($5 \times 10^6 - 1 \times 10^7$ cells/ml) of cells transformed Phm5-GFP constructs. The left-hand columns show low light DIC images. The right-hand columns show the GFP localisation of the constructs. The panel to the left shows Phm5-GFP localisations. The panel to the right shows Ub Phm5 GFP localisation. Images are representative of three replicate cultures. All strains were cultured in SC-Ura+25mg/L Met +2% glu medium and grown at 25°C. Scale bar represents 5 μ M.

In both 2-2 and the $\Delta gup1 \Delta chs6$ double mutant targeting of Phm5p appears to be correct, and the GFP construct is visualised in the vacuole. This suggests that no disruption of MVB sorting is occurring in this mutant. As a confirmation of this result, trafficking of UbPhm5-GFP is still seen in the vacuole. In a $\Delta fab1$ or $\Delta apl4$

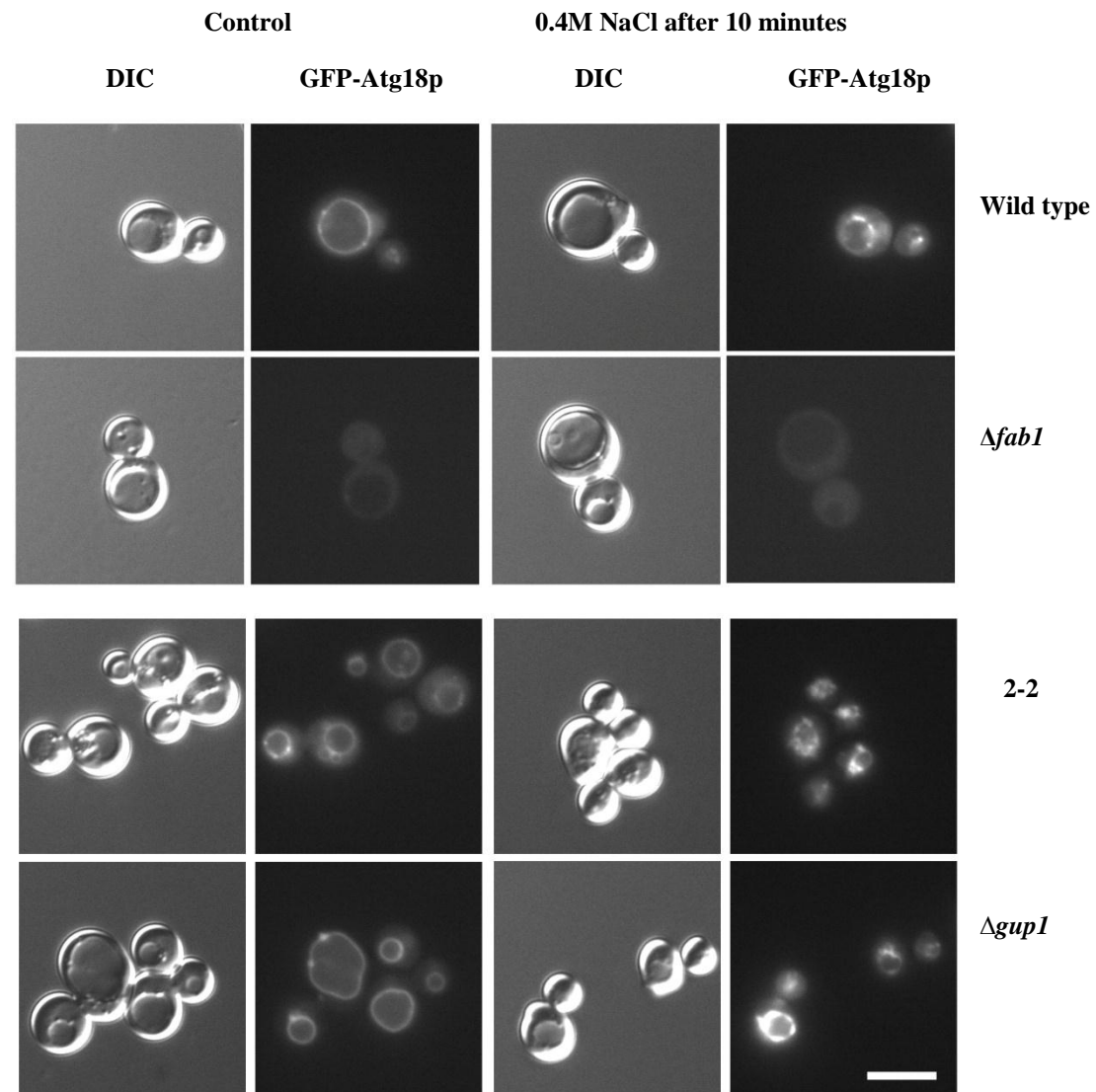
strain only the UbPhm5-GFP construct is sorted to the vacuole, Phm5-GFP is mis-sorted to the vacuole membrane (Shaw et al., 2003). To confirm this result with a different cargo, the localisation of Ste3-GFP was also examined since cargo specific trafficking defects are widespread in all eukaryotic systems.



It appears in Figure 4.40 that neither the isolated mutant nor the full knockout, possess a defect in the localisation of Ste3-GFP as it is correctly targeted to the vacuole. In some mutants of the Fab1p pathway, Ste3p is mistrafficked to the vacuole membrane or cytoplasm.

To see if $\Delta gup1$ may have a defect in $\text{PtdIns}(3,5)P_2$ metabolism the localisation of GFP-Atg18p, an effector of $\text{PtdIns}(3,5)P_2$, was also examined. Atg18p is usually found on the vacuole membrane when $\text{PtdIns}(3,5)P_2$ synthesis is normal.

Figure 4.41 Localisation of pUG36 GFP-Atg18p.



pUG36-GFP-ATG18P can be visualised on the vacuole membrane, and this localisation is increased when cells are subjected to a hyperosmotic stress. Shown above are fluorescence images of logarithmic phase cultures ($5 \times 10^6 - 1 \times 10^7$ cells/ml) of wildtype (top panel), $\Delta fab1$ (middle panel), 2-2 (middle panel), $\Delta gup1$ (bottom panel) transformed with pUG36-GFP-Atg18p. The left-hand panel shows localisation under control conditions. The right hand panel shows localisation under 0.4M NaCl conditions. The left hand columns show low light DIC images. The right-hand columns show GFP localisation. These images are representative of three replicate cultures. All strains were cultured in SC-Ura-Met+2% glu medium and grown at 25°C. Scale bar represents 5μM.

It appears that a gross defect in PtdIns(3,5) P_2 synthesis is not present in either of the strains; though more minor perturbations cannot be ruled out using this assay. Under normal conditions GFP-Atg18p can be clearly visualised on the vacuole membrane, and when the cell is given hyperosmotic stress the amount of GFP-Atg18p on the vacuole membrane increases as it does in wild-type cells.

It appears likely that Gup1p is not part of the PtdIns(3,5) P_2 or Fab1p pathway and may be playing an independent role in this process. It is likely that calcoflour sensitivity is due to a defect in the cell wall structure and not as a consequence of Chs3p trafficking.

Other mutants

Another mutant identified was 1-11, a disruption in the *GAS1* gene. This gene is already known to have a role in cell wall biosynthesis, as 1,3-beta-glucanoyltransferase which helps make 1,3 β glucan a major polysaccharide of the cell wall (Mouyna et al., 2000). *GAS1* mutants, in common with most mutants that affect cell wall biosynthesis, display a non-specific drug hypersensitivity phenotype and hence calcoflour sensitivity is likely to be a facet of this cell integrity defect rather than being a specific dysregulation of the Fab1p/ AP-1 complex pathway.

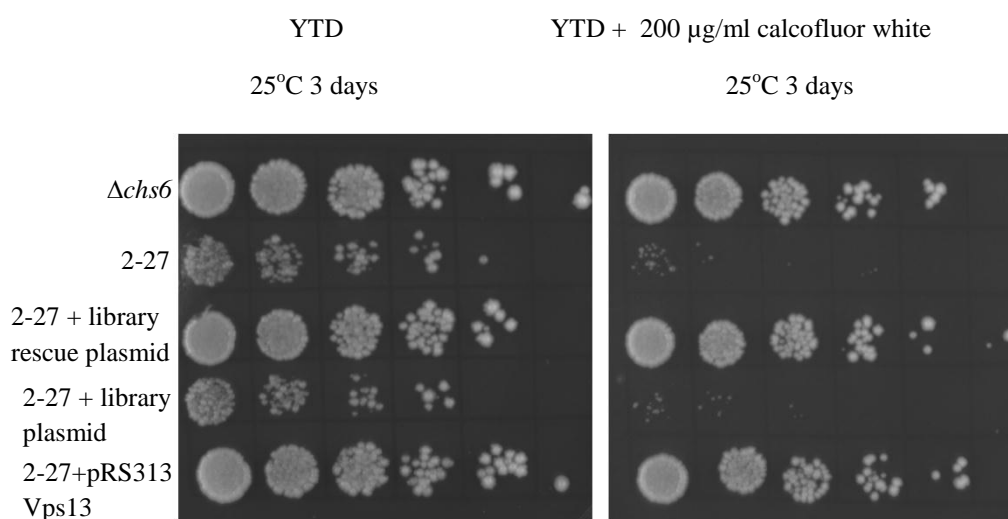
4.16 Mutant 2-27 is *VPS13*

As shown in previously 2-27 is an intriguing mutant because the calcoflour sensitivity of the strain can be overcome by expression of Fab1p in a plasmid as shown in Figure 4.30. This suggests the mutant may be of a gene that is part of the Fab1p or PtdIns(3,5) P_2 pathway. Expression of Apl2p or Apl4p on a plasmid cannot rescue 2-27. This strain also proved difficult to work with as it possesses a serious sporulation

defect; when sporulated, very few spores were produced and all proved inviable when dissected. This meant the mating type of the strain could not be changed easily. It has previously been noticed that $\Delta fab1$ strains also possess defects in sporulation although not to the extent of 2-27, as some viable spores can be produced.

It was difficult to isolate a plasmid that would rescue the calcofluor defects of the 2-27 mutant, as the strain appeared to be very sensitive to the drug, so a lower dosage of calcofluor (400 μ g/ml) was used. It was still difficult to get a plasmid to rescue and this raised the possibility that the mutation was present in a large gene, since larger genes are usually under-represented in genomic libraries. Eventually a plasmid was isolated that rescued the strain.

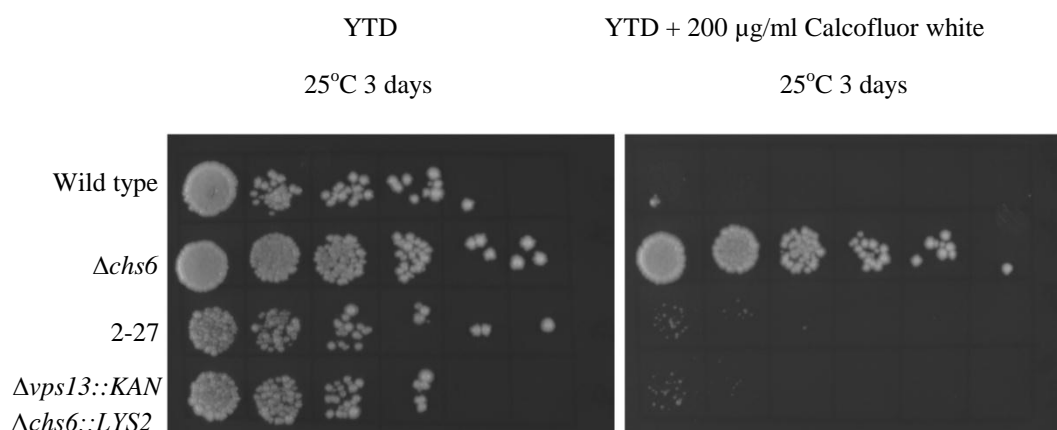
Figure 4.42 5X spot dilution of 2-27 rescues.



Various strains were grown to $\sim 1 \times 10^7$ cells/ml in YPD + 2% glu + G418 or SC-LYS+2% glu for double mutants. Dilution assay was carried out as described in methodology section. 2-27 was transformed with the plasmid from the library that rescued the strain. Another library plasmid was transformed into 2-27 to serve as a control. Cells were serially diluted five-fold then grown on YTD+2% glu agar plates or on the same plate but with 200 μ g/ml calcofluor white at 25°C for 3 days. Data represents three independent experiments.

As shown above in Figure 4.42, the plasmid isolated can rescue the 2-27 calcofluor sensitive phenotype. The plasmid was sequenced and found to contain a stretch of DNA encoding the *SDH2* and *VPS13* genes. From known functions of the genes, the mutant seemed likely to be a mutation in *VPS13* so a double mutant was made. At the same time a *VPS13* plasmid was obtained and used to transform into 2-27. As shown above, reintroduction of *VPS13* can rescue the 2-27 calcofluor sensitivity.

Figure 4.43 5X spot dilution of 2-27.

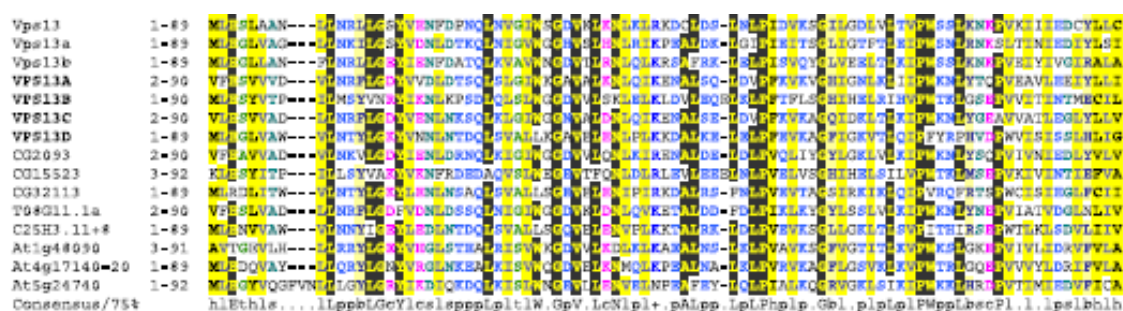


Various strains were grown to exponential phase till about $\sim 1 \times 10^7$ cells/ml in YPD + 2% glu + G418 or SC-LYS+2% glu for double mutants. Dilution assay was carried out as described in methodology section. Cells were serially diluted five-fold then grown on YTD+2% glu agar plates or on the same plate but with 200µg/ml calcofluor white at 25°C for 3 days. Data represents three independent experiments.

Like 2-27, the $\Delta vps13\Delta chs6$ double mutant is no longer calcofluor resistant and as shown below in Figure 4.43, bud scars are clearly visible. The deletion of *VPS13* was thus able to reverse the calcofluor resistance of $\Delta chs6$ cells in a specific fashion. This provides further evidence supporting the assertion that 2-27 does in fact contain a mutated version of *VPS13*. To obtain direct evidence, the *VPS13* gene from the 2-27 strain was isolated from genomic DNA and sequenced. The *VPS13* gene is around

9.5Kb and a single mutation in the sequence was found at E003K. This is a change from glutamate acid to Lysine right at the start of the gene which could be quite disruptive, particularly if this area contains a localisation signal or if it affects protein stability via the N-rule system. This is the same type of mutation observed in *GUP1*; consistent with the fact that a base change from G to an A is the most common type of mutation resulting from EMS treatment. As shown below in Figure 4.44 this residue in *VPS13* is conserved, particularly amongst fungi.

Figure 4.44 Sequence alignment of *Vps13* (From (Velayos-Baeza et al., 2004)).



Alignment of *Vps13p* from the following homologs: *S. cerevisiae*, *S. pombe* *Vps13a* and *Vps13b*, Human *Vps13A*, *Vps13B*, *Vps13C* and *Vps13D*, *D. melangastor* *CG2093*, *CG15523*, *CG32113*, *C. elegans* *T08G11.1*, "C25H3.11+8", *A. thaliana* *Atg48090*, "At4g17140-20" and *At5g24740*,

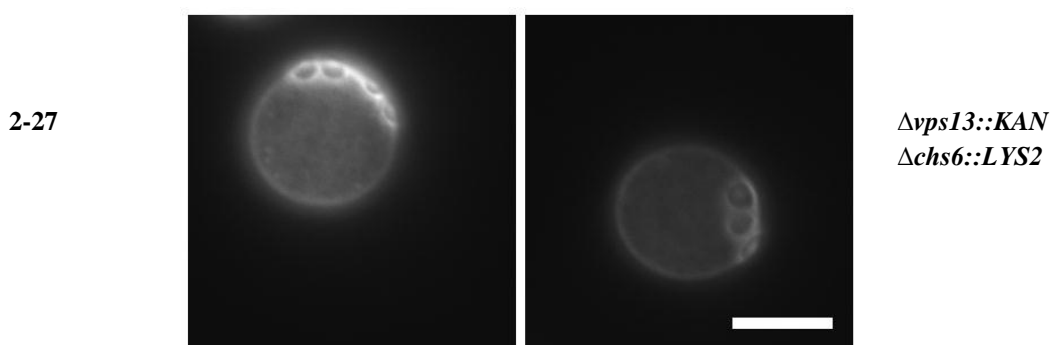
Vps13p has known homologs in higher eukaryotes, with several proteins showing similarity in *C. elegans*, *D. melangastor* and Humans. There are four human homologues of *VPS13*, and disruption of any of these genes causes Cohen syndrome, a disorder characterised by psychomotor retardation and retinal dystrophy (Kolehmainen et al., 2003). The human *Vps13p* proteins are associated with the Golgi. Most conservation of *Vps13p* is at the C and N terminal ends, suggesting these

are the most necessary for function; and this is where the mutation found is located. The sequence of Vps13p has previously been analysed and contains 25% charged residues (Glu, Asp, Arg and Lys) with a predicted pI of 5.23. It is also rich in residues found in α -helical coiled coils (Brickner and Fuller, 1997). It has been proposed that its sequence is suggestive of an extensive structural motif, although no heptad repeats longer than two to three turns are predicted (Brickner and Fuller, 1997). The protein has three potential transmembrane domains, although this is also doubtful because of hydrophilic and charged residues. No other motifs, domains or structural features have been predicted (Brickner and Fuller, 1997).

To see if $\Delta vps13$ strains shared any other phenotypes with $\Delta fab1$ strains, the mutant was put through a battery of tests for co-phenotypes.

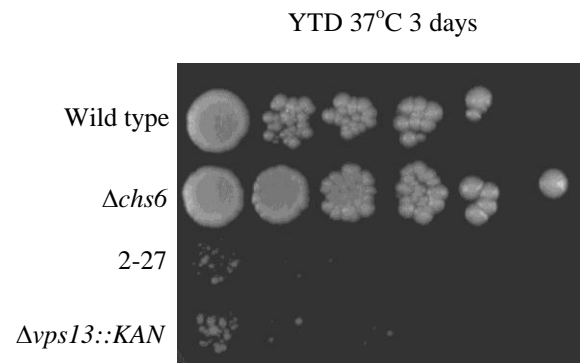
Figure 4.45 Calcofluor staining of 2-27 and $\Delta vps13\Delta chs6$.

Calcofluor staining



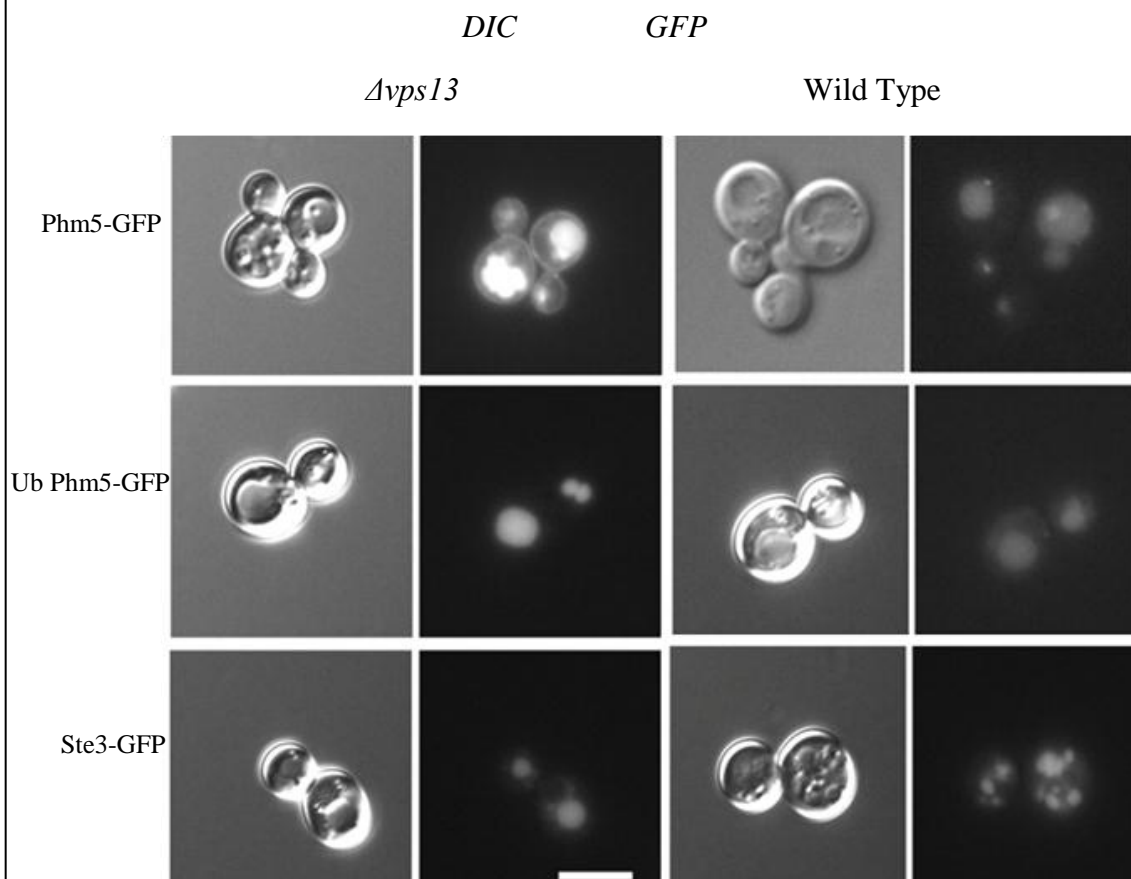
Shown above are fluorescence images of logarithmic phase cultures ($5 \times 10^6 - 1 \times 10^7$ cells/ml) of 2-27 (left hand panel) and $\Delta vps13::KAN \Delta chs6::LYS2$ (right hand panel) stained with calcofluor white for 10 minutes. The images show calcofluor staining visualised using a DAPI filter. These images are representative of three replicate cultures. All strains were cultured in SC-Lys+2% glu medium and grown at 25°C. Scale bar represents 5 μ M.

Figure 4.46 5X temperature sensitive spot dilution of 2-27.



Various strains were grown to exponential phase till about $\sim 1 \times 10^7$ cells/ml in YPD + 2% glu + G418 or SC-LYS+2% glu for double mutants. Dilution assay was carried out as described in methodology section. Cells were serially diluted five-fold then grown on YTD+2% glu agar plate at 37°C for 3 days. Data represents three independent experiments

Figure 4.47 MVB sorting in Δ vps13



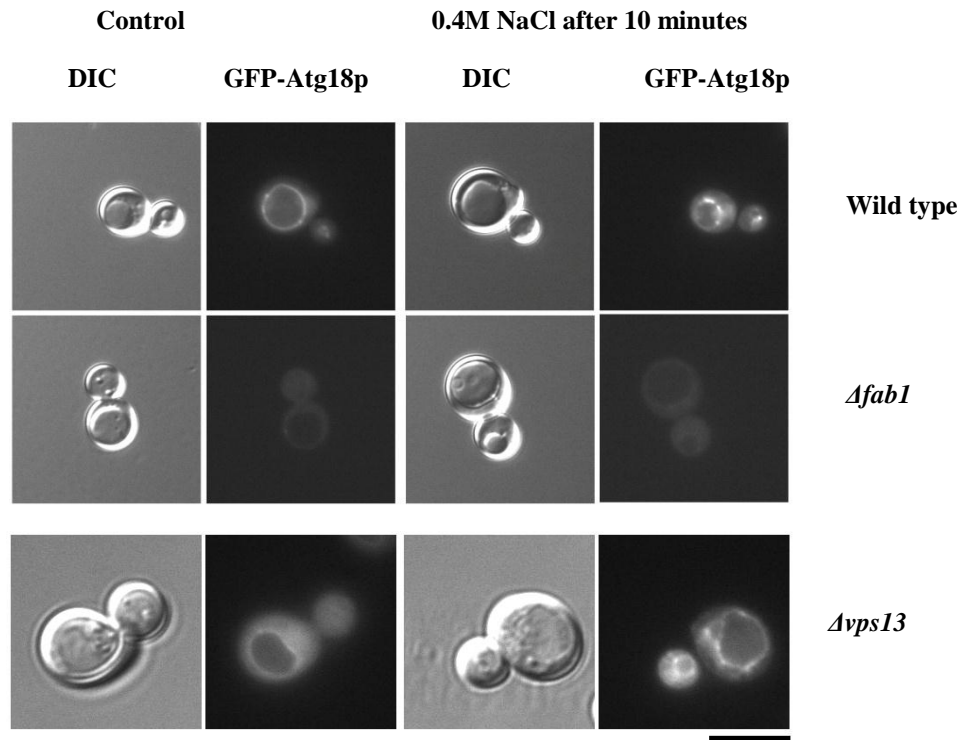
Phm5 GFP, UbPhm5 GFP and Ste3 GFP can be visualised in the vacuole. Shown above are fluorescence images of logarithmic phase cultures ($5 \times 10^6 - 1 \times 10^7$ cells/ml) of cells transformed with GFP constructs. The left-hand columns show low light DIC images. The right-hand columns show the GFP localisation of the constructs. Images are representative of three replicate cultures. All strains were cultured in SC-Ura+25mg/L Met +2% glu medium and grown at 25°C. Scale bar represents 5µM.

As shown in Figure 4.46 both 2-27 and $\Delta vps13$ are temperature sensitive at 37°C like *fab1*. It appears that $\Delta vps13$ does not possess the same defects in MVB sorting Ste3p as $\Delta fab1$; Ste3p is correctly localised in the strain (Figure 4.47). However there appears to be mis-localisation of Phm5p, partially to the cell surface in $\Delta vps13$ and although this is not the same mislocalisation as in $\Delta fab1$, the defect is corrected by ubiquitination of Phm5p. Ubiquitination dependent mislocalisation of Phm5p is so far only known to occur because of inactivation of the Fab1p pathway and this is strongly suggestive of link between Vps13p upstream of Fab1p and possibly AP-1.

In order to find out whether $\Delta vps13$ was likely to have a defect in PtdIns(3,5) P_2 metabolism, the localisation of pUG36 GFP-Atg18p, was also examined. Atg18p is usually found on the vacuole membrane when PtdIns(3,5) P_2 synthesis is normal. As shown in Figure 4.45 GFP-Atg18p can be visualised on the vacuole membrane under control conditions in $\Delta vps13$ cells but note that far more GFP-Atg18p is present in the cytoplasm as compared with wild-type; suggesting a defect in PtdIns(3,5) P_2 metabolism. This may be the consequence of reduced levels of PtdIns(3,5) P_2 . When cells are treated with a hyper osmotic stress, the levels of PtdIns(3,5) P_2 should increase, if no defects in its metabolism are present. More GFP-Atg18p seems to be on the vacuole after 0.9M NaCl stress, which may mean levels of PtdIns(3,5) P_2 can increase in this mutant. This assay will not rule out small interruptions to levels of PtdIns(3,5) P_2 so further inositol lipid labelling experiments would need to be

performed in order to see if Vps13p is a potential effector but an upstream role seems more likely.

Figure 4.48 GFP-Atg18p localisation in $\Delta vps13$



pUG36-ATG18GFP can be visualised on the vacuole membrane, and this localisation is increased when cells are subjected to a hyperosmotic stress. Shown above are fluorescence images of logarithmic phase cultures ($5 \times 10^6 - 1 \times 10^7$ cells/ml) of $\Delta vps13$ transformed with pUG36-ATG18. The left-hand panel shows localisation under control conditions. The right hand panel shows localisation under 0.4M NaCl conditions. The left hand columns show low light DIC images. The right-hand columns show GFP localisation. These images are representative of three replicate cultures. Strain was cultured in SC-Ura-Met+2% glu medium and grown at 25°C. Scale bar represents 5µM.

The data presented above seem to suggest that Vps13p may indeed be part of the Fab1p and PtdIns(3,5) P_2 pathway. Several phenotypes of $\Delta fab1$ cells are shared with $\Delta vps13$ cells. These include temperature sensitivity at 37 °C, a potential defect in MVB sorting of Phm5p, a defect in sporulation and a partial mis-localisation of GFP-Atg18p. All these phenotypes together, point to a role for Vps13p in the Fab1p

pathway. Further experiments including a retrograde trafficking assay and interaction studies could be performed in order to investigate the exact role of Vps13p.

4.17 Discussion

This chapter presents new evidence supporting a role for Fab1p and PtdIns(3,5) P_2 in regulation of the early endocytic system. This data suggests that both Fab1p and the AP-1 complex regulate trafficking from the recycling endosome to the TGN or vice versa. This confirms and extends previous work (Phelan et al., 2006). A likely model is as follows; Chs3p is normally transported to the cell surface by a novel protein coat, known as exomer, which is comprised of several proteins including Chs6p. In a $\Delta chs6$ mutant Chs3p is no longer specifically transported to the cell surface because Chs6p is needed to recruit Chs3p to the exomer complex; Chs3p instead endlessly cycles between the TGN and recycling endosome (PGE). When the AP-1 complex is simultaneously inactivated (via disruption of Fab1p or AP-1 function), then this internal sequestration of Chs3p is now disrupted and as Schekman observed, Chs3p is likely to build up at the recycling endosome (Valdivia et al., 2002). This concentration of Chs3p at the recycling endosome eventually allows some Chs3p to escape to the cell surface via mass action or non-specific membrane flow. This allows some chitin to be formed and is why, in a double mutant, we see reversion of the $\Delta chs6$ phenotypes. The route Chs3p takes back to the cell surface in this situation was also investigated. Triple mutants were made with a deletion of *PEP12* which controls entry into the pre vacuolar endosome (early/late endosome) and *VPS4* which would disrupt the pathway from the pre vacuolar endosome to the TGN. If Chs3p took either of these routes a triple $\Delta vps4 \Delta chs6 \Delta fab1$ mutant should become calcofluor resistant

again as the pathway to the cell surface would again be blocked. The results presented above indicate this is not the case and these triple mutant strains remain calcofluor sensitive. A triple mutant with the deletion of a classical secretion protein such as a *SEC* would be a good experiment to perform to rule out the possibility that Chs3p is finding a new route the cell surface through classical secretion from the Golgi via the exocyst. It would also allow confirmation of which pathway direction Fab1p is involved in, between the recycling endosome and TGN and whether in fact it is the retrograde pathway as evidence points to or the anteograde pathway. Unfortunately *SEC* mutants with a total block of secretion are inviable in yeast. Temperature sensitive constructs that become inactive at 37°C do exist, but these are unable to be used in this instance as a $\Delta fab1$ mutant is unable to grow at 37°C. One secretion mutant with *SEC22* disrupted could be used to perform this experiment as the deletion strain is viable, however attempts to perform this experiment were inconclusive.

The data discussed above point to the existence of a novel pathway that Chs3p is taking, in the $\Delta fab1\Delta chs6$ and $\Delta apl4\Delta chs6$ double mutants, to the cell surface. There is currently no known pathway in yeast from the recycling endosome to the cell surface. To further understand the novel route Chs3p is taking in $\Delta fab1\Delta chs6$ cells a screen could be performed to isolate another protein in this pathway. $\Delta fab1\Delta chs6$ cells could be mutagenised and the resultant colonies screened for strains that have brought back resistance to calcofluor. This would be relatively easy as plating the mutagenised cells onto plates containing calcofluor will only allow these mutants to grow. The tricky part of this experiment would be back crossing and complementation as it is a triple mutant involved, and all the mutations would have to isolated together in each spore; the chances of this are low and so the process of dissection would be tedious. It would also be time consuming to identify the mutation, as rescuing the

mutant with a yeast genomic library would make the cell calcofluor sensitive again. Loss of function is hard to look for as it involves identification of a tiny colony that is growing on one plate but not another. However, pictures of replica plates growing mutants with and without calcofluor could be taken, false coloured and overlaid using photoshop and the colonies growing only on the minus calcofluor plate identified or FACS used to isolate mutants, transformed with the library which has low fluorescence. FACS would certainly help to cut down the number of colonies that needed to be screened.

The role of Fab1p in the likely retrograde pathway from the recycling endosome to the TGN is dependent upon $\text{PtdIns}(3,5)P_2$. A Fab1p construct lacking the ability to make lipid cannot rescue the associated calcofluor sensitivity defect. This work has not identified the effector that mediates this process, but an extension of my screen should isolate such a gene in the end.

The work detailed in this chapter also shows that FACS is a better method for performing trafficking screens than plate-based assays. FACS allows thousands of cells to be screened and analysed in a matter of seconds. Not only their fluorescence is measured, but data about cellular shape and size is also collated, removing many false positives. Using FACS in this screen has been much better because it allowed concentration of mutants which brought back bud scars and calcofluor sensitivity directly. These mutants could easily be sorted by drawing gates around the appropriate populations on the graph. This enriched the number of mutants found in the resulting culture and cut down the amount of mutant plates that needed to be replica plated and colonies spot diluted. It also proved to be a better method because of the types of mutants that were isolated. Many of the group one mutants found by the traditional method clearly had defects in the cell wall, and this might have been

what was making the $\Delta chs6$ strain sensitive again, not disruption of the specific internal pathway of Chs3p localisation. Many more of the FACS sorted mutants appeared to be $\Delta fab1$ like with a large vacuole or large round cell. FACS allowed selection of mutants with a particular shape and size so it specifically sorted more correct cells rather than long misshaped cells with likely cell wall defects.

A successful trafficking screen will identify both known and novel components of the target pathway. Isolation of an *APL2* mutant helps to validate the screen conducted. *APL2* encodes a protein known to be involved in the specific localisation of Chs3p. It shows that it is possible to isolate components of the Fab1p dependent TGN to PGE pathway by the method used. This means it should also be possible to isolate further novel components by the same process.

Identifying the disrupted genes proved to be a difficult task. A library with better coverage and overlapping fragments would have helped speed up the process. A big problem was that many colonies when plated onto a calcofluor containing plate after transformation, still grew even though the plasmid they contained was not in fact rescuing the mutation. A way of overcoming this problem was discussed earlier and this method although time consuming has been found to work. This method could be used to carry on the work and identify some more of the interesting mutants. A screening method that would identify those mutants with defects in the cell wall that caused hypersensitivity, would also help focus our attentions on identifying the right kind of mutants. A way of doing this may be by backcrossing to see if the mutation on its own shows increased hypersensitivity to calcofluor.

The screen has identified two proteins, Gup1p and Gas1p which may be a consequence of defects in the cell wall. Gup1p is a membrane bound O-

acyltransferase but has been implicated in a wide range of functions including cell wall composition and integrity and the secretory/endocytic pathway (Bleve et al., 2011, Bonangelino et al., 2002). However, Gup1p has also been shown to interact genetically with several genes involved in chitin and β -1,6 glucan synthesis such as *SKT5*, an activator of chitin synthesis (Smits et al., 2001). Absence of Gup1p has been shown to create cells defective in cell wall composition that are sensitive to calcofluor and other enzymes that affect the cell wall, such as zymolyase. The amount of chitin present in the cell wall was measured and a $\Delta gup1$ mutant is found to have an increased level of chitin (Ferreira et al., 2006). So like $\Delta gas1$, it is likely that $\Delta gup1$ also shows calcofluor hypersensitivity. It is probable that the calcofluor sensitivity effect observed in 2-2 is independent of the Fab1p /AP-1 dependent pathway. Further supporting this are the results that *FAB1* over expression cannot rescue the $\Delta gup1 \Delta chs6$ mutant, and no defect in MVB sorting is observed. Recently Gup1p over expression has been shown to increase proliferation of intracellular membranes which contain both Golgi and ER proteins (Bleve et al., 2011). Deletion of *GUP1* also results in an increase of triglycerides and decrease in phospholipids synthesis (Oelkers et al., 2000). This raises the possibility that Gup1p may be implicated in the control of the ER membrane as this is the major site of lipid synthesis.

Vps13p is the most interesting mutant identified. *VPS13* is encoded by ORF *YLL040C* and is also known as *SOLI*. The gene is still classified as uncharacterised although it has been pulled out in several screens for defects in vacuolar sorting and targeting but its molecular function remains elusive (Bankaitis et al., 1986, Robinson et al., 1988, Rothman et al., 1989). More recently a role for the protein has emerged in Kex2p transport (Brickner and Fuller, 1997, Redding et al., 1996). Deletion of *VPS13* impairs the localisation of Kex2p at the TGN. Kex2p is a protease required for the production

of the mating pheromone α -factor. If Vps13p is not present, Kex2p is partially mislocalised to the pre-vacuolar endosome apparently because the retrieval of Kex2p from this endosome is much slower than normal. This implies that Vps13p is required for correct trafficking of the Kex2p cargo receptor; an as yet unidentified protein, back to the TGN (Brickner and Fuller, 1997). Vps13p has also been shown to missort CPY and lead to the increased vacuolar degradation of Vps10p, linking into the work in Chapter 3, suggesting that Vps13p might have a role in cargo specific retrieval of proteins back to the TGN. Targeting of Kex2p to the TGN is dependent on an aromatic TLS1 signal in its C-terminal tail; when this signal is mutated Kex2p is routed to the vacuole. Kex2p also possesses a TLS2 signal necessary for cycling between the PVC and TGN. Vps13p is thought to function by interaction with these signals. It is suggested that Vps13p antagonises the retention signal (TLS2) and promotes the function of the retrieval signal that acts at the PVC (Brickner and Fuller, 1997). Vps13p functions at both the TGN and PVC. Ste13p is also thought to contain similar signals as mentioned above (Brickner and Fuller, 1997)

It is likely that Vps13p is performing a similar role in the trafficking of Chs3p. It could be functioning at the TGN or recycling endosome/PGE or both. Vps13p may recognise a signal in Chs3p and promote its recycling or retrieval via recruitment of another complex such as AP-1 or Fab1p. The exomer complex is also known to transport Fus1p to the plasma membrane. It has now been found that Fus1p contains a IXTPK sequence in its cytosolic tail which is necessary for its direction to the plasma membrane (Barfield et al., 2009). Although none have been identified to date and sequence alignments with Kex2p did not reveal any sequence homology, it may be that Chs3p contains similar domains. Chs3p does contain an LITPK sequence in its second predicted cytosolic loop but mutation of the sequence does not affect transport

to the cell surface (Barfield et al., 2009). Mutation of Chs3p to see if any specific regions interact with Vps13p may reveal the process at work.

The fact that Fab1p can rescue the 2-27 strain and $\Delta vps13\Delta chs6$ double mutant makes it extremely likely that Vps13p can interact with the Fab1p, the AP-1 complex or PtdIns(3,5) P_2 in some fashion and suggests that all of these components act in the same pathway; the control of protein entry into the TGN via some form of retrograde trafficking pathway. Hence if either Vps13p, Fab1p or the AP-1 complex are inactivated then Chs3p can no longer enter the TGN and instead builds up at the recycling endosome (Snc1p positive compartment) where it again finds a new pathway to the cell surface. Further experiments are needed to clarify this role.

Localisation of Vps13p, components of the AP-1 complex, and Fab1p in wild-type and $\Delta chs6$ cells, could be performed by tagging each protein with GFP and examining microscopically. In order to understand the role of Vps13p, a $\Delta vps13\Delta chs6\Delta sec22$ triple mutant could also be generated to see if this brings back calcofluor resistance or not. It may be that in the $\Delta vps13\Delta chs6$ double mutant Chs3p builds up at the Golgi and finds a new route through classical secretion. A two hybrid screen could also be performed to see if interaction with Fab1p or the AP-1 complex does occur. A co-immunoprecipitation assay could also be performed to see if interaction occurs *in vivo*.

An expression assay could also be used to see if Vps13p can bind PtdIns(3,5) P_2 .

Levels of the lipid could also be measured in a $\Delta vps13$ strain to see if it does possess a defect in PtdIns(3,5) P_2 metabolism or is a potential effector, although the strain only appears to have a minor defect in GFP-Atg18p localisation.

Chapter 5

Vacuole Fragmentation.

5.1 Introduction

In order to survive a cell needs to be able to grow and adapt to changing conditions. When adverse environmental changes occur, the physiology of a cell also changes in response. The cell uses internal signals to activate stress response pathways. These pathways have been shown to activate in response to pH, osmotic stress and hydrostatic pressure changes (Dove and Johnson, 2007, Dove et al., 1999). As mentioned in Chapter 1 during hyper-osmotic stress, a transient 20 fold increase in PtdIns(3,5) P_2 levels is observed that is not seen in any of the other identified phosphoinositides (Dove et al., 1997). This increase has only been observed in fungi and plants, though at least one mammalian cell responds with a more modest increase in PtdIns(3,5) P_2 (Ikonov et al., 2001). A small increase in PtdIns3P is also seen due to increased Vps34p activity and is a prerequisite to the dramatic increase in PtdIns(3,5) P_2 levels that are catalysed by Fab1p activity. The increase in levels of PtdIns(3,5) P_2 are seen within seconds of stress and disappear at around 30-60 minutes; the intensity and duration of this response are proportional to the applied osmotic stress (Dove et al., 1997).

5.2. Vacuole fission.

During normal cellular growth and replication, vacuoles of *S. cerevisiae* undergo fusion and fission events in response to the cell cycle and in response to cellular

stress. The end point of many trafficking events in the yeast cell is the vacuole; it contains many proteases and is a site of degradation (Bowers and Stevens, 2005). Different machinery regulates fusion and fission events and they are antagonistically linked (Peters et al., 2004). Vacuole fission and fragmentation are required to be finely balanced in order to maintain cellular homeostasis.

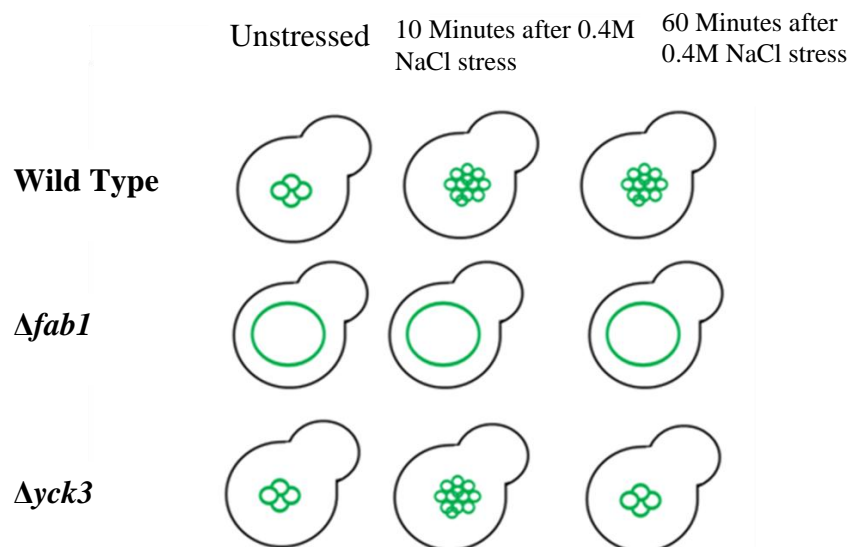
During cell division the vacuole is required to fragment into smaller vesicles which are then transported into the growing daughter cell. Inherited vacuolar vesicles then fuse during the later stages of cell division, to maintain a low copy number of the organelle (Ostrowicz et al., 2008).

Yeast vacuole fusion depends on Ypt7p a Rab GTPase, and the HOPS and SNARE complexes. Vacuole fusion comprises several different stages, all of which are tightly regulated. The first stage is priming, a process that requires ATP. During priming vacuoles are prepared for first contact. SNARE complexes present on the vacuole, are disassembled by Sec18p an ATPase. Vam7p a soluble SNARE remains partially bound to the vacuole, and Vps1p which binds to Vam3p on vacuoles is released, leaving the vacuolar SNAREs in an active position (Ostrowicz et al., 2008) . Tethering then proceeds, and is dependent on a fully assembled HOPS complex which forms a bridge between the vacuoles to be fused. Docking and fusion stages, then allow unpaired SNAREs, generated during priming to assemble across vacuole membranes. This happens through pairing of Q-SNAREs on one membrane with R-SNAREs on the other membrane, forming trans-complexes which bring and fuse opposing membranes allowing the vacuole contents to mix (Ostrowicz et al., 2008).

5.3. Vacuole fragmentation in response to stress

Duex and colleagues reported that the vacuoles of wild-type *S. cerevisiae* undergo regulated, PtdIns(3,5) P_2 dependent fragmentation into many smaller organelles when subjected to hyper-osmotic stress (Duex et al., 2006b). Vacuole fragmentation is not seen in cells deficient in PtdIns(3,5) P_2 , or cells that are unable to increase PtdIns(3,5) P_2 levels when given a hyper-osmotic stress, so Fab1p Vac7p, Vac14p and Fig4p are all necessary for vacuole fragmentation under hyper-osmotic stress (Duex et al., 2006b). This supports the idea that PtdIns(3,5) P_2 levels are increased under stress in order to carry out processes involving the vacuole.

Figure 5.1 Cartoon of vacuole fragmentation in response to stress.



Minutes after hyper-osmotic stress with 0.4M-1.0M NaCl, the vacuoles of wild-type cells fragment into a series of smaller vacuoles, however in *Fab1p* deficient cells the vacuoles are large and unlobed before and after application of the stress. Deletion of *YCK3* leads to a defect in the maintenance of vacuole fragmentation and after 60 minutes of hyperosmotic stress vacuoles re-fuse (Peplowska et al., 2007).

The reasons why the yeast vacuole undergoes fragmentation in response to hyper-osmotic stress are currently ill-defined. The once widely held belief that the vacuole acts as a water reservoir for the cytosol during hyper-osmotic stress is now questioned because both the cell and vacuole are now known to shrink with the same kinetics, which suggests they are osmotically continuous (Dove and Johnson, 2007). When cells are exposed to an osmotic stress, loss of water from the cell is observed. This produces a hypertonic cytoplasm, leading to a loss of water from the vacuole due to osmosis. It has been suggested that vacuolar water release is regulated by PtdIns(3,5) P_2 through control of a vacuolar-specific water channel. A vacuolar aquaporin has not yet been demonstrated in *S. cerevisiae*, but at least two aquaporins have been identified, *AQY1* and *AQY2*. Either of these may localize, in part, to the vacuole membrane (Meyrial et al., 2001). Further, most plant cells contain both plasma membrane and vacuolar aquaporins. These prevent the rapid dehydration and cell lysis that could occur when the osmolarity of the external environment changes, so similar mechanisms may occur in yeast (Soveral et al., 2006). PtdIns(3,5) P_2 may also regulate a vacuolar ion channel, therefore controlling the internal osmotic strength of the vacuole lumen. A decrease in ion flux out of the vacuole would help retain water that would otherwise be lost to the cytoplasm. PtdIns(3,5) P_2 has been shown to control the vacuolar ATPase and more recently it has been shown that vacuole acidification and fragmentation may be linked (Baars et al., 2007, Takeda et al., 2008). Indeed, a $\Delta fab1$ cell devoid of all PtdIns(3,5) P_2 also has a defect in vacuole acidification, suggesting a role for PtdIns(3,5) P_2 in vacuolar homeostasis. There is some evidence that acidification of the vacuole is also increased during hyper-osmotic stress although it is unclear if this is an active or passive process.

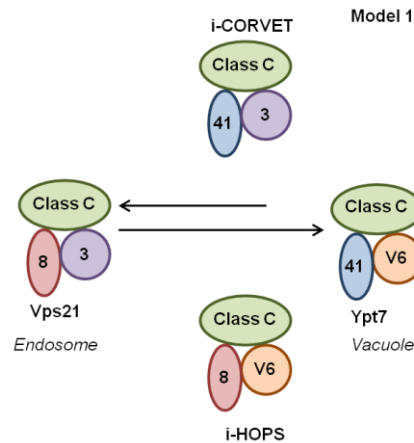
5.4. Process of vacuole Fragmentation.

The actual mechanism by which the fragmentation occurs is also unknown. One possibility is that it could occur through large-scale extrusion of the vacuole followed by scission. Another mechanism could be through a process of vesicle budding from the vacuole surface followed by fusion of these vesicles into a nascent vacuole. Some molecular components required for stress induced fission are known and include Fab1p and its upstream regulators, as well as Atg18p and Hsv2p, which are both known 7-bladed -propeller type PtdIns(3,5) P_2 effectors (PROPPINs) (Cooke et al., 1998, Dove et al., 2004, Efe et al., 2007).

5.5 The CORVET-HOPS complex.

Another potentially important protein complex in fragmentation is the HOPS/CORVET complex (Peplowska et al., 2007). The HOPS complex has been known for some time as a tethering complex, that “proof-reads” SNARE-SNARE interactions to ensure fidelity in vacuole-vacuole fusion in a Rab7 (Ypt7p) dependent fashion (Peplowska et al., 2007). Hence HOPS mediates the reverse process to Fab1p and PtdIns(3,5) P_2 . The HOPS complex has been shown to be able to swap out two of its subunits and become a new protein complex, known as CORVET. The CORVET complex mediates vacuole fission via Rab5 (Vps21p). Since CORVET interacts with Rab5 it could potentially mediate vacuole to PVE trafficking as well, suggesting that some link could exist between Fab1p / PtdIns(3,5) P_2 and CORVET (Peplowska et al., 2007).

Figure 5.2 HOPS/CORVET complex assembly.



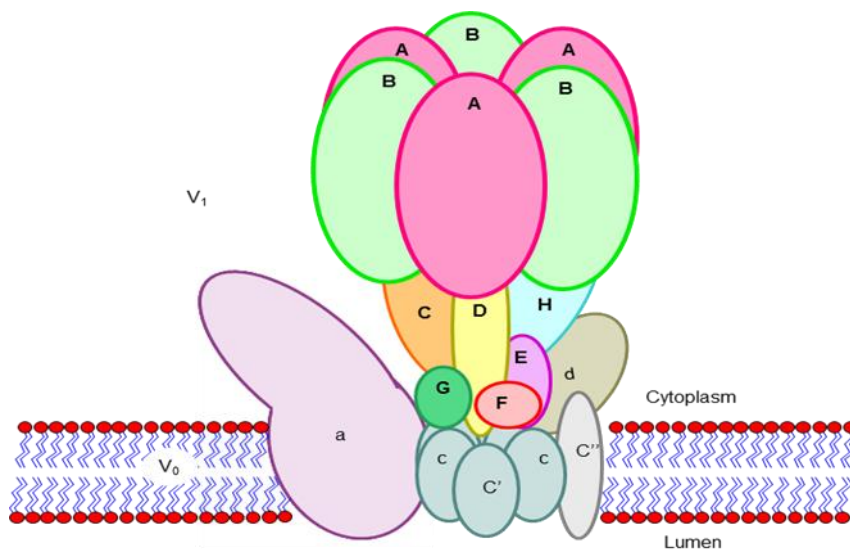
Interconversion from i-CORVET to CORVET is unidirectional (Figure modified from Peplowska et al 2007)

Both the HOPS and CORVET complexes share the subunits Vps11p, Vps16p, Vps18p and Vps33p. The remaining two subunits of the complex, determine if the complex is a Rab7 (Ypt7p) effector (HOPS complex) or a Rab5 (Vps21p) effector (CORVET complex). The HOPS complex contains Vps41p/Vam2p and Vam6p and CORVET the respective homologs of the HOPS specific proteins: Vps8p and Vps3p (Peplowska et al., 2007). Osmolytes generated during osmotic stress, functionally destabilise Ypt7p and the HOPS complex. This leads to subunit exchange and generation of the CORVET complex on vacuole membranes (Brett and Merz, 2008). Intermediate complexes as shown in Figure 5.2 are observed, which suggests that modular assembled tethering complexes define organelle biogenesis in the endocytic pathway (Peplowska et al., 2007). It will be intriguing to see whether the processes and machinery that control vacuole fragmentation are related to that underlying vacuole to late endosome (PVE) trafficking.

5.6. The V-ATPase

In addition, the vacuolar V-type H^+ ATPase has been demonstrated to also be required for PtdIns(3,5) P_2 -dependent vacuole fragmentation in response to hyper-osmotic stress, as indeed is the proton gradient (Baars et al., 2007). The V-ATPase is found in all eukaryotes, and is highly conserved between species. The *S. cerevisiae* V-ATPase has therefore been used as a model system and has many advantageous characteristics as mutants who lack V-ATPase subunits are still viable making study of the system easier (Sambade and Kane, 2004).

Figure 5.3. Diagram of the V-ATPase subunits.



The V-ATPase is made up from two sub complexes V₁ and the membrane bound V₀. Some of the subunits are tissue specific i.e. C''.

V₁ (A- Vma1p, B- Vma2p, C- Vma5p, D- Vma8p, E- Vma4p, F- Vma7p, G-Vma10p, H-Vma13p).

V₀ (a- Vph1p/Stv1p, c- Vma3p, c'-Vma11p, c''- Vma16p, d- Vma6p, e- Vma9p).

V-ATPases are able to acidify multiple organelles, mutants that lack V-ATPase activity have a distinctive set of growth defects. Mutants lacking a V-ATPase subunit are known as *vma* mutants and study of these mutants has revealed a much larger role for the V-ATPase (Sambade and Kane, 2004). These *vma* mutants are hypersensitive to multiple forms of oxidative stress so an antioxidant role for the V-ATPase has also been suggested.

Recent research by the Mayer lab has now linked the V-ATPase to the regulation of the vacuolar fission-fusion equilibrium (Baars et al., 2007). In the course of the normal cell cycle, the vacuole undergoes co-ordinated cycles of membrane fission and fusion involving both the HOPS and CORVET complexes. The Mayer lab identified a novel factor that impinges on the fusion-fission equilibrium which is the vacuolar H⁺-ATPase of V-ATPase. The V-ATPase performs two distinct roles during fusion and fission. Fusion of the vacuole needs the physical presence of the membrane sector of the V-ATPase, whilst fragmentation requires proton translocation by the V-ATPase (Baars et al., 2007). If the V-ATPase is disrupted by constitutive mutations or pharmacology so that it is no longer able to pump protons, then salt induced vacuole fragmentation is blocked (Baars et al., 2007). Another report has also noted that V-ATPase mutants display single vacuoles that do not undergo fragmentation in response to hyper-osmotic stress. It is believed that the vacuolar V(1)/V(0)-ATPase is involved in the release of the HOPS subunit Vps41p from vacuoles, further linking it with vacuole fragmentation and fusion (Bayer et al., 2003). Members of the V₁ sector are reported to be deficient in fragmentation under hyper-osmotic stress like what is observed in a $\Delta fab1$ strain.

A recent proteomics screen also identified several members of the V₁ sector as proteins which bind PtdIns(3,5)*P*₂; Vma1p, Vma2p, Vma4p, Vma5p (Catimel et al.,

2008). This is a very interesting development and strongly suggests that one of PtdIns(3,5) P_2 functions requires the V-ATPase and this possibly links with vacuolar fragmentation under hyper-osmotic stress.

5.7. Maintaining vacuole fragmentation.

A further clue to the machinery controlling the process of vacuole fragmentation, is provided by the $\Delta yck3$ mutant. This mutant initially displays vacuole fragmentation during hyper-osmotic stress as is seen in normal functioning wild-type cells.

However, after 10 minutes the vacuoles re-fuse. This raises the possibility that Yck3p, a vacuole membrane localised casein protein kinase, is required to maintain fragmentation of the yeast vacuole. Indeed Yck3p is involved in regulation of the HOPS/CORVET complex via phosphorylation of Vps41p, however, the role of this phosphorylation is not clear (LaGrassa and Ungermann, 2005).

5.8. Aims

This chapter aims to establish potential proteins which may be involved in the mechanism of stress induced vacuole fragmentation. Through the use of the lipid dye FM4-64 the requirement for members of the CORVET and V-ATPase complexes in vacuole fragmentation was examined.

5.9 Results

Screening of mutants who may play a role in vacuole fragmentation and be potential PtdIns(3,5) P_2 effectors was carried out to see if numbers of vacuoles inside the cell increase after 10 minutes of a 0.4M hyper-osmotic stress.

In some deletion strains it is harder to observe whether vacuole fragmentation is taking place as the vacuoles are too small. To overcome this problem strains with an additional deletion of *PEP4* a vacuolar protease were made. Deletion of *PEP4* increases the size of the vacuole and therefore makes microscopic visualisation easier.

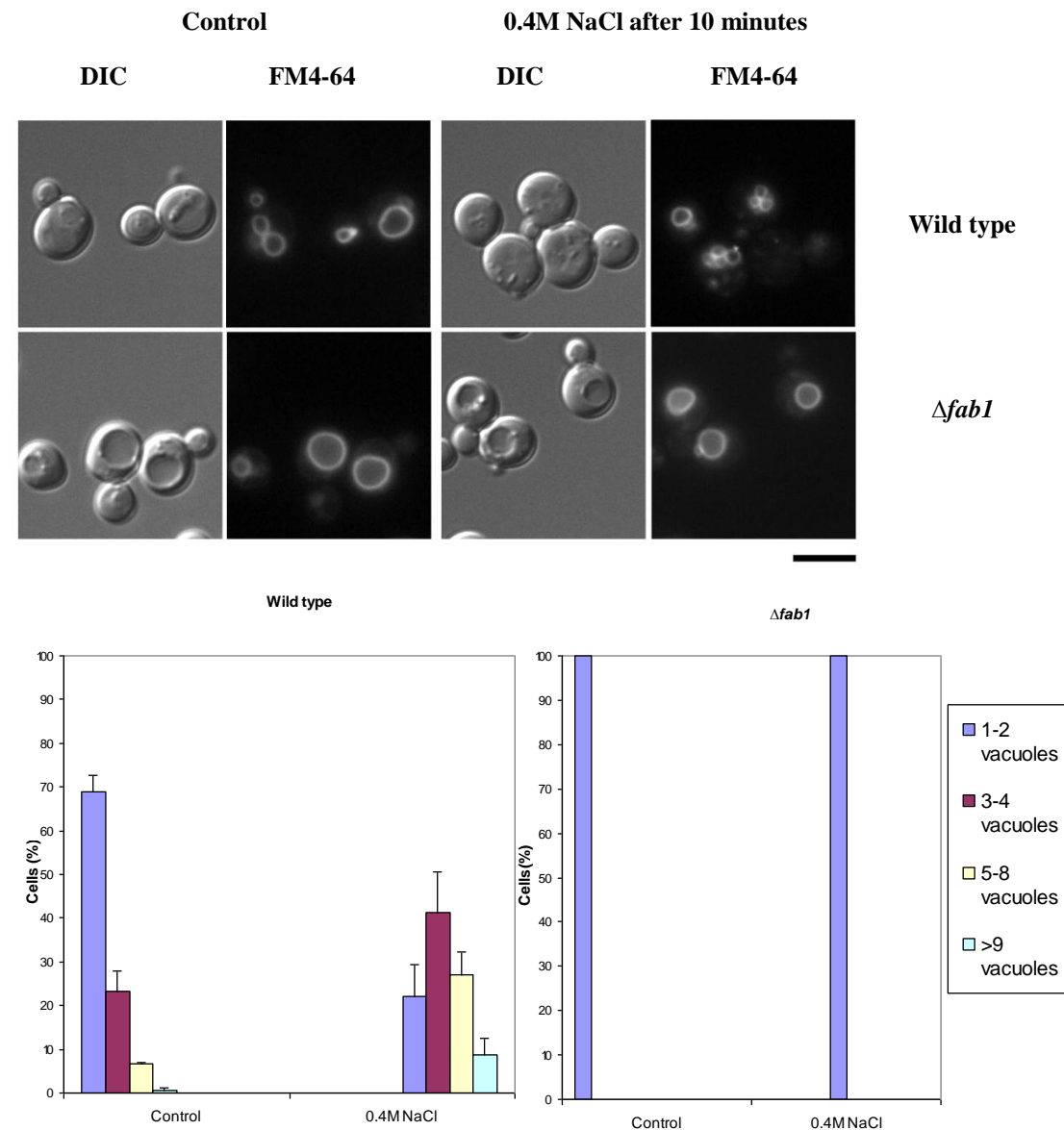
To begin, vacuole fragmentation was observed in controls of wild-type cells with a *PEP4* deletion and a $\Delta fab1$ strain. Strains were stained with FM4-64 as detailed in Chapter 2. They were then prepared for microscopy and cells were resuspended in either control microscope buffer or microscope buffer with 0.4M NaCl. Cells were visualised immediately or after 10 minutes for hyper-osmotically stressed samples.

As shown in Figure 5.4, FM4-64 is a reliable marker for the vacuole. In both strains the dye is endocytosed and can be visualised on the vacuolar membrane before and after treatment with 0.4M NaCl. The results indicate that the vacuoles of the $\Delta fab1$ strain are usually large and unlobed under control conditions. Cells that lack the Fab1p kinase are devoid of PtdIns(3,5) P_2 (Dove et al., 1997). This suggests that the lipid may be necessary in order to regulate the size and shape of vacuoles. This phenotype could be due to imbalance of the fusion-fission equilibrium, with the fusion reaction being favoured or could be due to a decrease in fission or fragmentation.

When $\Delta fab1$ are given hyper-osmotic stress treatment with 0.4M NaCl, the vacuoles still remain large and unlobed, no fragmentation of the vacuoles is observed. Again

the cells are completely devoid of $\text{PtdIns}(3,5)\text{P}_2$, the usual increase in this lipid induced by hyper-osmotic stress cannot happen.

Figure 5.4 Fragmentation controls



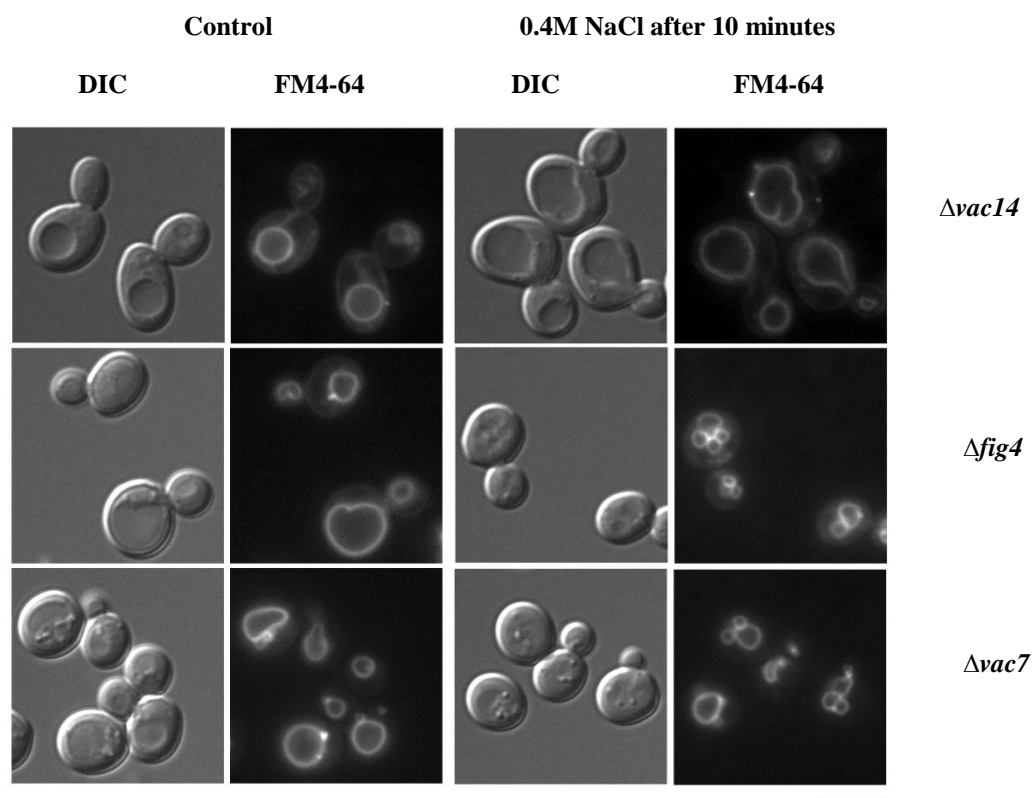
FM4-64 staining of vacuoles in wild-type and $\Delta fab1$ strains. Shown above are fluorescence images of logarithmic phase cultures ($5 \times 10^6 - 1 \times 10^7$ cells/ml) of wild-type (top panels) and $\Delta fab1$ (bottom panels) cells. The left-hand panels show cells under control conditions. The right-hand panels show cells after 10 minutes 0.4M NaCl stress. Left hand columns show low light DIC images. The right-hand columns show the RFP localisation of FM4-64 on the vacuole membrane. Both strains were cultured in YETD+2% glu medium with G418 for and were grown at 25°C. These images are representative of three replicate cultures. Scale bar represents 5 μM .

The number of vacuolar organelles in wild-type *S. cerevisiae* under control conditions is higher than that observed in the $\Delta fab1$ strain. A spread of the number of vacuoles per cell is seen, with some cells possessing up to 9 vacuoles. Vacuoles of wild-type cells, as expected, fragment into numerous smaller compartments with the majority of cells possessing at least 3-4 vacuoles, compared to 1-2 before stress. The number of cells with 1-2 vacuoles is reduced from around 68% to just 20% after treatment with 0.4M NaCl. The process of stress dependent vacuole fragmentation is functioning correctly in wild-type cells, as is the increase in PtdIns(3,5) P_2 levels observed under stress.

It has been reported that proteins involved in the activation of Fab1p and metabolism of PtdIns(3,5) P_2 should also be unable to fragment (Duex et al., 2006b). This is probably due to decreased levels of PtdIns(3,5) P_2 . The roles of Vac14p, Vac7p and Fig4p were investigated. If PtdIns(3,5) P_2 does indeed play a role in vacuole fragmentation, we would expect that cells with decreased levels of the lipid to also possess a defect in the hyper-osmotic stress response.

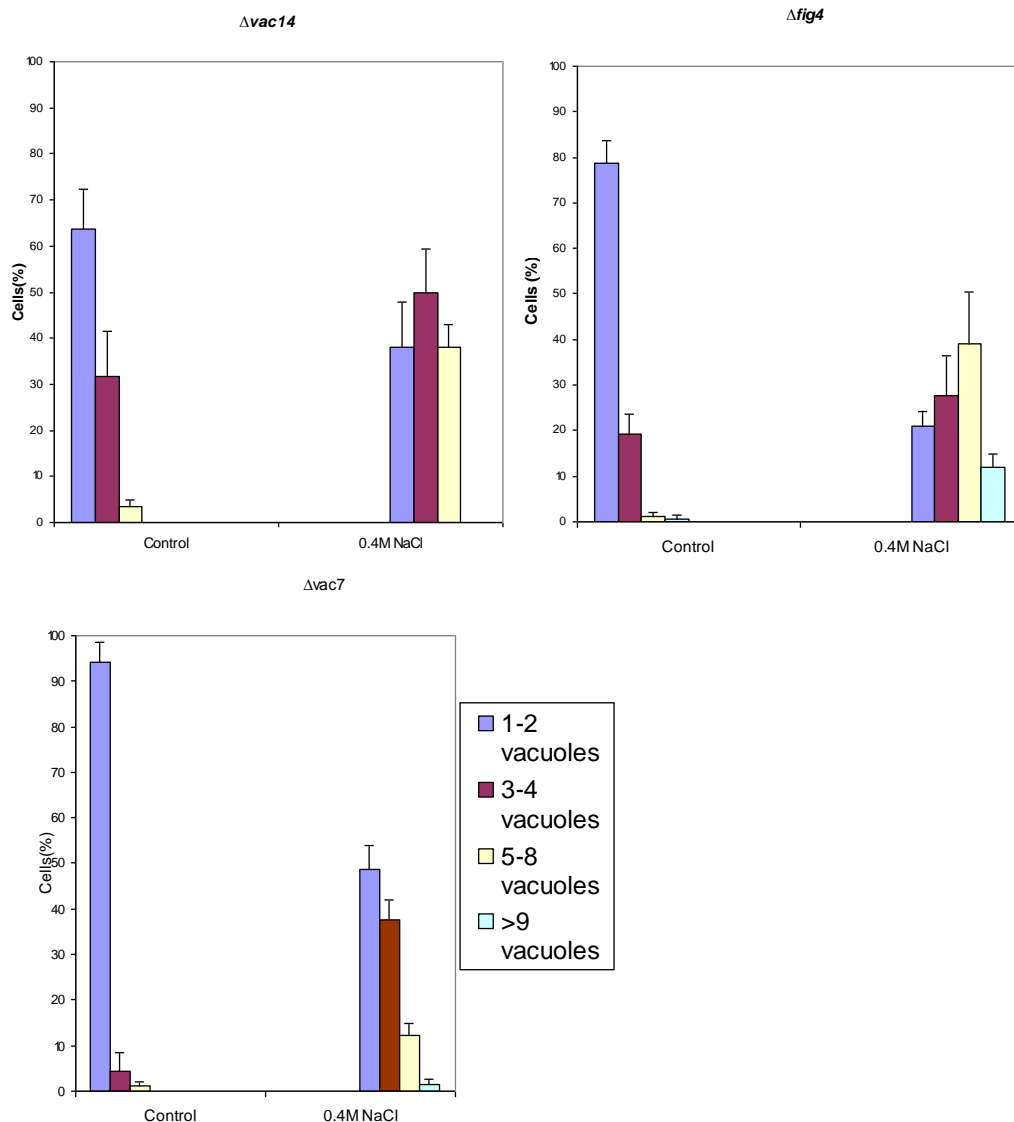
Vacuole numbers of each strain were examined and data grouped into number of vacuoles per cell. Graphs as shown below in Figure 5.6 were drawn to give a clearer indication of whether vacuole fragmentation was taking place in response to hyper-osmotic stress.

Figure 5.5 Fragmentation observed in *Fab1p* regulator mutants.



FM4-64 staining of vacuoles in $\Delta vac14$, $\Delta fig4$ and $\Delta vac7$ strains. Shown above are fluorescence images of logarithmic phase cultures ($5 \times 10^6 - 1 \times 10^7$ cells/ml), of $\Delta vac14$ (top panels), $\Delta fig4$ (middle panels) and $\Delta fab1$ (bottom panels). The left-hand panels show cells under control conditions. The right-hand panels show cells after 10 minutes 0.4M NaCl stress. Left hand columns show low light DIC images. The right-hand columns show the localisation of FM4-64 on the vacuole membrane. All strains were cultured in YETD+2% glu medium with G418 for and were grown at 25°C. These images are representative of three replicate cultures. Scale bar represents 5 μ M.

Figure 5.6 Graphs of fragmentation observed in *Fab1p* regulator mutants.

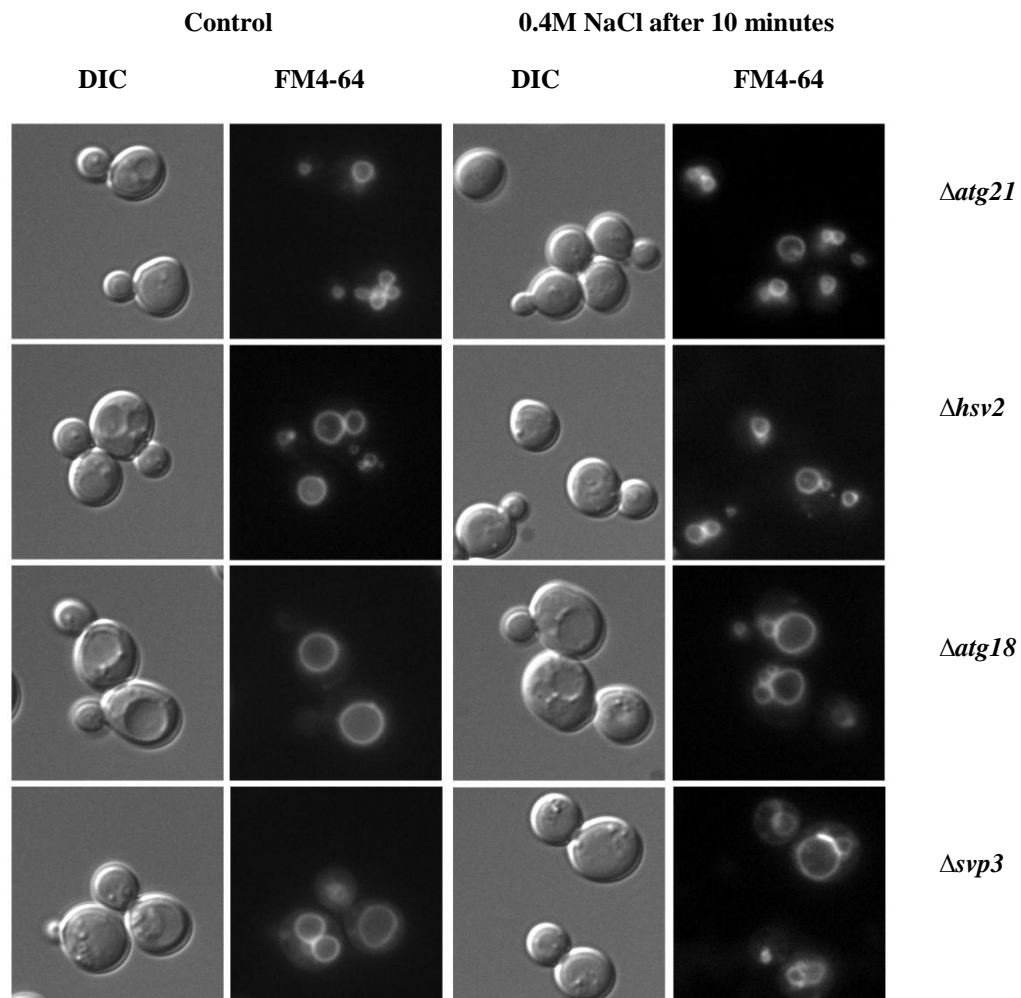


The results shown in Figures 5.5 and 5.6 are somewhat unclear, previously Vac14p mutant cells vacuoles have been reported not to fragment under a 0.4M NaCl stress, my data however suggests that the defect is partial. The percentage of cells with 1-2 vacuoles reduces from around 63% of cells to around 38% of cells. *Δvac14* are reported have an increase of PtdIns(3,5) P_2 levels in response to osmotic stress, although this is much lower than that seen in wild-type cells and is similar to basal levels (Bonangelino et al 2002). Levels of PtdIns3P are however higher than in wild-type, probably due to accumulation, as it is not being depleted by production of

PtdIns(3,5) P_2 . The small amounts of PtdIns(3,5) P_2 may be sufficient to allow some vacuole fragmentation to be carried out. Note however, that vacuoles of cells that have received 0.4M NaCl treatment are still large; they just have tiny vacuolar structures budding off. This may be due to a defect in the machinery involved in fragmentation, perhaps due to lower levels of PtdIns(3,5) P_2 in $\Delta vac14$ cells. Results may vary from reported results due to strain background or to the method of classification/counting. It appears that $\Delta fig4$ cells can carry out vacuole fragmentation in response to the hyper-osmotic stress. Under hyper osmotic stress conditions $\Delta fig4$ cells contain around 25% of wild-type levels of PtdIns(3,5) P_2 (Duex et al 2006b). Fig4p is reported to not only be an activator of Fab1p, but also to be a PtdIns(3,5) P_2 phosphatase, so levels of the lipid are not as low as in a $\Delta vac14$ strain. This would explain how vacuole fragmentation is still able to take place. Under control conditions levels of PtdIns(3,5) P_2 are again decreased, and the vacuole structure is enlarged and unlobed (Duex et al 2006b). This again suggest a link between PtdIns(3,5) P_2 levels and vacuole morphology. Interestingly it appears that the vacuoles of the $\Delta vac7$ strain fragment in a similar way to that of $\Delta fig4$, this suggests that maybe its role in activation of Fab1p may be similar to that of Fig4p. There is currently no known mammalian homolog for Vac7p so its role may be redundant, which suggests it may carry out a similar process to one of the other components involved in PtdIns(3,5) P_2 synthesis. However $\Delta vac7$ cells are reported to have no detectable levels of PtdIns(3,5) P_2 , and unlike in $\Delta vac14$ cells this doesn't change when the strain receives a hyper-osmotic stress (Bonangelino et al., 2002). Therefore as previously reported the vacuoles of $\Delta vac7$ cells would be expected not to fragment. This again may be a consequence of a different strain background, or perhaps even a suppression of the mutation; such suppressors have been reported to accumulate in *fab1* mutants many

times. Consistent with little detectable PtdIns(3,5) P_2 the vacuoles of $\Delta vac7$ cells are large and unlobed.

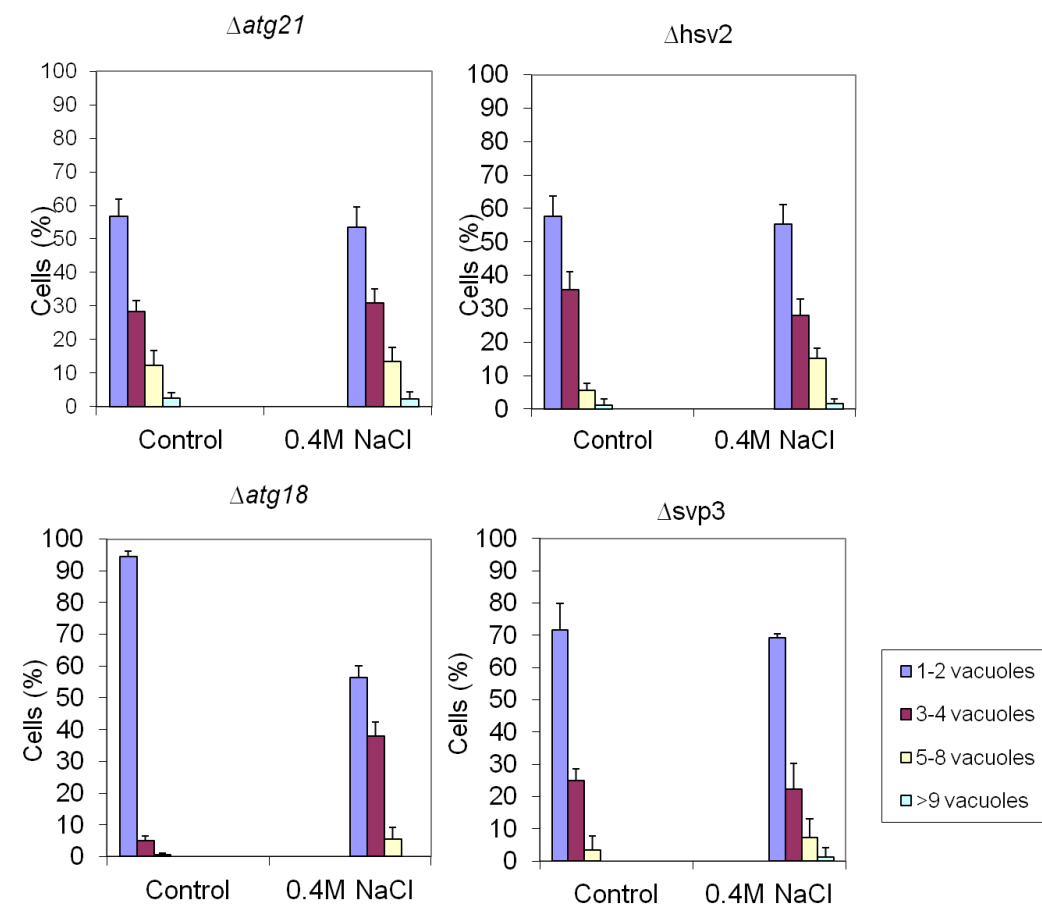
Figure 5.7 Fragmentation observed in PtdIns(3,5) P_2 effector mutants.



FM4-64 staining of vacuoles in $\Delta atg21$, $\Delta hsv2$, $\Delta atg18$ and $\Delta svp3$ strains. Shown above are fluorescence images of logarithmic phase cultures ($5 \times 10^6 - 1 \times 10^7$ cells/ml) of $\Delta atg21$ (top panels), $\Delta hsv2$ (second row panels), $\Delta atg18$ (third row panels) and $\Delta svp3$ (bottom panels). The left-hand panels show cells under control conditions. The right-hand panels show cells after 10 minutes 0.4M NaCl stress. Left hand columns show low light DIC images. The right-hand columns show the localisation of FM4-64 on the vacuole membrane. All strains were cultured in YETD+ G418 +2% glu medium and grown at 25°C. These images are representative of three replicate cultures. Scale bar represents 5 μ M.

Known PROPPIN domain containing effectors of PtdIns(3,5) P_2 were also examined for vacuole fragmentation. These strains should have normal levels of PtdIns(3,5) P_2 , if they are located downstream of Fab1p.

Figure 5.8 Graphs of vacuole fragmentation observed in PtdIns(3,5) P_2 effector mutants.



If the vacuoles of the mutants do not fragment in response to hyper-osmotic stress, it may suggest that the proteins are actually playing a role in this aspect of PtdIns(3,5) P_2 signalling. It would indicate that these effectors are required for vacuole fragmentation to occur. As with all phosphoinositides, PtdIns(3,5) P_2 requires effector

proteins in order to exert its effects so therefore, at least one effector protein should have a role in hyper-osmotic induced vacuole fragmentation (Michell et al., 2006)

Again the number of vacuoles before and after hyper osmotic stress was quantified; the results shown in Figures 5.7 and 5.8 suggest that Atg21p and Hsv2p may play a role in PtdIns(3,5) P_2 fragmentation as when either of the proteins is ablated, vacuoles no longer respond to hyper-osmotic shock and fragment properly. Unlike strains with decreased PtdIns(3,5) P_2 , the vacuoles of $\Delta atg21$ and $\Delta hsv2$ are not enlarged and unlobed under control conditions; suggesting they do not play a role in maintaining vacuole size or number under basal conditions. This suggests that the fusion-fission equilibrium is in the same position in these mutants, as in wild-type cells. The defect in vacuole fragmentation in response to hyper-osmotic stress must be because the proteins deleted are effectors necessary for the fragmentation of vacuoles to take place; since the levels of PtdIns(3,5) P_2 are normal in these cells and respond to stress normally (Dove, SK unpub).

The vacuoles of the $\Delta atg18$ strain appear large and unlobed both before and after hyper-osmotic stress. $\Delta atg18$ cells do not appear to undergo the process of vacuole fragmentation, suggesting that Atg18p is critical for the process and is an effector involved in this pathway. This is an intriguing result as the levels of PtdIns(3,5) P_2 have been measured in this strain and found to be higher than in wild-type cells. Unstressed cells contain 5-10 times more PtdIns(3,5) P_2 than wild-type cells and under stress four times more PtdIns(3,5) P_2 is observed (Dove et al 2004). This again suggests that Atg18p may be part of the machinery that controls stress induced vacuole fragmentation. The control result also strongly supports the idea that Atg18p is required for normal vacuole morphology as the increased levels of PtdIns(3,5) P_2

would suggest the strain should be highly fragmented if it is not involved in the process.

The results seen for $\Delta svp3$ are intriguing, although the vacuoles appear to fragment only slightly, they also do not seem to undergo the process correctly. As shown in Figure 5.7 the main vacuole remains large with smaller vacuoles budding off of one side. This looks like a partial defect and suggests that Svp3p may play a role in this process. In control conditions the vacuoles of $\Delta svp3$ are large but not unlobed; again a partial defect. Indeed, when radiolabelled levels of PtdIns(3,5) P_2 in $\Delta svp3$ are quantified, they are found to be increased (Dove, SK pers comm), which would point to the cell having increased vacuole fragmentation. This is therefore an intriguing result and likely to point to Svp3p having a role in vacuolar dynamics in response to stress.

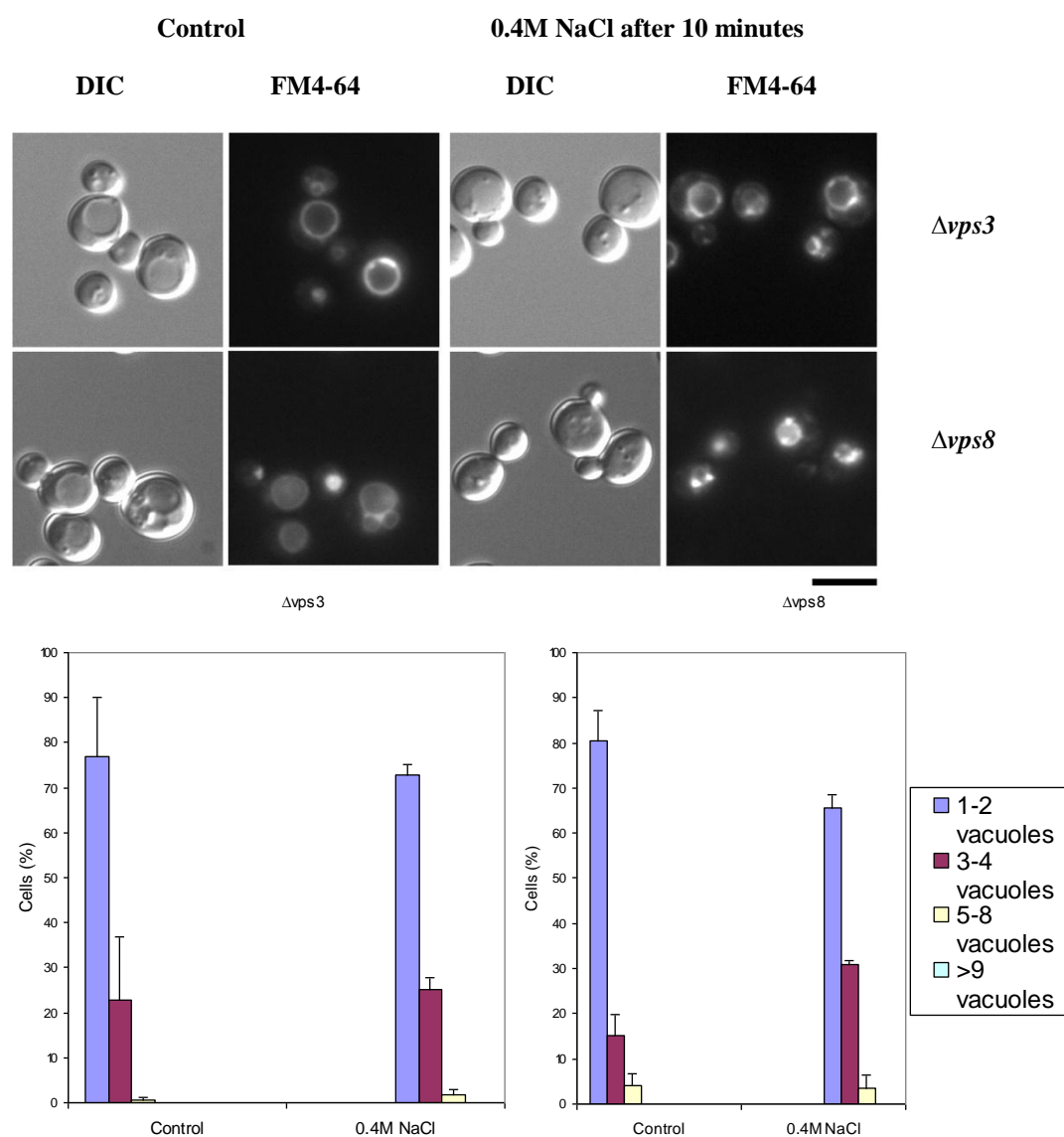
As discussed above the CORVET complex plays a crucial role in vacuole fragmentation during growth. To investigate whether the same components are responsible for micro vacuole fragmentation during hyper-osmotic stress, strains possessing a deletion of one of the two CORVET specific units of the HOPS/CORVET complex were studied. These cells should no longer be able to form complete CORVET complexes, and therefore be unable to undergo macro-fragmentation during the cell cycle (Peplowska et al., 2007).

As shown below in Figure 5.9 before stress, both $\Delta vps3$ and $\Delta vps8$ vacuoles are enlarged under normal conditions. Some cells possess unlobed vacuoles in both strains with $\Delta vps3$ cells possessing vacuoles that are less fragmented than wild-type. This suggests that in both of these strains vacuole fusion is favoured; this may be due

to shift of the equilibrium towards fusion, as the CORVET subunits required for fission are not present.

It appears that the vacuoles of the $\Delta vps3$ strain do not fragment when given a 0.4M NaCl stress. There is little change between control and hyper-osmotic conditions.

Figure 5.9 Fragmentation observed in CORVET mutants.



FM4-64 staining of vacuoles in $\Delta vps3$ and $\Delta vps8$ strains. Shown above are fluorescence images of logarithmic phase cultures ($5 \times 10^6 - 1 \times 10^7$ cells/ml) of $\Delta vps3$ (top panels), and $\Delta vps8$ (bottom panels). The left-hand panels show cells under control conditions. The right-hand panels show cells after 10 minutes 0.4M NaCl stress. Left hand columns show low light DIC images. The right-hand columns show the localisation of FM4-64 on the vacuole membrane. All strains were cultured in YETD+ G418 +2% *glu* medium and grown at 25°C. These images are representative of three replicate cultures. Scale bar represents 5 μ M.

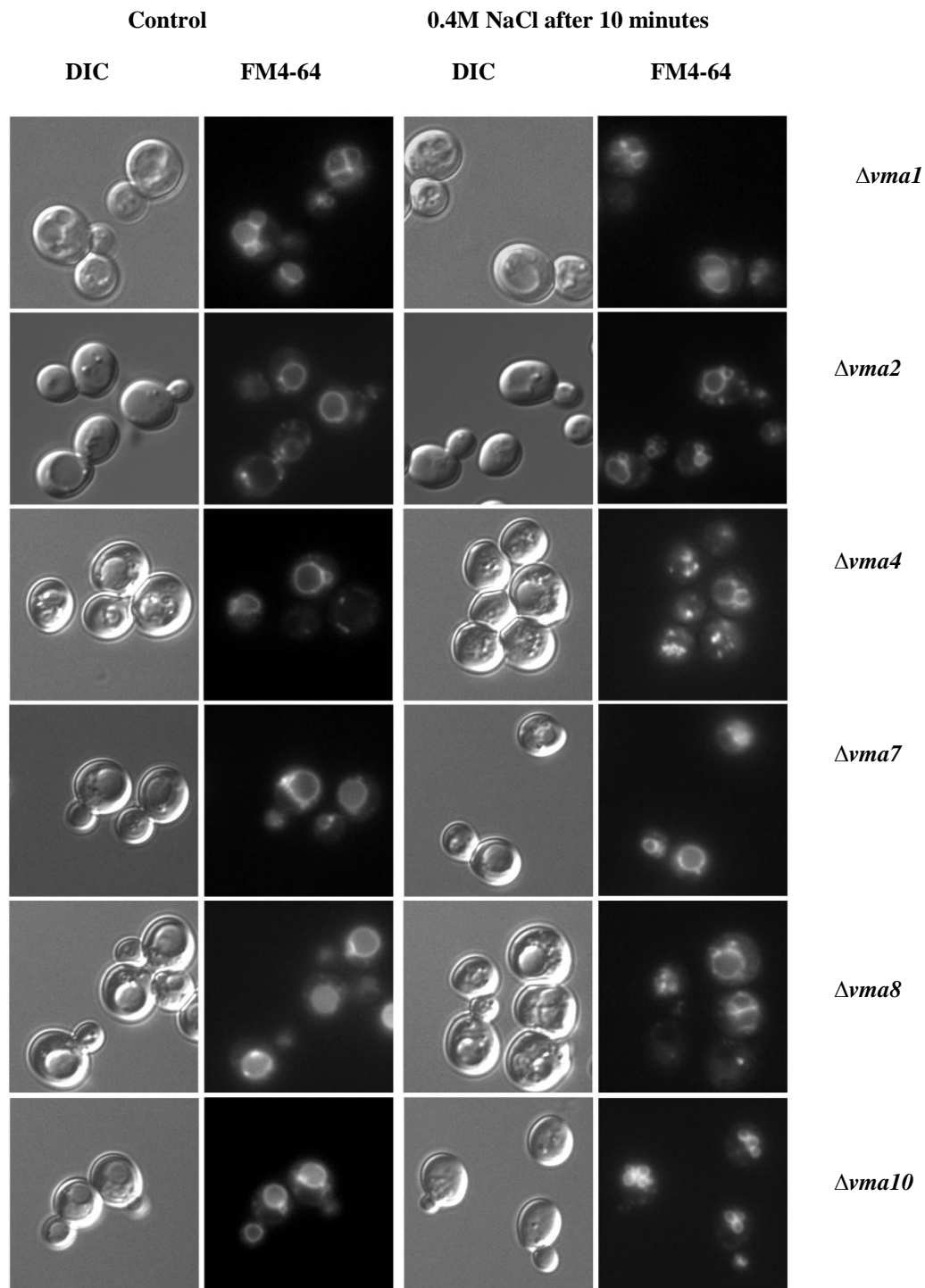
The $\Delta vps8$ strain undergoes some fragmentation although it does not appear to fragment as the wild-type strain does, and a large proportion of cells remain with only 1-2 vacuoles. When performing this experiment it was noticed that the process of fragmentation may be slower and requires a longer period of exposure to hyper-osmotic stress, suggesting that Vps8p may be involved in the dynamics of vacuole fragmentation, and enables the process to happen quickly. It may be that Vsp8p is linked to the process of sensing the cellular stress.

Both of the results above are consistent with the notion of a sharing of machinery between macro fragmentation during the cell cycle and the micro fragmentation in response to hyper-osmotic stress.

To investigate the role of the V-ATPase in vacuole fragmentation, mutants of various subunits of both the V_1 and V_0 complexes were examined.

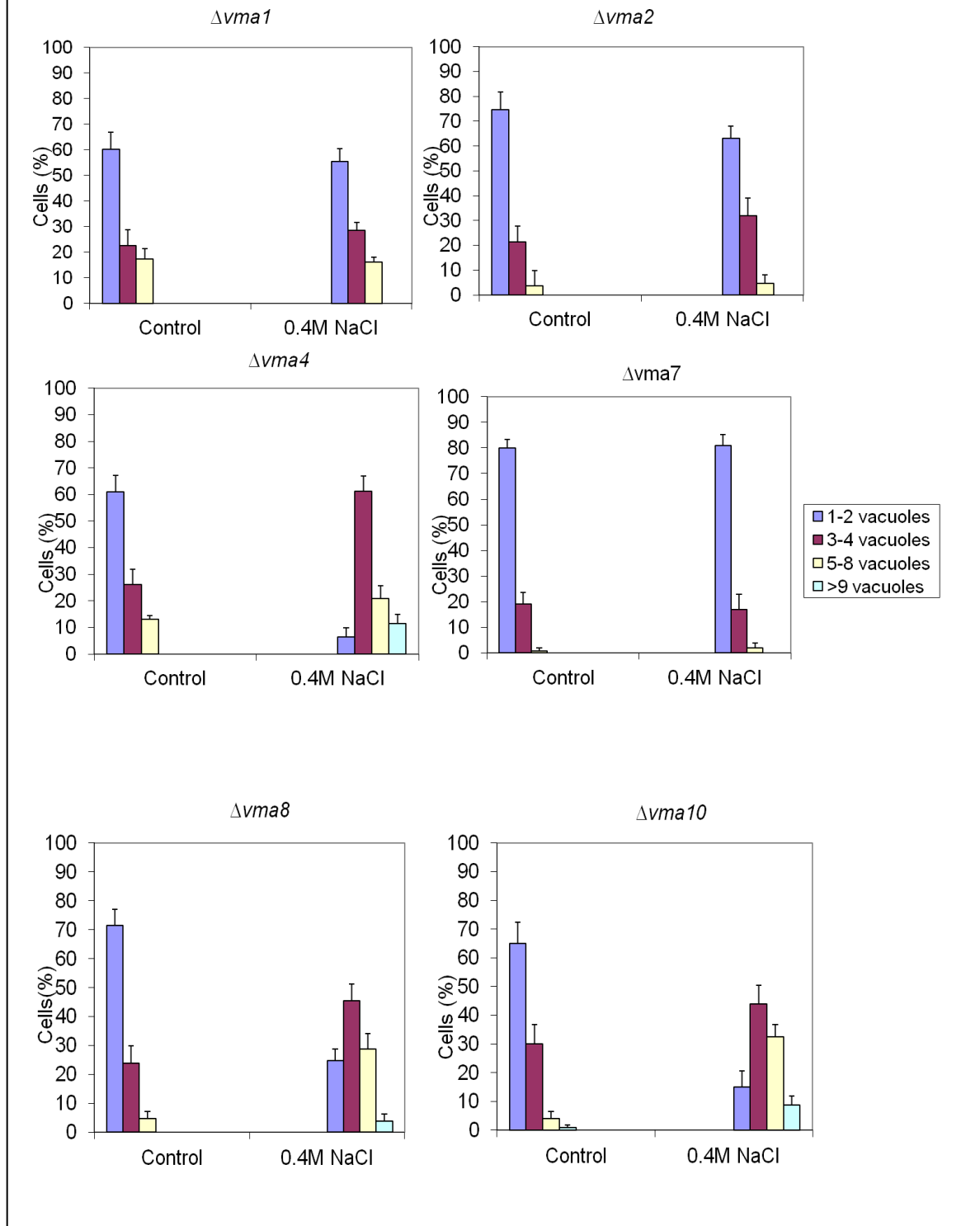
The V_1 domain is required for ATP hydrolysis, and is peripherally associated and contains tissue specific units. A central rotor axle is formed by units Vma8p and Vma7p, which interacts with the V_0 domain (Kane, 2005).

Figure 5.10 Fragmentation observed V_1 mutants.



FM4-64 staining of vacuoles in *Δvma1*, *Δvma2*, *Δvma4*, *Δvma7*, *Δvma8* and *Δvma10* strains. Shown above are fluorescence images of logarithmic phase cultures ($5 \times 10^6 - 1 \times 10^7$ cells/ml). The left-hand panels show cells under control conditions. The right-hand panels show cells after 10 minutes 0.4M NaCl stress. Left hand columns show low light DIC images. The right-hand columns show the localisation of FM4-64 on the vacuole membrane. All strains were cultured in YETD+ G418 +2% glu medium and grown at 25°C. These images are representative of three replicate cultures. Scale bar represents 5μM.

Figure 5.11 Graphs of vacuole fragmentation observed V_1 mutants.



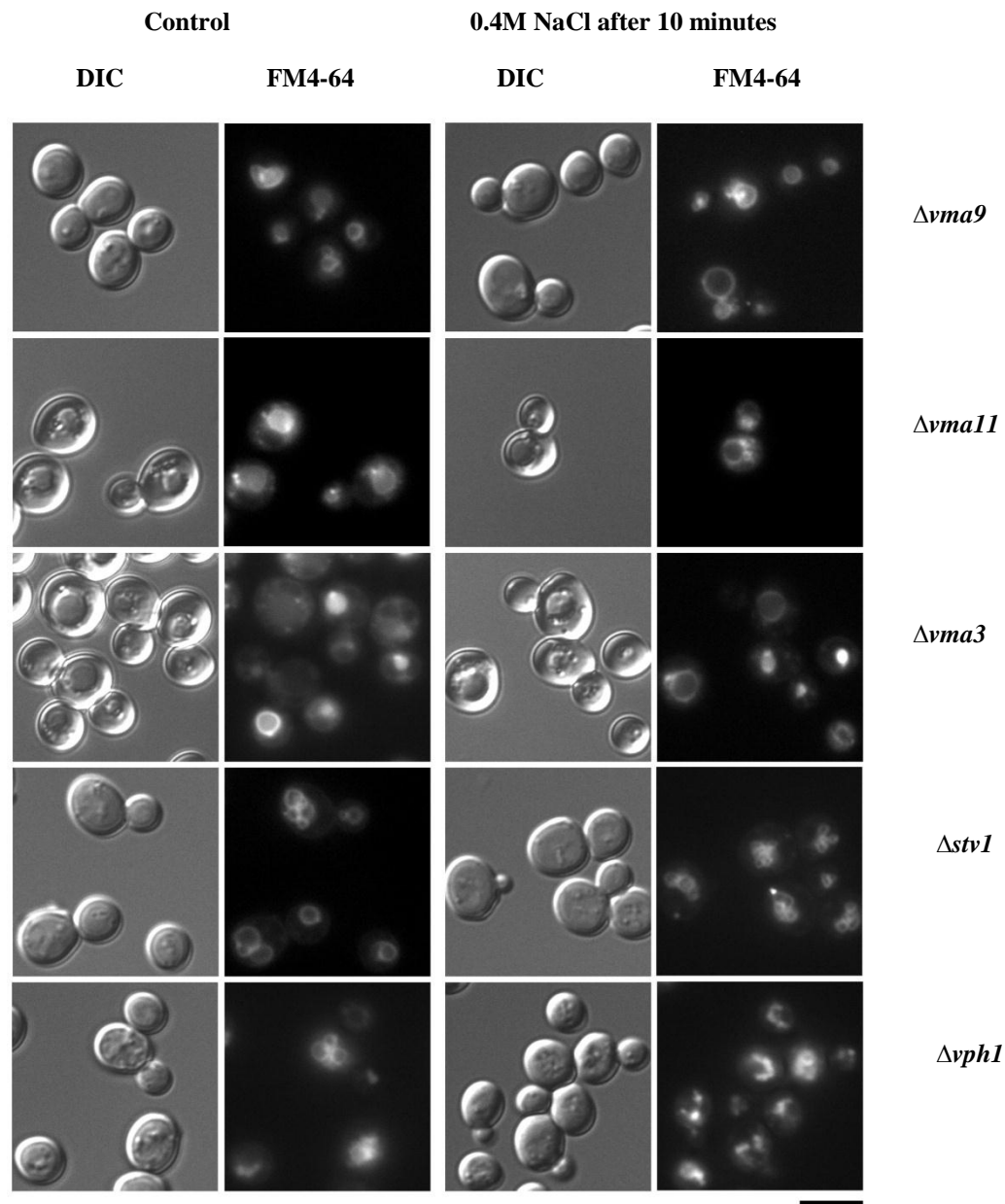
Figures 5.10 and 5.11 indicate that Vma7p, Vma2p and Vma1p may play a role in PtdIns(3,5) P_2 dependent fragmentation. Strains possessing a deletion in any of these genes either undergo no fragmentation in the case of $\Delta vma7$ or reduced fragmentation

in both $\Delta vma1$ and $\Delta vma2$ strains. This is an interesting result as both Vma1p and Vma2p have been reported to bind PtdIns(3,5) P_2 in the recent proteomics paper (Catimel et al., 2008). It would be interesting to see if expressed Vma1p, Vma2p or Vma7p bind PtdIns(3,5) P_2 selectively on lipid dot blots.

Vma4p is also reported to bind PtdIns(3,5) P_2 in the Catimel paper, however my results suggest that strains possessing a deletion of *VMA4* are still able to fragment. This means that Vma4p is unlikely to be a PtdIns(3,5) P_2 effector that is involved in vacuole fragmentation. This also agrees with data from the Mayer lab (Baars et al., 2007). Alternatively Vma4p may be involved in vacuole fusion.

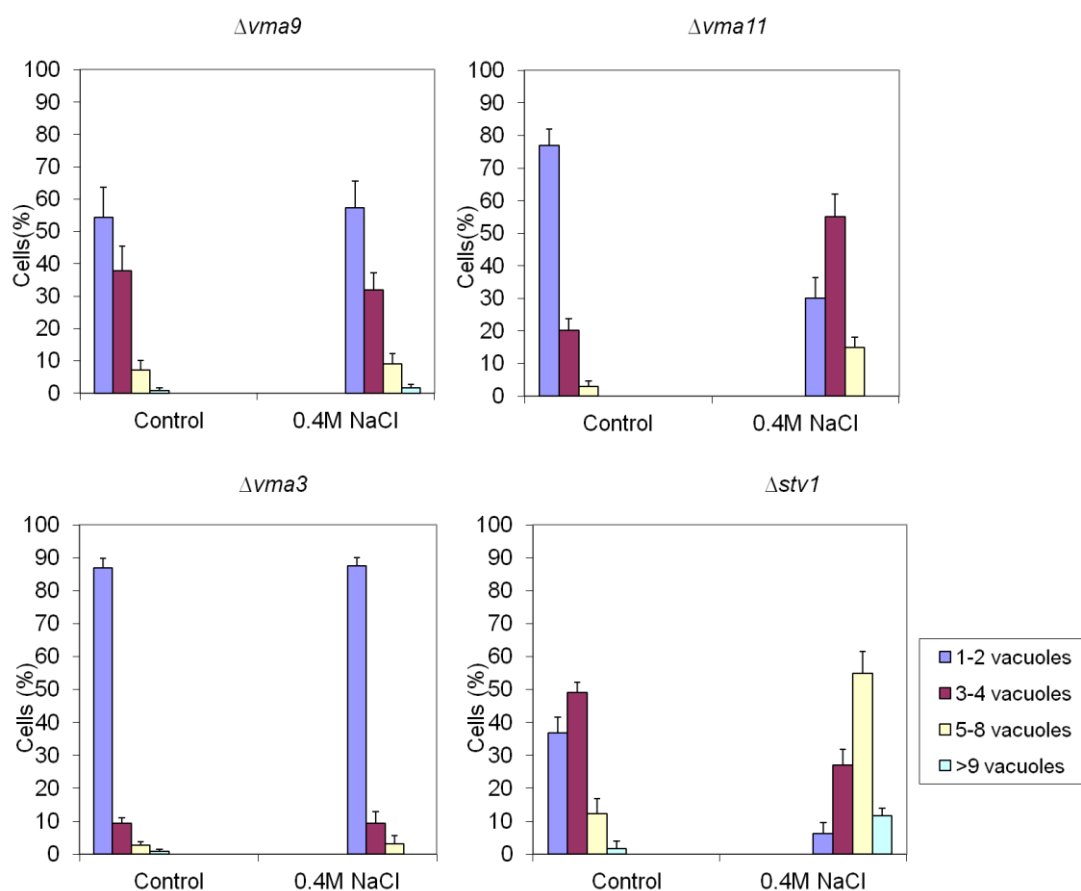
Members of the V_0 complex were also examined for a role in hyper-osmotic induced vacuole fragmentation. The V_0 complex is a membrane bound complex which is responsible for proton translocation. As shown in Figure 5.12 and the graphs shown in Figure 3.13 both Stv1p and Vph1p, which substitute for each other in the V_0 complex, fragment under hyper-osmotic stress. It also appears from the data that Vma11p does not have an effect on vacuole fragmentation. Cells deficient in Vma11p are still able to fragment when treated with a 0.4M NaCl stress.

Figure 5.12 Fragmentation observed V_0 mutants.



FM4-64 staining of vacuoles in *Δvma9*, *Δvma11*, *Δvma3*, *Δstv1* and *Δvph1* strains. Shown above are fluorescence images of logarithmic phase cultures ($5 \times 10^6 - 1 \times 10^7$ cells/ml.) The left-hand panels show cells under control conditions. The right-hand panels show cells after 10 minutes 0.4M NaCl stress. Left hand columns show low light DIC images. The right-hand columns show the localisation of FM4-64 on the vacuole membrane. All strains were cultured in YETD+ G418 +2% glu medium and grown at 25°C. These images are representative of three replicate cultures. Scale bar represents 5μM.

Figure 5.13 Graphs of vacuole fragmentation observed V_0 mutants.



Cells possessing a deletion of *VMA3* have previously been reported to not undergo hyper-osmotic induced vacuole fragmentation and the results in this study agree with this observation (Baars et al., 2007).

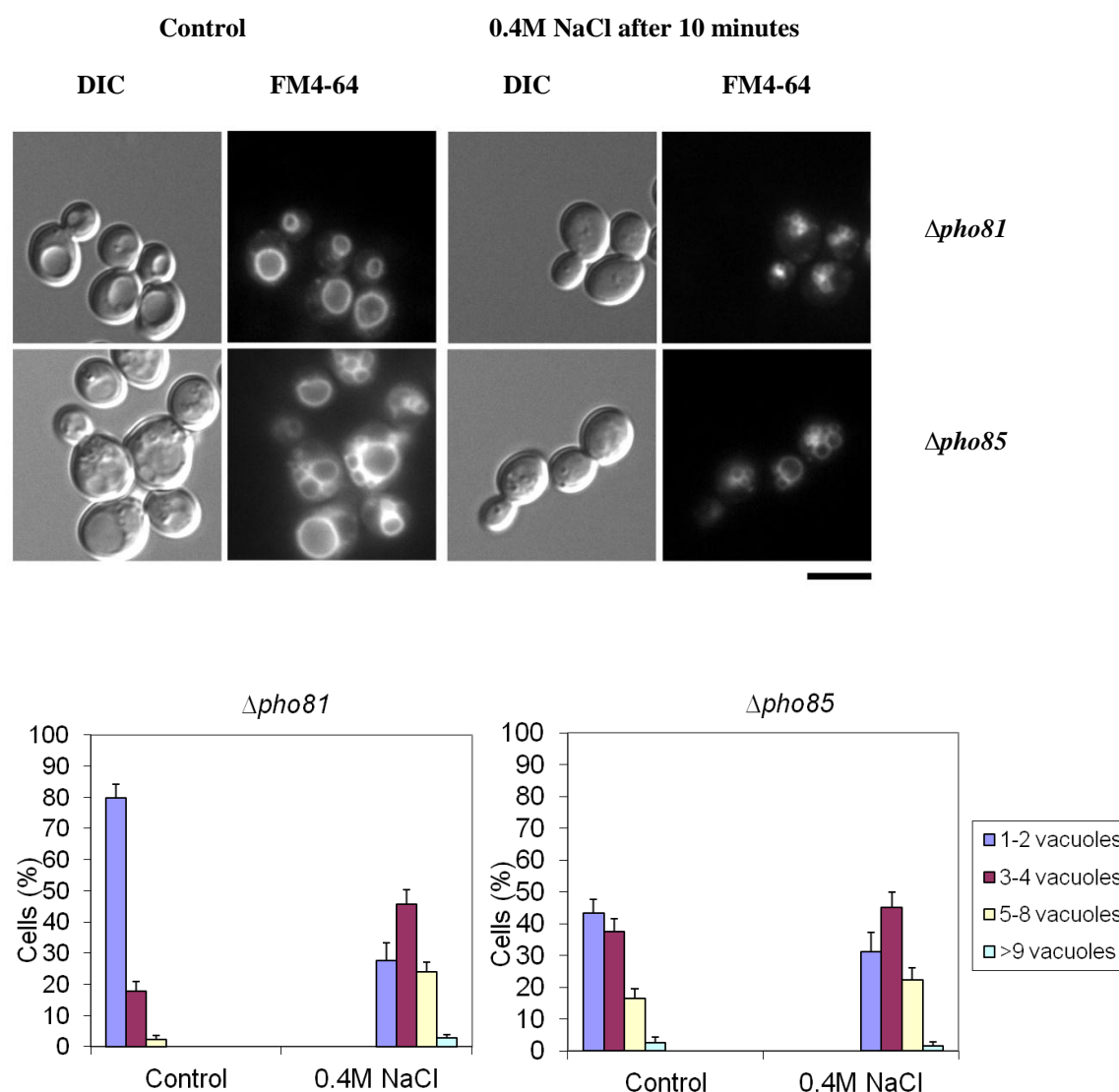
The data also suggests that another V_0 member is involved in vacuole fragmentation. In a $\Delta vma9$ strain cells do not appear to undergo fragmentation. The number of cells with just 1-2 vacuoles actually slightly increases. It is difficult to express membrane

proteins and do a dot blot to see if Vma9p binds PtdIns(3,5) P_2 but this would be a way of seeing if there is in fact any interaction with the lipid.

It is unknown what mechanism or component is used to sense hyper-osmotic stress and increase PtdIns(3,5) P_2 levels. Members of the *PHO* family were examined for defects in vacuole fragmentation as these proteins are involved in sensing and maintaining cellular homeostasis, so may allow the cell to react quickly to hyper-osmotic stress. Pho85p is a cyclin dependent kinase and associates with the cyclin Pho80p. Pho85p is known for its role in the PHO pathway that coordinates the response of yeast to phosphate starvation, but it has emerged that this cyclin-CDK complex may sense both nutrient and environmental stresses (Carroll and O Shea 2002). Pho81p is a CDK inhibitor which is bound to the Pho85p-Pho80p complex. It has been suggested that Pho85p appears to inform the cell the current environment is satisfactory (Carroll and O Shea 2002). It may therefore be performing the same role for hyper-osmotic stress.

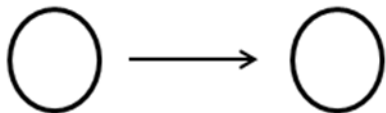
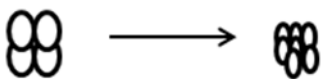
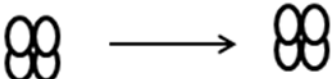

The results in Figure 5.14 indicate that deletion of *PHO81* OR *PHO85* have no effect on stress induced vacuole fragmentation and therefore are not involved in the process.

Figure 5.14 Fragmentation observed in other mutants.



FM4-64 staining of vacuoles in $\Delta pho81$ and $\Delta pho85$ strains. Shown above are fluorescence images of logarithmic phase cultures ($5 \times 10^6 - 1 \times 10^7$ cells/ml) of $\Delta pho81$ (top panels), and $\Delta pho85$ (bottom panels). The left-hand panels show cells under control conditions. The right-hand panels show cells after 10 minutes 0.4M NaCl stress. Left hand columns show low light DIC images. The right-hand columns show the localisation of FM4-64 on the vacuole membrane. All strains were cultured in YETD+ G418 +2% glu medium and grown at 25°C. These images are representative of three replicate cultures. Scale bar represents 5 μ M.

Table 5.1 Summary table

Phenotype	Genotype
	$\Delta fab1, \Delta vac14, \Delta atg18, \Delta vps3, \Delta vps8, \Delta vma7, \Delta vma3$
	Wild Type $\Delta fig4, \Delta vac7, \Delta vma4, \Delta vma8, \Delta vma10, \Delta vma11, \Delta pho81, \Delta pho85$
	$\Delta atg21, \Delta hsv2, \Delta vma1, \Delta vma2, \Delta vma9, \Delta stv1, \Delta vph1$
	$\Delta svp3$

5.10 Discussion.

This chapter presents results that indicate several novel proteins may be involved in PtdIns(3,5) P_2 dependent vacuole fragmentation. Mutants deleted for these genes, do not possess the machinery to undergo vacuole fragmentation as in wild-type cells.

It is likely that the machinery required for vacuole fission during normal cell cycle growth is also required for the micro-fragmentation of the vacuole under hyper-osmotic stress conditions. Evidence for this comes from mutation of the two specific CORVET sub units Vps3p and Vps8p. $\Delta vps3$ fails to undergo proper vacuole fragmentation, and $\Delta vps8$ shows a decrease and delay in the fragmentation response to hyper osmotic stress. It would be interesting to look at point mutations of these two genes to see if the same domains are required for the two processes. Labelling of these

mutants to observe levels of $\text{PtdIns}(3,5)P_2$ has revealed that the vacuole morphology defects are not a consequence of a failure to produce $\text{PtdIns}(3,5)P_2$ in the case of either mutant.

As previously reported a number of V-ATPase mutants have also been found to have a role in stress induced vacuole fragmentation (Baars et al., 2007). Additionally Vma9p, which hasn't previously been noted as showing defects in this process, has been shown to not undergo vacuole fragmentation. In further support for a role in not only vacuole acidification but vacuole fragmentation, several of the V-ATPase subunits have been suggested to bind $\text{PtdIns}(3,5)P_2$ i.e. Vma1p, Vma2p, Vma4p and Vma5p (Catimel et al., 2008). Attempts to express these proteins proved unsuccessful; not enough protein could be produced in order to see if any of these could bind $\text{PtdIns}(3,5)P_2$ in a dot blot or vesicle binding assay. Further work is required to see if these proteins do in fact bind $\text{PtdIns}(3,5)P_2$ and whether binding can regulate the V-ATPase under hyper-osmotic stress conditions.

Interestingly three proteins known to contain β propellers and are suggested $\text{PtdIns}(3,5)P_2$ effectors, have also been shown to have a role in vacuole fragmentation. Deletions of *ATG21*, *HSV2* and *ATG18* all lead to defects in stress induced vacuole fragmentation. This is an intriguing result as both $\Delta atg21$ and $\Delta hsv2$ are reported to not have defects in $\text{PtdIns}(3,5)P_2$ synthesis. Vacuole morphology in these mutants under control conditions is also normal; this suggests that the proteins may be part of the machinery required for stress induced fragmentation only. The $\Delta atg18$ strain has increased levels of $\text{PtdIns}(3,5)P_2$ under both normal and stress conditions, but vacuoles are large and unlobed in both control and stressed samples. Cells with increased levels of $\text{PtdIns}(3,5)P_2$ would be expected to have increased fragmentation but this is not seen. This suggests that Atg18p is required to both maintain vacuole

fission under control conditions and allow stress induced vacuole fragmentation. Atg18p may be part of the vacuolar machinery required before and after stress to control vacuole morphology. It would be interesting to see if Atg18p interacts and recruits Atg21p or Hsv2p to carry out stress induced vacuole fragmentation. Further work is needed in order to understand the role these proteins play. This can be through GFP localisation studies and pull down assays to see if any of the proteins interact with each other or PtdIns(3,5) P_2 through a dot blot assay. Atg18p is already known to bind PtdIns(3,5) P_2 . Again point mutagenesis of the genes could be used to see what part of the protein is necessary for vacuole fragmentation.

Chapter 6

PtdIns(3,5) P_2 and Svp3p/Art1p.

6.1 Introduction

PtdIns(3,5) P_2 is known to have roles at the vacuole particularly during times of cellular stress, it is also involved in various intracellular protein trafficking pathways. It is likely that PtdIns(3,5) P_2 is also implicated in processes or trafficking pathways, that involve the cell surface (discussed in chapter 4). This chapter explores how PtdIns(3,5) P_2 may be linked to the cell surface through a potential effector protein; Svp3p.

SVP3/ART1 was first identified as a potential effector of PtdIns(3,5) P_2 during a screen for yeast mutants which displayed a swollen vacuole phenotype. This characteristic is consistent with a defect in PtdIns(3,5) P_2 levels. Mutants displaying a large unlobed vacuole may be involved in PtdIns(3,5) P_2 generation, or be potential effectors (Dove et al., 2004). Δ *svp3* cells also share another phenotype of Δ *fab1* cells, temperature sensitivity that can be partially overcome with osmotic support (Dove et al., 2004). An increase in PtdIns(3,5) P_2 levels is normally observed at increased temperatures, as this can induce stress in yeast cells. In a Δ *fab1* strain, PtdIns(3,5) P_2 cannot be produced and the strain is unable to grow at 37°C (Dove et al., 2004). If a kinase dead version of Fab1p is present, the cell is still unable to make PtdIns(3,5) P_2 , but the phenotype can be overcome by adding sorbitol or salt to the growth medium. Adding extra osmolytes to the growth medium can also help Δ *svp3* cells overcome the temperature sensitivity defect. This gives an indication that there may be a defect with the cell wall or at the cell surface (Yamamoto et al., 1995).

SVP3 is a poorly characterised gene encoded by the *S.cerevisiae* ORF YOR22C, and is also known as *ART1*. The gene produces an 89 kDa protein, which has been shown to contain multiple PY motifs, and have similarity to mammalian arrestins (Lin et al., 2008). The PY motifs are known to be required for recruitment of a ubiquitin ligase, Rsp5p which in turn modifies the cargoes as well as the ARTs. This causes cargoes to be internalised and targeted to the vacuole for degradation (Lin et al., 2008). $\Delta fab1$ cells are known to have a defect in MVB sorting of ubiquitinated cargoes and defects in ubiquitination. When *FAB1* is deleted, certain MVB cargoes fail to be recognised and so are not sorted correctly in the intraluminal vesicles of the MVB (Shaw et al., 2003, Bryant et al., 1998, Odorizzi et al., 1998, Phelan et al., 2006). Svp3p may be the link between PtdIns(3,5) P_2 , ubiquitination and the cell surface (Katzmann et al., 2004, Phelan et al., 2006, Reggiori and Pelham, 2001). Svp3p is present in both yeast and filamentous fungi and has no known mammalian homologs, although sequence analysis has revealed nine ART family members in yeast that seem to share a conserved fold with mammalian arrestins (Lin et al., 2008).

Basal levels of PtdIns(3,5) P_2 in $\Delta svp3$ cells are around 5 to 10- fold higher than normal, and an increase of PtdIns(3,5) P_2 is observed when cells are treated with an osmotic stress (Dove, SK pers comm). This is similar to what is observed in another effector of PtdIns(3,5) P_2 ; Atg18p (Dove et al 2004). The increased levels of the lipid are however not a consequence of *FAB1* up regulation, since an over expression of *FAB1* does not substantially increase cellular levels of PtdIns(3,5) P_2 , because levels of the other accessory proteins are limiting. This suggests that Svp3p may also have some regulatory role in PtdIns(3,5) P_2 levels, similar to that of Atg18p and may be downstream of Fab1p.

When grown under standard conditions Svp3-GFP is localised to both the cytoplasm and an intense pool in the nucleus. When cells are treated with a hyperosmotic shock or heat stress, translocation occurs in less than a minute, to numerous small punctate 'granule like' structures. These structures are maintained for over an hour but reverse almost immediately if the stress is removed. This response still occurs in $\Delta fab1$ cells indicating that a second pathway, independent of Fab1p and PtdIns(3,5) P_2 also responds to hyper-osmotic stress and acts on Svp3p.

The aim of this Chapter is to find out the functions and mechanism of Svp3p stress induced translocation, as it is probable that this is what links PtdIns(3,5) P_2 to the cell surface.

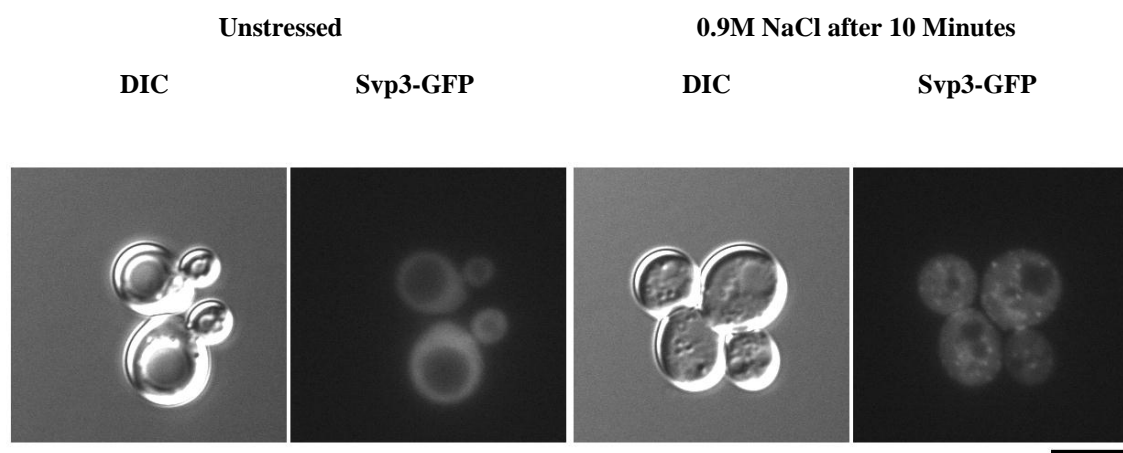
6.2 Localisation of Svp3p

SVP3 was cloned and tagged with GFP at its N terminal under the expression of a Met regulated promoter in a pUG36 plasmid. The construct was used to verify the localisation of Svp3p under both normal growth and hyper osmotic stress conditions. As shown in Figure 6.1, pUG36 Svp3-GFP behaves as described above. Svp3-GFP can be observed throughout the cytoplasm and more intensely in the nucleus of wild-type cells. When the cells receive a hyperosmotic stress Svp3p translocates to a series of punctae, which are observed throughout the cytoplasm and in the nucleus. This represents two pools of Svp3p that are both able to translocate when given a salt stress, suggesting a role for Svp3p in the stress response, and consistent with an increase in PtdIns(3,5) P_2 in response to stress. Svp3p may translocate into these tiny punctate structures because a stress related process, possibly ubiquitination, maybe

happening within these ‘granules’, which requires an increased concentration of Svp3p.

The translocation of Svp3-GFP occurs in both wild-type and $\Delta svp3$ cells. The construct is however easier to visualise in wild-type cells because they are not as slow growing and fragile, therefore all microscopy was carried out in wild-type cells.

Figure 6.1 Localisation of pUG36 Svp3-GFP

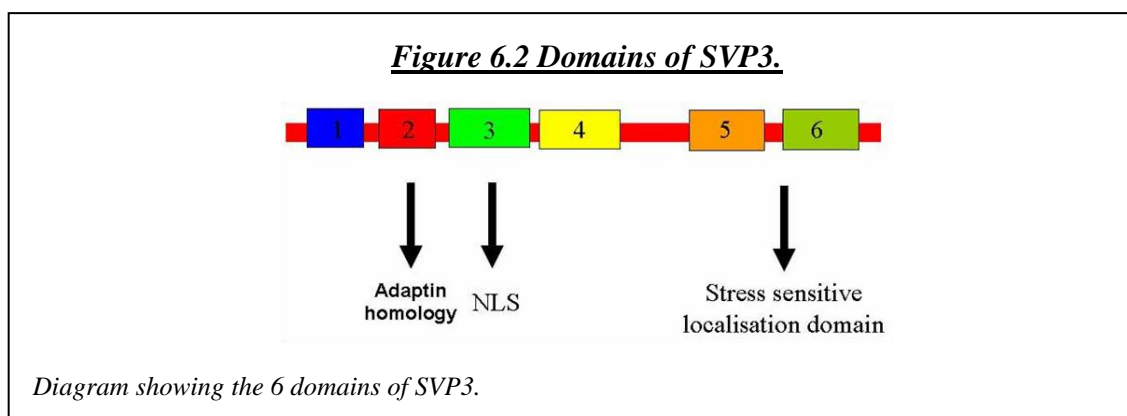


pUG36-Svp3 GFP can be visualised in the cytoplasm and nucleus under control conditions. When given a hyper osmotic stress Svp3-GFP forms punctae. Shown above are fluorescence images of logarithmic phase cultures ($5 \times 10^6 - 1 \times 10^7$ cells/ml) of wild-type cells transformed with pUG36 SVP3-GFP. The left-hand columns show low light DIC images. The right-hand columns show the GFP localisation of Svp3p. The panel to the left shows localisation under control conditions. The panel to the right shows localisation after treatment with 0.9M NaCl. Images are representative of three replicate cultures. All strains were cultured in SC-Ura+25mg/L Met +2% glu medium and grown at 25°C. Scale bar represents 5µM.

When *SVP3* was aligned, a series of conserved blocks of homology were observed as indicated in Figure 6.2. Domain 2 at the N terminus shows some homology to mammalian adaptins.

To discover what part of the *SVP3* gene was responsible for this stress driven translocation, truncation constructs were made where the *SVP3* gene had specific

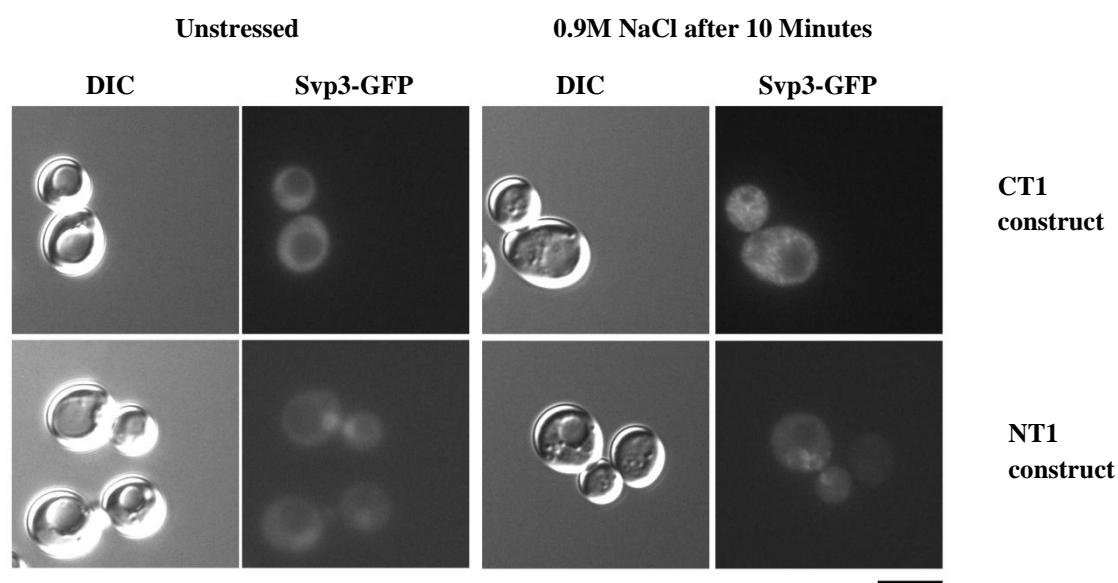
domains removed (Previously made in the Dove lab by Dr Steven Dove and Gavin McNee see Chapter 2 for methods).



All constructs previously examined lacking domain 3, had cytoplasmic localisation only, therefore this domain must contain the NLS. An Svp3^{NT1} GFP construct was used which only contains domains 1-4. An Svp3^{CT1}GFP construct only contains domains 5 and 6. The two constructs were examined under the microscope to see the effect of the truncations.

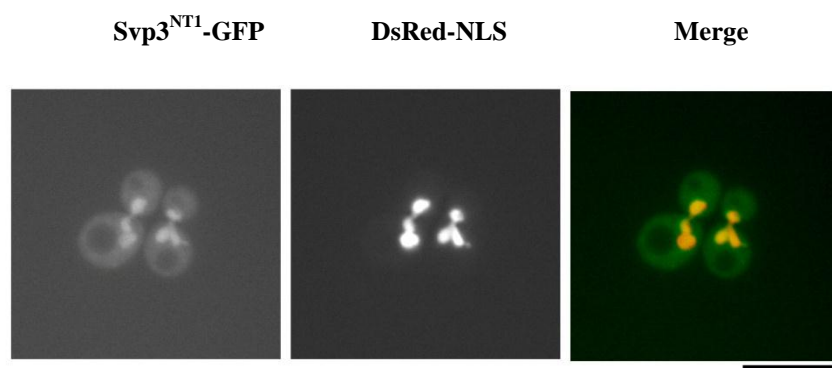
As shown in Figure 6.3 Svp3^{NT1}-GFP, is enriched within the nucleus. The majority of Svp3p that was localised to the cytoplasm in the wild-type construct, is no longer present. This implies that the domains deleted are crucial for normal localisation of Svp3p to the cytoplasm. The overall amount of Svp3-GFP also appears reduced in this strain, as the intensity of nuclear Svp3 –GFP doesn't seem to increase. This construct is stable as judged from GFP stability blots (Dove, SK unpub). When subjected to 0.9M NaCl osmotic stress, Svp3^{NT1}-GFP still translocates to punctae, however this is restricted to the nucleus. The punctae also appear larger than those of the wild-type Svp3-GFP construct. These results suggest domains 5 and 6 may contribute to stress induced translocation of Svp3p.

Figure 6.3 Localisation of pUG36 Svp3 CT1 and NT1.



pUG36-Svp3 GFP CT1 and NT1 constructs still translocate to punctae when given a salt tress. Shown above are fluorescence images of logarithmic phase cultures ($5 \times 10^6 - 1 \times 10^7$ cells/ml) of wild-type cells transformed with pUG36 Svp3^{CT1}-GFP(top panel) and pUG36 Svp3^{NT1}-GFP(bottom panel) The left-hand columns show low light DIC images. The right-hand columns show the GFP localisation of the Svp3-GFP constructs. The panels to the left show localisation under control conditions. The panels to the right show localisation after treatment with 0.9M NaCl. Images are representative of three replicate cultures. All strains were cultured in SC-Ura+25mg/L Met +2% glu medium and grown at 25°C. Scale bar represents 5 μ m.

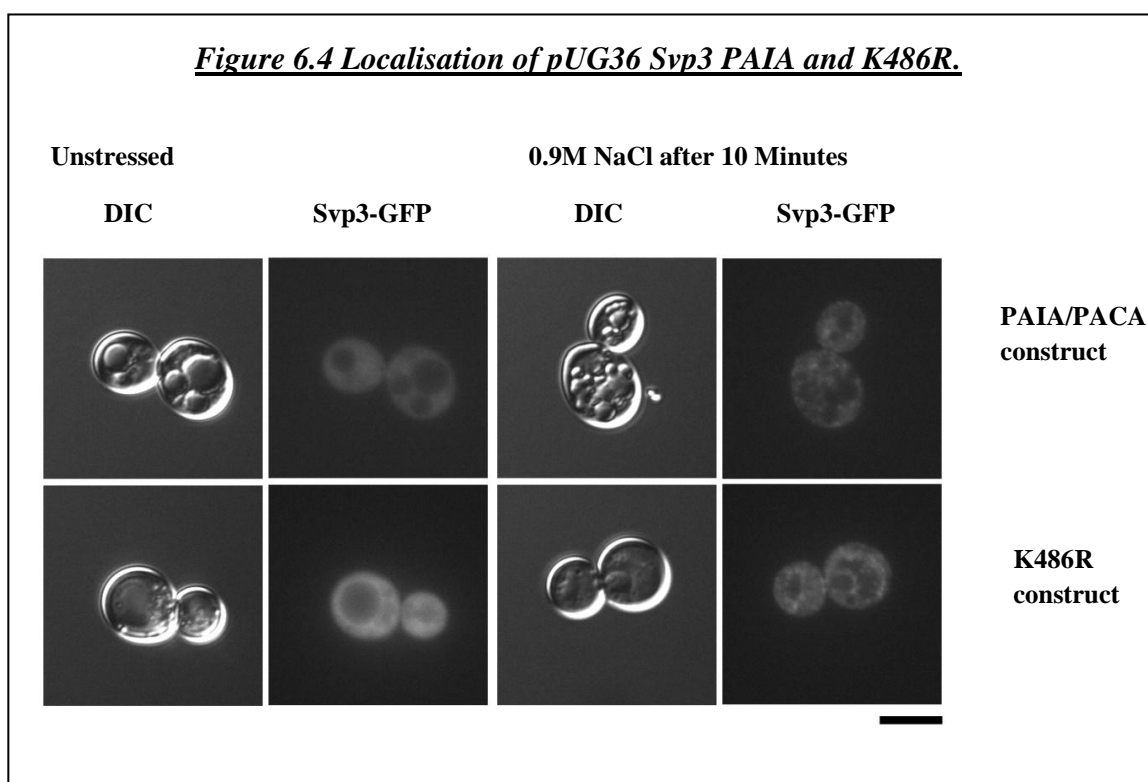
Previous data from Dr Steven Dove is shown below. The image shows the co-localisation of SVP^{NT1}-GFP with the nucleus marker DsRed-NLS.



The Svp3^{CT1}-GFP mutant no longer has the increased nuclear concentration of Svp3-GFP, as observed in the wild-type construct. This is because the domain necessary for nuclear localisation (domain 3) has been deleted. When the cells receive a 0.9M NaCl

stress Svp3^{CT1}-GFP still translocates to a series of punctae structures. However, it is hard to differentiate these from those seen for wild-type Svp3-GFP. Both of the above results suggest that the whole protein is not required for stress induced translocation to be carried out. It would be interesting to see the amounts of PtdIns(3,5)P₂ levels in Δ *svp3* strains possessing the constructs, to see if they are sufficient to rescue defects in the lipid.

A 2008 paper from the Emr group describing *ART1/SVP3*, details two mutants. They identify K486, a residue that becomes ubiquitinated, by Rsp5p. They also identified and mutated the PY motif which is also necessary for Svp3p ubiquitination (Lin et al., 2008). pUG36-Svp3 constructs bearing the above mutations were made using the Site overlap extension method (detailed in Chapter 2), to observe the roles of the residue/motif in stress dependent translocation of Svp3p.



pUG36-Svp3^{PAIA/PACA} and pUG36-Svp3^{K486R} constructs still translocate to punctae when given a salt stress. Shown above are fluorescence images of logarithmic phase cultures ($5 \times 10^6 - 1 \times 10^7$ cells/ml) of wild-type cells transformed with pUG36 Svp3^{PAIA/PACA} (top panel) and pUG36 Svp3^{K486R} (bottom panel). The left-hand columns show low light DIC images. The right-hand columns show the GFP localisation of the SVP3-GFP construct. The panels to the left show localisation under control conditions. The panels to the right show localisation after treatment with 0.9M NaCl. Images are representative of three replicate cultures. All strains were cultured in SC-Ura+25mg/L Met +2% glu medium and grown at 25°C. Scale bar represents 5µM.

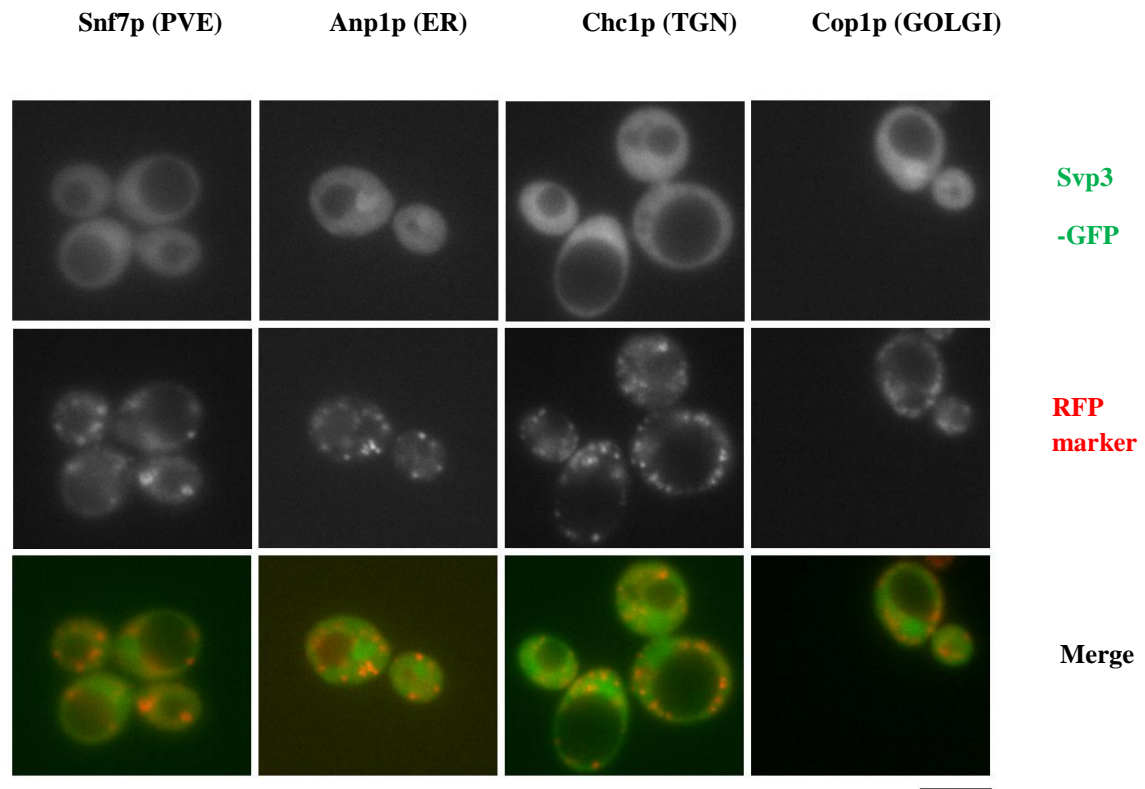
As shown in Figure 6.4 both Svp3^{PAIA/PACA}GFP and Svp3^{K486R}GFP translocate to punctae when the cells receive a hyper-osmotic stress. In both constructs this translocation is maintained as in wild-type cells. It is unclear whether either of these constructs have different localisations to wild-type Svp3-GFP. However under control conditions, neither construct seems to localise to the nucleus as fully as the wild-type Svp3-GFP construct.

To discover if there are any small differences with localisations of any of the constructs made, a series of co-localisations with known RFP markers were performed. This would allow identification of the compartment(s) the Svp3-GFP localises to.

As shown previously Svp3-GFP is observed in both the cytoplasm and intensely in the nucleus of wild-type cells. The pools of Svp3-GFP do not form punctae and so do not discreetly co-localise with the RFP marked compartments (Figure 6.4).

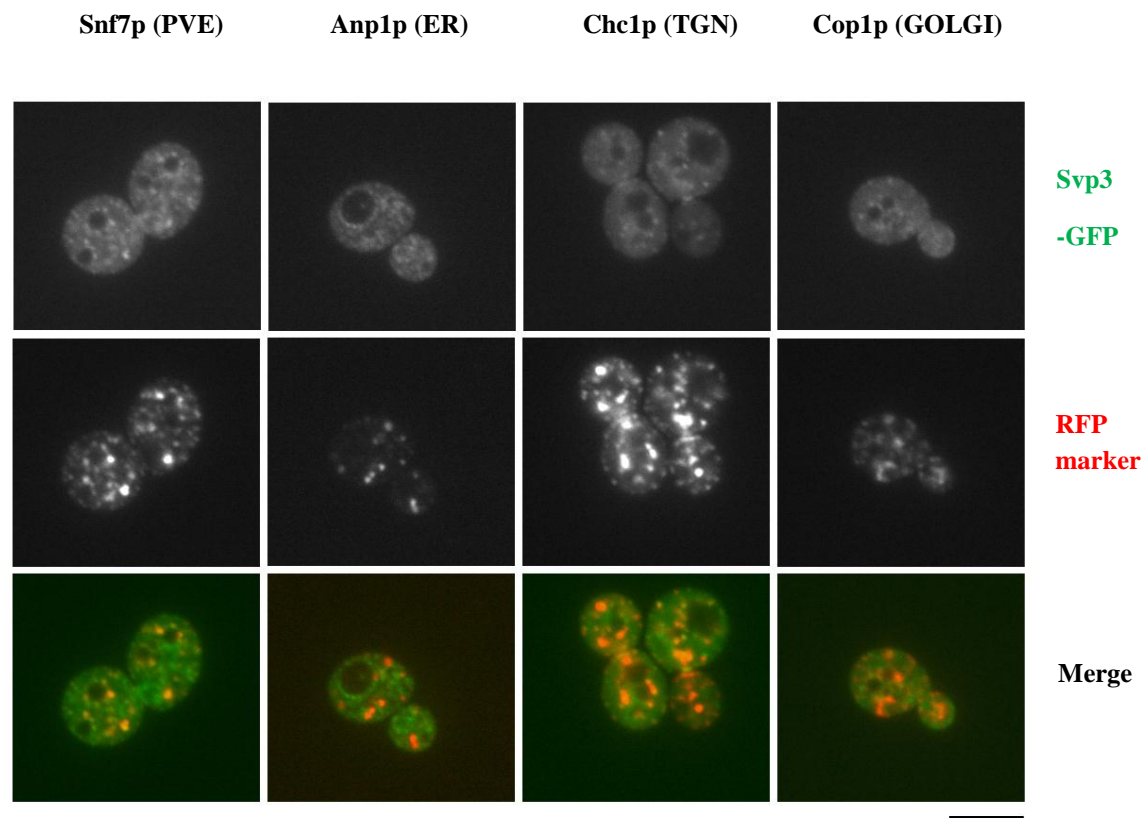
To observe what happens to Svp3-GFP when PtdIns(3,5)P₂ levels increase, cells were treated with a hyperosmotic stress. It could be seen that Svp3-GFP had translocated into a numerous small punctate compartments, as observed previously (Figure 6.6).

Figure 6.5 Co-localisation of GFP- Svp3p under control conditions.



In unstressed wild-type cells Svp3-GFP localises with both the cytoplasm and intensely in the nucleus. Shown above are fluorescence images of logarithmic phase cultures ($5 \times 10^6 - 1 \times 10^7$ cells/ml) of wild-type cells containing various RFP tagged proteins acting as markers (middle panels) transformed with pUG36 Svp3-GFP (top panels). The bottom panel shows a merge of both red and green images for co-localisation. Strains were cultured in SC-Ura+25mg/L Met +2% glu medium and grown at 25°C. These images are representative of three replicate cultures. Scale bar represents 5μM.

Figure 6.6 Co-localisation of GFP-Svp3p under stressed conditions.



59.6% ±7.9***	36.7% ±5.1***	72.1% ±16.4***	49.7% ±5.5***	Red co-localisation
23.2% ±1.7	14.9% ±5.4	24.3%±5.7	15.6% ±4.9	Random co-localisation
36.3% ±9.5	21.8% ±0.4	47.8%±15.2	34.2% ±7.9	Adjusted colocalisation

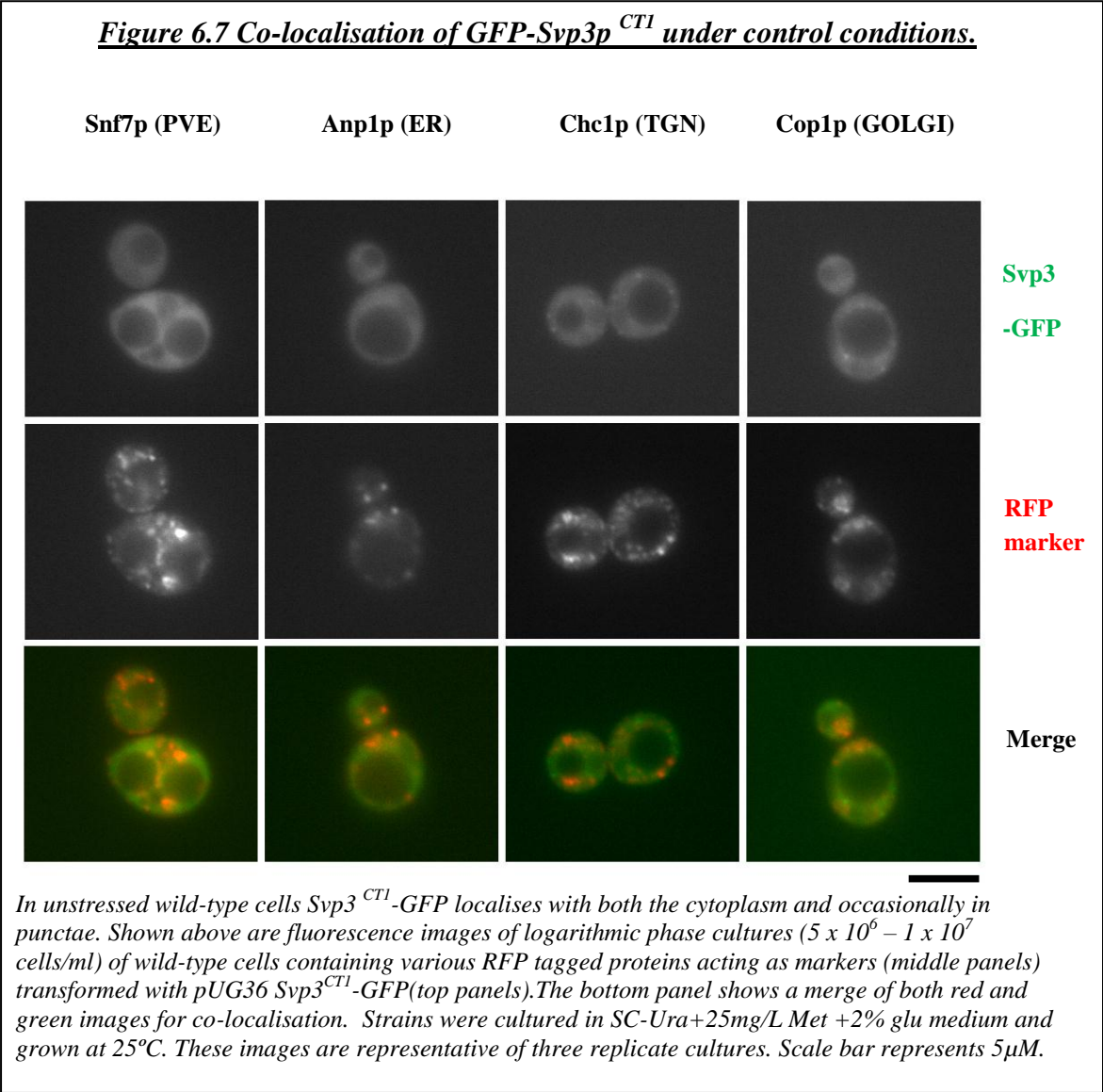
[Significantly different from random co-localiation: ***P<0.001]

In wild-type cells subjected to a 0.9M NaCl stress Svp3-GFP co localises with a number of RFP markers. Shown above are fluorescence images of logarithmic phase cultures ($5 \times 10^6 - 1 \times 10^7$ cells/ml) of wild-type cells containing various RFP tagged proteins acting as markers (middle panels) transformed with pUG36 SVP3-GFP(top panels). The bottom panel shows a merge of both red and green images for co-localisation. Strains were cultured in SC-Ura+25mg/L Met +2% glu medium and grown at 25°C. The cells were resuspended in 0.9M NaCl microscope buffer prior to microscopy. These images are representative of three replicate cultures. Scale bar represents 5µM.

The stress induced Svp3-GFP punctae compartments, do not fully co localise with one compartment alone. Significant co-localisation was observed with all four of the RFP markers examined. Note that co-localisations were carried out for RFP markers as the

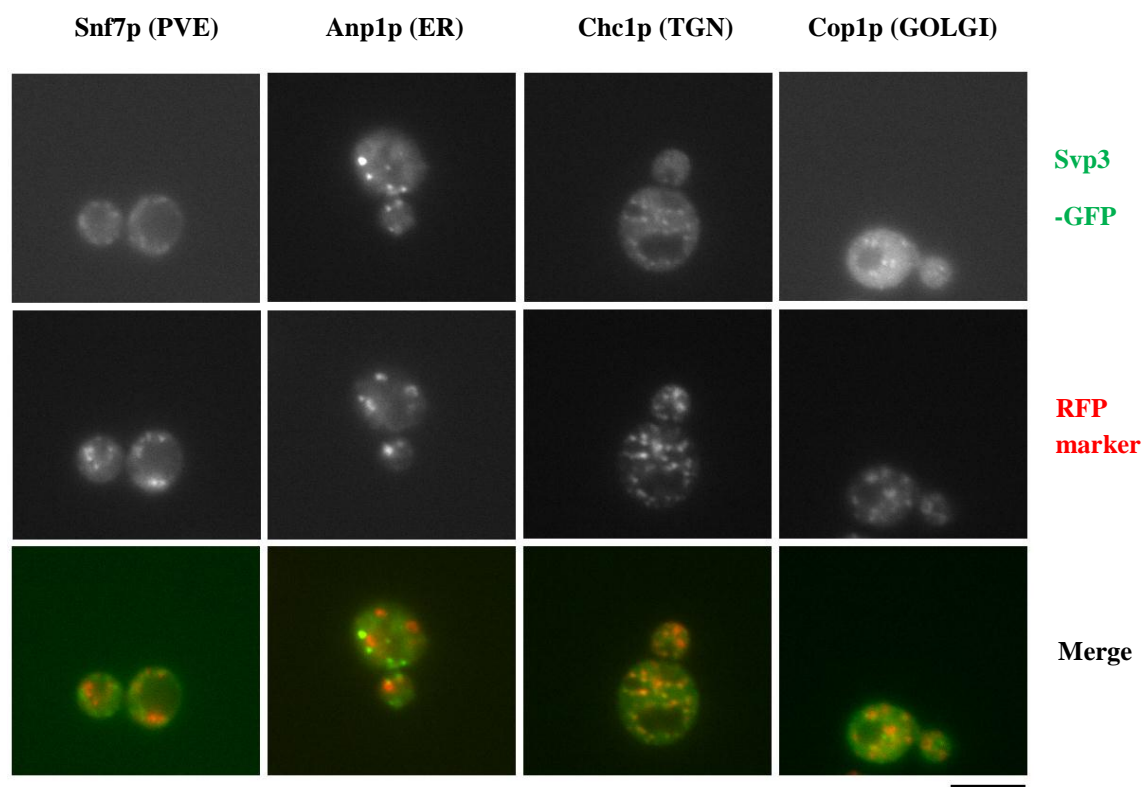
GFP punctae were too small and numerous to quantify in the same manner. Other techniques could have been applied but for consistency the method stated in Chapter 2 was applied.

To see whether any of the mutants had defects in stress induced translocation, co-localisations with the RFP markers were looked at for the other Svp3-GFP constructs.



Svp3^{CTI}-GFP construct localises to the cytoplasm under control conditions like wild-type Svp3-GFP.

Figure 6.8 Co-localisation of GFP- Svp3p^{CT1} under stressed conditions.



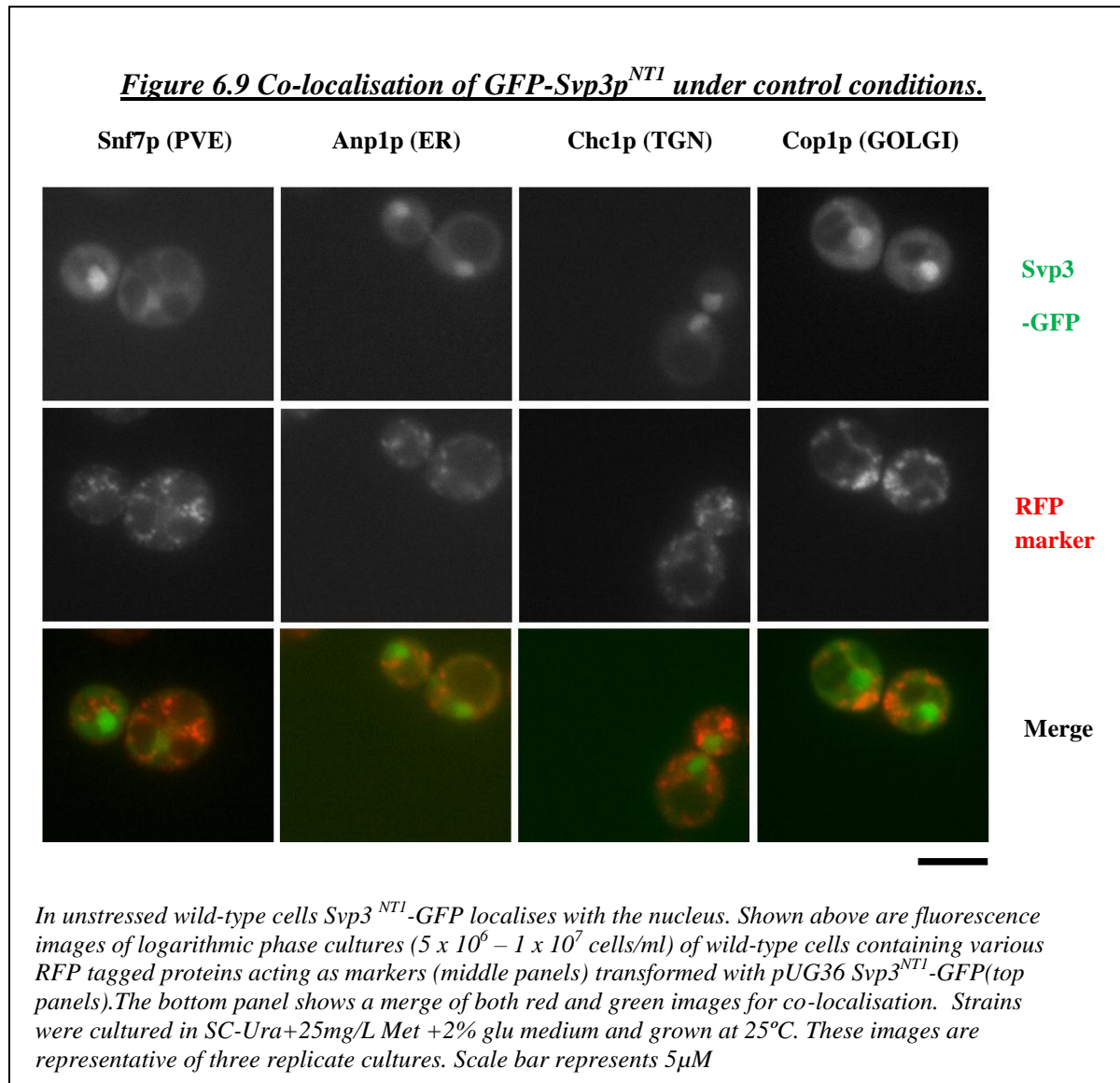
68.4% ±8.5***	33.49% ±0.5	58.2% ±2.5***	54.9% ±6.7***	Red co-localisation
27.4% ±4.6	19.7% ±6.4	29.0% ±1.5	25.1% ±5.1	Random co-localisation
41.0% ±3.9	13.8% ±6.9	29.2% ±3.7	29.7% ±1.6	Adjusted colocalisation

[Significantly different from random co-localisation: ***P<0.001, N/S not indicated]

In wild-type cells subjected to a 0.9M NaCl stress Svp3^{CT1}-GFP localises with a number of RFP markers. Shown above are fluorescence images of logarithmic phase cultures ($5 \times 10^6 - 1 \times 10^7$ cells/ml) of wild-type cells containing various RFP tagged proteins acting as markers (middle panels) transformed with pUG36 Svp3^{CT1}-GFP (top panels). The bottom panel shows a merge of both red and green images for co-localisation. Strains were cultured in SC-Ura+25mg/L Met +2% glu medium and grown at 25°C. The cells were resuspended in 0.9M NaCl microscope buffer prior to microscopy. These images are representative of three replicate cultures. Scale bar represents 5µM.

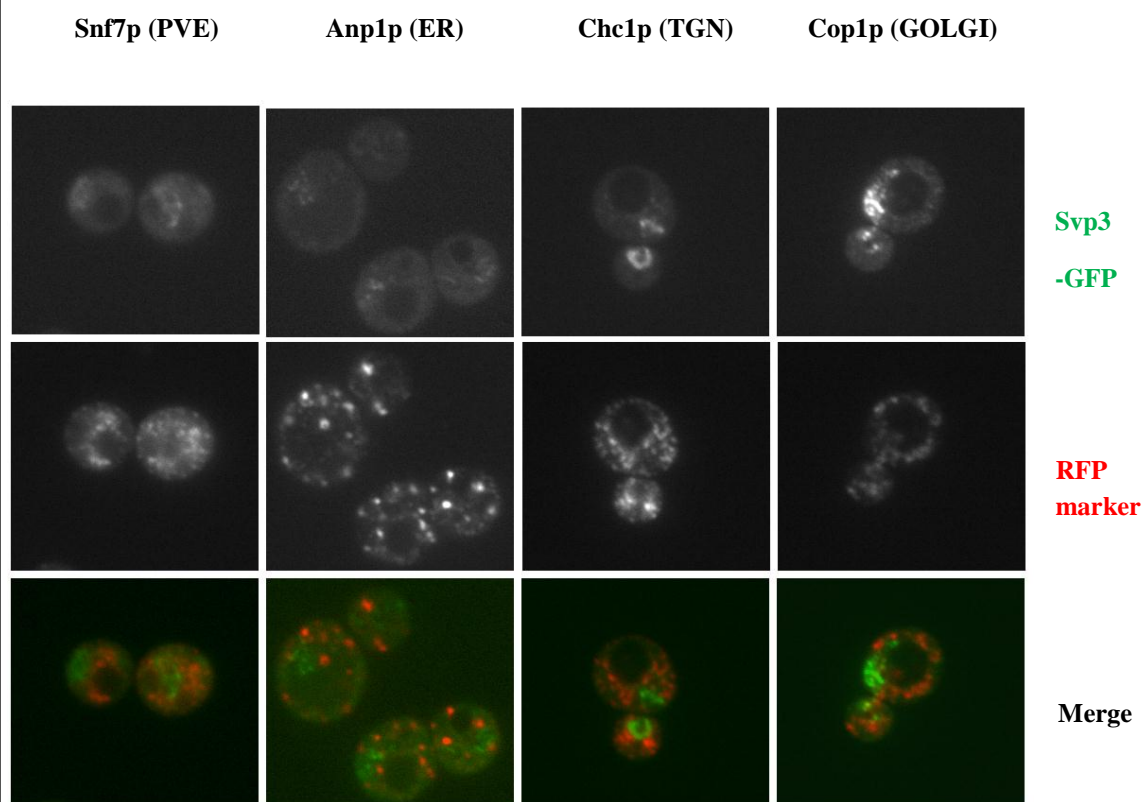
Under hyper osmotic stress, wild-type cells Svp3^{CT1}-GFP still translocates to smaller punctae compartments that fill the cell, however these appear to be less numerous than in wild-type Svp3-GFP. Significant colocalisation is still seen with three of the markers, Snf7p, Chc1p and Cop1p, however no significant co-localisation is observed with the Anp1p RFP marked compartments, which marks the ER. It appears

that one of the domains deleted in this construct is responsible for translocation of Svp3p to the ER compartment. The Svp3^{NT1} construct was also examined in the same way.



As shown in Figure 6.9, and as previously observed, in unstressed cells Svp3^{NT1}-GFP localises to the nucleus compartment only. No co-localisation is observed with any of the RFP markers examined.

Figure 6.10 Co-localisation of GFP-Svp3p^{NT1} under stressed conditions.



6.9% \pm 3.3	15.6% \pm 4.1	14.1% \pm 3.4	12.4% \pm 3.2	Red co-localisation
9.6% \pm 6.3	16.5% \pm 2.2	10.6% \pm 6.9	17.5% \pm 5.1	Random co-localisation
-2.8% \pm 3.0	-0.9% \pm 1.9	-3.5% \pm 3.5	-5.0% \pm 1.9	Adjusted colocalisation

[No significant difference was observed between co-localiations and random colocalisation data]

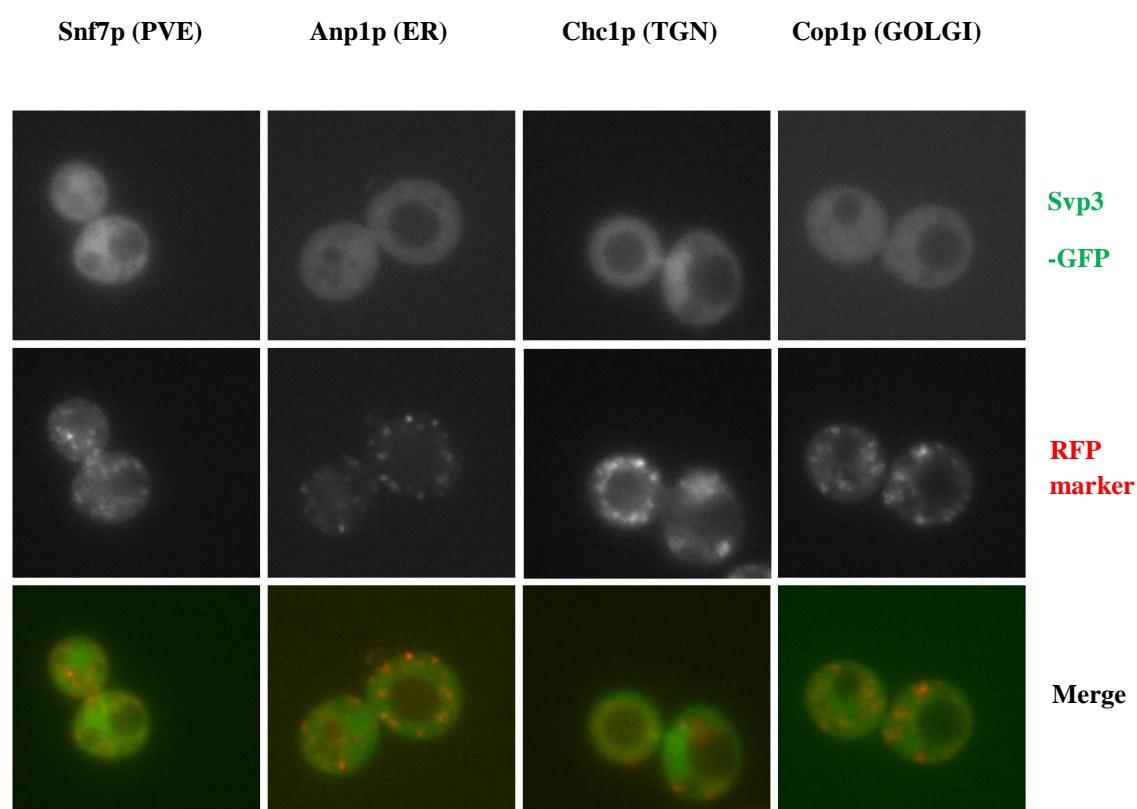
In wild-type cells subjected to a 0.9M NaCl stress Svp3^{NT1}-GFP does not co-localise with any of the RFP markers examined. Shown above are fluorescence images of logarithmic phase cultures (5×10^6 – 1×10^7 cells/ml) of wild-type cells containing various RFP tagged proteins acting as markers (middle panels) transformed with pUG36 Svp3-GFP(top panels).The bottom panel shows a merge of both red and green images for co-localisation. Strains were cultured in SC-Ura+25mg/L Met +2% glu medium and grown at 25°C. The cells were resuspended in 0.9M NaCl microscope buffer prior to microscopy. These images are representative of three replicate cultures. Scale bar represents 5 μ M.

Svp3^{NT1}-GFP still translocates to punctae when cells are subjected to a 0.9M NaCl stress. However no significant co-localisation is seen with any of the RFP markers

examined anymore as shown in Figure 6.10. The punctae translocation is restricted to the nucleus as the construct lacks the domain responsible for cytoplasm localisation and translocation. The punctae present after stress induced translocation appear to be morphologically different to those observed in wild-type Svp3-GFP. The punctate compartments are not as distinct and are somewhat enlarged. This may suggest that the domains deleted are also crucial for formation of some punctae and the regulation of the granular size.

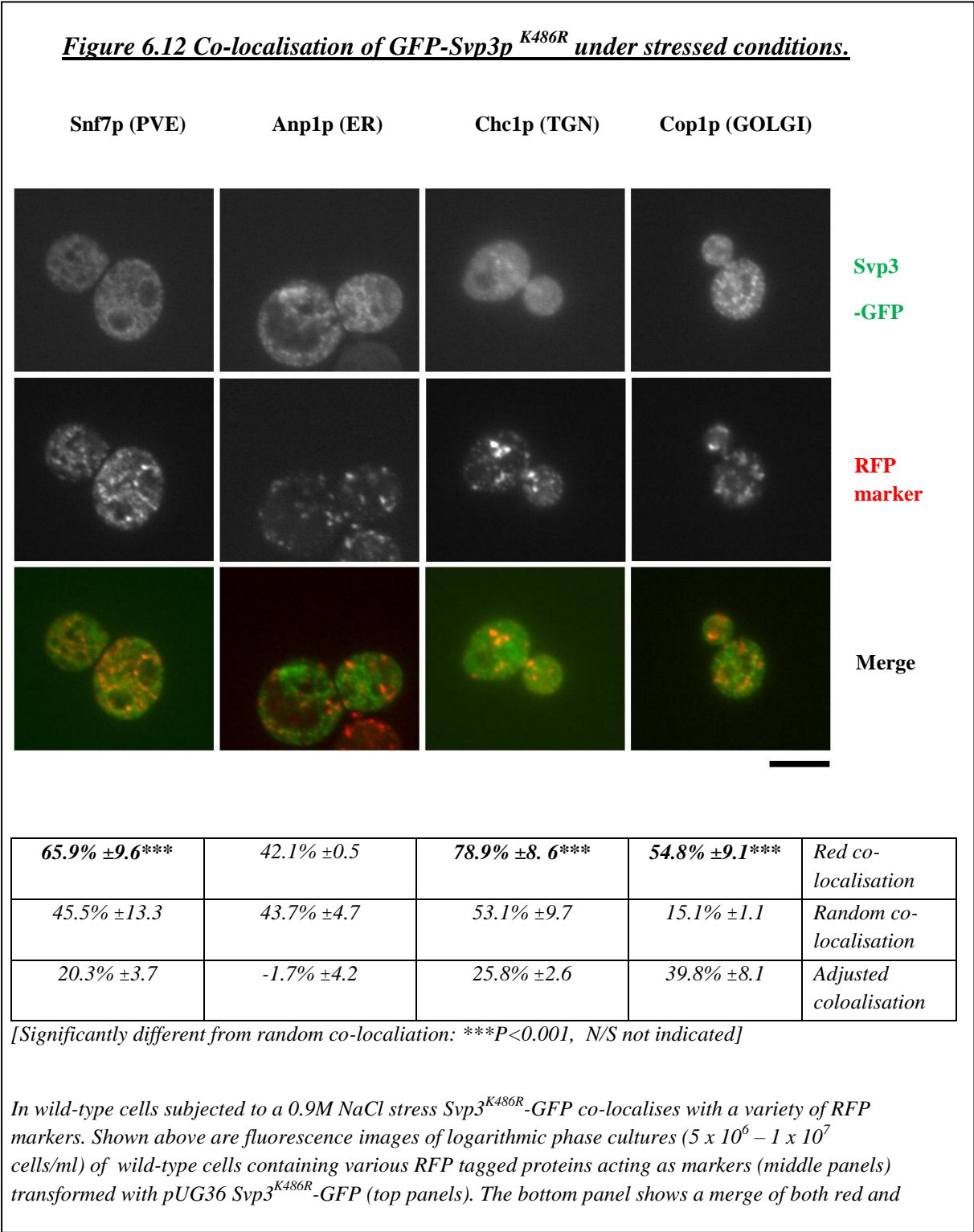
The localisation of the Svp3-GFP point mutations was also examined.

Figure 6.11 Co-localisation of GFP-Svp3p^{K486R} under control conditions.



In unstressed wild-type cells Svp3^{K486R}-GFP co localises with the nucleus. Shown above are fluorescence images of logarithmic phase cultures ($5 \times 10^6 - 1 \times 10^7$ cells/ml) of wild-type cells containing various RFP tagged proteins acting as markers (middle panels) transformed with Svp3^{K486R}-GFP (top panels). The bottom panel shows a merge of both red and green images for co-localisation. Strains were cultured in SC-Ura+25mg/L Met +2% glu medium and grown at 25°C. These images are representative of three replicate cultures. Scale bar represents 5µM.

As shown in Figure 6.11 under control conditions Svp3^{K486R} GFP localises to both the cytoplasm and the nucleus, although the nuclear signal appears to be weaker than in wild-type Svp3-GFP. Co-localisations with the RFP markers under hyper osmotic stress, were performed, to see if any difference in the translocation of Svp3^{K486R}GFP could be observed.

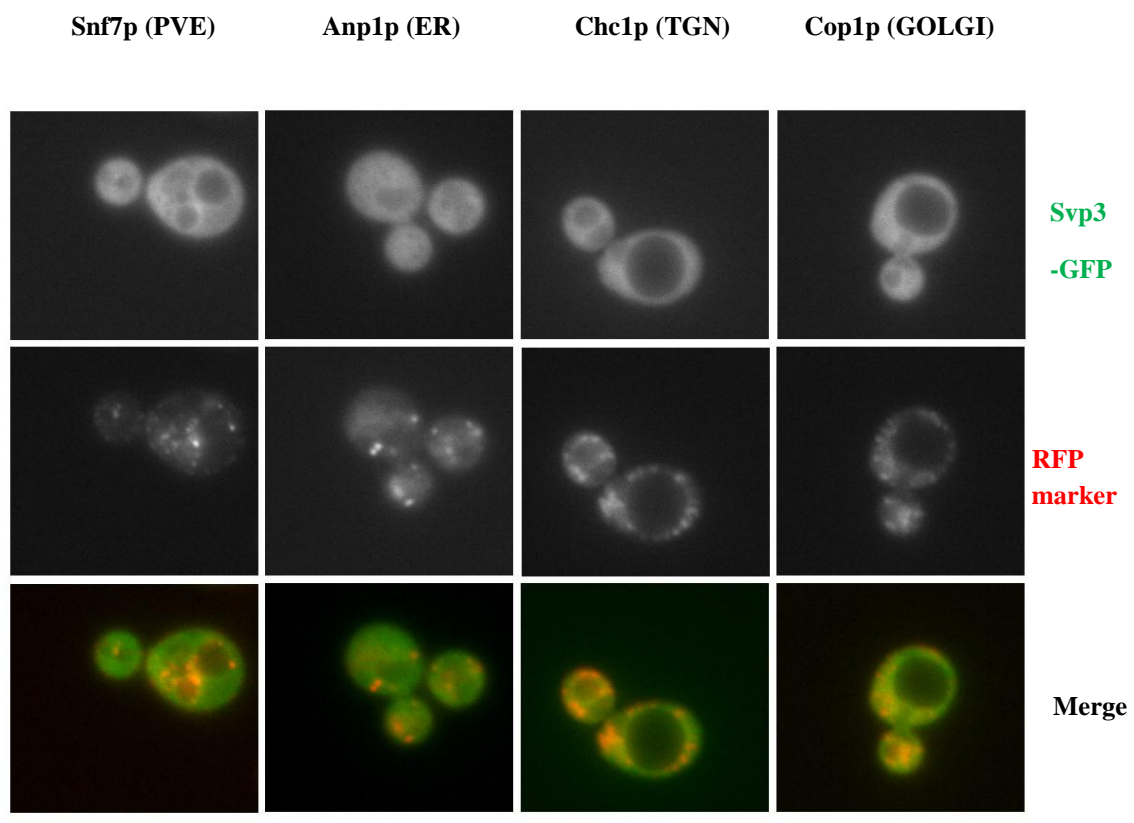


green images for co-localisation. Strains were cultured in SC-Ura+25mg/L Met +2% glu medium and grown at 25°C. The cells were resuspended in 0.9M NaCl microscope buffer prior to microscopy. These images are representative of three replicate cultures. Scale bar represents 5µM.

As shown in Figure 6.12 Svp3p^{K486R}-GFP still translocates to a number of small punctae when cells are treated with a 0.9M NaCl stress. Unlike the wild-type construct, there no longer appears to be significant co-localisation with the Anp1p RFP marker at the ER. Co-localisation decreases from 21.8% to -1.7%. This is a clear decrease; it suggests ubiquitination is necessary for translocation to the ER. Co-localisation with the Snf7p (20.4% vs 36.3%) and Chc1p (25.8% vs 47.8%) RFP markers is also decreased but is still significant. This may mean that ubiquitination is also necessary for Svp3p to efficiently translocate to the pre-vacuolar, endosome and TGN compartments. Translocation to the Golgi appears uninterrupted.

Localisation of the Svp3^{PAIA/PACA} GFP construct was also examined. This construct has a mutated PY motif at amino acids 678-681 (PPIY) and 689-692 (PPCY) so it can no longer bind to the WW domains of Rsp5, which is required for stress induced endocytosis of some cargoes, and is necessary to achieve Svp3p ubiquitination (Lin et al., 2008).

Figure 6.13 Co-localisation of GFP-Svp3p^{PAIA/PACA} under control conditions.



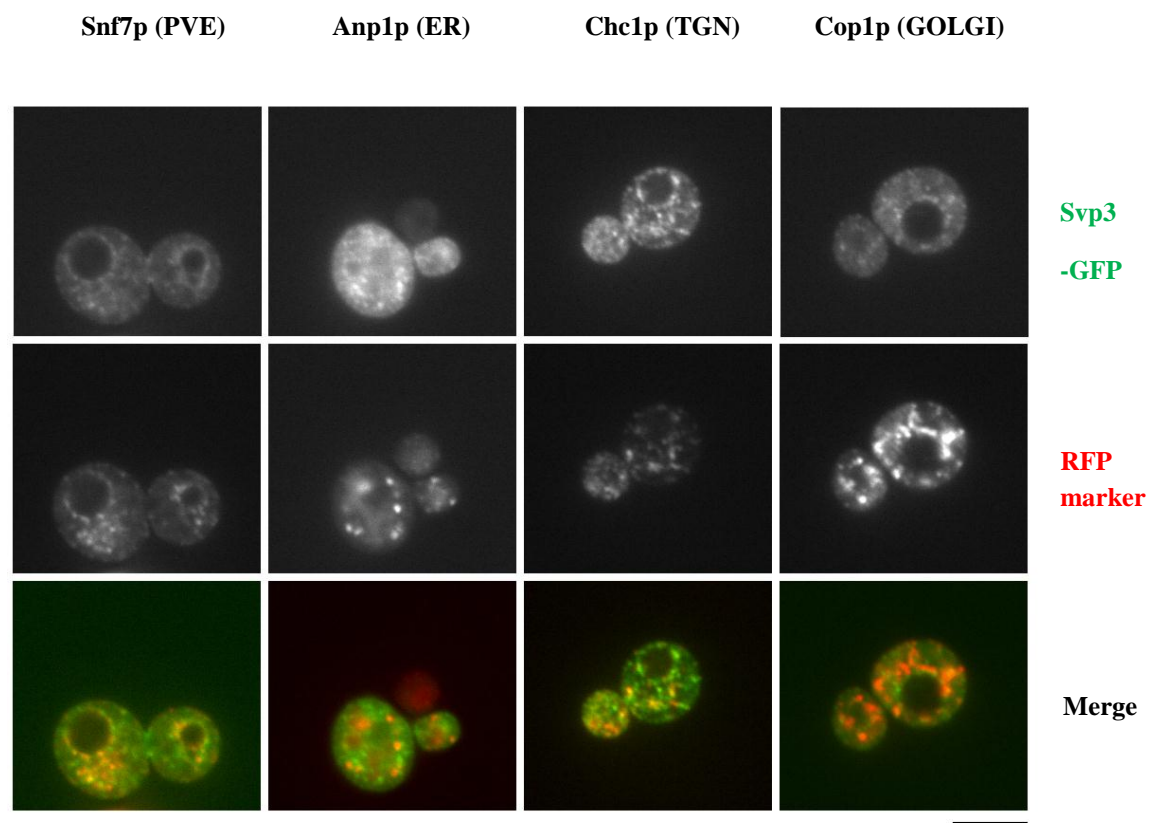
In unstressed wild-type cells Svp3^{PAIA/PACA}-GFP localises with the nucleus. Shown above are fluorescence images of logarithmic phase cultures ($5 \times 10^6 - 1 \times 10^7$ cells/ml) of wild-type cells containing various RFP tagged proteins acting as markers (middle panels) transformed with pUG36 Svp3^{PAIA/PACA} (top panels). The bottom panel shows a merge of both red and green images for co-localisation. Strains were cultured in SC-Ura+25mg/L Met +2% glu medium and grown at 25°C. These images are representative of three replicate cultures. Scale bar represents 5µM.

As shown in Figure 6.13 the localisation of Svp3^{PAIA/PACA}GFP is in the cytoplasm.

The construct is no longer observed intensely in the nucleus of wild-type cells, this suggest that the C- terminal PY motif along with the NLS signal is required for nuclear localisation of Svp3p.

Co-localisations were also carried out when the cells were subjected to hyper osmotic stress to see whether translocation of Svp3p is affected by mutation of the PY motif, results are shown in Figure 6.14.

Figure 6.14 Co-localisation of GFP-Svp3^{PAIA/PACA} under stressed conditions.



80.2% ±9.3***	47.9% ±2.3	84.8% ±3.9***	64.7% ±3.4***	Red co-localisation
49.5% ±4.8	37.1% ±0.9	50.1% ±11.1	31.9% ±9.9	Random co-localisation
30.6% ±4.5	10.8% ±3.1	34.7% ±9.9	32.8% ±6.5	Adjusted colocalisation

[Significantly different from random co-localiation: *** $P < 0.001$, N/S not indicated]

In wild-type cells subjected to a 0.9M NaCl stress Svp3^{PAIA/PACA}-GFP co-localises with a variety of RFP markers. Shown above are fluorescence images of logarithmic phase cultures ($5 \times 10^6 - 1 \times 10^7$ cells/ml) of wild-type cells containing various RFP tagged proteins acting as markers (middle panels) transformed with pUG36 Svp3^{PAIA/PACA}-GFP (top panels). The bottom panel shows a merge of both red and green images for co-localisation. Strains were cultured in SC-Ura+25mg/L Met +2% glu medium and grown at 25°C. The cells were resuspended in 0.9M NaCl microscope buffer prior to microscopy. These images are representative of three replicate cultures. Scale bar represents 5µM.

Svp3^{PAIA/PACA} GFP translocates to a number of punctate compartments, and significant co-localisations can be observed with three of the RFP markers examined (Snf7p, Cop1p and Chc1p). The construct however appears to have no significant co-

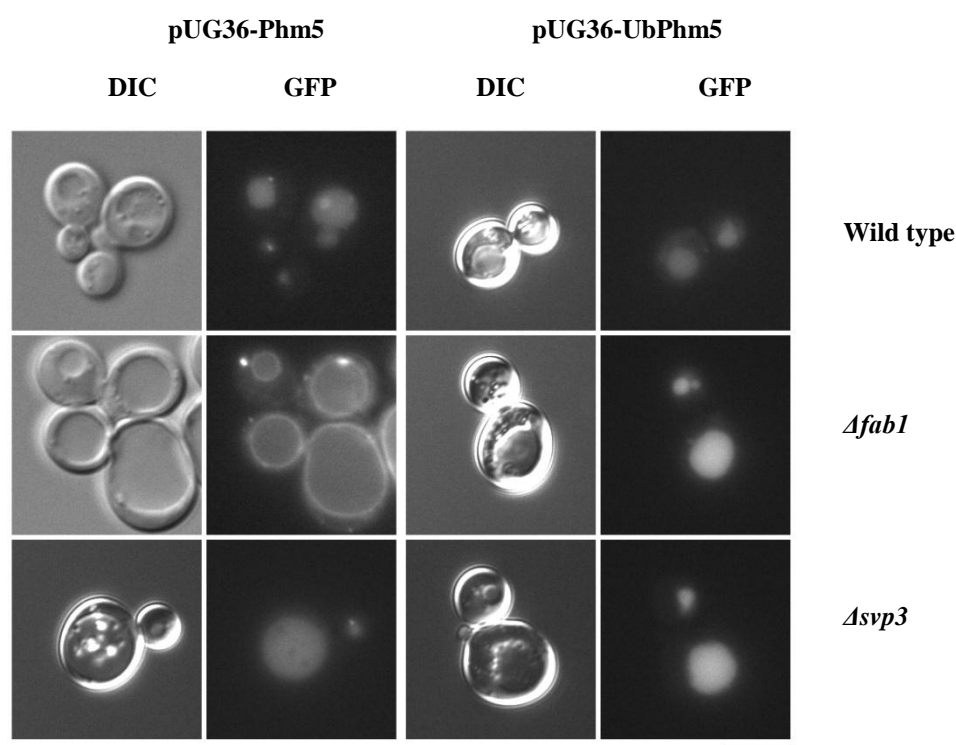
localisation with the Anp1p positive compartment, the ER. Levels are reduced to 10.8% compared to 31.8% in wild-type Svp3-GFP. Small decreases in co-localisation with the Snf7p (30.6% vs 36.3%) and Chc1p (34.7% vs 47.8%) markers are observed. Differences in these compartment co-localisations were also observed for the K486R mutant. Suggesting that ubiquitination is necessary for Svp3p to efficiently translocate to some compartments. It may also be the result of reduced interaction with Rsp5p due to mutation of the PY motifs.

As an additional note the addition of the Svp3-GFP plasmid seems to protect the vacuoles of wild-type cells against hyper osmotic shock. It seems to prevent the vacuoles from fragmenting into many smaller compartments that is normally observed. All the constructs seem to provide this protection suggesting that over expression of Svp3p can help prevent vacuole fragmentation. This may be due to decreased levels of $\text{PtdIns}(3,5)P_2$ present due to Svp3p over expression, as a Δsvp3 cell has increased levels of $\text{PtdIns}(3,5)P_2$ before and after stress. Another explanation could be that over expression of Svp3p allows the cell to regulate osmolytes during osmotic shock better. It may also be a secondary consequence of increased Svp3p levels. It is intriguing that this effect is observed in all the constructs, which may suggest that all the constructs are sufficient to decrease levels of $\text{PtdIns}(3,5)P_2$. Again labelling to see the effects of the constructs on lipid production would help to shed light on this matter.

To examine whether Δsvp3 cells have a defect in MVB sorting, an assay, using the MVB cargo Phm5-GFP, was conducted. As previously explained in Chapter 4, in wild-type cells Phm5p can be trafficked normally and is visualised inside the vacuole. In cells where trafficking is disrupted, Phm5-GFP is visualised on the vacuolar membrane. This is a property of Δfab1 cells and a consequence of a reduction of

PtdIns(3,5) P_2 levels. In $\Delta fab1$ cells, the trafficking defect can be overcome if a ubiquitinated Phm5-GFP construct is used. This suggests that the failure of $\Delta fab1$ cells to sort Phm5p correctly is due to the defect in ubiquitination. As discussed in the introduction Svp3p is known to interact with Rsp5p a protein involved in ubiquitination. Therefore it was examined whether $\Delta svp3$ cells shared the same defects in MVB sorting as $\Delta fab1$ cells. There may already be a role for Svp3p in ubiquitination and this might be what links the *SVP3* pathway with the *FAB1* pathway and PtdIns(3,5) P_2 .

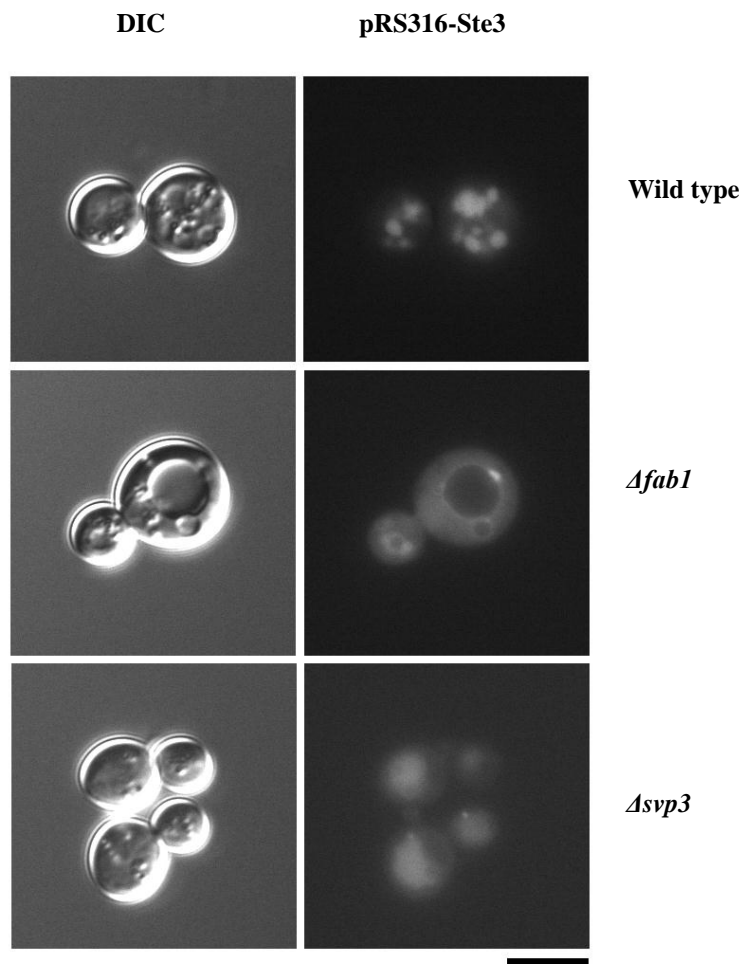
Figure 6.15 Localisation of pUG36 Phm5-GFP and pUG36 UbPhm5-GFP



pUG36-Phm5 can be visualised in the vacuole if trafficked correctly. Shown above are fluorescence images of logarithmic phase cultures ($5 \times 10^6 - 1 \times 10^7$ cells/ml) of wild-type (top panel), $\Delta fab1$ (middle panel) and $\Delta svp3$ (bottom panel) transformed with *pUG36-Phm5* (left hand panel) or *pUG36-UbPhm5* (right hand panel). The left-hand column shows low light DIC images. The right-hand column shows GFP localisation. These images are representative of three replicate cultures. All strains were cultured in SC-Ura+2% glu medium and grown at 25°C. Scale bar represents 5 μ M.

As shown in Figure 6.15 it appears that $\Delta svp3$ cells don't possess a defect in trafficking of Phm5-GFP, as both constructs can be correctly sorted to the vacuole. Another cargo that is also missorted in $PtdIns(3,5)P_2$ due to the defect in MVB sorting is Ste3-GFP so localisation of this construct was also examined.

Figure 6.16 Ste3-GFP localisation .



Ste3-GFP can be visualised in the vacuole if trafficked correctly. Shown above are fluorescence images of logarithmic phase cultures ($5 \times 10^6 - 1 \times 10^7$ cells/ml) of wild-type (top panel), $\Delta fab1$ (middle panel) and $\Delta svp3$ (bottom panel) transformed with pRS316-STE3-GFP. The left-hand column shows low light DIC images. The right-hand column shows GFP localisation. These images are representative of three replicate cultures. All strains were cultured in SC-His+2% glu medium and grown at 25°C. Scale bar represents 5μM.

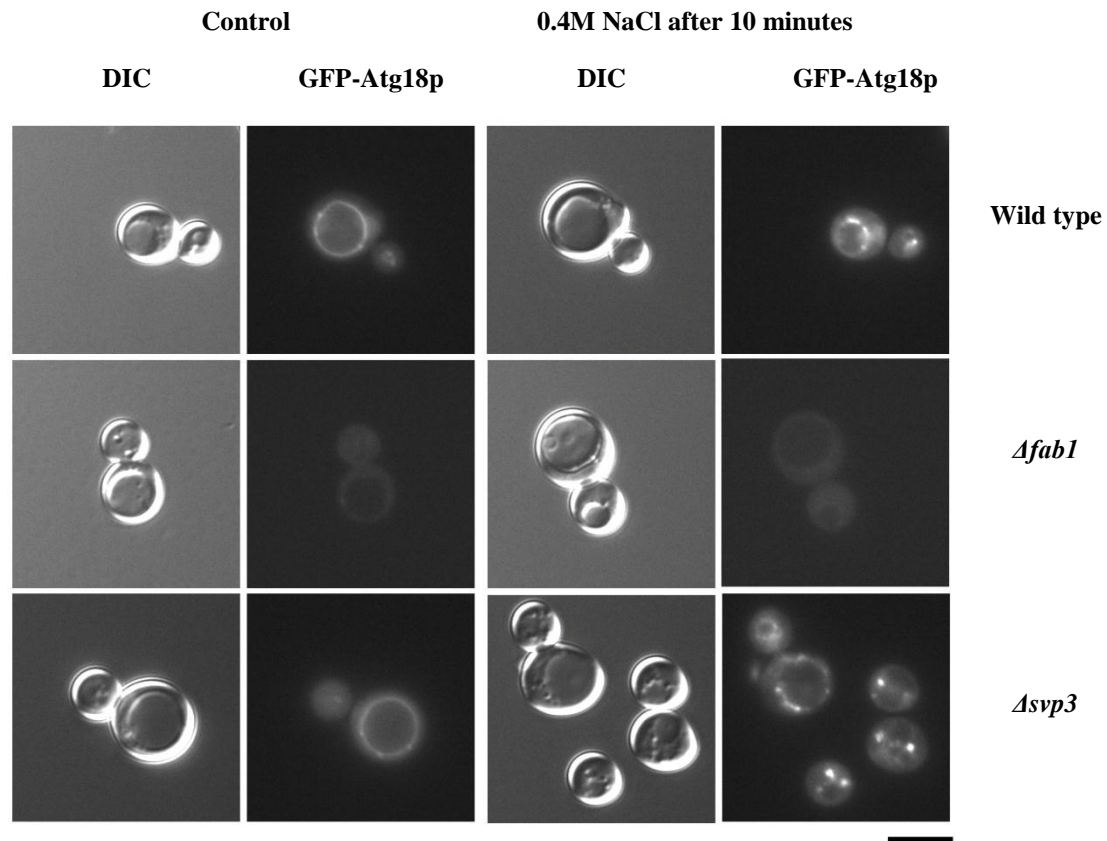
As shown in Figure 6.16 Ste3-GFP is trafficked correctly in the wild-type strain and therefore can be observed inside the vacuole. In $\Delta fab1$ cells, the trafficking of Ste3p is disrupted and Ste3-GFP becomes missorted. Ste3p is no longer correctly targeted to the vacuole and is instead visualised on the vacuole membrane. In $\Delta svp3$ cells it appears that the trafficking of Ste3-GFP is unaffected and it is still correctly targeted to the vacuole, where it is clearly visualised.

These experiments suggest that mutation of *SVP3* does not lead a defect in sorting at the MVB. It is likely that a defect in trafficking is not observed because levels of PtdIns(3,5) P_2 are not reduced, in fact they are increased. A defect would have still been observed if Svp3p was an effector involved in this process, therefore it is likely that Svp3p is not involved in MVB sorting.

Cells that have a defect in PtdIns(3,5) P_2 levels or are involved in the associated pathway often have a defect in the localisation of a potential PtdIns(3,5) P_2 effector protein Atg18p/Svp1p. Atg18p is also known to have a regulatory effect on PtdIns(3,5) P_2 levels. When labelled $\Delta atg18$ cells also have increased levels of PtdIns(3,5) P_2 with and without stress. The localisation of GFP-Atg18p was therefore examined in $\Delta svp3$ cells to see whether Svp3p may have a potential connection with the PtdIns(3,5) P_2 pathway.

As shown in Figure 6.17, in wild-type cells pUG36 GFP-Atg18p localises on the vacuole membrane. Small punctate structures coming off of the vacuole are also observed. When the cell is given a hyper-osmotic stress the amount of GFP-Atg18p on the vacuole membrane increases and is seen in bigger punctae structures, again coming off the vacuole.

Figure 6.17 Localisation of GFP-Atg18p.



*GFP-Atg18p can be visualised on the vacuole membrane, and this localisation is increased when cells are subjected to a hyperosmotic stress. Shown above are fluorescence images of logarithmic phase cultures ($5 \times 10^6 - 1 \times 10^7$ cells/ml) of wild-type (top panel), *Δfab1* (middle panel) and *Δsvp3* (bottom panel) transformed with pUG36-GFP-Atg18p. The left-hand panel shows localisation under control conditions. The right hand panel shows localisation under 0.4M NaCl conditions. The left hand columns show low light DIC images. The right-hand columns show GFP localisation. These images are representative of three replicate cultures. All strains were cultured in SC-Ura-Met+2% glu medium and grown at 25°C. Scale bar represents 5μM.*

In *Δfab1* cells GFP-Atg18p can no longer be visualised on the vacuole membrane and is instead observed diffusely throughout the cell, probably due to the strain being devoid of PtdIns(3,5) P_2 . This localisation is unchanged when the cell is treated with a 0.4M NaCl stress. The localisation of GFP-Atg18p in *Δsvp3* cells is similar to that observed in wild-type. Under control conditions GFP-Atg18p is again observed on the

vacuole membrane, with around three small punctae structures where fluorescence is increased. When $\Delta syp3$ cells are subjected to the 0.4M NaCl stress GFP-Atg18p again increases on the vacuole. The levels of GFP-Atg18p observed on the vacuole membrane are not as high as those observed in wild-type cells, but instead GFP is seen in much larger disc like punctae structures that protrude from the vacuole membrane. It seems that $\Delta syp3$ cells possess a slight defect in Atg18p localisation under stressed conditions, this is likely due to increased amounts of PtdIns(3,5) P_2 being present at an aberrant location. This may implicate Svp3p in the PtdIns(3,5) P_2 controlled stress response that may also involve Atg18p. It also helps explain the observation above that the Svp3-GFP constructs seem to protect the cell from vacuole fragmentation. Atg18p appears to be involved in vacuole fragmentation as observed in Chapter 5. Svp3p also seems to regulate localisation of Atg18p. Therefore increased levels of Svp3p will affect localisation of Atg18p to the vacuole, which may protect the cell from vacuole fragmentation.

6.3 Discussion

Data has been presented which suggests that the ubiquitination motif present in Svp3p is necessary for at least some of its localisation to Anp1p positive vesicles under salt stress. This is demonstrated through decreased significant localisation to the ER in all constructs examined. Intriguingly in the K486R mutant, which possesses a defect in ubiquitination, no significant co-localisation with this compartment is observed. ER localisation is also disrupted in the PY motif mutant. This suggests that when cells receive a hyper-osmotic stress, ubiquitination of Svp3p is necessary in order to translocate it to the ER.

In all the constructs examined apart from the NT1 mutant, which had no clear co-localisation with any of the RFP markers examined, translocation to the Cop1p RFP marked compartment; the Golgi, was uninterrupted.

Thus no link with the Fab1p pathway was firmly established for this protein, despite some intriguing evidence; including the mislocalisation of GFP-Atg18p, presumably caused by the hyper-elevated levels of PtdIns(3,5) P_2 . The problem has been that Svp3p is obviously regulated by multiple pathways and is subject to extremely complex signalling. My data alone suggests at least 3 modes of localisation and there could be more. This protein will be a fascinating subject for future study.

CHAPTER 7

Concluding remarks and future work.

7.1 Fab1p in the early endocytic system

It is now becoming clear, both from previous work in higher eukaryotes and also from the data presented here, that there is at least one role for Fab1p and PtdIns(3,5) P_2 in the early endocytic system; yet the precise molecular function of this pathway is proving hard to define. The major contribution my work makes to this issue is to link Fab1p function to Vps13p; because Vps13p is a conserved protein, that is thought to be Golgi resident and to affect both trafficking of some cargos in the early endocytic system and also the recycling of certain proteins from the forming MVB, back to the Golgi. This mirrors my data for Fab1p, because PtdIns(3,5) P_2 is influencing recycling of Chs3p between the Golgi and the PGE and also appears to influence the recycling of the M6R related protein, Mr11p. The latter result is important because recycling of Mr11p could now be used as a screen to isolate additional components of the Fab1p dependent late endosome to Golgi recycling system.

Vps13p appears to act upstream of Fab1p; since overexpression of this lipid kinase was able to correct the trafficking defects observed when Vps13p function was compromised. A similar relationship exists between Fab1p and AP-1, suggesting that Vps13p and AP-1 may work closely together in time and space. This bears further investigation and would have been my next set of experiments, if time had allowed. It would also be beneficial to examine levels of lipids in $\Delta vps13$ cells; because this was

what enabled Phelan et al (2002) to determine that the components of AP-1 were indeed upstream of Fab1p in Cps1p trafficking. A search for physical and genetic interactions between Vps13p and AP-1 is needed to define their precise relationship. We would also have liked to have spent more time defining where Chs3p is building up after double deletion of Chs6p and Fab1p; because this would define what role Fab1p plays in the early endocytic system, though it must be noted that decades of research have been insufficient to allow most researchers to agree on an exact role for AP-1. In order to study this question, epitope tagged Chs3p would have to be localised either by immuno-gold EM approaches, using antibodies labelled with different sized gold particles for marker proteins specific for each compartment; or by cell fractionation techniques, though a study by Scheckman's group using this latter approach did not take our knowledge much further.

It is also clear from my work that Fab1p may interact with retromer, but it is not an integral part of the core machinery and appears to only influence the trafficking of certain cargoes; in this case the M6R receptor like protein Mr11p. This might indicate an indirect role for Fab1p but what makes this less likely is the fact that Vac14p appears also to have a separate and distinct role in retromer function in yeast that appears to be independent of $\text{PtdIns}(3,5)P_2$. This probably explains the results observed in $\text{vac14}^{-/-}$ mice where M6R recycling was impaired and highlight the importance of checking any result by several methods; in this case mVac14 function is likely independent of PIKfyve, as it has proved from my studies in yeast.

The localisation of Vps13p would also answer a number of important questions in my system; especially if this localisation changes in cells where AP-1 or Fab1p function has been compromised. Notably, it would be a potential way of defining where the trafficking event mediated by Fab1p and AP-1 is likely to be occurring; in animal cells Vps13p seems to localise to the Golgi, though it is uncertain if the same is the case in the yeast system. One problem that was encountered working with Vps13p was its sheer size; the protein is encoded by an ORF that is over 9 kb in length and is one of the largest proteins in the whole genome of *S cerevisiae*.

Another set of experiments that certainly need to be extended, would be to ‘mine’ my mutant collection for more components of the novel Fab1p mediated pathway Chs3p recycling pathway. With hindsight, FACs analysis is a far more powerful method for pre-enrichment of mutants than classical plating techniques and also seemed to eliminate many of the cell wall mutants that seem to be the largest group of ‘false positives’ found in any screen relying on drug sensitivity. Transposon mutagenesis would also be used to increase the pool of mutants if time allowed; because of the ease of isolating the mutated gene versus the problems of determining it via complementation analysis using plasmid libraries.

7.2 Role of Svp3p

It seems clear from my work that Svp3p is likely to lie upstream of Fab1p; because of the hyper-elevation of PtdIns(3,5) P_2 synthesis observed in the $\Delta svp3$ mutant. Indeed, so perturbed is PtdIns(3,5) P_2 metabolism in $\Delta svp3$ cells that Atg18p is actually mislocalised during osmotic stress; to aberrant looking protrusions of the vacuole

membrane or a closely associated organelle. With hindsight, it seems obvious that Svp3p acts upstream of Fab1p but the similarity of the synthesis defect to that observed in $\Delta atg18$ cells initially lead earlier researchers to conclude that this might have been an effector of $\text{PtdIns}(3,5)P_2$. However, my experiments rule out the translocation of Svp3p being dependent upon $\text{PtdIns}(3,5)P_2$; indeed they suggest that even ubiquitin and Rsp5p binding are only part of the story and imply that Svp3p is binding to many different types of proteins or protein domains during hyper-osmotic stress. This assertion is borne out by the fact that a screen, looking for mutants that fail to translocate Svp3p, in which the entire set of viable *S. cerevisiae* deletion mutants were transformed with GFP-Svp3p and analysed for Svp3p stress induced translocation, failed to reveal a single mutant in which translocation was grossly impaired. This again suggests many targets and pathways that contribute to Svp3p translocation. My analysis of where Svp3p is translocating does indicate that it is binding to proteins in every conceivable compartment and suggests that this protein is part of some global stress pathway that is activated to bind proteins under conditions of cellular stress. Until a molecular role for Svp3p is defined, it will be hard to make further progress, and this is hampered by the fact it shows little homology to any other proteins. One clue to its function may lie in the prediction that part of Svp3p might fold like an arrestin; a series of proteins involved in the ‘down-regulation’ of G-protein coupled receptors after ligand activation in animal cells. This down-regulation results in internalisation of the receptor following phosphorylation, so it would be interesting to examine if Svp3p translocation follows on from any kind of phosphorylation. Previous work has examined a possible interaction with the Hog1p MAP-kinase pathway that is known to be activated by osmotic stress, but found that Svp3p translocation is normal in $\Delta hog1$ cells (Dove, SK unpub). Therefore, an easier

way of determining how Svp3p works would be to TAP tag Svp3p and look at which proteins are bound to Svp3p under basal conditions and under those of stress. As this analysis would also isolate binding proteins as bands on a gel, these proteins could not only be identified but also analysed by FTICR mass spectrometry for covalent modifications such as phosphorylation. Such an analysis is fairly simple once protein is available, although it is expensive. Indeed it has been used successfully in our lab to map phosphorylation sites on Vps41p (K Dong unpub).

References

- Alesutan, I. S., Ureche, O. N., Laufer, J., Klaus, F., Zurn, A., Lindner, R., Strutz-Seeböhm, N., Tavaré, J. M., Boehmer, C., Palmada, M., Lang, U. E., Seeböhm, G. & Lang, F. (2010) Regulation of the glutamate transporter EAAT4 by PIKfyve. **Cell Physiol Biochem**, 25, 187-94.
- Ali, B. R., Wasmeier, C., Lamoreux, L., Strom, M. & Seabra, M. C. (2004) Multiple regions contribute to membrane targeting of Rab GTPases. **J Cell Sci**, 117, 6401-12.
- Andrews, S., Stephens, L. R. & Hawkins, P. T. (2007) PI3K class IB pathway. **Sci STKE**, 2007, cm2.
- Auger, K. R., Carpenter, C. L., Cantley, L. C. & Varticovski, L. (1989) Phosphatidylinositol 3-kinase and its novel product, phosphatidylinositol 3-phosphate, are present in *Saccharomyces cerevisiae*. **J Biol Chem**, 264, 20181-4.
- Baars, T. L., Petri, S., Peters, C. & Mayer, A. (2007) Role of the V-ATPase in regulation of the vacuolar fission-fusion equilibrium. **Mol Biol Cell**, 18, 3873-82.
- Babst, M., Wendland, B., Estepa, E. J. & Emr, S. D. (1998) The Vps4p AAA ATPase regulates membrane association of a Vps protein complex required for normal endosome function. **Embo J**, 17, 2982-93.
- Backer, J. M. (2008) The regulation and function of Class III PI3Ks: novel roles for Vps34. **Biochem J**, 410, 1-17.
- Balla, T. (2006) Phosphoinositide-derived messengers in endocrine signaling. **J Endocrinol**, 188, 135-53.
- Bankaitis, V. A., Johnson, L. M. & Emr, S. D. (1986) Isolation of yeast mutants defective in protein targeting to the vacuole. **Proc Natl Acad Sci U S A**, 83, 9075-9.
- Banta, L. M., Robinson, J. S., Klionsky, D. J. & Emr, S. D. (1988) Organelle assembly in yeast: characterization of yeast mutants defective in vacuolar biogenesis and protein sorting. **J Cell Biol**, 107, 1369-83.
- Barfield, R. M., Fromme, J. C. & Schekman, R. (2009) The exomer coat complex transports Fus1p to the plasma membrane via a novel plasma membrane sorting signal in yeast. **Mol Biol Cell**, 20, 4985-96.
- Barth, H., Meiling-Wesse, K., Epple, U. D. & Thumm, M. (2001) Autophagy and the cytoplasm to vacuole targeting pathway both require Aut10p. **FEBS Lett**, 508, 23-8.
- Barth, H., Meiling-Wesse, K., Epple, U. D. & Thumm, M. (2002) Mailp is essential for maturation of proaminopeptidase I but not for autophagy. **FEBS Lett**, 512, 173-9.
- Bayer, M. J., Reese, C., Buhler, S., Peters, C. & Mayer, A. (2003) Vacuole membrane fusion: V0 functions after trans-SNARE pairing and is coupled to the Ca²⁺-releasing channel. **J Cell Biol**, 162, 211-22.
- Berwick, D. C., Dell, G. C., Welsh, G. I., Heesom, K. J., Hers, I., Fletcher, L. M., Cooke, F. T. & Tavaré, J. M. (2004) Protein kinase B phosphorylation of PIKfyve regulates the trafficking of GLUT4 vesicles. **J Cell Sci**, 117, 5985-93.
- Bleve, G., Di Sansebastiano, G. P. & Grieco, F. (2011) Over-expression of functional *Saccharomyces cerevisiae* GUP1, induces proliferation of intracellular membranes containing ER and Golgi resident proteins. **Biochim Biophys Acta**, 1808, 733-44.
- Bonangelino, C. J., Catlett, N. L. & Weisman, L. S. (1997) Vac7p, a novel vacuolar protein, is required for normal vacuole inheritance and morphology. **Mol Cell Biol**, 17, 6847-58.
- Bonangelino, C. J., Nau, J. J., Duex, J. E., Brinkman, M., Wurmser, A. E., Gary, J. D., Emr, S. D. & Weisman, L. S. (2002) Osmotic stress-induced increase of phosphatidylinositol 3,5-bisphosphate requires Vac14p, an activator of the lipid kinase Fab1p. **J Cell Biol**, 156, 1015-28.
- Bonifacino, J. S. & Hurley, J. H. (2008) Retromer. **Curr Opin Cell Biol**, 20, 427-36.
- Botelho, R. J., Efe, J. A., Teis, D. & Emr, S. D. (2008) Assembly of a Fab1 phosphoinositide kinase signaling complex requires the Fig4 phosphoinositide phosphatase. **Mol Biol Cell**, 19, 4273-86.
- Bowers, K. & Stevens, T. H. (2005) Protein transport from the late Golgi to the vacuole in the yeast *Saccharomyces cerevisiae*. **Biochim Biophys Acta**, 1744, 438-54.
- Brachmann, C. B., Davies, A., Cost, G. J., Caputo, E., Li, J., Hieter, P. & Boeke, J. D. (1998) Designer deletion strains derived from *Saccharomyces cerevisiae* S288C: a useful set of strains and plasmids for PCR-mediated gene disruption and other applications. **Yeast**, 14, 115-32.
- Brett, C. L., Donowitz, M. & Rao, R. (2006) Does the proteome encode organellar pH? **FEBS Lett**, 580, 717-9.

- Brett, C. L. & Merz, A. J. (2008) Osmotic regulation of Rab-mediated organelle docking. **Curr Biol**, 18, 1072-7.
- Brickner, J. H. & Fuller, R. S. (1997) SOI1 encodes a novel, conserved protein that promotes TGN-endosomal cycling of Kex2p and other membrane proteins by modulating the function of two TGN localization signals. **J Cell Biol**, 139, 23-36.
- Bryant, N. J., Piper, R. C., Weisman, L. S. & Stevens, T. H. (1998) Retrograde traffic out of the yeast vacuole to the TGN occurs via the prevacuolar/endosomal compartment. **J Cell Biol**, 142, 651-63.
- Bulawa, C. E. (1993) Genetics and molecular biology of chitin synthesis in fungi. **Annu Rev Microbiol**, 47, 505-34.
- Burda, P., Padilla, S. M., Sarkar, S. & Emr, S. D. (2002) Retromer function in endosome-to-Golgi retrograde transport is regulated by the yeast Vps34 PtdIns 3-kinase. **J Cell Sci**, 115, 3889-900.
- Cabezas, A., Pattni, K. & Stenmark, H. (2006) Cloning and subcellular localization of a human phosphatidylinositol 3-phosphate 5-kinase, PIKfyve/Fab1. **Gene**, 371, 34-41.
- Cantley, L. C. (2002) The phosphoinositide 3-kinase pathway. **Science**, 296, 1655-7.
- Carlton, J., Bujny, M., Peter, B. J., Oorschot, V. M., Rutherford, A., Mellor, H., Klumperman, J., McMahon, H. T. & Cullen, P. J. (2004) Sorting nexin-1 mediates tubular endosome-to-TGN transport through coincidence sensing of high-curvature membranes and 3-phosphoinositides. **Curr Biol**, 14, 1791-800.
- Carricaburu, V., Lamia, K. A., Lo, E., Favereaux, L., Payraastre, B., Cantley, L. C. & Rameh, L. E. (2003) The phosphatidylinositol (PI)-5-phosphate 4-kinase type II enzyme controls insulin signaling by regulating PI-3,4,5-trisphosphate degradation. **Proc Natl Acad Sci U S A**, 100, 9867-72.
- Catimel, B., Schieber, C., Condrón, M., Patsiouras, H., Connolly, L., Catimel, J., Nice, E. C., Burgess, A. W. & Holmes, A. B. (2008) The PI(3,5)P₂ and PI(4,5)P₂ interactomes. **J Proteome Res**, 7, 5295-313.
- Cereghino, J. L., Marcusson, E. G. & Emr, S. D. (1995) The cytoplasmic tail domain of the vacuolar protein sorting receptor Vps10p and a subset of VPS gene products regulate receptor stability, function, and localization. **Mol Biol Cell**, 6, 1089-102.
- Chaung, H. M., Hong, C. H., Chiang, C. P., Lin, S. K., Kuo, Y. S., Lan, W. H. & Hsieh, C. C. (1996) Comparison of calcium phosphate cement mixture and pure calcium hydroxide as direct pulp-capping agents. **J Formos Med Assoc**, 95, 545-50.
- Chen, C., Dewaele, S., Braeckman, B., Desmyter, L., Verstraelen, J., Borgonie, G., Vanfleteren, J. & Contreras, R. (2003) A high-throughput screening system for genes extending life-span. **Exp Gerontol**, 38, 1051-63.
- Chow, C. Y., Zhang, Y., Dowling, J. J., Jin, N., Adamska, M., Shiga, K., Szigeti, K., Shy, M. E., Li, J., Zhang, X., Lupski, J. R., Weisman, L. S. & Meisler, M. H. (2007) Mutation of FIG4 causes neurodegeneration in the pale tremor mouse and patients with CMT4J. **Nature**, 448, 68-72.
- Chuang, J. S. & Schekman, R. W. (1996) Differential trafficking and timed localization of two chitin synthase proteins, Chs2p and Chs3p. **J Cell Biol**, 135, 597-610.
- Clague, M. J., Urbe, S. & De Lartigue, J. (2009) Phosphoinositides and the endocytic pathway. **Exp Cell Res**, 315, 1627-31.
- Cooke, F. T., Dove, S. K., McEwen, R. K., Painter, G., Holmes, A. B., Hall, M. N., Michell, R. H. & Parker, P. J. (1998) The stress-activated phosphatidylinositol 3-phosphate 5-kinase Fab1p is essential for vacuole function in *S. cerevisiae*. **Curr Biol**, 8, 1219-22.
- Cooper, A. A. & Stevens, T. H. (1996) Vps10p cycles between the late-Golgi and prevacuolar compartments in its function as the sorting receptor for multiple yeast vacuolar hydrolases. **J Cell Biol**, 133, 529-41.
- Copic, A., Starr, T. L. & Schekman, R. (2007) Ent3p and Ent5p exhibit cargo-specific functions in trafficking proteins between the trans-Golgi network and the endosomes in yeast. **Mol Biol Cell**, 18, 1803-15.
- Corvera, S. (2001) Phosphatidylinositol 3-kinase and the control of endosome dynamics: new players defined by structural motifs. **Traffic**, 2, 859-66.
- Costaguta, G., Duncan, M. C., Fernandez, G. E., Huang, G. H. & Payne, G. S. (2006) Distinct roles for TGN/endosome epsin-like adaptors Ent3p and Ent5p. **Mol Biol Cell**, 17, 3907-20.
- Cowles, C. R., Odorizzi, G., Payne, G. S. & Emr, S. D. (1997) The AP-3 adaptor complex is essential for cargo-selective transport to the yeast vacuole. **Cell**, 91, 109-18.
- Cozier, G. E., Carlton, J., McGregor, A. H., Gleeson, P. A., Teasdale, R. D., Mellor, H. & Cullen, P. J. (2002) The phox homology (PX) domain-dependent, 3-phosphoinositide-mediated association

- of sorting nexin-1 with an early sorting endosomal compartment is required for its ability to regulate epidermal growth factor receptor degradation. **J Biol Chem**, 277, 48730-6.
- Cui, X., De Vivo, I., Slany, R., Miyamoto, A., Firestein, R. & Cleary, M. L. (1998) Association of SET domain and myotubularin-related proteins modulates growth control. **Nat Genet**, 18, 331-7.
- Cullen, P. J. (2008) Endosomal sorting and signalling: an emerging role for sorting nexins. **Nat Rev Mol Cell Biol**, 9, 574-82.
- Cullen, P. J., Cozier, G. E., Banting, G. & Mellor, H. (2001) Modular phosphoinositide-binding domains--their role in signalling and membrane trafficking. **Curr Biol**, 11, R882-93.
- Czech, M. P. (2003) Dynamics of phosphoinositides in membrane retrieval and insertion. **Annu Rev Physiol**, 65, 791-815.
- D'angelo, G., Vicinanza, M., Di Campli, A. & De Matteis, M. A. (2008) The multiple roles of PtdIns(4)P -- not just the precursor of PtdIns(4,5)P₂. **J Cell Sci**, 121, 1955-63.
- Darsow, T., Katzmann, D. J., Cowles, C. R. & Emr, S. D. (2001) Vps41p function in the alkaline phosphatase pathway requires homo-oligomerization and interaction with AP-3 through two distinct domains. **Mol Biol Cell**, 12, 37-51.
- De Camilli, P., Chen, H., Hyman, J., Panepucci, E., Bateman, A. & Brunger, A. T. (2002) The ENTH domain. **FEBS Lett**, 513, 11-8.
- De Duve, C. (1971) Tissue fractionation. Past and present. **J Cell Biol**, 50, 20d-55d.
- De Lartigue, J., Polson, H., Feldman, M., Shokat, K., Tooze, S. A., Urbe, S. & Clague, M. J. (2009) PIKfyve regulation of endosome-linked pathways. **Traffic**, 10, 883-93.
- Dong, X. P., Shen, D., Wang, X., Dawson, T., Li, X., Zhang, Q., Cheng, X., Zhang, Y., Weisman, L. S., Dellling, M. & Xu, H. (2010) PI(3,5)P₂ controls membrane trafficking by direct activation of mucolipin Ca(2+) release channels in the endolysosome. **Nat Commun**, 1, 38.
- Dove, S. K., Cooke, F. T., Douglas, M. R., Sayers, L. G., Parker, P. J. & Michell, R. H. (1997) Osmotic stress activates phosphatidylinositol-3,5-bisphosphate synthesis. **Nature**, 390, 187-92.
- Dove, S. K., Dong, K., Kobayashi, T., Williams, F. K. & Michell, R. H. (2009) Phosphatidylinositol 3,5-bisphosphate and Fab1p/PIKfyve under PPI_n endo-lysosome function. **Biochem J**, 419, 1-13.
- Dove, S. K. & Johnson, Z. E. (2007) Our FABulous VACation: a decade of phosphatidylinositol 3,5-bisphosphate. **Biochem Soc Symp**, 129-39.
- Dove, S. K., Mcewen, R. K., Cooke, F. T., Parker, P. J. & Michell, R. H. (1999) Phosphatidylinositol 3,5-bisphosphate: a novel lipid that links stress responses to membrane trafficking events. **Biochem Soc Trans**, 27, 674-7.
- Dove, S. K., Mcewen, R. K., Mayes, A., Hughes, D. C., Beggs, J. D. & Michell, R. H. (2002) Vac14 controls PtdIns(3,5)P₂ synthesis and Fab1-dependent protein trafficking to the multivesicular body. **Curr Biol**, 12, 885-93.
- Dove, S. K., Piper, R. C., Mcewen, R. K., Yu, J. W., King, M. C., Hughes, D. C., Thuring, J., Holmes, A. B., Cooke, F. T., Michell, R. H., Parker, P. J. & Lemmon, M. A. (2004) Svp1p defines a family of phosphatidylinositol 3,5-bisphosphate effectors. **Embo J**, 23, 1922-33.
- Duex, J. E., Nau, J. J., Kauffman, E. J. & Weisman, L. S. (2006a) Phosphoinositide 5-phosphatase Fig 4p is required for both acute rise and subsequent fall in stress-induced phosphatidylinositol 3,5-bisphosphate levels. **Eukaryot Cell**, 5, 723-31.
- Duex, J. E., Tang, F. & Weisman, L. S. (2006b) The Vac14p-Fig4p complex acts independently of Vac7p and couples PI3,5P₂ synthesis and turnover. **J Cell Biol**, 172, 693-704.
- Dumas, J. J., Merithew, E., Sudharshan, E., Rajamani, D., Hayes, S., Lawe, D., Corvera, S. & Lambright, D. G. (2001) Multivalent endosome targeting by homodimeric EEA1. **Mol Cell**, 8, 947-58.
- Efe, J. A., Botelho, R. J. & Emr, S. D. (2007) Atg18 regulates organelle morphology and Fab1 kinase activity independent of its membrane recruitment by phosphatidylinositol 3,5-bisphosphate. **Mol Biol Cell**, 18, 4232-44.
- Eugster, A., Pecheur, E. I., Michel, F., Winsor, B., Letourneur, F. & Friant, S. (2004) Ent5p is required with Ent3p and Vps27p for ubiquitin-dependent protein sorting into the multivesicular body. **Mol Biol Cell**, 15, 3031-41.
- Farquhar, M. G. & Palade, G. E. (1998) The Golgi apparatus: 100 years of progress and controversy. **Trends Cell Biol**, 8, 2-10.
- Feldmann, H. (2005) *Yeast Molecular genetics. 10: Yeast growth and cell cycle*. University of Munich.
- Ferguson, C. J., Lenk, G. M. & Meisler, M. H. (2009) Defective autophagy in neurons and astrocytes from mice deficient in PI(3,5)P₂. **Hum Mol Genet**, 18, 4868-78.

- Ferreira, C., Silva, S., Van Voorst, F., Aguiar, C., Kielland-Brandt, M. C., Brandt, A. & Lucas, C. (2006) Absence of Gup1p in *Saccharomyces cerevisiae* results in defective cell wall composition, assembly, stability and morphology. **FEMS Yeast Res**, 6, 1027-38.
- Ford, M. G., Mills, I. G., Peter, B. J., Vallis, Y., Praefcke, G. J., Evans, P. R. & McMahon, H. T. (2002) Curvature of clathrin-coated pits driven by epsin. **Nature**, 419, 361-6.
- Franke, T. F. & Cantley, L. C. (1997) Apoptosis. A Bad kinase makes good. **Nature**, 390, 116-7.
- Franke, T. F., Kaplan, D. R., Cantley, L. C. & Toker, A. (1997) Direct regulation of the Akt proto-oncogene product by phosphatidylinositol-3,4-bisphosphate. **Science**, 275, 665-8.
- Friant, S., Pecheur, E. I., Eugster, A., Michel, F., Lefkir, Y., Nourrisson, D. & Letourneur, F. (2003) Ent3p Is a PtdIns(3,5)P₂ effector required for protein sorting to the multivesicular body. **Dev Cell**, 5, 499-511.
- Funamoto, S., Milan, K., Meili, R. & Firtel, R. A. (2001) Role of phosphatidylinositol 3' kinase and a downstream pleckstrin homology domain-containing protein in controlling chemotaxis in dictyostelium. **J Cell Biol**, 153, 795-810.
- Gary, J. D., Sato, T. K., Stefan, C. J., Bonangelino, C. J., Weisman, L. S. & Emr, S. D. (2002) Regulation of Fab1 phosphatidylinositol 3-phosphate 5-kinase pathway by Vac7 protein and Fig4, a polyphosphoinositide phosphatase family member. **Mol Biol Cell**, 13, 1238-51.
- Gary, J. D., Wurmser, A. E., Bonangelino, C. J., Weisman, L. S. & Emr, S. D. (1998) Fab1p is essential for PtdIns(3)P 5-kinase activity and the maintenance of vacuolar size and membrane homeostasis. **J Cell Biol**, 143, 65-79.
- Gaulhier, J. M., Simonsen, A., D'arrigo, A., Bremnes, B., Stenmark, H. & Aasland, R. (1998) FYVE fingers bind PtdIns(3)P. **Nature**, 394, 432-3.
- Gehring, E. M., Lam, R. S., Siraskar, G., Koutsouki, E., Seeböhm, G., Ureche, O. N., Ureche, L., Baltaev, R., Tavares, J. M. & Lang, F. (2009a) PIKfyve upregulates CFTR activity. **Biochem Biophys Res Commun**, 390, 952-7.
- Gehring, E. M., Zurn, A., Klaus, F., Laufer, J., Sopjani, M., Lindner, R., Strutz-Seeböhm, N., Tavares, J. M., Boehmer, C., Palmada, M., Lang, U. E., Seeböhm, G. & Lang, F. (2009b) Regulation of the glutamate transporter EAAT2 by PIKfyve. **Cell Physiol Biochem**, 24, 361-8.
- Gillooly, D. J., Morrow, I. C., Lindsay, M., Gould, R., Bryant, N. J., Gaulhier, J. M., Parton, R. G. & Stenmark, H. (2000) Localization of phosphatidylinositol 3-phosphate in yeast and mammalian cells. **Embo J**, 19, 4577-88.
- Godi, A., Di Campli, A., Konstantakopoulos, A., Di Tullio, G., Alessi, D. R., Kular, G. S., Daniele, T., Marra, P., Lucocq, J. M. & De Matteis, M. A. (2004) FAPPs control Golgi-to-cell-surface membrane traffic by binding to ARF and PtdIns(4)P. **Nat Cell Biol**, 6, 393-404.
- Groves, M. R., Hanlon, N., Turowski, P., Hemmings, B. A. & Barford, D. (1999) The structure of the protein phosphatase 2A PR65/A subunit reveals the conformation of its 15 tandemly repeated HEAT motifs. **Cell**, 96, 99-110.
- Han, B. K. & Emr, S. D. (2011) Phosphoinositide [PI(3,5)P₂] lipid-dependent regulation of the general transcriptional regulator Tup1. **Genes Dev**, 25, 984-95.
- Harrington, B. J. & Raper, K. B. (1968) Use of a fluorescent brightener to demonstrate cellulose in the cellular slime molds. **Appl Microbiol**, 16, 106-13.
- Hauke, V. & Schatz, G. (1997) Import of proteins into mitochondria and chloroplasts. **Trends Cell Biol**, 7, 103-6.
- Hettema, E. H., Lewis, M. J., Black, M. W. & Pelham, H. R. (2003) Retromer and the sorting nexins Snx4/41/42 mediate distinct retrieval pathways from yeast endosomes. **Embo J**, 22, 548-57.
- Hierro, A., Rojas, A. L., Rojas, R., Murthy, N., Effantin, G., Kajava, A. V., Steven, A. C., Bonifacino, J. S. & Hurley, J. H. (2007) Functional architecture of the retromer cargo-recognition complex. **Nature**, 449, 1063-7.
- Horazdovsky, B. F., Davies, B. A., Seaman, M. N., Mclaughlin, S. A., Yoon, S. & Emr, S. D. (1997) A sorting nexin-1 homologue, Vps5p, forms a complex with Vps17p and is required for recycling the vacuolar protein-sorting receptor. **Mol Biol Cell**, 8, 1529-41.
- Huh, W. K., Falvo, J. V., Gerke, L. C., Carroll, A. S., Howson, R. W., Weissman, J. S. & O'shea, E. K. (2003) Global analysis of protein localization in budding yeast. **Nature**, 425, 686-91.
- Ikonomov, O. C., Fligger, J., Sbrissa, D., Dondapati, R., Mlak, K., Deeb, R. & Shisheva, A. (2009a) Kinesin adapter JLP links PIKfyve to microtubule-based endosome-to-trans-Golgi network traffic of furin. **J Biol Chem**, 284, 3750-61.
- Ikonomov, O. C., Sbrissa, D., Fligger, J., Delvecchio, K. & Shisheva, A. (2010) ArPIKfyve regulates Sac3 protein abundance and turnover: disruption of the mechanism by Sac3I41T mutation causing Charcot-Marie-Tooth 4J disorder. **J Biol Chem**, 285, 26760-4.

- Ikonomov, O. C., Sbrissa, D., Mlak, K., Deeb, R., Fligger, J., Soans, A., Finley, R. L., Jr. & Shisheva, A. (2003) Active PIKfyve associates with and promotes the membrane attachment of the late endosome-to-trans-Golgi network transport factor Rab9 effector p40. **J Biol Chem**, 278, 50863-71.
- Ikonomov, O. C., Sbrissa, D. & Shisheva, A. (2001) Mammalian cell morphology and endocytic membrane homeostasis require enzymatically active phosphoinositide 5-kinase PIKfyve. **J Biol Chem**, 276, 26141-7.
- Ikonomov, O. C., Sbrissa, D. & Shisheva, A. (2009b) YM201636, an inhibitor of retroviral budding and PIKfyve-catalyzed PtdIns(3,5)P₂ synthesis, halts glucose entry by insulin in adipocytes. **Biochem Biophys Res Commun**, 382, 566-70.
- Isakoff, S. J., Cardozo, T., Andreev, J., Li, Z., Ferguson, K. M., Abagyan, R., Lemmon, M. A., Aronheim, A. & Skolnik, E. Y. (1998) Identification and analysis of PH domain-containing targets of phosphatidylinositol 3-kinase using a novel in vivo assay in yeast. **Embo J**, 17, 5374-87.
- Itoh, T., Koshiba, S., Kigawa, T., Kikuchi, A., Yokoyama, S. & Takenawa, T. (2001) Role of the ENTH domain in phosphatidylinositol-4,5-bisphosphate binding and endocytosis. **Science**, 291, 1047-51.
- Jackson, J. G., Kreisberg, J. I., Koterba, A. P., Yee, D. & Brattain, M. G. (2000) Phosphorylation and nuclear exclusion of the forkhead transcription factor FKHR after epidermal growth factor treatment in human breast cancer cells. **Oncogene**, 19, 4574-81.
- Jefferies, H. B., Cooke, F. T., Jat, P., Boucheron, C., Koizumi, T., Hayakawa, M., Kaizawa, H., Ohishi, T., Workman, P., Waterfield, M. D. & Parker, P. J. (2008) A selective PIKfyve inhibitor blocks PtdIns(3,5)P₂ production and disrupts endomembrane transport and retroviral budding. **EMBO Rep**, 9, 164-70.
- Jeffries, T. R., Dove, S. K., Michell, R. H. & Parker, P. J. (2004) PtdIns-specific MPR pathway association of a novel WD40 repeat protein, WIPI49. **Mol Biol Cell**, 15, 2652-63.
- Jin, N., Chow, C. Y., Liu, L., Zolov, S. N., Bronson, R., Davisson, M., Petersen, J. L., Zhang, Y., Park, S., Duex, J. E., Goldowitz, D., Meisler, M. H. & Weisman, L. S. (2008) VAC14 nucleates a protein complex essential for the acute interconversion of PI3P and PI(3,5)P₂ in yeast and mouse. **Embo J**, 27, 3221-34.
- Joly, M., Kazlauskas, A. & Corvera, S. (1995) Phosphatidylinositol 3-kinase activity is required at a postendocytic step in platelet-derived growth factor receptor trafficking. **J Biol Chem**, 270, 13225-30.
- Jones, D. R., Bultsma, Y., Keune, W. J., Halstead, J. R., Elouarrat, D., Mohammed, S., Heck, A. J., D'santos, C. S. & Divecha, N. (2006) Nuclear PtdIns5P as a transducer of stress signaling: an in vivo role for PIP4Kbeta. **Mol Cell**, 23, 685-95.
- Jorgensen, M. U., Emr, S. D. & Winther, J. R. (1999) Ligand recognition and domain structure of Vps10p, a vacuolar protein sorting receptor in *Saccharomyces cerevisiae*. **Eur J Biochem**, 260, 461-9.
- Kama, R., Robinson, M. & Gerst, J. E. (2007) Btn2, a Hook1 ortholog and potential Batten disease-related protein, mediates late endosome-Golgi protein sorting in yeast. **Mol Cell Biol**, 27, 605-21.
- Kanai, F., Liu, H., Field, S. J., Akbary, H., Matsuo, T., Brown, G. E., Cantley, L. C. & Yaffe, M. B. (2001) The PX domains of p47phox and p40phox bind to lipid products of PI(3)K. **Nat Cell Biol**, 3, 675-8.
- Kane, P. M. (2005) Close-up and genomic views of the yeast vacuolar H⁺-ATPase. **J Bioenerg Biomembr**, 37, 399-403.
- Katzmann, D. J., Sarkar, S., Chu, T., Audhya, A. & Emr, S. D. (2004) Multivesicular body sorting: ubiquitin ligase Rsp5 is required for the modification and sorting of carboxypeptidase S. **Mol Biol Cell**, 15, 468-80.
- Kay, B. K., Yamabhai, M., Wendland, B. & Emr, S. D. (1999) Identification of a novel domain shared by putative components of the endocytic and cytoskeletal machinery. **Protein Sci**, 8, 435-8.
- Kihara, A., Noda, T., Ishihara, N. & Ohsumi, Y. (2001) Two distinct Vps34 phosphatidylinositol 3-kinase complexes function in autophagy and carboxypeptidase Y sorting in *Saccharomyces cerevisiae*. **J Cell Biol**, 152, 519-30.
- Kirchhausen, T. (1999) Adaptors for clathrin-mediated traffic. **Annu Rev Cell Dev Biol**, 15, 705-32.
- Klaus, F., Gehring, E. M., Zurn, A., Laufer, J., Lindner, R., Strutz-Seeböhm, N., Tavaré, J. M., Rothstein, J. D., Boehmer, C., Palmada, M., Gruner, I., Lang, U. E., Seeböhm, G. & Lang, F. (2009a) Regulation of the Na⁽⁺⁾-coupled glutamate transporter EAAT3 by PIKfyve. **Neurochem Int**, 54, 372-7.

- Klaus, F., Laufer, J., Czarkowski, K., Strutz-Seeböhm, N., Seeböhm, G. & Lang, F. (2009b) PIKfyve-dependent regulation of the Cl⁻ channel ClC-2. **Biochem Biophys Res Commun**, 381, 407-11.
- Kolehmainen, J., Black, G. C., Saarinen, A., Chandler, K., Clayton-Smith, J., Traskelin, A. L., Perveen, R., Kivitiö-Kallio, S., Norio, R., Warburg, M., Fryns, J. P., De La Chapelle, A. & Lehesjoki, A. E. (2003) Cohen syndrome is caused by mutations in a novel gene, COH1, encoding a transmembrane protein with a presumed role in vesicle-mediated sorting and intracellular protein transport. **Am J Hum Genet**, 72, 1359-69.
- Kong, A. M., Horan, K. A., Sriratanana, A., Bailey, C. G., Collyer, L. J., Nandurkar, H. H., Shisheva, A., Layton, M. J., Rasko, J. E., Rowe, T. & Mitchell, C. A. (2006) Phosphatidylinositol 3-phosphate [PtdIns3P] is generated at the plasma membrane by an inositol polyphosphate 5-phosphatase: endogenous PtdIns3P can promote GLUT4 translocation to the plasma membrane. **Mol Cell Biol**, 26, 6065-81.
- Krick, R., Henke, S., Tolstrup, J. & Thumm, M. (2008) Dissecting the localization and function of Atg18, Atg21 and Ygr223c. **Autophagy**, 4, 896-910.
- Krick, R., Tolstrup, J., Appelles, A., Henke, S. & Thumm, M. (2006) The relevance of the phosphatidylinositolphosphat-binding motif FRRGT of Atg18 and Atg21 for the Cvt pathway and autophagy. **FEBS Lett**, 580, 4632-8.
- Lagrassa, T. J. & Ungermann, C. (2005) The vacuolar kinase Yck3 maintains organelle fragmentation by regulating the HOPS tethering complex. **J Cell Biol**, 168, 401-14.
- Lecompte, O., Poch, O. & Laporte, J. (2008) PtdIns5P regulation through evolution: roles in membrane trafficking? **Trends Biochem Sci**, 33, 453-60.
- Lemmon, M. A. (2008) Membrane recognition by phospholipid-binding domains. **Nat Rev Mol Cell Biol**, 9, 99-111.
- Lemmon, M. A. & Ferguson, K. M. (2000) Signal-dependent membrane targeting by pleckstrin homology (PH) domains. **Biochem J**, 350 Pt 1, 1-18.
- Lenk, G. M., Ferguson, C. J., Chow, C. Y., Jin, N., Jones, J. M., Grant, A. E., Zolov, S. N., Winters, J. J., Giger, R. J., Dowling, J. J., Weisman, L. S. & Meisler, M. H. (2011) Pathogenic mechanism of the FIG4 mutation responsible for Charcot-Marie-Tooth disease CMT4J. **PLoS Genet**, 7, e1002104.
- Li, G., D'souza-Schorey, C., Barbieri, M. A., Roberts, R. L., Klippel, A., Williams, L. T. & Stahl, P. D. (1995) Evidence for phosphatidylinositol 3-kinase as a regulator of endocytosis via activation of Rab5. **Proc Natl Acad Sci U S A**, 92, 10207-11.
- Li, S. C. & Kane, P. M. (2009) The yeast lysosome-like vacuole: endpoint and crossroads. **Biochim Biophys Acta**, 1793, 650-63.
- Lin, C. H., Macgurn, J. A., Chu, T., Stefan, C. J. & Emr, S. D. (2008) Arrestin-related ubiquitin-ligase adaptors regulate endocytosis and protein turnover at the cell surface. **Cell**, 135, 714-25.
- Lindmo, K. & Stenmark, H. (2006) Regulation of membrane traffic by phosphoinositide 3-kinases. **J Cell Sci**, 119, 605-14.
- Longtine, M. S., Mckenzie, A., 3rd, Demarini, D. J., Shah, N. G., Wach, A., Brachet, A., Philippsen, P. & Pringle, J. R. (1998) Additional modules for versatile and economical PCR-based gene deletion and modification in *Saccharomyces cerevisiae*. **Yeast**, 14, 953-61.
- Manheit, J.E., Cowan, D.F. & Moore, D.G. (1984) Rapid detection of fungi in tissues using calcofluor white and fluorescence microscopy. **Arch Pathol Lab Med**, 108, 616-618.
- Marcusson, E. G., Horazdovsky, B. F., Cereghino, J. L., Gharakhanian, E. & Emr, S. D. (1994) The sorting receptor for yeast vacuolar carboxypeptidase Y is encoded by the VPS10 gene. **Cell**, 77, 579-86.
- Marks, M. S., Ohno, H., Kirchhausen, T. & Bonracino, J. S. (1997) Protein sorting by tyrosine-based signals: adapting to the Ys and wherefore. **Trends Cell Biol**, 7, 124-8.
- Martelli, A. M., Cocco, L., Capitani, S., Miscia, S., Papa, S. & Manzoli, F. A. (2007) Nuclear phosphatidylinositol 3,4,5-trisphosphate, phosphatidylinositol 3-kinase, Akt, and PTEN: emerging key regulators of anti-apoptotic signaling and carcinogenesis. **Eur J Histochem**, 51 Suppl 1, 125-31.
- Matern, H., Yang, X., Andrulis, E., Sternglanz, R., Trepte, H. H. & Gallwitz, D. (2000) A novel Golgi membrane protein is part of a GTPase-binding protein complex involved in vesicle targeting. **Embo J**, 19, 4485-92.
- McEwen, R. K., Dove, S. K., Cooke, F. T., Painter, G. F., Holmes, A. B., Shisheva, A., Ohya, Y., Parker, P. J. & Michell, R. H. (1999) Complementation analysis in PtdInsP kinase-deficient yeast mutants demonstrates that *Schizosaccharomyces pombe* and murine Fab1p

- homologshomologues are phosphatidylinositol 3-phosphate 5-kinases. **J Biol Chem**, 274, 33905-12.
- Mellman, I. & Warren, G. (2000) The road taken: past and future foundations of membrane traffic. **Cell**, 100, 99-112.
- Meyrial, V., Laize, V., Gobin, R., Ripoche, P., Hohmann, S. & Tacnet, F. (2001) Existence of a tightly regulated water channel in *Saccharomyces cerevisiae*. **Eur J Biochem**, 268, 334-43.
- Michell, R. H., Heath, V. L., Lemmon, M. A. & Dove, S. K. (2006) Phosphatidylinositol 3,5-bisphosphate: metabolism and cellular functions. **Trends Biochem Sci**, 31, 52-63.
- Misra, S. & Hurley, J. H. (1999) Crystal structure of a phosphatidylinositol 3-phosphate-specific membrane-targeting motif, the FYVE domain of Vps27p. **Cell**, 97, 657-66.
- Mitchell, R. S., Chaudhuri, R., Lindwasser, O. W., Tanaka, K. A., Lau, D., Murillo, R., Bonifacino, J. S. & Guatelli, J. C. (2008) Competition model for upregulation of the major histocompatibility complex class II-associated invariant chain by human immunodeficiency virus type 1 Nef. **J Virol**, 82, 7758-67.
- Mitra, P., Zhang, Y., Rameh, L. E., Ivshina, M. P., Mccollum, D., Nunnari, J. J., Hendricks, G. M., Kerr, M. L., Field, S. J., Cantley, L. C. & Ross, A. H. (2004) A novel phosphatidylinositol(3,4,5)P3 pathway in fission yeast. **J Cell Biol**, 166, 205-11.
- Mollapour, M., Phelan, J. P., Millson, S. H., Piper, P. W. & Cooke, F. T. (2006) Weak acid and alkali stress regulate phosphatidylinositol bisphosphate synthesis in *Saccharomyces cerevisiae*. **Biochem J**, 395, 73-80.
- Mouyna, I., Fontaine, T., Vai, M., Monod, M., Fonzi, W. A., Diaquin, M., Popolo, L., Hartland, R. P. & Latge, J. P. (2000) Glycosylphosphatidylinositol-anchored glucanotransferases play an active role in the biosynthesis of the fungal cell wall. **J Biol Chem**, 275, 14882-9.
- Mumberg, D., Muller, R. & Funk, M. (1994) Regulatable promoters of *Saccharomyces cerevisiae*: comparison of transcriptional activity and their use for heterologous expression. **Nucleic Acids Res**, 22, 5767-8.
- Munier-Lehmann, H., Mauxion, F. & Hoflack, B. (1996) Function of the two mannose 6-phosphate receptors in lysosomal enzyme transport. **Biochem Soc Trans**, 24, 133-6.
- Murray, J. L., Mavrikakis, M., Mcdonald, N. J., Yilla, M., Sheng, J., Bellini, W. J., Zhao, L., Le Doux, J. M., Shaw, M. W., Luo, C. C., Lippincott-Schwartz, J., Sanchez, A., Rubin, D. H. & Hodge, T. W. (2005) Rab9 GTPase is required for replication of human immunodeficiency virus type 1, filoviruses, and measles virus. **J Virol**, 79, 11742-51.
- Nicot, A. S., Fares, H., Payraastre, B., Chisholm, A. D., Labouesse, M. & Laporte, J. (2006) The phosphoinositide kinase PIKfyve/Fab1p regulates terminal lysosome maturation in *Caenorhabditis elegans*. **Mol Biol Cell**, 17, 3062-74.
- Nicot, A. S. & Laporte, J. (2008) Endosomal phosphoinositides and human diseases. **Traffic**, 9, 1240-9.
- Niedenthal, R. K., Riles, L., Johnston, M. & Hegemann, J. H. (1996) Green fluorescent protein as a marker for gene expression and subcellular localization in budding yeast. **Yeast**, 12, 773-86.
- Noda, T., Suzuki, K. & Ohsumi, Y. (2002) Yeast autophagosomes: de novo formation of a membrane structure. **Trends in Cell Biology**, 12, 231-5.
- Obara, K., Sekito, T., Niimi, K. & Ohsumi, Y. (2008) The Atg18-Atg2 complex is recruited to autophagic membranes via phosphatidylinositol 3-phosphate and exerts an essential function. **J Biol Chem**, 283, 23972-80.
- Obara, K., Sekito, T. & Ohsumi, Y. (2006) Assortment of phosphatidylinositol 3-kinase complexes--Atg14p directs association of complex I to the pre-autophagosomal structure in *Saccharomyces cerevisiae*. **Mol Biol Cell**, 17, 1527-39.
- Odorizzi, G., Babst, M. & Emr, S. D. (1998) Fab1p PtdIns(3)P 5-kinase function essential for protein sorting in the multivesicular body. **Cell**, 95, 847-58.
- Odorizzi, G., Babst, M. & Emr, S. D. (2000) Phosphoinositide signaling and the regulation of membrane trafficking in yeast. **Trends Biochem Sci**, 25, 229-35.
- Oelkers, P., Tinkelenberg, A., Erdeniz, N., Cromley, D., Billheimer, J. T. & Sturley, S. L. (2000) A lecithin cholesterol acyltransferase-like gene mediates diacylglycerol esterification in yeast. **J Biol Chem**, 275, 15609-12.
- Ortiz, D. & Novick, P. J. (2006) Ypt32p regulates the translocation of Chs3p from an internal pool to the plasma membrane. **Eur J Cell Biol**, 85, 107-16.
- Osborne, S. L., Wen, P. J., Boucheron, C., Nguyen, H. N., Hayakawa, M., Kaizawa, H., Parker, P. J., Vitale, N. & Meunier, F. A. (2008) PIKfyve negatively regulates exocytosis in neurosecretory cells. **J Biol Chem**, 283, 2804-13.

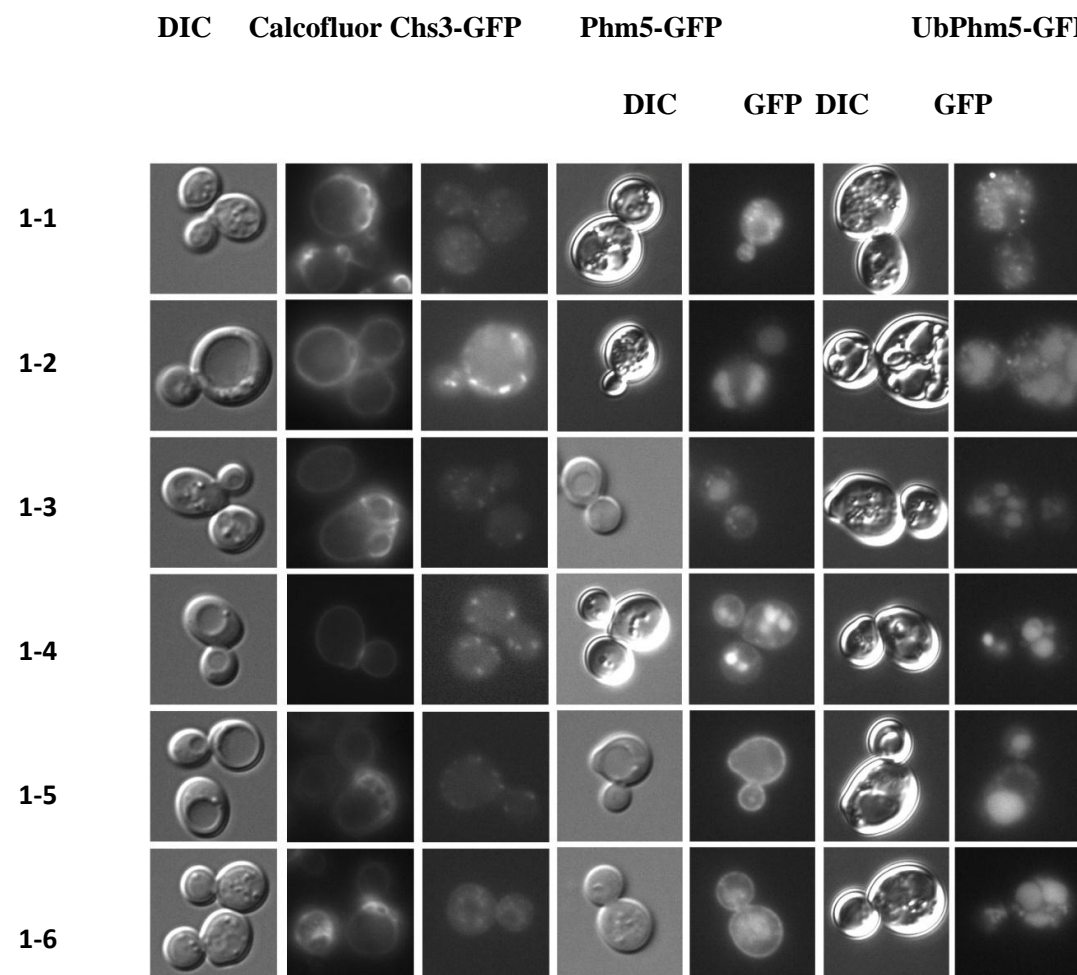
- Ostrowicz, C. W., Meiringer, C. T. & Ungermann, C. (2008) Yeast vacuole fusion: a model system for eukaryotic endomembrane dynamics. **Autophagy**, 4, 5-19.
- Palade, G. (1975) Intracellular aspects of the process of protein synthesis. **Science**, 189, 347-58.
- Paroutis, P., Touret, N. & Grinstein, S. (2004) The pH of the secretory pathway: measurement, determinants, and regulation. **Physiology (Bethesda)**, 19, 207-15.
- Pelham, H. R. (1999) SNAREs and the secretory pathway-lessons from yeast. **Exp Cell Res**, 247, 1-8.
- Pelham, H. R. (2002) Insights from yeast endosomes. **Curr Opin Cell Biol**, 14, 454-62.
- Peplowska, K., Markgraf, D. F., Ostrowicz, C. W., Bange, G. & Ungermann, C. (2007) The CORVET tethering complex interacts with the yeast Rab5 homolog Vps21 and is involved in endo-lysosomal biogenesis. **Dev Cell**, 12, 739-50.
- Peters, C., Baars, T. L., Buhler, S. & Mayer, A. (2004) Mutual control of membrane fission and fusion proteins. **Cell**, 119, 667-78.
- Phelan, J. P., Millson, S. H., Parker, P. J., Piper, P. W. & Cooke, F. T. (2006) Fab1p and AP-1 are required for trafficking of endogenously ubiquitinated cargoes to the vacuole lumen in *S. cerevisiae*. **J Cell Sci**, 119, 4225-34.
- Piper, R. C., Bryant, N. J. & Stevens, T. H. (1997) The membrane protein alkaline phosphatase is delivered to the vacuole by a route that is distinct from the VPS-dependent pathway. **J Cell Biol**, 138, 531-45.
- Piper, R. C., Cooper, A. A., Yang, H. & Stevens, T. H. (1995) VPS27 controls vacuolar and endocytic traffic through a prevacuolar compartment in *Saccharomyces cerevisiae*. **J Cell Biol**, 131, 603-17.
- Piper, R. C. & Luzio, J. P. (2001) Late endosomes: sorting and partitioning in multivesicular bodies. **Traffic**, 2, 612-21.
- Prescianotto-Baschong, C. & Riezman, H. (2002) Ordering of compartments in the yeast endocytic pathway. **Traffic**, 3, 37-49.
- Proikas-Cezanne, T., Waddell, S., Gaugel, A., Frickey, T., Lupas, A. & Nordheim, A. (2004) WIPI-1alpha (WIPI49), a member of the novel 7-bladed WIPI protein family, is aberrantly expressed in human cancer and is linked to starvation-induced autophagy. **Oncogene**, 23, 9314-25.
- Raiborg, C., Rusten, T. E. & Stenmark, H. (2003) Protein sorting into multivesicular endosomes. **Curr Opin Cell Biol**, 15, 446-55.
- Rameh, L. E., Tolias, K. F., Duckworth, B. C. & Cantley, L. C. (1997) A new pathway for synthesis of phosphatidylinositol-4,5-bisphosphate. **Nature**, 390, 192-6.
- Raymond, C. K., Howald-Stevenson, I., Vater, C. A. & Stevens, T. H. (1992) Morphological classification of the yeast vacuolar protein sorting mutants: evidence for a prevacuolar compartment in class E vps mutants. **Mol Biol Cell**, 3, 1389-402.
- Redding, K., Brickner, J. H., Marschall, L. G., Nichols, J. W. & Fuller, R. S. (1996) Allele-specific suppression of a defective trans-Golgi network (TGN) localization signal in *Kex2p* identifies three genes involved in localization of TGN transmembrane proteins. **Mol Cell Biol**, 16, 6208-17.
- Reggiori, F. & Pelham, H. R. (2001) Sorting of proteins into multivesicular bodies: ubiquitin-dependent and -independent targeting. **Embo J**, 20, 5176-86.
- Robinson, F. L. & Dixon, J. E. (2006) Myotubularin phosphatases: policing 3-phosphoinositides. **Trends Cell Biol**, 16, 403-12.
- Robinson, J. S., Klionsky, D. J., Banta, L. M. & Emr, S. D. (1988) Protein sorting in *Saccharomyces cerevisiae*: isolation of mutants defective in the delivery and processing of multiple vacuolar hydrolases. **Mol Cell Biol**, 8, 4936-48.
- Roncero, C., Valdivieso, M. H., Ribas, J. C. & Duran, A. (1988) Effect of calcofluor white on chitin synthases from *Saccharomyces cerevisiae*. **J Bacteriol**, 170, 1945-9.
- Rothman, J. E. & Wieland, F. T. (1996) Protein sorting by transport vesicles. **Science**, 272, 227-34.
- Rothman, J. H., Howald, I. & Stevens, T. H. (1989) Characterization of genes required for protein sorting and vacuolar function in the yeast *Saccharomyces cerevisiae*. **EMBO J**, 8, 2057-65.
- Rudge, S. A., Anderson, D. M. & Emr, S. D. (2004) Vacuole size control: regulation of PtdIns(3,5)P₂ levels by the vacuole-associated Vac14-Fig4 complex, a PtdIns(3,5)P₂-specific phosphatase. **Mol Biol Cell**, 15, 24-36.
- Ruiz-Herrera, J., Xoconostle-Cazares, B., Reynaga-Pena, C. G., Leon-Ramirez, C. & Carabez-Trejo, A. (2006) Immunolocalization of chitin synthases in the phytopathogenic dimorphic fungus *Ustilago maydis*. **FEMS Yeast Res**, 6, 999-1009.
- Rusten, T. E., Filimonenko, M., Rodahl, L. M., Stenmark, H. & Simonsen, A. (2007a) ESCRTing autophagic clearance of aggregating proteins. **Autophagy**, 4.

- Rusten, T. E., Rodahl, L. M., Pattni, K., Englund, C., Samakovlis, C., Dove, S., Brech, A. & Stenmark, H. (2006) Fab1 phosphatidylinositol 3-phosphate 5-kinase controls trafficking but not silencing of endocytosed receptors. **Mol Biol Cell**, 17, 3989-4001.
- Rusten, T. E., Vaccari, T., Lindmo, K., Rodahl, L. M., Nezis, I. P., Sem-Jacobsen, C., Wendler, F., Vincent, J. P., Brech, A., Bilder, D. & Stenmark, H. (2007b) ESCRTs and Fab1 regulate distinct steps of autophagy. **Curr Biol**, 17, 1817-25.
- Rutherford, A. C., Traer, C., Wassmer, T., Pattni, K., Bujny, M. V., Carlton, J. G., Stenmark, H. & Cullen, P. J. (2006) The mammalian phosphatidylinositol 3-phosphate 5-kinase (PIKfyve) regulates endosome-to-TGN retrograde transport. **J Cell Sci**, 119, 3944-57.
- Sambade, M. & Kane, P. M. (2004) The yeast vacuolar proton-translocating ATPase contains a subunit homologous to the *Manduca sexta* and bovine e subunits that is essential for function. **J Biol Chem**, 279, 17361-5.
- Sanchatjate, S. & Schekman, R. (2006) Chs5/6 complex: a multiprotein complex that interacts with and conveys chitin synthase III from the trans-Golgi network to the cell surface. **Mol Biol Cell**, 17, 4157-66.
- Sankaran, V. G., Klein, D. E., Sachdeva, M. M. & Lemmon, M. A. (2001) High-affinity binding of a FYVE domain to phosphatidylinositol 3-phosphate requires intact phospholipid but not FYVE domain oligomerization. **Biochemistry**, 40, 8581-7.
- Santos, B. & Snyder, M. (2003) Specific protein targeting during cell differentiation: polarized localization of Fus1p during mating depends on Chs5p in *Saccharomyces cerevisiae*. **Eukaryot Cell**, 2, 821-5.
- Sbrissa, D., Ikonomov, O. C. & Shisheva, A. (2000) PIKfyve lipid kinase is a protein kinase: downregulation of 5'-phosphoinositide product formation by autophosphorylation. **Biochemistry**, 39, 15980-9.
- Sbrissa, D., Ikonomov, O. C. & Shisheva, A. (2002) Phosphatidylinositol 3-phosphate-interacting domains in PIKfyve. Binding specificity and role in PIKfyve. Endomembrane localization. **J Biol Chem**, 277, 6073-9.
- Sbrissa, D., Ikonomov, O. C. & Shisheva, A. (2005) Analysis of potential binding of the recombinant Rab9 effector p40 to phosphoinositide-enriched synthetic liposomes. **Methods Enzymol**, 403, 696-705.
- Sbrissa, D., Ikonomov, O. C., Strakova, J., Dondapati, R., Mlak, K., Deeb, R., Silver, R. & Shisheva, A. (2004) A mammalian ortholog of *Saccharomyces cerevisiae* Vac14 that associates with and up-regulates PIKfyve phosphoinositide 5-kinase activity. **Mol Cell Biol**, 24, 10437-47.
- Schekman, R. & Orci, L. (1996) Coat proteins and vesicle budding. **Science**, 271, 1526-33.
- Schekman, R. W. (1994) Regulation of membrane traffic in the secretory pathway. **Harvey Lect**, 90, 41-57.
- Schill, N. J. & Anderson, R. A. (2009) Out, in and back again: PtdIns(4,5)P(2) regulates cadherin trafficking in epithelial morphogenesis. **Biochem J**, 418, 247-60.
- Schimmoller, F. & Riezman, H. (1993) Involvement of Ypt7p, a small GTPase, in traffic from late endosome to the vacuole in yeast. **J Cell Sci**, 106 (Pt 3), 823-30.
- Schmid, S. L. (1997) Clathrin-coated vesicle formation and protein sorting: an integrated process. **Annu Rev Biochem**, 66, 511-48.
- Seals, D. F., Eitzen, G., Margolis, N., Wickner, W. T. & Price, A. (2000) A Ypt/Rab effector complex containing the Sec1 homolog Vps33p is required for homotypic vacuole fusion. **Proc Natl Acad Sci U S A**, 97, 9402-7.
- Seaman, M. N. (2005) Recycle your receptors with retromer. **Trends Cell Biol**, 15, 68-75.
- Seaman, M. N., Marcusson, E. G., Cereghino, J. L. & Emr, S. D. (1997) Endosome to Golgi retrieval of the vacuolar protein sorting receptor, Vps10p, requires the function of the VPS29, VPS30, and VPS35 gene products. **J Cell Biol**, 137, 79-92.
- Seaman, M. N., Mc Caffery, J. M. & Emr, S. D. (1998) A membrane coat complex essential for endosome-to-Golgi retrograde transport in yeast. **J Cell Biol**, 142, 665-81.
- Seeböhm, G., Strutz-Seeböhm, N., Birkin, R., Dell, G., Bucci, C., Spinoso, M. R., Baltaev, R., Mack, A. F., Korniyuchuk, G., Choudhury, A., Marks, D., Pagano, R. E., Attali, B., Pfeufer, A., Kass, R. S., Sanguinetti, M. C., Tavare, J. M. & Lang, F. (2007) Regulation of endocytic recycling of KCNQ1/KCNE1 potassium channels. **Circ Res**, 100, 686-92.
- Shaw, J. D., Hama, H., Sohrabi, F., Dewald, D. B. & Wendland, B. (2003) PtdIns(3,5)P2 is required for delivery of endocytic cargo into the multivesicular body. **Traffic**, 4, 479-90.
- Sherman, F. (2002) Getting started with yeast. **Methods Enzymol**, 350, 3-41.
- Shisheva, A. (2001) PIKfyve: the road to PtdIns 5-P and PtdIns 3,5-P(2). **Cell Biol Int**, 25, 1201-6.

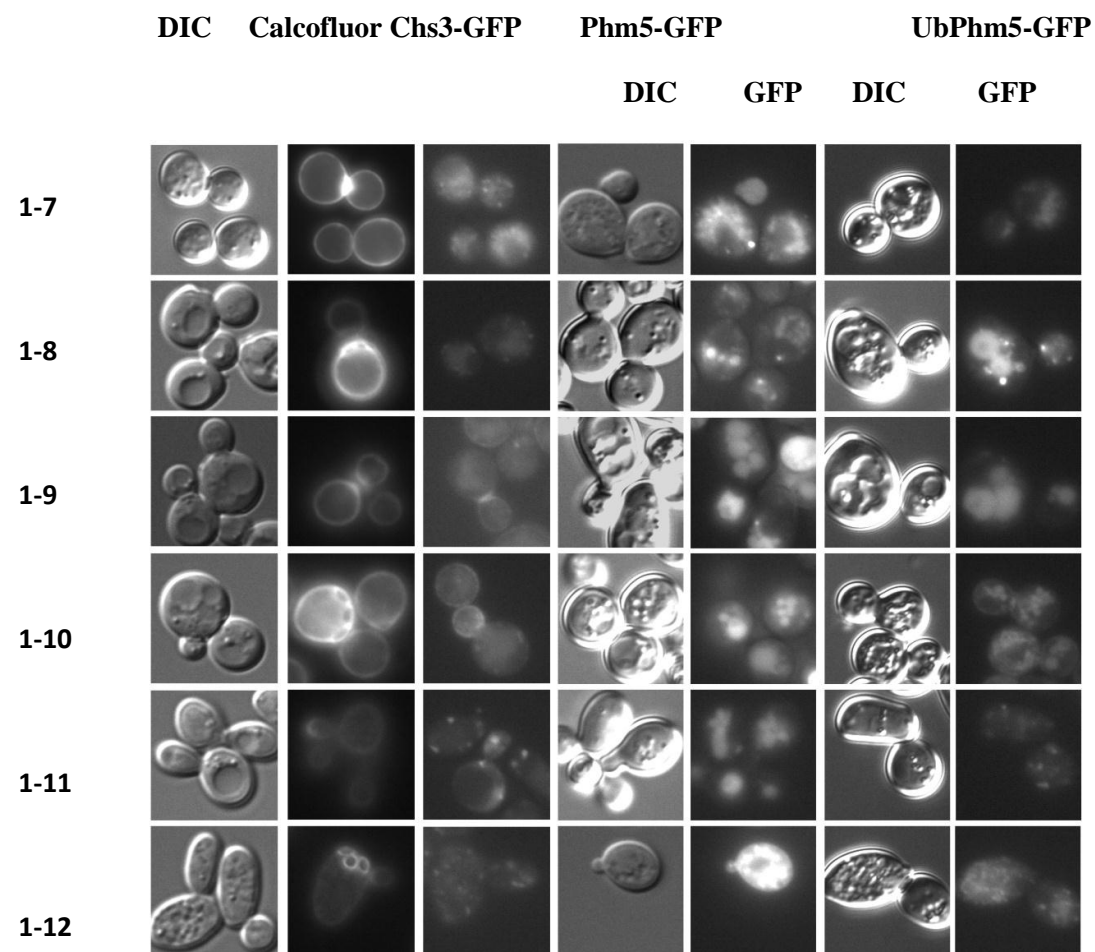
- Shojaiefard, M., Strutz-Seeböhm, N., Tavaré, J. M., Seeböhm, G. & Lang, F. (2007) Regulation of the Na(+), glucose cotransporter by PIKfyve and the serum and glucocorticoid inducible kinase SGK1. **Biochem Biophys Res Commun**, 359, 843-7.
- Sikorski, R. S. & Hieter, P. (1989) A system of shuttle vectors and yeast host strains designed for efficient manipulation of DNA in *Saccharomyces cerevisiae*. **Genetics**, 122, 19-27.
- Smits, G. J., Van Den Ende, H. & Klis, F. M. (2001) Differential regulation of cell wall biogenesis during growth and development in yeast. **Microbiology**, 147, 781-94.
- Song, X., Xu, W., Zhang, A., Huang, G., Liang, X., Virbasius, J. V., Czech, M. P. & Zhou, G. W. (2001) Phox homology domains specifically bind phosphatidylinositol phosphates. **Biochemistry**, 40, 8940-4.
- Sopjani, M., Kunert, A., Czarkowski, K., Klaus, F., Laufer, J., Foller, M. & Lang, F. (2009) Regulation of the Ca(2+) channel TRPV6 by the kinases SGK1, PKB/Akt, and PIKfyve. **J Membr Biol**, 233, 35-41.
- Soveral, G., Veiga, A., Loureiro-Dias, M. C., Tanghe, A., Van Dijck, P. & Moura, T. F. (2006) Water channels are important for osmotic adjustments of yeast cells at low temperature. **Microbiology**, 152, 1515-21.
- Stack, J. H., Dewald, D. B., Takegawa, K. & Emr, S. D. (1995) Vesicle-mediated protein transport: regulatory interactions between the Vps15 protein kinase and the Vps34 PtdIns 3-kinase essential for protein sorting to the vacuole in yeast. **J Cell Biol**, 129, 321-34.
- Starai, V. J., Thorngren, N., Fratti, R. A. & Wickner, W. (2005) Ion regulation of homotypic vacuole fusion in *Saccharomyces cerevisiae*. **J Biol Chem**, 280, 16754-62.
- Stenmark, H., Aasland, R. & Driscoll, P. C. (2002) The phosphatidylinositol 3-phosphate-binding FYVE finger. **FEBS Lett**, 513, 77-84.
- Stenmark, H., Aasland, R., Toh, B. H. & D'arrigo, A. (1996) Endosomal localization of the autoantigen EEA1 is mediated by a zinc-binding FYVE finger. **J Biol Chem**, 271, 24048-54.
- Stephens, L. R., Jackson, T. R. & Hawkins, P. T. (1993) Agonist-stimulated synthesis of phosphatidylinositol(3,4,5)-trisphosphate: a new intracellular signalling system? **Biochim Biophys Acta**, 1179, 27-75.
- Strahl, T. & Thorner, J. (2007) Synthesis and function of membrane phosphoinositides in budding yeast, *Saccharomyces cerevisiae*. **Biochim Biophys Acta**, 1771, 353-404.
- Stromhaug, P. E., Reggiori, F., Guan, J., Wang, C. W. & Klionsky, D. J. (2004) Atg21 is a phosphoinositide binding protein required for efficient lipidation and localization of Atg8 during uptake of aminopeptidase I by selective autophagy. **Mol Biol Cell**, 15, 3553-66.
- Strutz-Seeböhm, N., Shojaiefard, M., Christie, D., Tavaré, J., Seeböhm, G. & Lang, F. (2007) PIKfyve in the SGK1 mediated regulation of the creatine transporter SLC6A8. **Cell Physiol Biochem**, 20, 729-34.
- Takeda, K., Cabrera, M., Rohde, J., Bausch, D., Jensen, O. N. & Ungermann, C. (2008) The vacuolar V1/V0-ATPase is involved in the release of the HOPS subunit Vps41 from vacuoles, vacuole fragmentation and fusion. **FEBS Lett**, 582, 1558-63.
- Taylor, G. S., Maehama, T. & Dixon, J. E. (2000) Myotubularin, a protein tyrosine phosphatase mutated in myotubular myopathy, dephosphorylates the lipid second messenger, phosphatidylinositol 3-phosphate. **Proc Natl Acad Sci U S A**, 97, 8910-5.
- Teter, S. A. & Klionsky, D. J. (2000) Transport of proteins to the yeast vacuole: autophagy, cytoplasm-to-vacuole targeting, and role of the vacuole in degradation. **Semin Cell Dev Biol**, 11, 173-9.
- Tosch, V., Rohde, H. M., Tronchere, H., Zanoteli, E., Monroy, N., Kretz, C., Dondaine, N., Payrastré, B., Mandel, J. L. & Laporte, J. (2006) A novel PtdIns3P and PtdIns(3,5)P2 phosphatase with an inactivating variant in centronuclear myopathy. **Hum Mol Genet**, 15, 3098-106.
- Touchberry, C. D., Bales, I. K., Stone, J. K., Rohrberg, T. J., Parekar, N. K., Nguyen, T., Fuentes, O., Liu, X., Qu, C. K., Andresen, J. J., Valdivia, H. H., Brotto, M. & Wacker, M. J. (2010) Phosphatidylinositol 3,5-bisphosphate (PI(3,5)P2) potentiates cardiac contractility via activation of the ryanodine receptor. **J Biol Chem**, 285, 40312-21.
- Trautwein, M., Schindler, C., Gauss, R., Dengjel, J., Hartmann, E. & Spang, A. (2006) Arf1p, Chs5p and the ChAPs are required for export of specialized cargo from the Golgi. **Embo J**, 25, 943-54.
- Trilla, J. A., Duran, A. & Roncero, C. (1999) Chs7p, a new protein involved in the control of protein export from the endoplasmic reticulum that is specifically engaged in the regulation of chitin synthesis in *Saccharomyces cerevisiae*. **J Cell Biol**, 145, 1153-63.
- Tsien, R. Y. (1998) The green fluorescent protein. **Annu Rev Biochem**, 67, 509-44.
- Tsuruta, F., Green, E. M., Rousset, M. & Dolmetsch, R. E. (2009) PIKfyve regulates CaV1.2 degradation and prevents excitotoxic cell death. **J Cell Biol**, 187, 279-94.

- Urbanowski, J. L. & Piper, R. C. (2001) Ubiquitin sorts proteins into the intraluminal degradative compartment of the late-endosome/vacuole. **Traffic**, 2, 622-30.
- Valdivia, R. H., Baggott, D., Chuang, J. S. & Schekman, R. W. (2002) The yeast clathrin adaptor protein complex 1 is required for the efficient retention of a subset of late Golgi membrane proteins. **Dev Cell**, 2, 283-94.
- Valdivia, R. H. & Schekman, R. (2003) The yeasts Rho1p and Pkc1p regulate the transport of chitin synthase III (Chs3p) from internal stores to the plasma membrane. **Proc Natl Acad Sci U S A**, 100, 10287-92.
- Velayos-Baeza, A., Vettori, A., Copley, R. R., Dobson-Stone, C. & Monaco, A. P. (2004) Analysis of the human VPS13 gene family. **Genomics**, 84, 536-49.
- Vicinanza, M., D'angelo, G., Di Campli, A. & De Matteis, M. A. (2008a) Function and dysfunction of the PI system in membrane trafficking. **Embo J**, 27, 2457-70.
- Vicinanza, M., D'angelo, G., Di Campli, A. & De Matteis, M. A. (2008b) Phosphoinositides as regulators of membrane trafficking in health and disease. **Cell Mol Life Sci**, 65, 2833-41.
- Vida, T. A. & Emr, S. D. (1995) A new vital stain for visualizing vacuolar membrane dynamics and endocytosis in yeast. **J Cell Biol**, 128, 779-92.
- Wang, C. W., Hamamoto, S., Orci, L. & Schekman, R. (2006) Exomer: A coat complex for transport of select membrane proteins from the trans-Golgi network to the plasma membrane in yeast. **J Cell Biol**, 174, 973-83.
- Warren, G. & Wickner, W. (1996) Organelle inheritance. **Cell**, 84, 395-400.
- Wassmer, T., Attar, N., Bujny, M. V., Oakley, J., Traer, C. J. & Cullen, P. J. (2007) A loss-of-function screen reveals SNX5 and SNX6 as potential components of the mammalian retromer. **J Cell Sci**, 120, 45-54.
- Weisman, L. S. (2003) Yeast vacuole inheritance and dynamics. **Annu Rev Genet**, 37, 435-60.
- Weisman, L. S., Emr, S. D. & Wickner, W. T. (1990) Mutants of *Saccharomyces cerevisiae* that block intervacuole vesicular traffic and vacuole division and segregation. **Proc Natl Acad Sci U S A**, 87, 1076-80.
- Whitley, P., Reaves, B. J., Hashimoto, M., Riley, A. M., Potter, B. V. & Holman, G. D. (2003) Identification of mammalian Vps24p as an effector of phosphatidylinositol 3,5-bisphosphate-dependent endosome compartmentalization. **J Biol Chem**, 278, 38786-95.
- Whyte, J. R. & Munro, S. (2001) A yeast homolog of the mammalian mannose 6-phosphate receptors contributes to the sorting of vacuolar hydrolases. **Curr Biol**, 11, 1074-8.
- Yamamoto, A., Dewald, D. B., Boronenkov, I. V., Anderson, R. A., Emr, S. D. & Koshland, D. (1995) Novel PI(4)P 5-kinase homologue, Fab1p, essential for normal vacuole function and morphology in yeast. **Mol Biol Cell**, 6, 525-39.
- Zhang, Y., Zolov, S. N., Chow, C. Y., Slutsky, S. G., Richardson, S. C., Piper, R. C., Yang, B., Nau, J. J., Westrick, R. J., Morrison, S. J., Meisler, M. H. & Weisman, L. S. (2007) Loss of Vac14, a regulator of the signaling lipid phosphatidylinositol 3,5-bisphosphate, results in neurodegeneration in mice. **Proc Natl Acad Sci U S A**, 104, 17518-23.
- Ziman, M., Chuang, J. S. & Schekman, R. W. (1996) Chs1p and Chs3p, two proteins involved in chitin synthesis, populate a compartment of the *Saccharomyces cerevisiae* endocytic pathway. **Mol Biol Cell**, 7, 1909-19.
- Ziman, M., Chuang, J. S., Tsung, M., Hamamoto, S. & Schekman, R. (1998) Chs6p-dependent anterograde transport of Chs3p from the chitosome to the plasma membrane in *Saccharomyces cerevisiae*. **Mol Biol Cell**, 9, 1565-76.

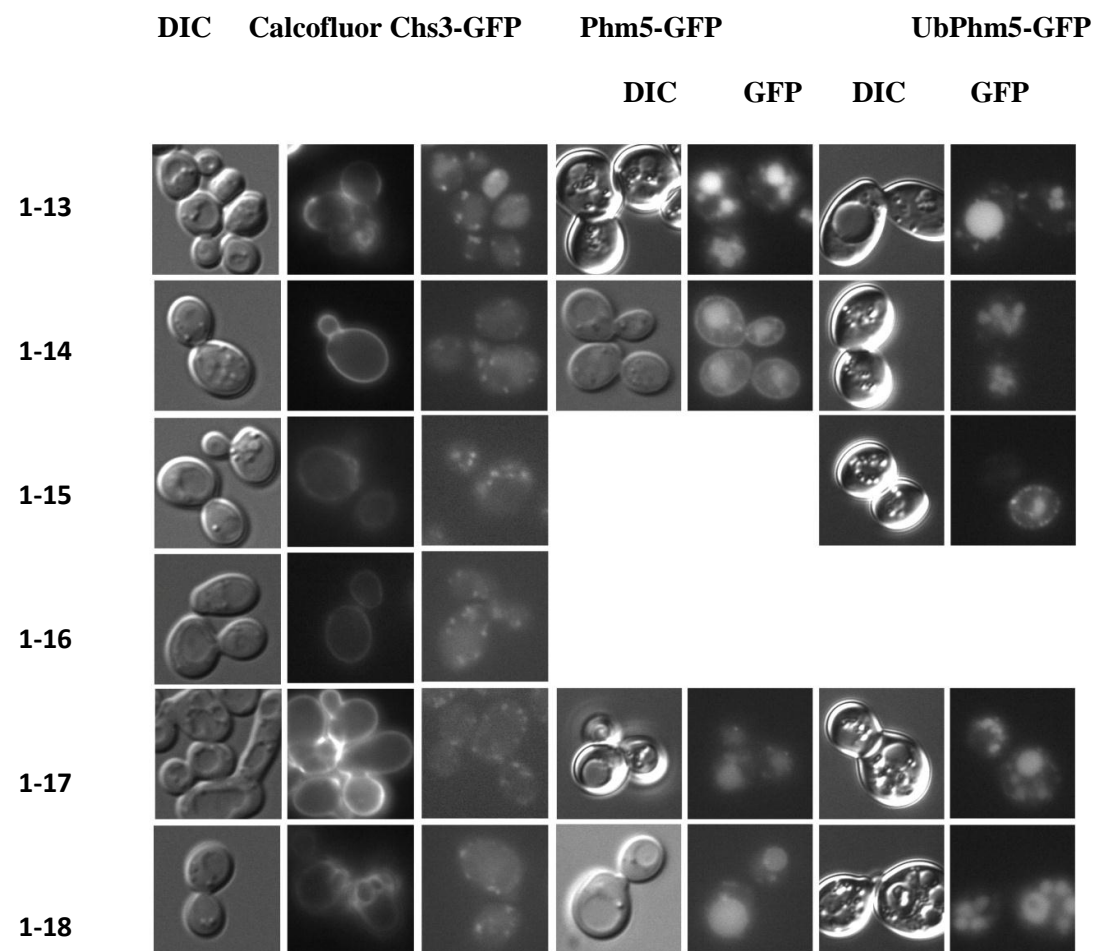
Appendix 1: Visulisation of the mutants. **EMS mutants 1-1 to 1-6**



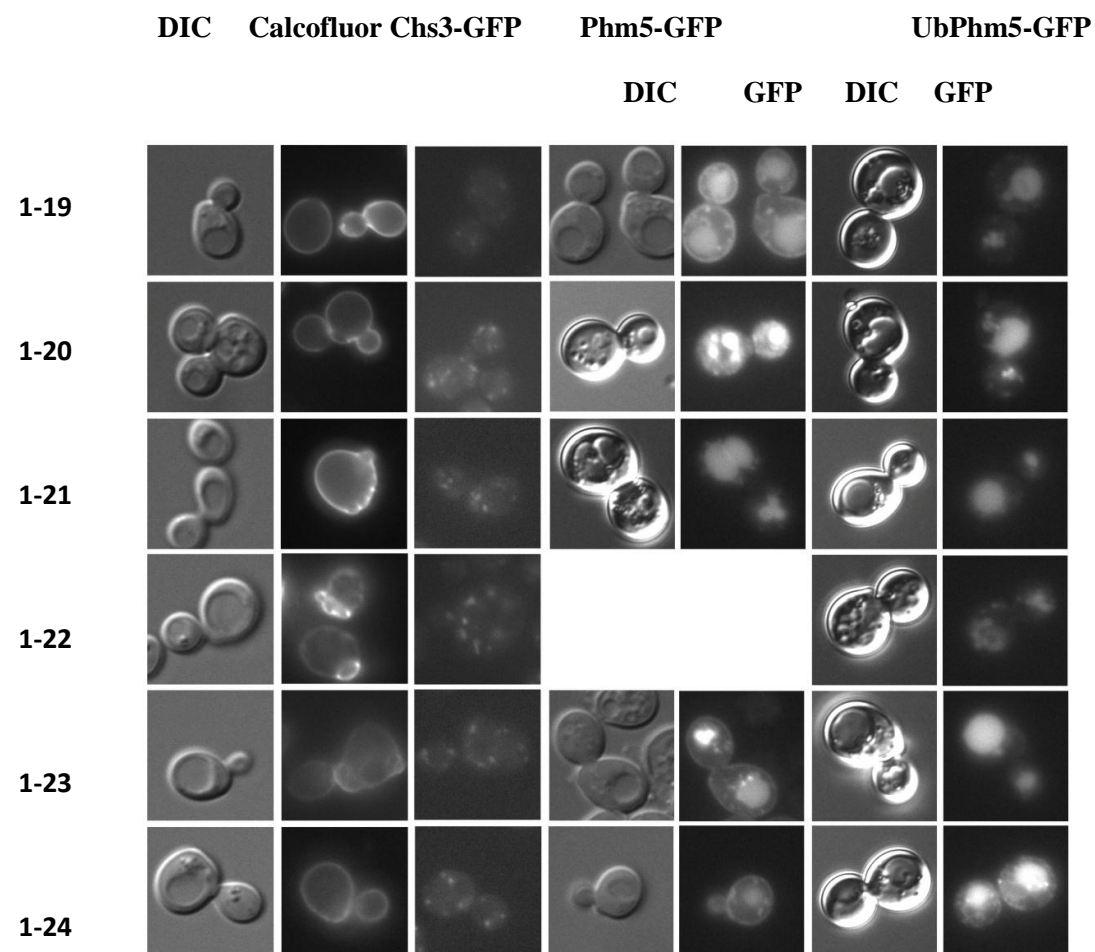
EMS mutants 1-7 to 1-12



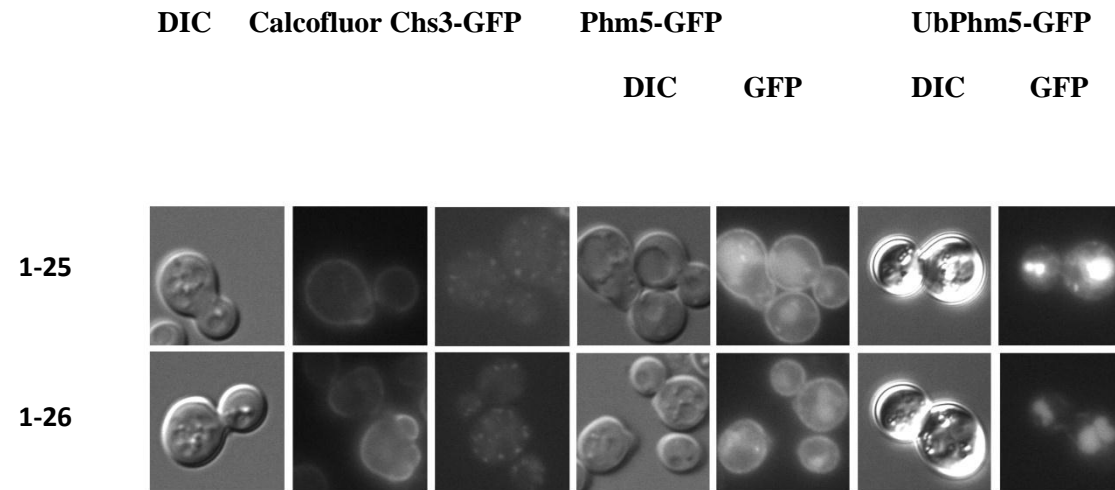
EMS mutants 1-13 to 1-18



EMS mutants 1-19 to 1-24

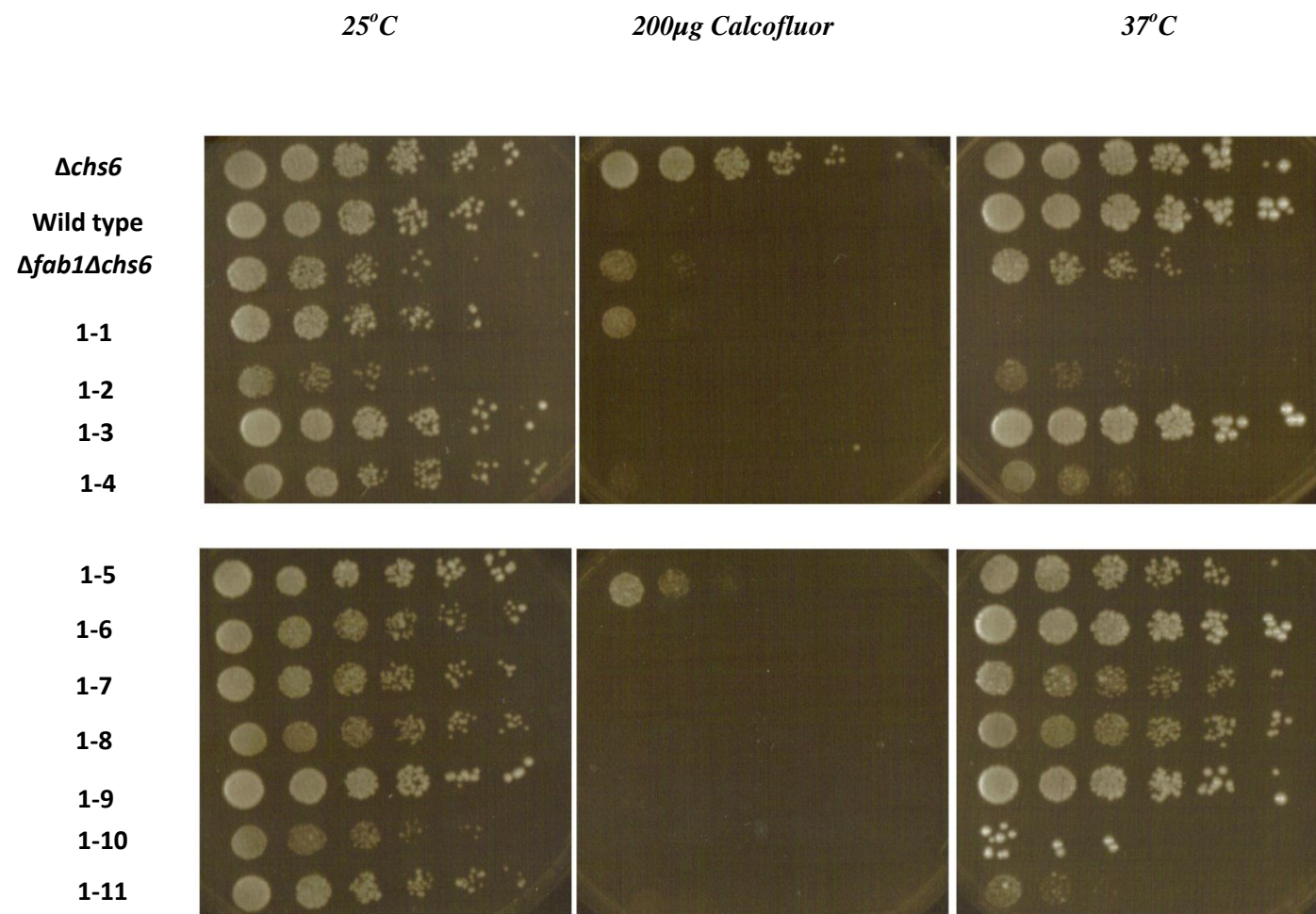


EMS mutants 1-25 to 1-26



Fluorescence images of logarithmic phase cultures ($5 \times 10^6 - 1 \times 10^7$ cells/ml) of mutant cells transformed with the indicated GFP constructs.. These images are representative of three replicate cultures. All strains were cultured in SC-His, Sc-Ura or YETD G418 media+2% glu medium and grown at 25°C. All panels represent 11μM.

Appendix 2: Spot dilutions of the Mutants



Spot dilutions of Mutants

25°C

200µg Calcofluor

37°C

1-12

1-13

1-14

1-15

1-16

1-17

1-18

1-19

1-20

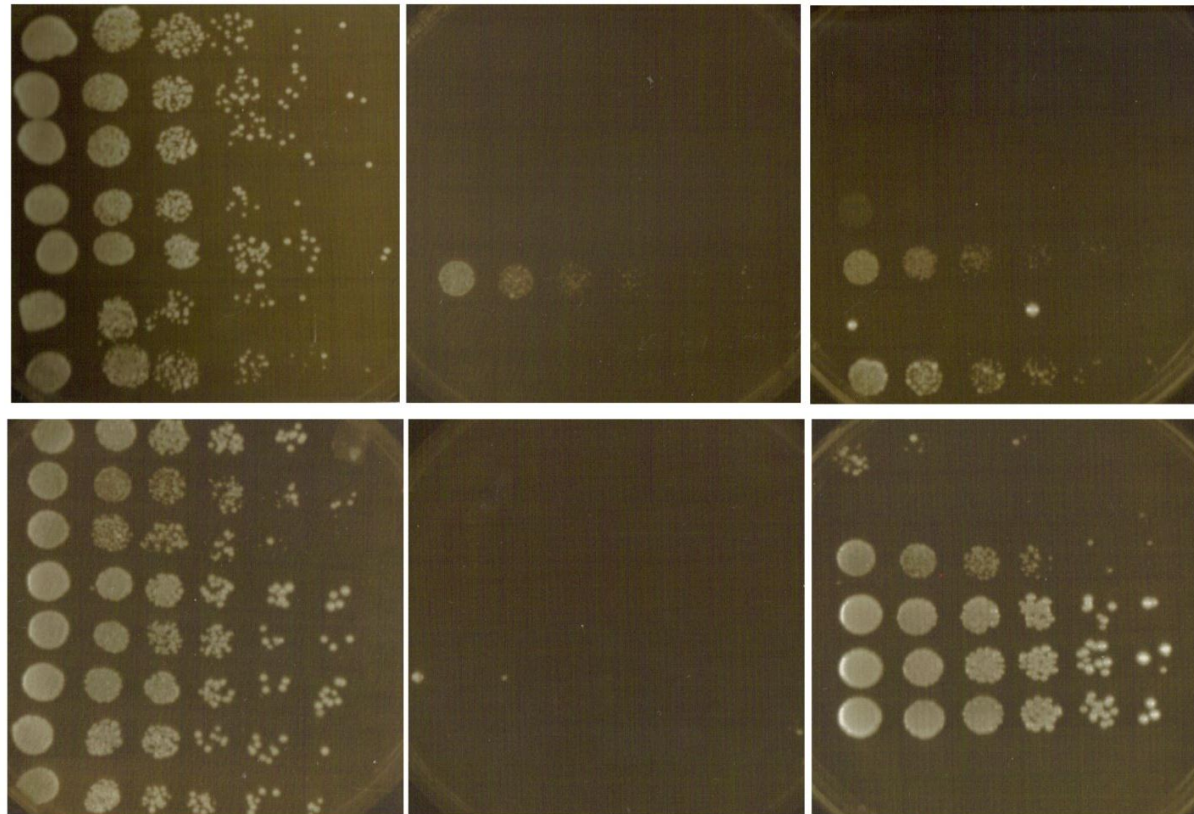
1-21

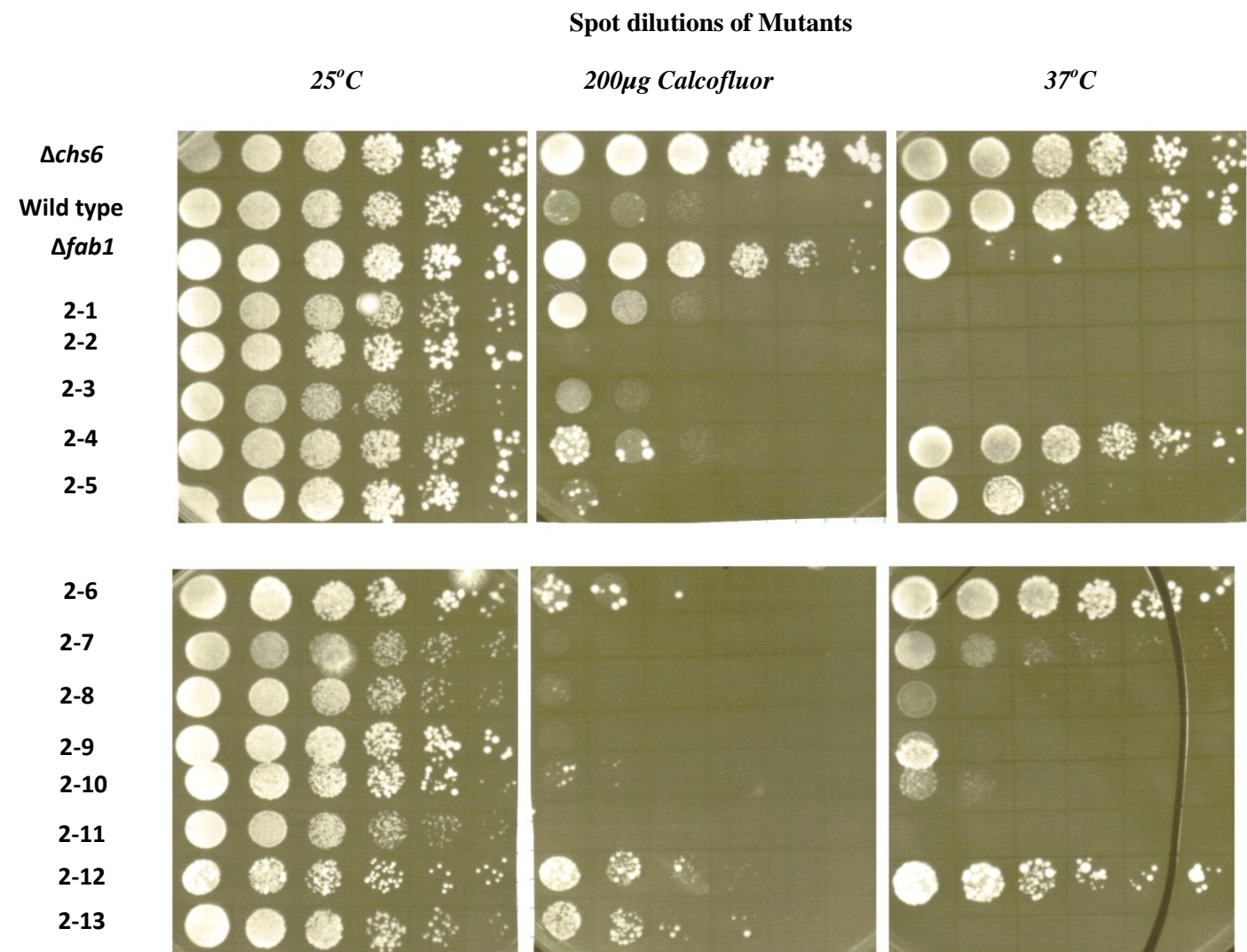
1-22

1-23

1-24

1-25





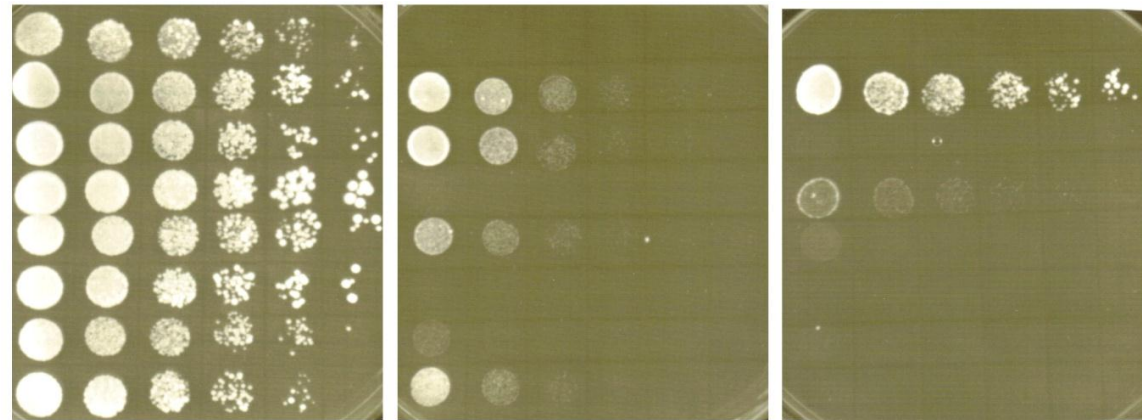
Spot dilutions of Mutants

25°C

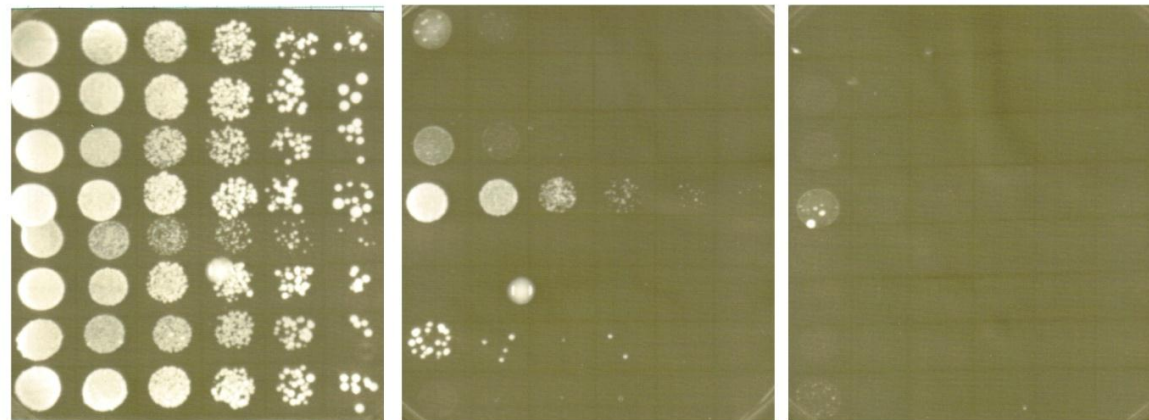
200µg Calcofluor

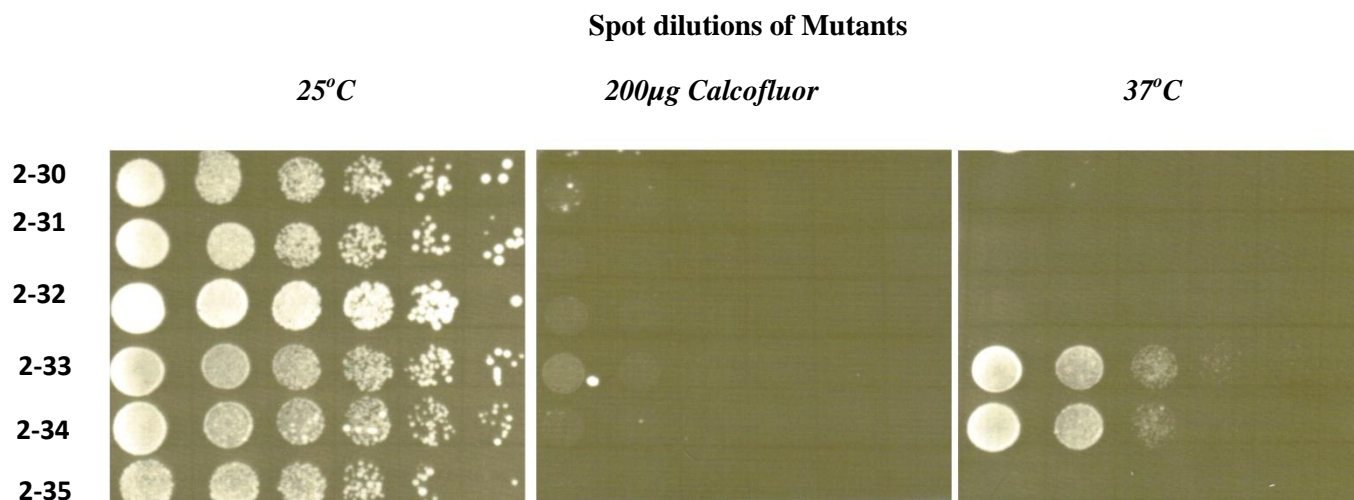
37°C

2-14
2-15
2-16
2-17
2-18
2-19
2-20
2-21



2-22
2-23
2-24
2-25
2-26
2-27
2-28
2-29





Mutant strains were grown to exponential phase till about $\sim 1 \times 10^7$ cells/ml in YPD + 2% glu for wild type cells or added G418 for mutants. Dilution assay was carried out as described in methodology section. Cells were serially diluted five-fold then grown on YTD+2% glu agar plates or on the same plate but with 200µg/ml calcofluor white at 25°C and on YETD plates at 37°C for 3 days.

Appendix 3: Complementation analysis of mutants

Complementation analysis carried out as described in Chapter 2. The mutants in the first column indicate those that have mating type a. Those highlighted in grey could not be successfully backcrossed and therefore matings have not been carried out. Strains in rows represent the α mating type mutants.

Mutant	1-1	1-2	1-3	1-4	1-5	1-6	1-7	1-8	1-9	1-10	1-11	1-12	1-13	1-14	1-15	1-16	1-17	1-18	1-19	1-20	1-21	1-22	1-23	1-24	1-25	1-26
1-1	X	-	-	-	-	-	-	-	-	-	-	-	-	-	-	-	-	-	-	-	-	-	-	-	-	-
1-2	-	X	-	-	-	-	-	-	-	-	-	-	-	-	-	-	-	-	-	-	-	-	-	-	-	-
1-3	-	-	X	-	-	-	-	-	-	-	-	-	-	-	-	-	-	-	-	-	-	-	-	-	-	-
1-4	-	-	-	X	-	-	-	-	-	-	-	-	-	-	-	-	-	-	-	-	-	-	-	-	-	-
1-5	-	-	-	-	X	-	-	-	-	-	-	-	-	-	-	-	-	-	-	-	-	-	-	-	-	-
1-6	-	-	-	-	-	X	-	-	-	-	-	-	-	-	-	-	-	-	-	-	-	-	-	-	-	-
1-7	-	-	-	-	-	-	X	-	-	-	-	-	-	-	-	-	-	-	-	-	-	-	-	-	-	-
1-8	-	-	-	-	-	-	-	X	-	-	-	-	-	-	-	-	-	-	-	-	-	-	-	-	-	-
1-9	-	-	-	-	-	-	-	-	X	-	-	-	-	-	-	-	-	-	-	-	-	-	-	-	-	-
1-10	-	-	-	-	-	-	-	-	-	X	-	-	-	-	-	-	-	-	-	-	-	-	-	-	-	-
1-11																										
1-12	-	-	-	-	-	-	-	-	-	-	-	X	-	-	-	-	-	-	-	-	-	-	-	-	-	-
1-13	-	-	-	-	-	-	-	-	-	-	-	-	X	-	-	-	-	-	-	-	-	-	-	-	-	-
1-14	-	-	-	-	-	-	-	-	-	-	-	-	-	X	-	-	-	-	-	-	-	-	-	-	-	-
1-15	-	-	-	-	-	-	-	-	-	-	-	-	-	-	X	-	-	-	-	-	-	-	-	-	-	-
1-16	-	-	-	-	-	-	-	-	-	-	-	-	-	-	-	X	-	-	-	-	-	-	-	-	-	-
1-17	-	-	-	-	-	-	-	-	-	-	-	-	-	-	-	-	X	-	-	-	-	-	-	-	-	-
1-18	-	-	-	-	-	-	-	-	-	-	-	-	-	-	-	-	-	X	-	-	-	-	-	-	-	-
1-19	-	-	-	-	-	-	-	-	-	-	-	-	-	-	-	-	-	-	X	-	-	-	-	-	-	-
1-20	-	-	-	-	-	-	-	-	-	-	-	-	-	-	-	-	-	-	-	X	-	-	-	-	-	-
1-21	-	-	-	-	-	-	-	-	-	-	-	-	-	-	-	-	-	-	-	-	X	-	-	-	-	-
1-22	-	-	-	-	-	-	-	-	-	-	-	-	-	-	-	-	-	-	-	-	-	X	-	-	-	-
1-23	-	-	-	-	-	-	-	-	-	-	-	-	-	-	-	-	-	-	-	-	-	-	X	-	-	-
1-24	-	-	-	-	-	-	-	-	-	-	-	-	-	-	-	-	-	-	-	-	-	-	-	X	-	-
1-25	-	-	-	-	-	-	-	-	-	-	-	-	-	-	-	-	-	-	-	-	-	-	-	-	X	-
1-26	-	-	-	-	-	-	-	-	-	-	-	-	-	-	-	-	-	-	-	-	-	-	-	-	-	X

Mutant	2-1	2-2	2-3	2-4	2-5	2-6	2-7	2-8	2-9	2-10	2-11	2-12	2-13
1-1	-	-	-	-	-	-	-	-	-	-	-	-	-
1-2	-	-	-	-	-	-	-	-	-	-	-	-	-
1-3	-	-	-	-	-	-	-	-	-	-	-	-	-
1-4	-	-	-	-	-	-	-	-	-	-	-	-	-
1-5	-	-	-	-	-	-	-	-	-	-	-	-	-
1-6	-	-	-	-	-	-	-	-	-	-	-	-	-
1-7	-	-	-	-	-	-	-	-	-	-	-	-	-
1-8	-	-	-	-	-	-	-	-	-	-	-	-	-
1-9	-	-	-	-	-	-	-	-	-	-	-	-	-
1-10	-	-	-	-	-	-	-	-	-	-	-	-	-
1-11													
1-12	-	-	-	-	-	-	-	-	-	-	-	-	-
1-13	-	-	-	-	-	-	-	-	-	-	-	-	-
1-14	-	-	-	-	-	-	-	-	-	-	-	-	-
1-15	-	-	-	-	-	-	-	-	-	-	-	-	-
1-16	-	-	-	-	-	-	-	-	-	-	-	-	-
1-17	-	-	-	-	-	-	-	-	-	-	-	-	-
1-18	-	-	-	-	-	-	-	-	-	-	-	-	-
1-19	-	-	-	-	-	-	-	-	-	-	-	-	-
1-20	-	-	-	-	-	-	-	-	-	-	-	-	-
1-21	-	-	-	-	-	-	-	-	-	-	-	-	-
1-22	-	-	-	-	-	-	-	-	-	-	-	-	-
1-23	-	-	-	-	-	-	-	-	-	-	-	-	-
1-24	-	-	-	-	-	-	-	-	-	-	-	-	-
1-25	-	-	-	-	-	-	-	-	-	-	-	-	-
1-26	-	-	-	-	-	-	-	-	-	-	-	-	-

Mutant	2-14	2-15	2-16	2-17	2-18	2-19	2-20	2-21	2-22	2-23	2-24	2-25	2-26	2-27	2-28	2-29	2-30	2-31	2-32	2-33	2-34	2-35
1-1	-	-	-	-	-	-	-	-	-	-	-	-	-	-	-	-	-	-	-	-	-	-
1-2	-	-	-	-	-	-	-	-	-	-	-	-	-	-	-	-	-	-	-	-	-	-
1-3	-	-	-	-	-	-	-	-	-	-	-	-	-	-	-	-	-	-	-	-	-	-
1-4	-	-	-	-	-	-	-	-	-	-	-	-	-	-	-	-	-	-	-	-	-	-
1-5	-	-	-	-	-	-	-	-	-	-	-	-	-	-	-	-	-	-	-	-	-	-
1-6	-	-	-	-	-	-	-	-	-	-	-	-	-	-	-	-	-	-	-	-	-	-
1-7	-	-	-	-	-	-	-	-	-	-	-	-	-	-	-	-	-	-	-	-	-	-
1-8	-	-	-	-	-	-	-	-	-	-	-	-	-	-	-	-	-	-	-	-	-	-
1-9	-	-	-	-	-	-	-	-	-	-	-	-	-	-	-	-	-	-	-	-	-	-
1-10	-	-	-	-	-	-	-	-	-	-	-	-	-	-	-	-	-	-	-	-	-	-
1-11																						
1-12	-	-	-	-	-	-	-	-	-	-	-	-	-	-	-	-	-	-	-	-	-	-
1-13	-	-	-	-	-	-	-	-	-	-	-	-	-	-	-	-	-	-	-	-	-	-
1-14	-	-	-	-	-	-	-	-	-	-	-	-	-	-	-	-	-	-	-	-	-	-
1-15	-	-	-	-	-	-	-	-	-	-	-	-	-	-	-	-	-	-	-	-	-	-
1-16	-	-	-	-	-	-	-	-	-	-	-	-	-	-	-	-	-	-	-	-	-	-
1-17	-	-	-	-	-	-	-	-	-	-	-	-	-	-	-	-	-	-	-	-	-	-
1-18	-	-	-	-	-	-	-	-	-	-	-	-	-	-	-	-	-	-	-	-	-	-
1-19	-	-	-	-	-	-	-	-	-	-	-	-	-	-	-	-	-	-	-	-	-	-
1-20	-	-	-	-	-	-	-	-	-	-	-	-	-	-	-	-	-	-	-	-	-	-
1-21	-	-	-	-	-	-	-	-	-	-	-	-	-	-	-	-	-	-	-	-	-	-
1-22	-	-	-	-	-	-	-	-	-	-	-	-	-	-	-	-	-	-	-	-	-	-
1-23	-	-	-	-	-	-	-	-	-	-	-	-	-	-	-	-	-	-	-	-	-	-
1-24	-	-	-	-	-	-	-	-	-	-	-	-	-	-	-	-	-	-	-	-	-	-
1-25	-	-	-	-	-	-	-	-	-	-	-	-	-	-	-	-	-	-	-	-	-	-
1-26	-	-	-	-	-	-	-	-	-	-	-	-	-	-	-	-	-	-	-	-	-	-

Mutant	1-1	1-2	1-3	1-4	1-5	1-6	1-7	1-8	1-9	1-10	1-11	1-12	1-13	1-14	1-15	1-16	1-17	1-18	1-19	1-20	1-21	1-22	1-23	1-24	1-25	1-26
2-1	-	-	-	-	-	-	-	-	-	-	-	-	-	-	-	-	-	-	-	-	-	-	-	-	-	-
2-2	-	-	-	-	-	-	-	-	-	-	-	-	-	-	-	-	-	-	-	-	-	-	-	-	-	-
2-3	-	-	-	-	-	-	-	-	-	-	-	-	-	-	-	-	-	-	-	-	-	-	-	-	-	-
2-4	-	-	-	-	-	-	-	-	-	-	-	-	-	-	-	-	-	-	-	-	-	-	-	-	-	-
2-5	-	-	-	-	-	-	-	-	-	-	-	-	-	-	-	-	-	-	-	-	-	-	-	-	-	-
2-6	-	-	-	-	-	-	-	-	-	-	-	-	-	-	-	-	-	-	-	-	-	-	-	-	-	-
2-7	-	-	-	-	-	-	-	-	-	-	-	-	-	-	-	-	-	-	-	-	-	-	-	-	-	-
2-8	-	-	-	-	-	-	-	-	-	-	-	-	-	-	-	-	-	-	-	-	-	-	-	-	-	-
2-9	-	-	-	-	-	-	-	-	-	-	-	-	-	-	-	-	-	-	-	-	-	-	-	-	-	-
2-10	-	-	-	-	-	-	-	-	-	-	-	-	-	-	-	-	-	-	-	-	-	-	-	-	-	-
2-11	-	-	-	-	-	-	-	-	-	-	-	-	-	-	-	-	-	-	-	-	-	-	-	-	-	-
2-12	Y																									
2-13	-	-	-	-	-	-	-	-	-	-	-	-	-	-	-	-	-	-	-	-	-	-	-	-	-	-
2-14	-	-	-	-	-	-	-	-	-	-	-	-	-	-	-	-	-	-	-	-	-	-	-	-	-	-
2-15	-	-	-	-	-	-	-	-	-	-	-	-	-	-	-	-	-	-	-	-	-	-	-	-	-	-
2-16	-	-	-	-	-	-	-	-	-	-	-	-	-	-	-	-	-	-	-	-	-	-	-	-	-	-
2-17	-	-	-	-	-	-	-	-	-	-	-	-	-	-	-	-	-	-	-	-	-	-	-	-	-	-
2-18	-	-	-	-	-	-	-	-	-	-	-	-	-	-	-	-	-	-	-	-	-	-	-	-	-	-
2-19	-	-	-	-	-	-	-	-	-	-	-	-	-	-	-	-	-	-	-	-	-	-	-	-	-	-
2-20	-	-	-	-	-	-	-	-	-	-	-	-	-	-	-	-	-	-	-	-	-	-	-	-	-	-
2-21	-	-	-	-	-	-	-	-	-	-	-	-	-	-	-	-	-	-	-	-	-	-	-	-	-	-
2-22	-	-	-	-	-	-	-	-	-	-	-	-	-	-	-	-	-	-	-	-	-	-	-	-	-	-
2-23	-	-	-	-	-	-	-	-	-	-	-	-	-	-	-	-	-	-	-	-	-	-	-	-	-	-
2-24	-	-	-	-	-	-	-	-	-	-	-	-	-	-	-	-	-	-	-	-	-	-	-	-	-	-
2-25	-	-	-	-	-	-	-	-	-	-	-	-	-	-	-	-	-	-	-	-	-	-	-	-	-	-
2-26	-	-	-	-	-	-	-	-	-	-	-	-	-	-	-	-	-	-	-	-	-	-	-	-	-	-
2-27																										
2-28	-	-	-	-	-	-	-	-	-	-	-	-	-	-	-	-	-	-	-	-	-	-	-	-	-	-
2-29																										
2-30	-	-	-	-	-	-	-	-	-	-	-	-	-	-	-	-	-	-	-	-	-	-	-	-	-	-
2-31	-	-	-	-	-	-	-	-	-	-	-	-	-	-	-	-	-	-	-	-	-	-	-	-	-	-

2-32	-	-	-	-	-	-	-	-	-	-	-	-	-	-	-	-	-	-	-	-	-	-	-	-	-	-	-
2-33	-	-	-	-	-	-	-	-	-	-	-	-	-	-	-	-	-	-	-	-	-	-	-	-	-	-	-
2-34	-	-	-	-	-	-	-	-	-	-	-	-	-	-	-	-	-	-	-	-	-	-	-	-	-	-	-
2-35																											

Mutant	2-1	2-2	2-3	2-4	2-5	2-6	2-7	2-8	2-9	2-10	2-11	2-12	2-13
2-1	X	-	-	-	-	-	-	-	-	-	-	-	-
2-2	-	X	-	-	-	-	-	-	-	-	-	-	-
2-3	-	-	X	-	-	-	-	-	-	-	-	-	-
2-4	-	-	-	X	-	-	-	-	-	-	-	-	-
2-5	-	-	-	-	X	-	-	-	-	-	-	-	-
2-6	-	-	-	-	-	X	-	-	-	-	-	-	-
2-7	-	-	-	-	-	-	X	-	-	-	-	-	-
2-8	-	-	-	-	-	-	-	X	-	-	-	-	-
2-9	-	-	-	-	-	-	-	-	X	-	-	-	-
2-10	-	-	-	-	-	-	-	-	-	X	-	-	-
2-11	-	-	-	-	-	-	-	-	-	-	X	-	-
2-12													
2-13	-	-	-	-	-	-	-	-	-	-	-	-	X
2-14	-	-	-	-	-	-	-	-	-	-	-	-	-
2-15	-	-	-	-	-	-	-	-	-	-	-	-	-
2-16	-	-	-	-	-	-	-	-	-	-	-	-	-
2-17	-	-	-	-	-	-	-	-	-	-	-	-	-
2-18	-	-	-	-	-	-	-	-	-	-	-	-	-
2-19	-	-	-	-	-	-	-	-	-	-	-	-	-
2-20	-	-	-	-	-	-	-	-	-	-	-	-	-
2-21	-	-	-	-	-	-	-	-	-	-	-	-	-
2-22	-	-	-	-	-	-	-	-	-	-	-	-	-
2-23	-	-	-	-	-	-	-	-	-	-	-	-	-
2-24	-	-	-	-	-	-	-	-	-	-	-	-	-
2-25	-	-	-	-	-	-	-	-	-	-	-	-	-

2-26	-	-	-	-	-	-	-	-	-	-	-	-	-
2-27													
2-28	-	-	-	-	-	-	-	-	-	-	-	-	-
2-29													
2-30	-	-	-	-	-	-	-	-	-	-	-	-	-
2-31	-	-	-	-	-	-	-	-	-	-	-	-	-
2-32	-	-	-	-	-	-	-	-	-	-	-	-	-
2-33	-	-	-	-	-	-	-	-	-	-	-	-	-
2-34	-	-	-	-	-	-	-	-	-	-	-	-	-
2-35													

Mutant	2-14	2-15	2-16	2-17	2-18	2-19	2-20	2-21	2-22	2-23	2-24	2-25	2-26	2-27	2-28	2-29	2-30	2-31	2-32	2-33	2-34	2-35
2-1	-	-	-	-	-	-	-	-	-	-	-	-	-	-	-	-	-	-	-	-	-	-
2-2	-	-	-	-	-	-	-	-	-	-	-	-	-	-	-	-	-	-	-	-	-	-
2-3	-	-	-	-	-	-	-	-	-	-	-	-	-	-	-	-	-	-	-	-	-	-
2-4	-	-	-	-	-	-	-	-	-	-	-	-	-	-	-	-	-	-	-	-	-	-
2-5	-	-	-	-	-	-	-	-	-	-	-	-	-	-	-	-	-	-	-	-	-	-
2-6	-	-	-	-	-	-	-	-	-	-	-	-	-	-	-	-	-	-	-	-	-	-
2-7	-	-	-	-	-	-	-	-	-	-	-	-	-	-	-	-	-	-	-	-	-	-
2-8	-	-	-	-	-	-	-	-	-	-	-	-	-	-	-	-	-	-	-	-	-	-
2-9	-	-	-	-	-	-	-	-	-	-	-	-	-	-	-	-	-	-	-	-	-	-
2-10	-	-	-	-	-	-	-	-	-	-	-	-	-	-	-	-	-	-	-	-	-	-
2-11	-	-	-	-	-	-	-	-	-	-	-	-	-	-	-	-	-	-	-	-	-	-
2-12																						
2-13	-	-	-	-	-	-	-	-	-	-	-	-	-	-	-	-	-	-	-	-	-	-
2-14	X	-	-	-	-	-	-	-	-	-	-	-	-	-	-	-	-	-	-	-	-	-
2-15	-	X	-	-	-	-	-	-	-	-	-	-	-	-	-	-	-	-	-	-	-	-
2-16	-	-	X	-	-	-	-	-	-	-	-	-	-	-	-	-	-	-	-	-	-	-
2-17	-	-	-	X	-	-	-	-	-	-	-	-	-	-	-	-	-	-	-	-	-	-
2-18	-	-	-	-	X	-	-	-	-	-	-	-	-	-	-	-	-	-	-	-	-	-
2-19	-	-	-	-	-	X	-	-	-	-	-	-	-	-	-	-	-	-	-	-	-	-

2-20	-	-	-	-	-	-	X	-	-	-	-	-	-	-	-	-	-	-	-	-	-	-
2-21	-	-	-	-	-	-	-	X	-	-	-	-	-	-	-	-	-	-	-	-	-	-
2-22	-	-	-	-	-	-	-	-	X	-	-	-	-	-	-	-	-	-	-	-	-	-
2-23	-	-	-	-	-	-	-	-	-	X	-	-	-	-	-	-	-	-	-	-	-	-
2-24	-	-	-	-	-	-	-	-	-	-	X	-	-	-	-	-	-	-	-	-	-	-
2-25	-	-	-	-	-	-	-	-	-	-	-	X	-	-	-	-	-	-	-	-	-	-
2-26	-	-	-	-	-	-	-	-	-	-	-	-	X	-	-	-	-	-	-	-	-	-
2-27																						
2-28	-	-	-	-	-	-	-	-	-	-	-	-	-	-	X	-	-	-	-	-	-	-
2-29																						
2-30	-	-	-	-	-	-	-	-	-	-	-	-	-	-	-	X	-	-	-	-	-	-
2-31	-	-	-	-	-	-	-	-	-	-	-	-	-	-	-	-	X	-	-	-	-	-
2-32	-	-	-	-	-	-	-	-	-	-	-	-	-	-	-	-	-	X	-	-	-	-
2-33	-	-	-	-	-	-	-	-	-	-	-	-	-	-	-	-	-	-	X	-	-	-
2-34	-	-	-	-	-	-	-	-	-	-	-	-	-	-	-	-	-	-	-	X	-	-
2-35																						